

# **Translating iterative reconstruction for CT to the clinic**

**A.M. den Harder**

Translating iterative reconstruction for CT to the clinic  
PhD thesis, Utrecht University, The Netherlands  
ISBN: 978-90-393-6851-0  
Copyright: Annemarie den Harder, 2017

The copyright of the articles that have been published or accepted for publication has been transferred to the respective journals. No part of this thesis may be reproduced without the written permission from the author, or, when appropriate, from the publishers of the publications.

Layout: Roy Sanders, Utrecht  
Cover design: Willemijn den Harder, Zwolle ([www.willemijndenharder.com](http://www.willemijndenharder.com))

# Translating iterative reconstruction for CT to the clinic

**Invoering van iteratieve reconstructie  
voor CT in de patiëntenzorg**  
(met een samenvatting in het Nederlands)

Proefschrift

ter verkrijging van de graad van doctor aan de Universiteit Utrecht  
op gezag van de rector magnificus, prof.dr. G.J. van der Zwaan,  
ingevolge het besluit van het college voor promoties  
in het openbaar te verdedigen  
op dinsdag 24 oktober 2017 des middags te 4.15 uur

door

Adriana Maria den Harder  
geboren op 12 december 1990 te Ouderkerk aan de Amstel

Promotoren: Prof. dr. T. Leiner  
Prof. dr. P.A. de Jong  
Copromotor: Dr. R.P.J. Budde

The research described in this thesis was partly funded by the Dutch Organization for Health Research and Development (grant number 837001403).

Financial support by the Dutch Heart Foundation for the publication of this thesis is gratefully acknowledged. Additional financial support for the publication of this thesis was generously provided by Philips Healthcare, Bayer and ChipSoft.



## Content

1.0	General introduction and outline of the thesis	9
-----	--	---

---

### Part I

#### Clinical implementation of iterative reconstruction in cardiac CT

---

1.1	Dose reduction with iterative reconstruction for coronary CT angiography: a systematic review and meta-analysis. <i>British Journal of Radiology 2016</i>	21
1.2	Dose reduction for coronary calcium scoring with hybrid and model-based iterative reconstruction: an ex vivo study. <i>International Journal of Cardiovascular Imaging 2014</i>	41
1.3	Finding the optimal dose reduction and iterative reconstruction level for coronary calcium scoring: a within patients analysis. <i>Journal of Cardiovascular Computed Tomography 2016</i>	59
1.4	Submillisievert coronary calcium quantification using model-based iterative reconstruction: a within patient analysis. <i>European Journal of Radiology 2016</i>	79

---

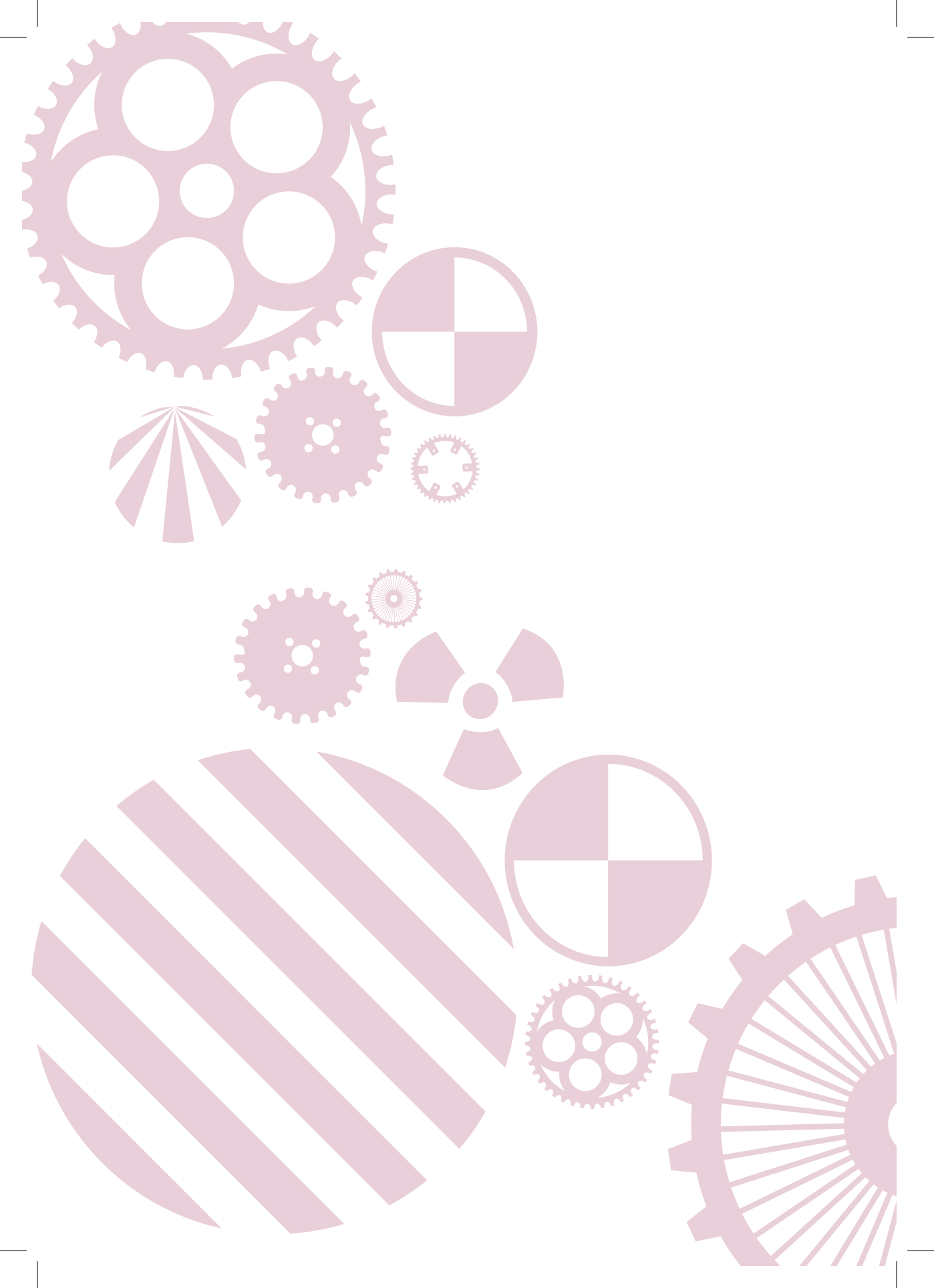
### Part 2

#### Clinical implementation of iterative reconstruction in thoraco-abdominal CT

---

2.1	Achievable dose reduction using iterative reconstruction for chest computed tomography: A systematic review. <i>European Journal of Radiology 2015</i>	101
2.2	Pulmonary nodule volumetry at different low CT radiation dose levels with hybrid and model-based iterative reconstruction: a within patient analysis. <i>Journal of Computer Assisted Tomography 2016</i>	119
2.3	Effect of radiation dose reduction and iterative reconstruction on computer-aided detection of pulmonary nodules: Intra-individual comparison. <i>European Journal of Radiology 2016</i>	137
2.4	Aortic Valve and Thoracic Aortic Calcification Measurements: How Low Can We Go in Radiation Dose? <i>Journal of Computer Assisted Tomography 2017</i>	153
2.5	Radiation dose reduction for CT assessment of urolithiasis using iterative reconstruction: a prospective intra-individual study. <i>European Radiology 2017</i>	173

<b>Part 3</b>		
<b>Clinical implementation of iterative reconstruction in pediatric CT</b>		
3.1	Hybrid and model-based iterative reconstruction for pediatric computed tomography. <i>AJR American Journal of Roentgenology 2015</i>	195
3.2	Radiation dose reduction in pediatric great vessel stent computed tomography using iterative reconstruction: a phantom study. <i>PLoS One 2017</i>	217
<b>Part 4</b>		
<b>The rationale and need for CT prior to cardiac surgery</b>		
4.1	Frequency of abnormal findings on routine chest radiography before cardiac surgery. <i>Submitted</i>	233
4.2	Can routine chest radiography be used to diagnose mild COPD? A nested case-control study <i>European Journal of Radiology 2017</i>	247
4.3	Effect of Computed Tomography before Cardiac Surgery on Surgical Strategy, Mortality and Stroke. <i>European Journal of Radiology 2016</i>	265
4.4	Ultra low-dose chest ct with iterative reconstructions as an alternative to conventional chest x-ray prior to heart surgery (CRICKET study): Rationale and design of a multicenter randomized trial. <i>Journal of Cardiovascular Computed Tomography 2016</i>	283
<b>Part 5</b>		
<b>Discussion</b>		
5.1	Summary	297
5.2	General Discussion	303
	Dutch summary (Nederlandse samenvatting)	319
	Acknowledgements (Dankwoord)	327
	Curriculum Vitae	333
	List of publications	337



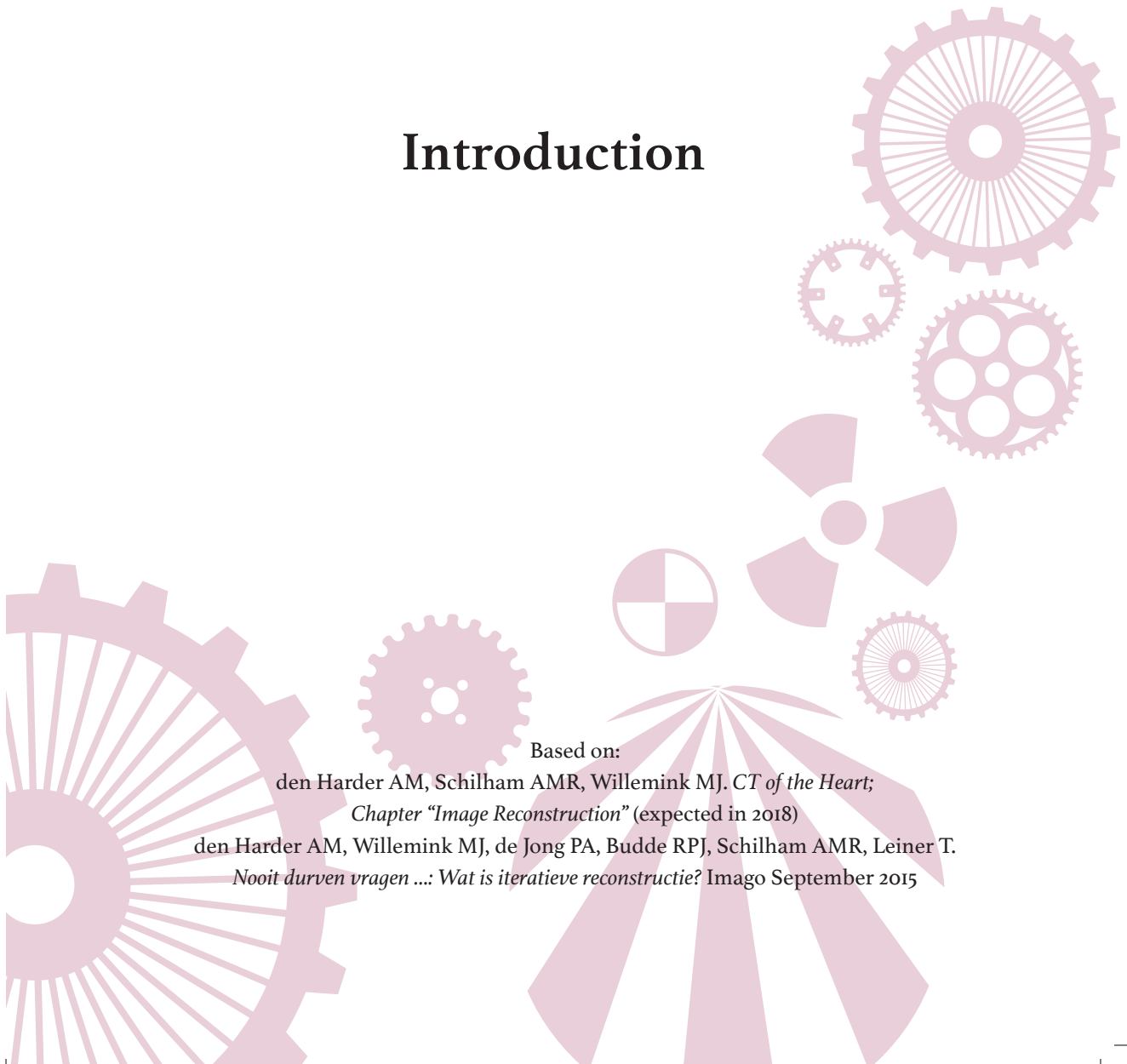
# Chapter 1.0

## Introduction

Based on:

den Harder AM, Schilham AMR, Willeminck MJ. *CT of the Heart*;  
*Chapter "Image Reconstruction"* (expected in 2018)

den Harder AM, Willeminck MJ, de Jong PA, Budde RPJ, Schilham AMR, Leiner T.  
*Nooit durven vragen ...: Wat is iteratieve reconstructie?* Imago September 2015



The number of CT examinations has increased tremendously over the years. The estimated number of annual CT examinations in the United States of America (USA) increased from 3 million in 1980 to 62 million in 1996 [1] and 82 million in 2016 [2]. In the Netherlands this number increased from 400,000 in 1991 to 1.4 million CT examinations in 2014 [3]. Compared to other BeNeLux countries Belgium and Luxembourg where more than twice as many CT examinations are performed per 100,000 inhabitants the number in the Netherlands is still low [4]. The associated radiation exposure brings a small risk of cancer later in life [1,5,6]. Most evidence regarding excess cancer risk from radiation exposure is based on information about atomic bomb survivors. Studies investigating dose levels below 10 mSv, a typical dose for CT examinations, are scarce. However, an often used calculation is that for a 1 Sv (1000 mSv) increase in radiation exposure the excess risk of death from cancer increases with 5%, thus for a CT scan of 1 mSv, an individual will incur 0.005% additional risk above the background cancer risk of 40% [7,8]. Several measures can be taken to reduce this risk. First and foremost CT examinations should only be performed when there is a proper indication and if other non-invasive imaging cannot provide the same information [9]. The American College of Radiology has published several appropriateness criteria to assist clinicians to order the appropriate imaging examination [10,11]. If applied correctly, this can result in a significant reduction in the number of CT examinations [12]. If a CT is needed, imaging should be limited to the correct body part and image acquisition protocols should be optimized for example by only acquiring necessary imaging phases. Furthermore, several developments in both CT hardware and software have been made to reduce the radiation dose [13]. This arises from the ALARA principle of radiation protection. ALARA is an acronym for “As Low As Reasonably Achievable” and is applied when ionizing radiation is used [14]. This thesis focuses on a recently introduced technical development with great promise to reduce CT radiation dose, namely the use of iterative reconstruction.

## **Image Reconstruction**

Image reconstruction is the formation of images based on CT projection data. During a CT-acquisition, x-ray photons travel from the CT tube to the detector. Once they hit the detector, x-ray photons are converted to light photons which are converted to an electrical signal. The electrical signal scales with the intensity of the detected x-rays. Based on the signals the detector receives, a

signal intensity profile is created which displays the number of signals with a specific intensity. All signals together received from a certain beam angle form a projection. The signal intensity profiles of each projection are transformed into x-ray attenuation values. If an object is placed between the CT tube and the detector, a decreased electrical signal is measured, which reflects an increase of the total x-ray attenuation along the line between the detector and the tube. Projection data can be stored in a two-dimensional image which is called a sinogram because of its sinusoid shape (*Figure 1*). The collection of projection data in a sinogram is called the raw data set, which can be used to reconstruct an image.

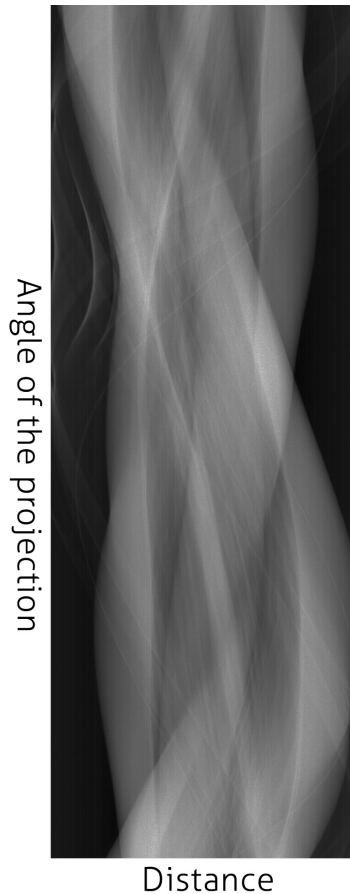
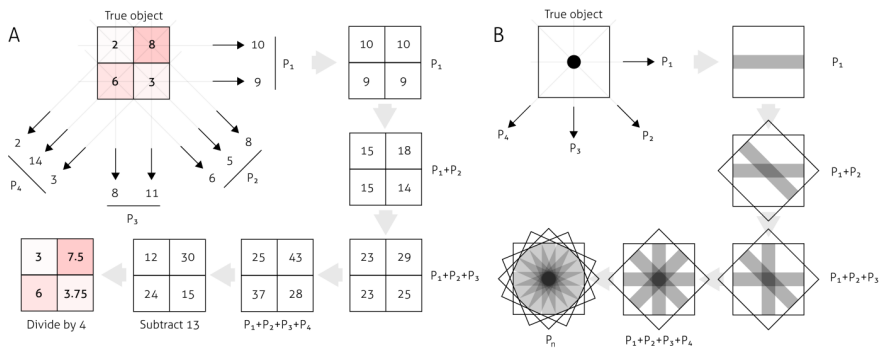


Figure 1 – Sinogram of a cardiac CT acquisition.

Although for each projection the total sum of attenuation values is known, the exact positions of those values along the projection are unknown. To compute an image from those values the total sum of attenuations is averaged over the different pixels on the projection line. It is possible to get an approximation of the numbers based on the total sum of attenuation values. To this aim, the values are smeared out across the projection and the different projections are summed and renormalized by dividing the total amount by the number of projections. Increasing the number of projections will lead to a better approximation of the true object. However, even with hundreds of projections the image will still remain an approximation and with this simple back projection the final image will be blurred (*Figure 2*). A convolution kernel is necessary for mathematical filtering to improve the approximation. Convolution takes the values of neighboring pixels into account with certain weights based on the distance. Depending on the kernel this can result in a smooth or a sharp image and everything in between. After the convolution kernel is applied to the projection data, back projection is performed to create an image.



**Figure 2**– Schematic explanation of back projection (A). The upper left matrix indicates the measured attenuation values of the true object. In this example there are four pixels and four projections are acquired at different angles ( $P_1$  to  $P_4$ ). The first projection ( $P_1$ ) shows the measured attenuation from left to right and the other projections ( $P_2$  to  $P_4$ ) are rotated by 45 degrees. The values are smeared out across the projection. For example the 10 in  $P_1$  is divided by two (number of pixels) therefore a five is allocated to each pixel. While in  $P_2$  the 8 and 6 are not divided because this are projections of a single pixel. Subsequently the projections are summed. Finally the numbers are divided by the number of projections, which is four. The final reconstruction is shown in the left lower corner. Increasing numbers of projections improves the quality of the approximated final reconstruction. On the right an example is shown with an image of a cylinder (B).

A commonly used reconstruction method is filtered back projection (FBP), in which a convolution kernel is applied to the projection data, followed by a back projection as explained above. This method works well in most situations, however at low radiation doses and in large patients FBP produces noisy images. To reduce the amount of noise, iterative reconstruction algorithms have been developed [15]. A form of iterative reconstruction was first described in the '70s under the name algebraic reconstruction [16]. Due to the limited computational power at that time it was not suitable for clinical practice. The first step of iterative reconstruction is an FBP. From the images derived from the FBP, new projection data are generated based on prior information concerning the scanner geometry, the x-ray spectrum, the detector characteristics and a noise model. Subsequently the new projection data are compared to the original projection data and corrections in noise modelling are performed. This process is repeated (iterated) several times. Each time the newly generated projection data will represent a closer match to the original projection data. This iteration process can be repeated until the differences are very small, or until a certain number of iterations is reached. This process is also called model-based iterative reconstruction. A simplified, less time-consuming method is hybrid iterative reconstruction. In hybrid iterative reconstruction noise is iteratively filtered in the projection domain and in the image domain without multiple iterations in forward and backward projection steps. In image-based iterative reconstruction noise is only reduced in the image domain. In both hybrid and image-based iterative reconstruction no forward projection steps are performed based on the acquired image resulting in less computational demanding algorithms.

### **Dose reduction with iterative reconstruction**

Iterative reconstruction in itself does not reduce the radiation dose. However, the associated reduction in noise makes it possible to acquire images with improved image quality when using the same dose (*Figure 3*) or to acquire images at a lower radiation dose level with an objective image quality comparable to FBP at routine dose levels [17]. From 2009 onwards all major vendors introduced iterative reconstruction algorithms for CT [15]. Initially only hybrid algorithms were marketed, later on followed by more advanced model-based algorithms. Currently more than 10 different algorithms are available, which are listed in *Table 1* [18,19]. The exact working mechanism of those algorithms is proprietary information.



**Figure 3** – Example of improved objective image quality with iterative reconstruction. Abdominal CT acquisition in a 77-year old male with a body mass index of 32 kg/m<sup>2</sup>. The FBP reconstruction (left) shows substantial noise which decreases after application of hybrid (middle) and model-based (right) reconstruction. All images were reconstructed from the same acquisition at 120 kV and 195 mA. Radiation dose: dose length product (DLP) 470.8 mGy\*cm, volumetric CT dose index (CTDIvol) 8.2 mGy, effective dose 7.3 mSv

**Table 1** – Overview of the currently available iterative reconstruction algorithms.

Algorithm	Abbreviation	Vendor	Type
Adaptive Iterative Dose Reduction	AIDR	Toshiba	Hybrid
Adaptive Iterative Dose Reduction 3D	AIDR 3D	Toshiba	Hybrid
Adaptive Statistical Iterative Reconstruction	ASiR	GE	Hybrid
Adaptive Statistical Iterative Reconstruction	ASiR-V	GE	Hybrid
Advanced Modeled Iterative Reconstruction	ADMIRE	Siemens	Hybrid
Forward projected model-based Iterative Reconstruction SoluTion	FIRST	Toshiba	Model-based
iDose <sup>4</sup>	iDose	Philips	Hybrid
Iterative Model Reconstruction	IMR	Philips	Model-based
Iterative Reconstruction in Image Space	IRIS	Siemens	Hybrid
Model-Based Iterative Reconstruction	MBIR-Veo	GE	Model-based
Sinogram-Affirmed Iterative Reconstruction	SAFIRE	Siemens	Hybrid

## Outline of thesis

Experimental assessment of iterative reconstruction showed that the radiation dose can be reduced while preserving objective image quality compared to a routine dose acquisition reconstructed with FBP [17]. The next step, which is the first aim of this thesis, was to investigate whether those initial promising results can be applied in a routine clinical setting by investigating the effect of iterative reconstruction on commonly used imaging-based quantification methods and on diagnostic accuracy (*Part 1 – 3*). The potential radiation dose reduction with iterative reconstruction to submillisievert dose levels also offers the opportunity to replace conventional imaging with low dose CT for certain indications. Therefore, the second aim of this thesis was to investigate if iterative reconstruction should be applied in the field of imaging prior to cardiac surgery, by replacing the conventional preoperative chest radiograph by a low dose chest CT (*Part 4*).

### *Part I Clinical implementation of iterative reconstruction in cardiac CT*

A systematic review and meta-analysis was performed to investigate the extent to which iterative reconstruction is capable of actual radiation dose reduction and image quality (**chapter 1.1**). Phantom studies have reported a possible effect of iterative reconstruction and dose reduction on the coronary calcium score. The coronary calcium score measures the extent and density of calcifications in the coronary arteries, which reflects the burden of atherosclerosis. It is a predictor for the risk of future cardiovascular events [20]. To measure the effect of dose and iterative reconstruction on the coronary calcium score, 15 ex-vivo human hearts were scanned at different dose levels and reconstructed with both hybrid and model-based iterative reconstruction (**chapter 1.2**). In this thesis, the results of this ex-vivo study were translated to the clinic by performing a within-patient study. In this study 30 patients underwent a routine dose acquisition for clinical purposes, followed by three reduced dose acquisitions at 40%, 60% and 80% decreased dose. Different iterative reconstruction algorithms and levels were applied, and the findings are reported in **chapters 1.3 and 1.4**.

*Part II Clinical implementation of iterative reconstruction in thoraco-abdominal CT*

A systematic review of previous studies investigating iterative reconstruction for chest is provided in **chapter 2.1**. Subsequently, the same within patient design as described above in which patients underwent both a routine dose and three low dose CT acquisitions was applied. For chest CT, this was done in patients with known pulmonary nodules. Since those patients often receive multiple follow-up CT examinations, radiation dose is an important concern. The effect of dose reduction and iterative reconstruction on pulmonary nodule volumetry and computer-aided detection was investigated in **chapters 2.2 and 2.3**, respectively. Besides coronary calcifications, aortic valve calcifications and thoracic aortic calcifications are predictors of adverse cardiovascular outcomes. Therefore the influence of dose and reconstruction were also investigated for aortic valve and thoracic aorta calcifications in **chapter 2.4**. Urinary stones can be detected with both ultrasonography and CT. The advantage of CT is the higher sensitivity and specificity, and the potential to detect extra-urinary causes of flank pain. The potential to reduce the radiation dose in patients with urinary stones was studied in **chapter 2.5**.

*Part III Clinical implementation of iterative reconstruction in pediatric CT*

Medical radiation exposure is especially worrisome in children, because they are more radiosensitive and have a longer lifetime to develop radiation-induced effects. In **chapter 3.1** the possibilities, advantages and disadvantages of radiation dose reduction with iterative reconstruction in pediatric CT are discussed. Children with aortic coarctation are most frequently treated with stent implantation and receive regular follow-up with CT. In **chapter 3.2** the potential dose reduction with iterative reconstruction for CT angiography of aortic coarctation stents is investigated in an in vitro study.

*Part IV The rationale and need for CT prior to cardiac surgery*

Preoperative imaging before cardiac surgery is widely performed using conventional chest radiography. In **chapter 4.1** a retrospective cohort study is performed to assess the frequency and type of abnormalities on preoperative chest radiographs and whether these findings directly impacted surgery. A frequently reported abnormality is the suspicion of chronic obstructive pulmonary disease (COPD), however it is unclear whether this can be accurately detected on chest radiography. Therefore in **chapter 4.2** a nested case-control study is performed to assess the diagnostic accuracy of chest radiography for mild COPD with

spirometry as reference standard. CT provides more detailed preoperative information compared to chest radiography. Especially the location and extent of aortic calcifications, an important predictor of postoperative strokes, are more clearly depicted using CT. This is important, because the ascending aorta is clamped during surgery to initiate cardiopulmonary bypass. The resulting intraoperative manipulation of the aorta might provoke mobilization of atherothrombotic material and calcifications from the aortic wall, which can result in an embolic stroke [21]. Calcifications in the ascending aorta are often not accurately depicted on chest radiography, due to the 2D nature. The more extensive information about aortic calcifications provided by a CT examination might be relevant for clinical management by choosing a different surgical strategy in patients with calcifications in the ascending aorta. For example, a different cannulation site in an area free of calcification can be preferred. This can hypothetically result in better patient outcomes by reducing postoperative strokes. Therefore, in **chapter 4.3** a systematic review was performed to assess if a preoperative CT can be used to optimize the surgical strategy with the aim of reducing the incidence of postoperative strokes and mortality. This systematic review was the basis of a multicenter randomized controlled trial which is currently conducted to assess if a chest CT before cardiac surgery can decrease the postoperative stroke rate by optimizing the surgical strategy. The rationale and design of this trial is reported in **chapter 4.4**.

## References

- [1] Brenner DJ, Hall EJ, Computed tomography--an increasing source of radiation exposure. *N Engl J Med* 2007;357(22):2277-84.
- [2] IMV, Information for the Decisions Ahead, 2016 CT Market Outlook Report. 2016.
- [3] Rijksinstituut voor Volksgezondheid en Milieu (RIVM), Trends in het aantal CT-onderzoeken. ;2017/03/28.
- [4] European Commission, Healthcare resource statistics - technical resources and medical technology. ;2017(4/21).
- [5] Smith-Bindman R, Lipson J, Marcus R, et al., Radiation dose associated with common computed tomography examinations and the associated lifetime attributable risk of cancer. *Arch Intern Med* 2009;169(22):2078-86.
- [6] Berrington de Gonzalez A, Mahesh M, Kim KP, et al., Projected cancer risks from computed tomographic scans performed in the United States in 2007. *Arch Intern Med* 2009;169(22):2071-7.
- [7] Lin EC, Radiation risk from medical imaging. *Mayo Clin Proc* 2010;85(12):1142-1146.
- [8] Sasieni PD, Shelton J, Ormiston-Smith N, Thomson CS, Silcocks PB, What is the lifetime risk of developing cancer?: the effect of adjusting for multiple primaries. *Br J Cancer* 2011;105(3):460-5.
- [9] Malone J, Guleria R, Craven C, et al., Justification of diagnostic medical exposures: some practical issues. Report of an International Atomic Energy Agency Consultation. *Br J Radiol* 2012;85(1013):523-38.
- [10] Sheng AY, Castro A, Lewiss RE, Awareness, Utilization, and Education of the ACR Appropriateness Criteria: A Review and Future Directions. *J Am Coll Radiol* 2016;13(2):131-6.
- [11] Emergency Department Patients With Chest Pain Writing Panel, Rybicki FJ, Udelson JE, et al., 2015 ACR/ACC/AHA/AATS/ACEP/ASNC/NASCI/SAEM/SCCT/SCMR/SCPC/SNMMI/STR/STS Appropriate Utilization of Cardiovascular Imaging in Emergency Department Patients With Chest Pain: A Joint Document of the American College of Radiology Appropriateness Criteria Committee and the American College of Cardiology Appropriate Use Criteria Task Force. *J Am Coll Radiol* 2016;13(2):e1-e29.
- [12] Hadley JL, Agola J, Wong P, Potential impact of the American College of Radiology appropriateness criteria on CT for trauma. *AJR Am J Roentgenol* 2006;186(4):937-42.
- [13] Lell MM, Wildberger JE, Alkadhi H, Damilakis J, Kachelriess M, Evolution in Computed Tomography: The Battle for Speed and Dose. *Invest Radiol* 2015;50(9):629-44.
- [14] Frush DP, Applegate K, Computed tomography and radiation: understanding the issues. *J Am Coll Radiol* 2004;1(2):113-9.
- [15] Willemink MJ, de Jong PA, Leiner T, et al., Iterative reconstruction techniques for computed tomography Part 1: technical principles. *Eur Radiol* 2013;23(6):1623-31.

- [16] Fleischmann D, Boas F.E., Computed tomography-old ideas and new technology. *Eur Radiol* 2011;21(3):510-7.
- [17] Willeminck MJ, Leiner T, de Jong PA, et al., Iterative reconstruction techniques for computed tomography part 2: initial results in dose reduction and image quality. *Eur Radiol* 2013;23(6):1632-42.
- [18] den Harder AM, Willeminck MJ, de Jong PA, et al., New horizons in cardiac CT. *Clin Radiol* 2016;71(8):758-67.
- [19] Maeda E, Tomizawa N, Kanno S, et al., Subjective and objective evaluation of 10-30% dose reduced coronary artery phantom scans reconstructed with Forward projected model-based Iterative Reconstruction SoluTion (FIRST). *Data Brief* 2016;10:210-4.
- [20] Polonsky TS, McClelland RL, Jorgensen NW, et al., Coronary artery calcium score and risk classification for coronary heart disease prediction. *JAMA* 2010;303(16):1610-6.
- [21] Selim M, Perioperative stroke. *N Engl J Med* 2007;356(7):706-13.



# Chapter I.I

## *Part I Cardiac*

### **Dose reduction with iterative reconstruction for coronary computed tomography angiography: a systematic review and meta-analysis**

Annemarie M. den Harder, Martin J. Willemink, Quirina M.B. de Ruiter,  
Pim A. de Jong, Arnold M.R. Schilham, Gabriel P. Krestin,  
Tim Leiner, Ricardo P.J. Budde

British Journal of Radiology 2016; DOI 10.1259/bjr.20150068



## **Abstract**

### *Objectives*

To investigate the achievable radiation dose reduction for coronary computed tomography angiography (CCTA) with iterative reconstruction (IR) in adults and the effects on image quality.

### *Methods*

PubMed and EMBASE were searched and original articles concerning IR for CCTA in adults using prospective ECG-triggering were included. Primary outcome was the effective dose using filtered back projection (FBP) and IR. Secondary outcome was the effect of IR on objective and subjective image quality.

### *Results*

The search yielded 1,616 unique articles of which 10 studies (1,042 patients) were included. The pooled routine effective dose with FBP was 4.2 (95% CI 3.5 – 5.0) mSv. A dose reduction of 48% to a pooled effective dose of 2.2 (95% CI 1.3 – 3.1) mSv using IR was reported. Noise, contrast-to-noise ratio (CNR) and subjective image quality were equal or improved in all but one study while signal-to-noise ratio (SNR) was decreased in two studies with IR at reduced dose.

### *Conclusion*

IR allows for CCTA acquisition with an effective dose of 2.2 mSv with preserved objective and subjective image quality.

## Introduction

The number of computed tomography (CT) examinations has increased rapidly over the past decades leading to increased radiation exposure [1]. This is especially a concern for coronary CT angiography (CCTA) since retrospectively electrocardiogram (ECG)-gated CCTA used to be associated with relatively high radiation doses of more than 10 mSv[2]. These high CCTA radiation doses have led to the development of new techniques like prospective ECG-triggering, high pitch spiral acquisition and more recently iterative reconstruction (IR) to reduce radiation dose [3]. Despite these advances, radiation dose remains an important issue for CCTA because the number of indications and eligible patients has increased rapidly over the past few years [4-6].

IR offers the possibility to reduce radiation dose and was already used on the first CT systems [7,8]. However, due to the limited computational power at that time it could not be used in clinical practice. With recent improvements in computer processing, IR has become feasible in a clinical setting. Currently, the most commonly used reconstruction technique is filtered back projection (FBP), which is a fast reconstruction technique that suffers from impaired image quality when radiation dose is lowered. IR is a noise-suppressing technique that allows for a decrease in radiation dose compared to FBP while maintaining image [9].

Recently new IR algorithms were introduced which led to a surge in the number of publications. Therefore, we present the results of a systematic review and meta-analysis to determine the achievable radiation dose reduction for prospective ECG-gated CCTA acquisitions using IR. Furthermore the effect of IR on objective and subjective image quality was investigated.

## Methods

### *Search*

A systematic search in PubMed and EMBASE was performed on the 2nd of May 2014 for studies investigating IR for CCTA without a publication date limitation. English language restriction was applied. Synonyms for 'IR techniques' and 'CT' were combined. The search syntax is provided in the Appendix 1. Duplicates were removed. Hereafter a manual search of the reference lists of included articles and review articles was performed after which review articles were removed.

*Inclusion and exclusion criteria*

All articles were screened by two authors (AH and MW). In case of discrepancy a consensus had to be reached between authors on whether to include the study. Original research articles concerning IR techniques for CCTA using prospective ECG-triggering were included. Studies comparing routine dose acquisitions with FBP to reduced dose acquisitions with IR using the same CT system, contrast medium and dose modulation techniques were included while studies investigating only one dose level without comparison to FBP were excluded. Furthermore studies only investigating non-enhanced CCTA, ex-vivo, in-vitro and animal studies as well as studies performed in children were excluded. Case reports and reviews were excluded as well. Case reports were defined as studies including less than five patients.

*Data extraction*

Data were extracted to a standardized data sheet, which included first author, title, publication date, journal, study design, participant characteristics, reconstruction technique, scan indication, type of scan, type of CT system, and reported dose and image quality measurements.

The primary outcome was the effective dose reduction with IR. The effective dose was calculated as the dose-length product (DLP) times the conversion factor for chest CT (0.014 mSv/(mGy/cm)) [10]. This conversion factor was chosen because it was the most commonly used conversion factor in the included articles. In case a different conversion factor was used, the effective dose was recalculated using the DLP. If the effective dose was reported without conversion factor or DLP, the corresponding author was contacted. The corresponding authors were also contacted if both the effective dose and the DLP were not reported.

Secondary outcome was the influence of IR on objective and subjective image quality. Noise, contrast-to-noise ratio (CNR) and signal-to-noise ratio (SNR) were investigated. Image quality was specified as improved, equal or deteriorated compared to FBP. Improved was defined as a statistically significant improvement of image quality with IR compared to FBP. Non-significant differences were classified as the same and a significant decrease in image quality was classified as deteriorated. If multiple IR levels were studied, the IR level with the most favorable outcome was used for further analysis.

From each article the mean and the standard deviation (SD) of the effective dose was extracted. If only the median and the interquartile range (IQR) were reported, the mean and SD were recalculated. The median was considered to

be equal to the mean if the number of patients exceeded 25 [11]. The IQR was converted to the SD using the formula  $1.35 * SD = IQR$ .

### *Statistical analysis*

Statistical analysis was performed using SPSS (version 20.0 for Microsoft Windows) and the RStudio statistical environment (version 0.98.1025, RStudio, Inc., 2009-2013) with 'meta' package (version 3.7-1) [12]. For every study a mean and 95% confidence interval was calculated. Heterogeneity was assessed by the I<sup>2</sup> statistic and random effect models were used in case of large inter-study variance (I<sup>2</sup>≥65%). Results were presented as mean with 95% confidence interval. Both the normal dose data with FBP and the reduced dose data with IR were calculated and pooled. A two-tailed p-value below 0.05 was considered statistically significant.

## **Results**

### *Study selection*

In total 2,556 articles were identified. A flowchart is provided in *Figure 1*. After removing of duplicates 1,616 articles were screened based on title and abstract. Sixteen-hundred-six articles were excluded because the articles did not investigate IR for CT (n=1,338), were non-cardiac (n=196), were not in-vivo (n=16), were pediatric studies (n=4), only concerned non-contrast enhanced coronary CT (n=5), only 1 dose level investigated (n=26), used retrospective ECG-gating (n=14), used different CT systems for the FBP and IR group (n=5), used automatic exposure control only in the IR group (n=1) or used a different contrast medium for the IR group (n=1). Articles investigating 1 dose level are mentioned in Appendix 2. Ten articles remained with a total of 1,042 patients. One corresponding author was contacted because reported information about radiation dose was insufficient [13].

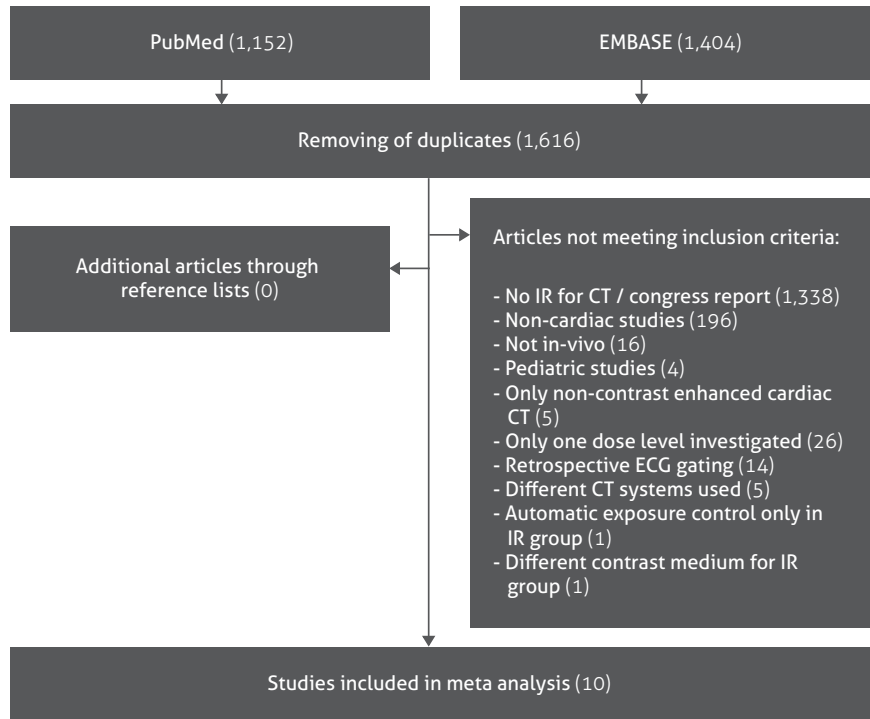


Figure 1 – Flowchart of included studies.

### Study characteristics

The baseline characteristics are provided in *Table 1*. Studies were published in 2011 (n=1), 2012 (n=3), 2013 (n=5) and 2014 (n=1). Different IR techniques were used namely Adaptive Statistical Iterative Reconstruction (ASIR, GE Healthcare, n=3), Sinogram-Affirmed Iterative Reconstruction (SAFIRE, Siemens Healthcare, n=3), iDose (Philips Healthcare, n=2), Iterative Reconstruction in Image Space (IRIS, Siemens Healthcare, n=1) and Adaptive Iterative Dose Reduction (Toshiba Medical Systems, AIDR, n=1). One study compared Model-Based Iterative Reconstruction (MBIR-Veo, GE Healthcare) with ASIR [14], since FBP was replaced by ASIR as the clinically implemented routine reconstruction method. CT systems used were Aquilion One (n=1), Brilliance iCT (n=2), Discovery HD 750 (n=3) and SOMATOM Definition Flash (n=4).

The median number of patients per study was 74 (range 20 – 338). In total, data of 1,042 patients were included in this study. Most studies (n=7) used different study

populations to compare FBP with IR, however three studies compared different dose levels in the same patients [14-16]. This was achieved by using data from only one source of a dual source CT scanner [15] or by making additional scans of the same patient [14,16]. Mean BMI varied between studies from 23.9 to 33.8 kg/m<sup>2</sup> with heart rates of 57 to 74 beats per minute. The contrast rate and volume was the same between the FBP and IR groups in all studies. In three studies tube current modulation was used [15-17].

*Effective dose*

Inter-study variance was high for effective dose pooling (I<sup>2</sup> 98.9%) therefore random effects models were used. In three studies the effective dose was (re) calculated using the DLP because the effective dose was not provided or calculated with a different conversion factor [15,16,18]. The pooled routine effective dose using FBP was 4.2 (95% CI 3.5 – 5.0) mSv. At reduced dose level using IR the pooled effective dose was 2.2 (95% CI 1.3 – 3.1) mSv (Figure 2).

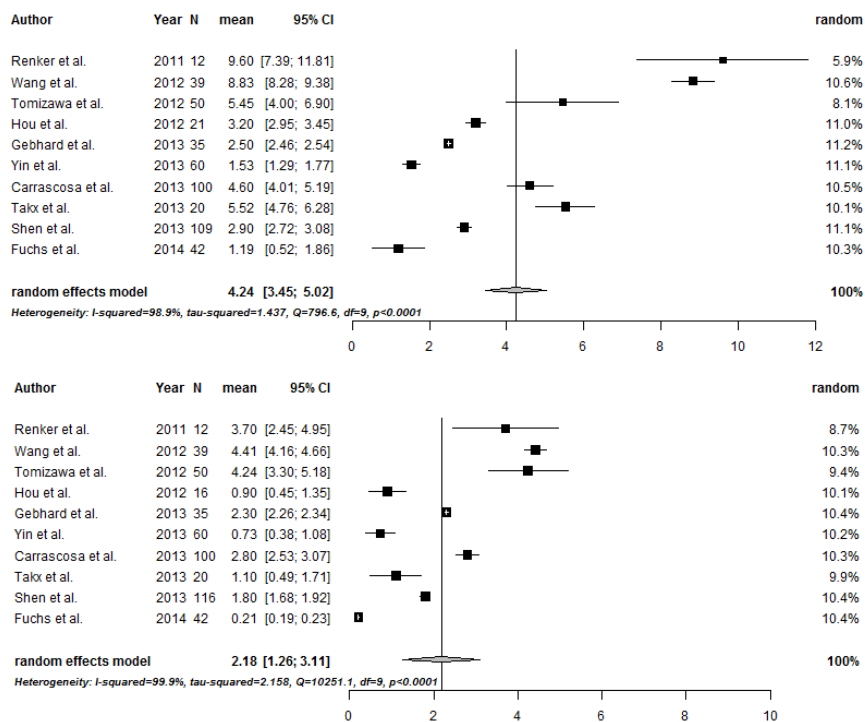
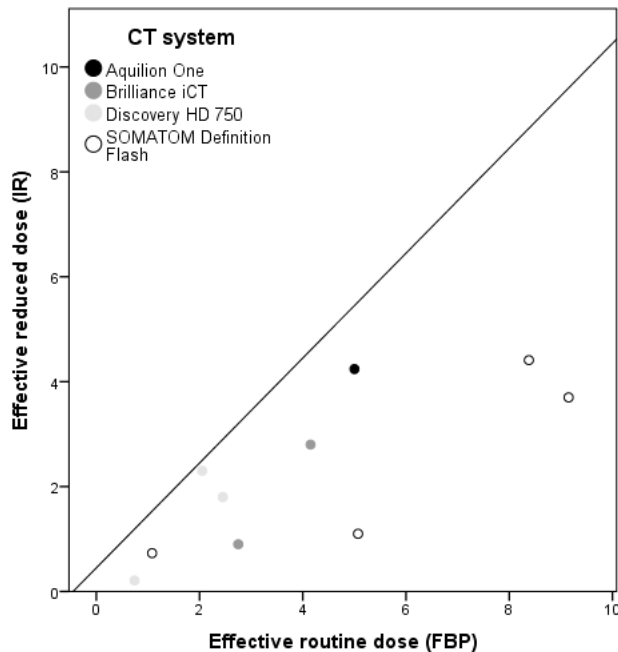


Figure 2 – Forest plot of routine effective dose with FBP (upper panel) and the reduced effective dose using IR (lower panel) with pooled estimate. N=number of patients

Standard effective dose varied highly between studies from 1.2 – 9.6 mSv while differences were smaller with IR (0.2 – 4.4 mSv). The relationship between routine effective dose and reduced effective dose for each CT system is illustrated in *Figure 3*.



**Figure 3** – Relationship between normal effective dose and reduced effective dose in studies comparing multiple dose levels. FBP Filtered Back Projection; IR Iterative Reconstruction

### *Image quality*

Objective image quality was scored using image noise ( $n=10$ ), contrast-to-noise ratio (CNR,  $n = 6$ ) and/or signal-to-noise ratio (SNR,  $n = 8$ ). Subjective image quality was scored by two observers in all studies, mostly by using a Likert scale. The results are shown in *Table 1*.

Noise was improved ( $n = 4$ ) or equal ( $n = 5$ ) with IR at reduced dose compared to FBP at routine dose in all but one study [15]. CNR was equal ( $n = 5$ ) in all but one study while SNR was improved ( $n = 1$ ), equal ( $n = 5$ ) or deteriorated ( $n = 2$ ) with IR at reduced dose.

Table 1 – Baseline characteristics of the included studies.

Author	Study characteristics		Image quality			Routine dose group			Reduced dose group								
	Year of publication	Total number of patients	IR technique	Noise	CNR	SNR	Subjective image quality	BMI (routine dose group, kg/m <sup>2</sup> )	Number of patients	Tube current	Tube voltage (kV)	Mean effective dose (normal, mSv)	BMI (reduced dose group, kg/m <sup>2</sup> )	Number of patients	Tube current	Tube voltage (kV)	Mean effective dose (reduced, mSv)
Renker et al.[19]	2011	24	IRIS	+	NR	NR	+	30.7	12	NR	120	9.6	30.2	12	NR	80/100	3.7
Wang et al.[21]	2012	78	SAFIRE	+/-	+/-	+/-	+/-	31.7	39	354-430 mAs	120	8.8	32.3	39	286-370 mAs	100	4.4
Tomizawa et al.[18]	2012	100	AIDR	+	+/-	+/-	+/-	24.0	50	483 mA	120	5.5	23.9	50	289 mA	120	4.2
Hou et al.[13]	2012	110	iDose	+/-	+/-	+/-	+/-	25.1	21	210 mAs	120	3.2	25.5	16	65 mAs	120	0.9
Gebhard et al.[22]	2013	70	ASIR	+	+/-	+/-	+	33.8	35	646 mA	116	2.5	32.9	35	633 mA	112	2.3
Yin et al.[16]	2013	60	SAFIRE	+/-	+/-	+/-	+/-	NR	60	320-400 mAs	80-120	1.5	NR	60	160-200 mAs	80-120	0.7
Carrascosa et al.[17]	2013	200	iDose	+/-	NR	NR	+/-	27.2	100	203 mAs	119	4.6	26.3	100	196mAs	109	2.8
Takx et al.[15]	2013	20	SAFIRE	-	-	-	-	33.1	20	331 mAs	100-120	5.5	33.1	20	66 mAs	100-120	1.1
Shen et al.[23]	2013	338	ASIR	+/-	NR	-	+	25.5	109	600 mA	120	2.9	25.2	116	300 mA	120	1.8
Fuchs et al.[14]	2014	42	ASIR / MBIR	+	NR	+	+/-	25.2	42	450-700 mA	100-120	1.2	25.2	42	150-210 mA	80-100	0.2

IR = iterative reconstruction, + = improved with IR, +/- = no difference, - = decreased with IR, NR = not reported, CNR = contrast-to-noise ratio, SNR = signal-to-noise ratio

Subjective image quality was improved ( $n = 3$ ) or equal ( $n = 6$ ) in all but one study [15]. Furthermore, Renker et al.[19] and Takx et al.[15] reported that IR resulted in a reduction of blooming artifacts. The study of Takx and colleagues [15] was the only study reporting a decrease in both objective and subjective image quality which was possibly due to the large dose reduction (80%, compared to a median dose reduction of 50% in the other included studies).

## Discussion

This meta-analysis showed that dose reduction is feasible using IR techniques for CCTA with preserved image quality compared to conventional FBP techniques. Our results, indicating an achievable dose reduction of 48%, are in the range of dose reductions reported in a prior systematic review [20]. Forty-nine studies were included and reported achievable dose reduction varied from 23% to 76%. In that review, data were not pooled and only the percentage of achieved dose reduction for each study was reported. In this previous review CCTA was not specifically studied since the review focused on all body regions. Also, no meta-analysis was performed. Furthermore, a lot of included studies concerned ex vivo data, new IR algorithms have become available and a substantial number of new studies have been published about IR for CT since the publication of the aforementioned review [20].

In the present review the effective dose reported in individual studies was pooled. Furthermore, only effective dose was used with the most commonly used conversion factor to achieve a uniform quantity to report dose. As can be seen in the forest plots (*Figure 2*), effective doses varied widely between studies. Also the 95% confidence interval was high in some studies. This is partly due to the variation in BMI between study samples but also shows the differences in routine scan protocols between hospitals.

Most studies did not report whether the dose of the localizer and bolus tracking images were included in the effective dose, which might have influenced results. However, the additional dose of the localizer and bolus tracking images might be small and therefore less likely to have influenced the dose significantly.

All major vendors have developed and are marketing a variety of slightly different IR algorithms. One study found an ultra-low dose of 0.2 mSv in patients with a mean BMI of 25.2 kg/m<sup>2</sup> using MBIR, which is a model-based IR algorithm [14]. All other studies investigated less advanced hybrid IR algorithms. Therefore with the development of model-based IR algorithms the radiation dose is expected to decrease even further.

This study has several limitations. First, due to our strict in- and exclusion criteria, we excluded many articles. By only including articles using the same CT system, contrast medium and scan parameters (except for variation in tube voltage and/or current to create dose reduction) for both the routine dose scan and the reduced dose scan it was possible to investigate the true potential of IR. Second, there are different quantities to report dose but only effective dose was used in the current study. Volume computed tomography dose index (CTDIvol) might be more appropriate because it is independent of anatomical length and dose conversion factors. In this review the effective dose was used since most studies only reported DLP and/or effective dose. We felt this was appropriate because using a standard conversion factor eliminated the influence of different conversion factors. A conversion factor of 0.014 was used because this was the most commonly used factor in the included articles. However, this factor was designed for chest rather than cardiac CT and a different conversion factor might therefore be more appropriate. Efforts were made to ensure effective dose data concerned only CCTA studies and did not include non enhanced acquisitions, however this cannot be guaranteed and could be a potential limitation. Third, we used an English language restriction.

A major limitation is the inability to determine if the diagnostic accuracy remains acceptable at reduced dose levels. Since this was not reported in most studies, we were not able to investigate this. Therefore, the current meta-analysis only provides an overview of dose reductions reported in the literature and does not focus on diagnostic acceptability. However, it is difficult to investigate the diagnostic accuracy due to IR alone, since this is also influenced by factors as the used CT system and other dose reduction techniques.

Ideally different dose levels should be compared within patients. However, performing multiple scans in one patient can lead to difficulties with contrast enhancement. This explains why only two studies performed additional scans for research purposes in the same patients [14,16]. Another study tried to simulate a within patient comparison by using data from one detector of a dual source CT system [15].

This meta-analysis provides the possible dose reduction with IR as reported in the literature. However, the lowest possible dose remains unclear. Most studies only investigated one or two different dose levels and we found that it is feasible to reduce the dose below 3 mSv using prospective ECG-triggering and state-of-the-art CT systems. Other dose reduction techniques have been developed in the past years like automatic tube current modulation, which was used in only

three of the included studies. It is likely that radiation dose can be reduced even further by combining techniques. Future research investigating dose reduction with IR should focus on radiation doses of 3 mSv and lower. Furthermore we recommend a uniform way of reporting radiation dose. Both CTDIvol and DLP should be reported, making it possible to calculate the effective dose with a consistent conversion factor. Also authors should be clear about whether scout views and non-enhanced scans were included in the total reported dose.

In conclusion, this meta-analysis provides an overview of currently available dose reduction for CCTA with IR. Pooled data suggested that CCTA acquisition with an effective dose below 3 mSv is possible with preserved image quality. Future research should determine if radiation dose can be reduced even further with model-based IR techniques.

## Appendix I

### *Search syntax PubMed*

(((((iterative[Title/Abstract]) AND reconstruction[Title/Abstract])) OR (((iterative[Title/Abstract]) AND dose[Title/Abstract]) AND reduction[Title/Abstract])) OR (((((((ASIR[Title/Abstract]) OR iDose[Title/Abstract]) OR IRIS[Title/Abstract]) OR AIDR[Title/Abstract]) OR IMR[Title/Abstract]) OR MBIR[Title/Abstract]) OR Veo[Title/Abstract]) OR SAFIRE[Title/Abstract]) OR ADMIRE[Title/Abstract]))) AND (((CT [Title/Abstract] OR “Tomography, X-Ray Computed” [Mesh] OR “Cone-Beam Computed Tomography” [Mesh] OR “Four-Dimensional Computed Tomography” [Mesh] OR “Spiral Cone-Beam Computed Tomography” [Mesh] OR “Tomography Scanners, X-Ray Computed” [Mesh] OR “Tomography, Spiral Computed” [Mesh]))) OR ((computed[Title/Abstract]) AND tomography[Title/Abstract])) Filters: English

### *Search syntax EMBASE*

((((iterative:ab,ti AND reconstruction:ab, ti) OR (iterative:ab,ti AND dose:ab,ti AND reduction:ab,ti) OR (ASIR:ab,ti OR iDose:ab,ti OR IRIS:ab,ti OR AIDR:ab,ti OR IMR:ab,ti OR MBIR:ab,ti OR Veo:ab,ti OR SAFIRE:ab,ti OR ADMIRE:ab,ti)) AND ((computed:ab,ti AND tomography:ab,ti) OR (CT:ab,ti OR ‘tomography, x-ray computed’:ab,ti OR ‘cone-beam computed tomography’:ab,ti OR ‘four-dimensional computed tomography’:ab,ti OR ‘spiral cone-beam computed tomography’: ab,ti OR ‘tomography scanners, x-ray computed’:ab, ti OR ‘tomography, spiral computed’:ab,ti))) AND [english]/lim

## Appendix 2

### *List of excluded studies investigating one dose level.*

Leipsic J., LaBounty T.M., Heilbron B., Min J.K., Mancini G.B.J., Lin F.Y., et al. Adaptive statistical iterative reconstruction: assessment of image noise and image quality in coronary CT angiography. *Am J Roentgenol* 2010;195(3):649-654

Renker M., Nance Jr. J.W., Schoepf U.J., O'Brien T.X., Zwerner P.L., Meyer M., et al. Evaluation of heavily calcified vessels with coronary CT angiography: Comparison of iterative and filtered back projection image reconstruction. *Radiology* 2011;260(2):390-399

Bittencourt M.S., Schmidt B., Seltmann M., Muschiol G., Ropers D., Daniel W.G., et al. Iterative reconstruction in image space (IRIS) in cardiac computed tomography: Initial experience. *Int J Card Imaging* 2011;27(7):1081-1087

Tatsugami F, Matsuki M, Nakai G, Inada Y, Kanazawa S, Takeda Y, et al. The effect of adaptive iterative dose reduction on image quality in 320-detector row CT coronary angiography. *Br J Radiol* 2012 Aug;85(1016):e378-82

Pontone G, Andreini D, Bartorelli AL, Bertella E, Mushtaq S, Foti C, et al. Feasibility and diagnostic accuracy of a low radiation exposure protocol for prospective ECG-triggering coronary MDCT angiography. *Clin Radiol* 2012 Mar;67(3):207-215

Oda S, Utsunomiya D, Funama Y, Yonenaga K, Namimoto T, Nakaura T, et al. A hybrid iterative reconstruction algorithm that improves the image quality of low-tube-voltage coronary CT angiography. *AJR Am J Roentgenol* 2012 May;198(5):1126-1131

Hosch W, Stiller W, Mueller D, Gitsioudis G, Welzel J, Dadrach M, et al. Reduction of radiation exposure and improvement of image quality with BMI-adapted prospective cardiac computed tomography and iterative reconstruction. *Eur J Radiol* 2012 Nov;81(11):3568-3576

Maffei E, Martini C, Rossi A, Mollet N, Lario C, Castiglione Morelli M, et al. Diagnostic accuracy of second-generation dual-source computed tomography coronary angiography with iterative reconstructions: a real-world experience. *Radiol Med* 2012 Aug;117(5):725-738

Utsunomiya D, Weigold WG, Weissman G, Taylor AJ. Effect of hybrid iterative reconstruction technique on quantitative and qualitative image analysis at 256-slice prospective gating cardiac CT. *Eur Radiol* 2012 Jun;22(6):1287-1294

Morsbach F, Desbiolles L, Plass A, Leschka S, Schmidt B, Falk V, et al. Stenosis quantification in coronary CT angiography: impact of an integrated circuit detector with iterative reconstruction. *Invest Radiol* 2013 Jan;48(1):32-40

Gebhard C, Fiechter M, Fuchs TA, Stehli J, Muller E, Stahli BE, et al. Coronary artery stents: influence of adaptive statistical iterative reconstruction on image quality using 64-HDCT. *Eur Heart J Cardiovasc Imaging* 2013 Oct;14(10):969-977

Hou Y, Zheng J, Wang Y, Yu M, Vembar M, Guo Q. Optimizing radiation dose levels in prospectively electrocardiogram-triggered coronary computed tomography angiography using iterative reconstruction techniques: a phantom and patient study. *PLoS One* 2013;8(2):e56295

Eisentopf J, Achenbach S, Ulzheimer S, Layritz C, Wuest W, May M, et al. Low-dose dual-source CT angiography with iterative reconstruction for coronary artery stent evaluation. *JACC Cardiovasc Imaging* 2013 Apr;6(4):458-465

Yin WH, Lu B, Hou ZH, Li N, Han L, Wu YJ, et al. Detection of coronary artery stenosis with sub-milliSievert radiation dose by prospectively ECG-triggered high-pitch spiral CT angiography and iterative reconstruction. *Eur Radiol* 2013 Nov;23(11):2927-2933

Hassan T.A., Abdalaal M. Coronary CT angiography with iterative reconstruction in early triage of patients with acute chest pain. *Egypt J Radiol Nucl Med* 2013;44(4):755-763

Yoo RE, Park EA, Lee W, Shim H, Kim YK, Chung JW, et al. Image quality of adaptive iterative dose reduction 3D of coronary CT angiography of 640-slice CT: comparison with filtered back-projection. *Int J Cardiovasc Imaging* 2013 Mar;29(3):669-676

Schuhbaeck A, Achenbach S, Layritz C, Eisentopf J, Hecker F, Pflederer T, et al. Image quality of ultra-low radiation exposure coronary CT angiography with an effective dose <0.1 mSv using high-pitch spiral acquisition and raw data-based iterative reconstruction. *Eur Radiol* 2013 Mar;23(3):597-606

Wuest W, May MS, Scharf M, Layritz C, Eisentopf J, Ropers D, et al. Stent evaluation in low-dose coronary CT angiography: effect of different iterative reconstruction settings. *J Cardiovasc Comput Tomogr* 2013 Sep-Oct;7(5):319-325

Fuchs TA, Fiechter M, Gebhard C, Stehli J, Ghadri JR, Kazakauskaitė E, et al. CT coronary angiography: impact of adapted statistical iterative reconstruction (ASIR) on coronary stenosis and plaque composition analysis. *Int J Cardiovasc Imaging* 2013 Mar;29(3):719-724

Nakaura T, Kidoh M, Sakaino N, Utsunomiya D, Oda S, Kawahara T, et al. Low contrast- and low radiation dose protocol for cardiac CT of thin adults at 256-row CT: usefulness of low tube voltage scans and the hybrid iterative reconstruction algorithm. *Int J Cardiovasc Imaging* 2013 Apr;29(4):913-923

Kropil P, Bigdeli AH, Nagel HD, Antoch G, Cohnen M. Impact of Increasing Levels of Advanced Iterative Reconstruction on Image Quality in Low-Dose Cardiac CT Angiography. *Rofo* 2014 Jan 23

Spears JR, Schoepf UJ, Henzler T, Joshi G, Moscariello A, Vliegenthart R, et al. Comparison of the effect of iterative reconstruction versus filtered back projection on cardiac CT postprocessing. *Acad Radiol* 2014 Mar;21(3):318-324

Wang R, Schoepf UJ, Wu R, Nance JW, Jr, Lv B, Yang H, et al. Diagnostic accuracy of coronary CT angiography: comparison of filtered back projection and iterative reconstruction with different strengths. *J Comput Assist Tomogr* 2014 Mar-Apr;38(2):179-184

Zhou Q, Jiang B, Dong F, Huang P, Liu H, Zhang M. Computed Tomography Coronary Stent Imaging With Iterative Reconstruction: A Trade-off Study Between Medium Kernel and Sharp Kernel. *J Comput Assist Tomogr* 2014 Mar 19

Hou Y, Ma Y, Fan W, Wang Y, Yu M, Vembar M, et al. Diagnostic accuracy of low-dose 256-slice multi-detector coronary CT angiography using iterative reconstruction in patients with suspected coronary artery disease. *Eur Radiol* 2014 Jan;24(1):3-11

Takx RA, Willeminck MJ, Nathoe HM, Schilham AM, Budde RP, de Jong PA, et al. The effect of iterative reconstruction on quantitative computed tomography assessment of coronary plaque composition. *Int J Cardiovasc Imaging* 2014 Jan;30(1):155-163

## References

- [1] Brenner DJ, Hall EJ, Computed tomography--an increasing source of radiation exposure. *N Engl J Med* 2007;357(22):2277-84.
- [2] Hausleiter J, Meyer T, Hermann F, et al., Estimated radiation dose associated with cardiac CT angiography. *JAMA* 2009;301(5):500-7.
- [3] Earls JP, Leipsic J, Cardiac computed tomography technology and dose-reduction strategies. *Radiol Clin North Am* 2010;48(4):657-74.
- [4] Gallagher MJ, Ross MA, Raff GL, Goldstein JA, O'Neill WW, O'Neil B, The diagnostic accuracy of 64-slice computed tomography coronary angiography compared with stress nuclear imaging in emergency department low-risk chest pain patients. *Ann Emerg Med* 2007;49(2):125-36.
- [5] Gruettner J, Fink C, Walter T, et al., Coronary computed tomography and triple rule out CT in patients with acute chest pain and an intermediate cardiac risk profile. Part I: impact on patient management. *Eur J Radiol* 2013;82(1):100-5.
- [6] Goldstein JA, Chinnaiyan KM, Abidov A, et al., The CT-STAT (Coronary Computed Tomographic Angiography for Systematic Triage of Acute Chest Pain Patients to Treatment) trial. *J Am Coll Cardiol* 2011;58(14):1414-22.
- [7] Xu J, Mahesh M, Tsui BM, Is iterative reconstruction ready for MDCT? *J Am Coll Radiol* 2009;6(4):274-6.
- [8] Herman GT, Lent A, Rowland SW, ART: mathematics and applications. A report on the mathematical foundations and on the applicability to real data of the algebraic reconstruction techniques. *J Theor Biol* 1973;42(1):1-32.
- [9] Willemink MJ, de Jong PA, Leiner T, et al., Iterative reconstruction techniques for computed tomography Part I: technical principles. *Eur Radiol* 2013;23(6):1623-31.
- [10] American Association of Physicists in Medicine, The measurement, reporting and management of radiation dose in CT: report of AAPM Task Group 23 of the Diagnostic Imaging Council CT Committee. 2008(Accessed June 2014).
- [11] Hozo SP, Djulbegovic B, Hozo I, Estimating the mean and variance from the median, range, and the size of a sample. *BMC Med Res Methodol* 2005;5:13.
- [12] R Foundation, The R Foundation for Statistical Computing. 2002;2014(09/30).
- [13] Hou Y, Xu S, Guo W, Vembar M, Guo Q, The optimal dose reduction level using iterative reconstruction with prospective ECG-triggered coronary CTA using 256-slice MDCT. *Eur J Radiol* 2012;81(12):3905-11.
- [14] Fuchs TA, Stehli J, Bull S, et al., Coronary computed tomography angiography with model-based iterative reconstruction using a radiation exposure similar to chest X-ray examination. *Eur Heart J* 2014.

- [15] Takx RA, Schoepf UJ, Moscariello A, et al., Coronary CT angiography: comparison of a novel iterative reconstruction with filtered back projection for reconstruction of low-dose CT-Initial experience. *Eur J Radiol* 2013;82(2):275-80.
- [16] Yin WH, Lu B, Li N, et al., Iterative reconstruction to preserve image quality and diagnostic accuracy at reduced radiation dose in coronary CT angiography: an intraindividual comparison. *JACC Cardiovasc Imaging* 2013;6(12):1239-49.
- [17] Carrascosa P, Rodriguez-Granillo GA, Capunay C, Deviggiano A, Low-dose CT coronary angiography using iterative reconstruction with a 256-slice CT scanner. *World J Cardiol* 2013;5(10):382-6.
- [18] Tomizawa N, Nojo T, Akahane M, Torigoe R, Kiryu S, Ohtomo K, AdaptiveIterative Dose Reduction in coronary CT angiography using 320-row CT: assessment of radiation dose reduction and image quality. *J Cardiovasc Comput Tomogr* 2012;6(5):318-24.
- [19] Renker M., Ramachandra A., Schoepf U.J., et al., Iterative image reconstruction techniques: Applications for cardiac CT. *J Cardiovasc Comput Tomogr* 2011;5(4):225-30.
- [20] Willemink MJ, Leiner T, de Jong PA, et al., Iterative reconstruction techniques for computed tomography part 2: initial results in dose reduction and image quality. *Eur Radiol* 2013;23(6):1632-42.
- [21] Wang R, Schoepf UJ, Wu R, et al., Image quality and radiation dose of low dose coronary CT angiography in obese patients: sinogram affirmed iterative reconstruction versus filtered back projection. *Eur J Radiol* 2012;81(11):3141-5.
- [22] Gebhard C, Fuchs TA, Fiechter M, et al., Image quality of low-dose CCTA in obese patients: impact of high-definition computed tomography and adaptive statistical iterative reconstruction. *Int J Cardiovasc Imaging* 2013;29(7):1565-74.
- [23] Shen J, Du X, Guo D, et al., Prospective ECG-triggered coronary CT angiography: clinical value of noise-based tube current reduction method with iterative reconstruction. *PLoS One* 2013;8(5):e65025.



# Chapter 1.2

## *Part I Cardiac*

### **Dose reduction for coronary calcium scoring with hybrid and model-based iterative reconstruction: an ex-vivo study**

Annemarie M. den Harder, Martin J. Willeminck, Ronald L.A.W. Bleys,  
Pim A. de Jong, Ricardo P.J. Budde, Arnold M.R. Schilham, Tim Leiner

The International Journal of Cardiovascular Imaging 2014; DOI 10.1007/s10554-014-0434-8

## Abstract

### *Purpose*

To determine the influence of dose reduction on coronary calcium scoring using hybrid and model-based iterative reconstruction (IR) techniques.

### *Methods*

Fifteen ex-vivo hearts were scanned in a phantom representing an average adult person at routine dose and three levels of dose reduction; 27%, 55% and 82% reduced-dose, respectively. All images were reconstructed using filtered back-projection (FBP), hybrid IR (iDose<sup>4</sup>, levels 1, 4 and 7) as well as model-based IR (IMR, levels 1, 2 and 3). Agatston, mass and volume scores as well as the objective image quality found with iDose<sup>4</sup> and IMR were compared to the FBP reconstruction (routine dose).

### *Results*

With FBP calcium scores remained unchanged at 82% reduced dose. With IR Agatston scores differed significantly at routine dose, using IMR level 3 and iDose<sup>4</sup> level 7, and at 82% reduced dose, using IMR levels 1 to 3 and iDose<sup>4</sup> level 7. The maximum median difference was 5.3%. Mass remained unchanged at reduced dose levels while volume was significantly lower at 82% reduced dose with IMR (maximum median difference 5.0%).

Objective image quality improved with IR, at 82% reduced dose the CNR of iDose<sup>4</sup> level 7 was similar to the reference dose CNR, and IMR levels 1 to 3 resulted in an even higher CNR.

### *Conclusion*

Calcium scores were not affected by radiation-dose reduction with FBP and low levels of iDose<sup>4</sup>. Objective image quality increased significantly using iDose<sup>4</sup> and IMR. Therefore low level iDose<sup>4</sup> has the potential to reduce radiation-dose of coronary calcium scoring with up to 82%.

## Introduction

Cardiovascular disease is the leading cause of death in developed countries [1]. Prognosis on the risk of a future cardiovascular event can be made based on the amount of coronary calcium as assessed with cardiac computed tomography (CT) [2]. Coronary artery calcifications can be quantified with cardiac CT as the Agatston score, calcification mass and volume.

Cardiac CT examinations are associated with a small risk for radiation-induced carcinogenesis [3]. Although the radiation dose used in cardiac CT-scans decreased significantly over the past years, cardiac CT-scans are commonly performed and therefore dose remains an important concern, especially since recent guidelines recommend cardiac CT examinations to assess coronary calcifications even for asymptomatic adults at low-to-intermediate and intermediate cardiovascular risk [4-6].

Iterative reconstruction (IR) is a possible solution to lower radiation dose for CT imaging [5,7-9]. Recently, IR algorithms came available for clinical use and have been demonstrated to reduce radiation dose while preserving the image quality compared to the reconstruction by filtered back projection (FBP) [10]. In the current study two recently introduced IR algorithms were compared to FBP. The first is iDose<sup>4</sup> (*Philips Healthcare, Best, The Netherlands*), a hybrid reconstruction technique that iterates in both the projection (raw) data domain and the image domain [11]. Dose reductions of up to 76% have been reported with preserved image quality compared to a corresponding routine dose CT-scan [12].

The second algorithm studied is a prototype version of a novel model-based IR technique called iterative model-based reconstruction (IMR, *Philips Healthcare, Best, The Netherlands*) and became recently available [13]. This algorithm models both the CT system optics and geometry and uses forward and backward reconstruction steps and is therefore an advanced model-based IR technique.

Because IMR is more advanced than iDose<sup>4</sup>, even more dose reduction might be achievable with IMR. An initial study showed significant noise reduction and contrast-to-noise improvements [14].

The strength of iDose<sup>4</sup> and IMR is defined in different levels of noise reduction. A higher level implicates more noise reduction. There are seven levels of noise reduction for iDose<sup>4</sup> and three levels for IMR.

The purpose of this ex-vivo study was to determine to which extent radiation dose can be reduced using iDose<sup>4</sup> or IMR without affecting coronary calcium scoring and risk assessment using the extent of coronary calcification as quantified with the Agatston score, calcification mass and volume. Different levels of dose

reduction were used within the same hearts to determine the influence of dose reduction on coronary calcium scoring. Furthermore, the effects of iDose<sup>4</sup> and IMR on objective image quality, compared to FBP at routine dose were assessed.

## Methods

For this study 15 ex-vivo hearts from deceased subjects were included. All patients signed informed consent during life to donate their entire body to science for educational and research purposes. The hearts were fixed in 3%-formaldehyde and placed in a commercially available anthropomorphic chest phantom (*QRM GmbH, Moehrendorf, Germany*) [15] for CT imaging.

### *CT protocol*

Image acquisition was performed using a 256-slice CT scanner (Brilliance iCT, *Philips Healthcare, Best, The Netherlands*). Five hearts were scanned twice to evaluate interscan reproducibility. The following parameters were used for image acquisition: matrix size 512x512; 128x0.625 mm collimation and a tube voltage of 120 kV. Different mAs-values were used to expose the heart to different radiation dose levels. In total four radiation dose levels were evaluated: routine dose (4.12 mGy), a 27% reduced dose protocol (2.99 mGy), a 55% reduced dose protocol (1.87 mGy) and an 82% reduced dose protocol (0.75 mGy). Standard sequential cardiac CT protocols were used with a simulated 60 beats per minute electrocardiogram signal. No contrast agents were used.

### *CT image reconstruction*

All 15 ex-vivo hearts were imaged at the four dose levels as previous described and reconstructed at 3 mm slice thickness and a field-of view (FOV) of 160 mm with FBP, iDose<sup>4</sup> (levels 1, 4 and 7) and IMR (levels 1, 2 and 3) on the same workstation (Extended Brilliance Workspace version 4.5.5.1035, *Philips Healthcare, Best, The Netherlands*). The 'Cardiac Routine' kernel was used for all reconstructions. The reconstructed 3 mm slices were sent to an offline CT workstation (*Philips Healthcare, the Netherlands*) for further analysis.

### *Calcium score*

The extent of coronary calcification was determined using the Agatston score, calcification mass and volume. All plaques related to the coronary arteries with a density higher than 130 Hounsfield Units (HU) and an area  $\geq 1 \text{ mm}^2$  were included and scored as previously described by *Agatston et al* [16,17].

The total calcium score of calcifications was determined. All measurements were performed using commercially available semiautomatic software on the workstation (Cardiac Calcium Scoring, Heartbeat CS, *Philips Healthcare, Best, The Netherlands*). By placing a cursor in a calcified area and by clicking with the mouse, the user instructed the software to automatically delineate the calcified area and quantified the Agatston score, calcification mass and calcification volume. A single observer assessed the calcium scores. All reconstructions per dose level were assessed at the same time to ensure that the same calcifications were measured.

The number of reclassifications from predefined Agatston categories was investigated. The following risk groups based on Agatston score were used: 0 (normal); 1-10 (low); 11-100 (low-intermediate); 101-400 (intermediate); >400 (high).

#### *Image quality*

Objective image quality was assessed using contrast-to-noise ratio (CNR) and signal-to-noise ratio (SNR). To this end, a homogenous region of interest (ROI) with a diameter of 18 mm was drawn within the spine and the lung and the mean HU and the standard deviation (SD) were determined. The CNR was computed using the following equation:

$$\text{CNR} = \frac{\text{Density (Spine)} - \text{Density (Lung)}}{\sqrt{\frac{1}{2} \times (\text{SD (Spine)}^2 + \text{SD (Lung)}^2)}}$$

The SNR was defined as the ratio between the mean HU and the SD of the same ROI.

#### *Statistical analysis*

Statistical analysis was performed using SPSS (version 20.0 for Microsoft Windows). The Shapiro-Wilk test was used to identify normally distributed data. Data were compared using the Friedman test and post-hoc analyses were performed with the Wilcoxon signed ranks test. A p-value below 0.05 was considered statistically significant for the Friedman test and a Bonferroni correction was made for the post-hoc Wilcoxon test with a significance level set at a p-value below 0.007. Values are given as medians with interquartile ranges unless otherwise stated. Interscan variability was measured using the intraclass correlation coefficient as well as a Bland-Altman plot.

## Results

### *Calcium score*

The median Agatston score at routine dose reconstructed with FBP was 397 (interquartile range 212 – 1413). An example of the different reconstruction techniques and parameters is shown in *Figure 1*. The measured Agatston scores, calcification masses and volumes are listed in *Table 1*. The Agatston score, calcification mass and volume at all dose levels in all reconstruction methods were compared to the reference dose protocol reconstructed with FBP. The results are shown in *Figure 2*.

At routine dose a significantly lower average Agatston score was found with IMR level 3 (median difference 1.7%, 6.8 Agatston units) and iDose<sup>4</sup> level 7 (median difference 1.5%, 6.0 Agatston units) compared to FBP ( $p < 0.007$ ). At 27% and 55% reduced dose no differences with FBP (routine dose) were found ( $p > 0.007$ ). At 82% reduced dose significantly lower Agatston scores were found with IMR levels 1 to 3 and iDose<sup>4</sup> level 7. The average differences were 5.2% (20.7 Agatston units), 5.3% (21.0 Agatston units) and 5.2% (20.7 Agatston units) with IMR levels 1 to 3 respectively and 3.6% (14.3 Agatston units) with iDose<sup>4</sup> level 7.

Calcium mass was compared to the acquisition at routine dose reconstructed with FBP. With the three reduced dose levels no significant differences were found for all reconstruction methods. At routine dose a small but statistically significant increase in mass with IMR levels 2 and 3 was found ( $p < 0.007$ ). The median difference was 1.9% (2.3 mg) and 2.0% (2.4 mg) respectively.

Statistically significantly lower calcium volumes compared to FBP (routine dose) were found at 82% reduced dose using IMR levels 1 to 3 ( $p < 0.007$ ). The median difference was 4.4% (14.7 mm<sup>3</sup>), 4.7% (15.8 mm<sup>3</sup>) and 5.0% (16.8 mm<sup>3</sup>) respectively. There were two reclassifications from risk groups based on Agatston scores. One changed from low to normal at 82% reduced dose (iDose<sup>4</sup> levels 1, 4 and 7). One changed from intermediate to high at 27% reduced dose (iDose<sup>4</sup> levels 1, 4 and 7) and routine dose (iDose<sup>4</sup> levels 4 and 7).

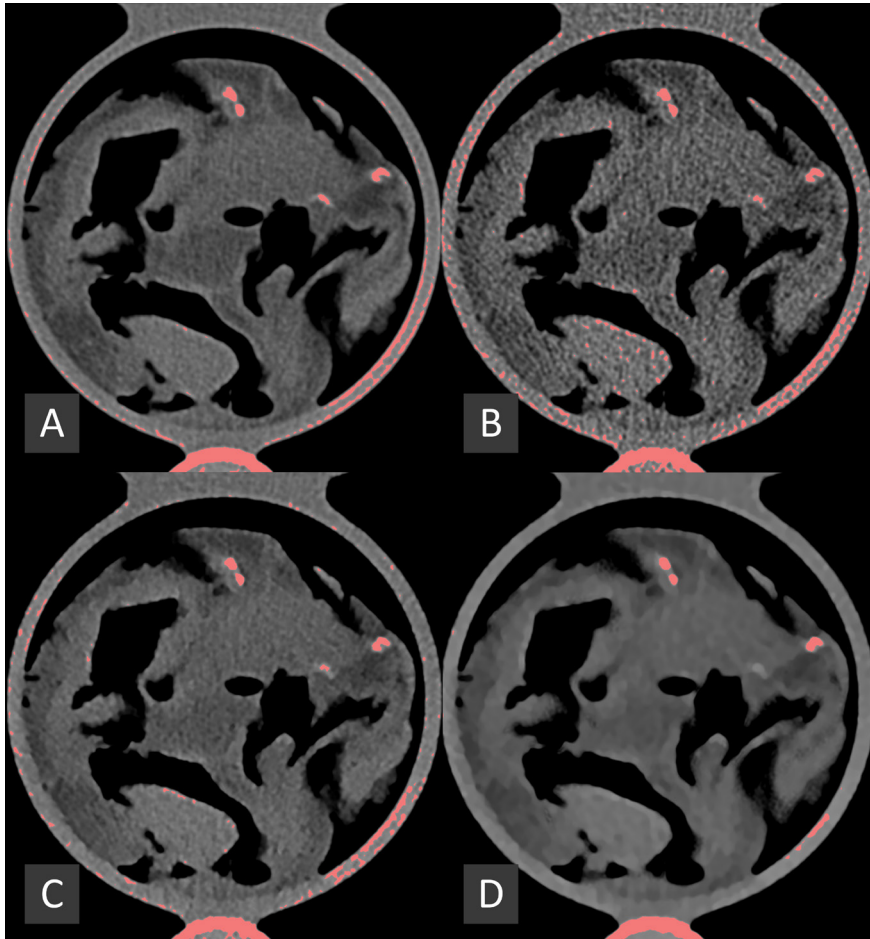


Figure 1 – Example images reconstructed with the different reconstruction techniques and parameters at reference dose reconstructed with filtered back-projection (A) and at 82% reduced dose reconstructed with filtered back-projection (B), iDose<sup>4</sup> level 7 (C) and IMR level 3 (D).

Table 1 – Agatston score, calcification mass and volume per reconstruction method and per dose level. Values are presented as medians (interquartile range).

	FBP	iDose <sup>4</sup> level 1	iDose <sup>4</sup> level 4	iDose <sup>4</sup> level 7	IMR level 1	IMR level 2	IMR level 3
<b>Routine dose</b>							
Agatston score	397 (212 - 1413)	397 (211 - 1411)	397 (212 - 1398)	398 (210 - 1387)* p=0.005	373 (207 - 1391)	405 (206 - 1390)	410 (206 - 1389)* p=0.005
Mass	122 (61 - 410)	122 (6 - 411)	122 (60 - 411)	121 (58 - 411)	109 (61 - 415)	124 (63 - 416)* p=0.001	123 (61 - 416)* p=0.001
Volume	335 (173 - 1115)	323 (172 - 1115)	321 (172 - 1111)	322 (172 - 1105)	307 (173 - 1102)	336 (171 - 1099)	335 (172 - 1096)
<b>27% reduced dose</b>							
Agatston score	395 (218 - 1443)	395 (216 - 1442)	395 (214 - 1439)	398 (210 - 1428)	400 (213 - 1417)	400 (213 - 1415)	401 (213 - 1415)
Mass	122 (65 - 416)	122 (64 - 416)	122 (63 - 417)	121 (62 - 417)	123 (64 - 421)	123 (64 - 422)	123 (64 - 422)
Volume	379 (185 - 1134)	378 (181 - 1132)	366 (178 - 1126)	357 (177 - 1120)	367 (178 - 1120)	369 (178 - 1118)	370 (179 - 1119)
<b>55% reduced dose</b>							
Agatston score	391 (214 - 1376)	389 (212 - 1368)	386 (208 - 1348)	395 (204 - 1339)	384 (211 - 1325)	391 (211 - 1325)	393 (211 - 1324)
Mass	120 (62 - 393)	119 (60 - 392)	117 (57 - 392)	116 (54 - 392)	118 (56 - 395)	118 (55 - 396)	118 (56 - 396)
Volume	356 (188 - 1071)	346 (184 - 1067)	323 (177 - 1057)	317 (171 - 1049)	309 (180 - 1038)	320 (180 - 1035)	320 (181 - 1032)
<b>82% reduced dose</b>							
Agatston score	392 (230 - 1462)	390 (221 - 1448)	385 (211 - 1428)	380 (205 - 1395)* p=0.005	376 (201 - 1401)* p=0.003	376 (199 - 1399)* p=0.003	377 (198 - 1403)* p=0.004
Mass	122 (67 - 417)	121 (56 - 415)	121 (55 - 414)	120 (53 - 412)	121 (49 - 414)	121 (48 - 415)	121 (48 - 416)
Volume	415 (203 - 1136)	320 (197 - 1132)	317 (189 - 1122)	312 (178 - 1095)	308 (175 - 1083)* p=0.005	307 (172 - 1082)* p=0.004	309 (170 - 1078)* p=0.003

\*Significant difference compared to FBP at routine dose. Abbreviations: FBP = filtered back projection; IMR = iterative model reconstruction

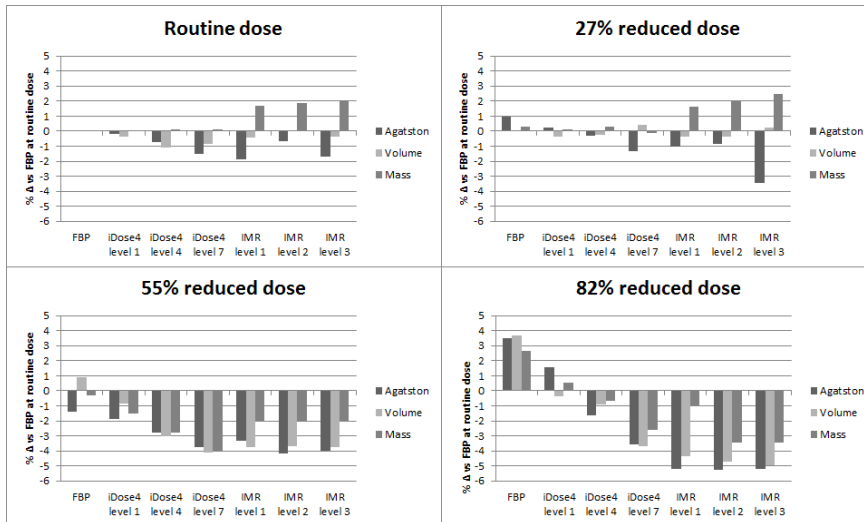


Figure 2 – Difference in Agatston score, calcification volume and mass between reconstruction methods. Differences are expressed as median percentage difference compared to FBP (at routine dose). Abbreviations: FBP = filtered back projection; IMR = iterative model reconstruction

### Objective image quality

The measured CNR and SNR values are listed in Table 2. The CNR at different dose levels and with different reconstruction methods is shown in Figure 3. The Friedman test was significant and post-hoc analysis was performed. The CNR and SNR measured with different reconstruction methods were compared per dose level and were significantly different at all dose levels between reconstruction methods. The CNR and SNR decreased significantly using FBP at the reduced dose protocols.

CNR and SNR on all dose levels in every reconstruction method were compared to the reference dose protocol reconstructed with FBP. Both CNR and SNR were significantly higher in both iDose<sup>4</sup> and IMR at all levels at routine dose compared to FBP ( $p < 0.007$ ). Also, IMR levels 1 to 3 reached a significantly higher CNR and SNR on all reduced dose protocols compared to the FBP reconstruction at routine dose. The difference between iDose<sup>4</sup> at reduced dose protocols and FBP at routine dose was significant for all comparisons except for iDose<sup>4</sup> level 1 (at 27% dose reduction) and iDose<sup>4</sup> level 7 (at 82% dose reduction). The CNR and SNR found with iDose<sup>4</sup> level 1 with 27%, 55% and 82% dose reduction and with

Table 2 – CNR and SNR per dose level and per reconstruction method. Values are presented as medians (interquartile range).

	FBP	iDose <sup>a</sup> level 1	iDose <sup>a</sup> level 4	iDose level <sup>b</sup> 7	IMR level 1	IMR level 2	IMR level 3
<b>CNR</b>							
Routine dose	53.8 (50.6 - 56.2)	60.1 (56.5 - 62.8)	75.5 (70.5 - 78.9)	117.3 (109.1 - 121.9)	161.1 (158.1 - 172.9)	194.0 (189.3 - 206.4)	233.3 (228.0 - 248.7)
27% dose reduction	45.9 (43.3 - 50.5)	51.3 (48.2 - 56.4)	64.8 (60.0 - 70.7)	99.6 (91.9 - 109.5)	146.4 (132.2 - 155.6)	180.0 (160.3 - 193.1)	221.0 (195.1 - 238.2)
55% dose reduction	36.3 (32.0 - 39.1)	40.5 (35.7 - 43.7)	50.7 (44.5 - 54.7)	78.8 (68.5 - 85.4)	113.9 (104.7 - 127.3)	139.4 (129.0 - 158.0)	175.5 (162.4 - 195.6)
82% dose reduction	24.7 (23.1 - 25.3)	28.0 (26.2 - 28.7)	35.1 (32.7 - 35.8)	54.4 (50.3 - 56.4)	83.0 (79.5 - 87.2)	103.0 (95.7 - 107.9)	127.8 (115.5 - 132.8)
<b>SNR Spine</b>							
Routine dose	5.8 (5.2 - 6.0)	6.4 (5.8 - 6.7)	8.1 (7.3 - 8.4)	12.4 (11.3 - 12.8)	17.4 (16.2 - 18.7)	20.7 (20.0 - 22.8)	25.2 (24.3 - 27.4)
27% dose reduction	4.9 (4.6 - 5.5)	5.5 (5.1 - 6.1)	6.9 (6.4 - 7.7)	10.7 (9.9 - 11.9)	16.0 (14.0 - 16.8)	19.7 (16.8 - 20.7)	24.7 (20.3 - 27.3)
55% dose reduction	3.7 (3.4 - 4.1)	4.1 (3.9 - 4.6)	5.2 (4.9 - 5.8)	7.9 (7.4 - 9.0)	12.1 (10.8 - 13.5)	14.9 (12.2 - 16.5)	18.6 (15.9 - 20.9)
82% dose	2.6 (2.4 - 2.8)	3.0 (2.7 - 3.2)	3.7 (3.4 - 4.0)	5.7 (5.1 - 6.3)	9.0 (8.2 - 9.4)	11.0 (9.7 - 12.2)	13.6 (11.3 - 15.4)

Abbreviations: FBP = filtered back projection; IMR = iterative model-based reconstruction

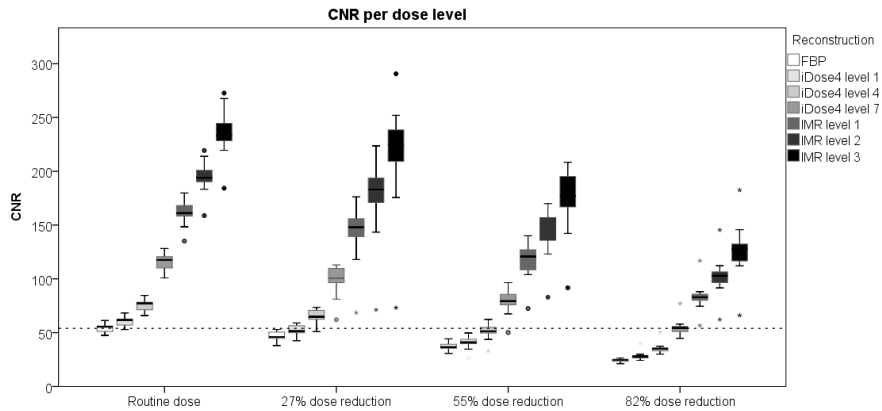


**Figure 3** – CNR per dose level. Reference line represents the median CNR with FBP (at routine dose). Abbreviations: CNR = contrast-to-noise ratio; FBP = filtered back projection; IMR = iterative model reconstruction; ● outlier (more than 1.5 box lengths); \* extreme outlier (more than 3 box lengths)

iDose<sup>4</sup> level 4 at 55% and 82% dose reduction were lower compared to FBP at routine dose.

At the lowest dose level (82% reduction) there was a median decrease in CNR of 54% for FBP, 48% and 35% for iDose<sup>4</sup> levels 1 and 4 respectively and a median increase in CNR of 1% for iDose<sup>4</sup> level 7 and 54%, 91% and 238% for IMR levels 1 to 3 respectively compared to FBP at routine dose.

#### *Interscan variability*

Five hearts were scanned twice to measure interscan variability. FBP reconstructions were used to measure the interscan variability. Bland-Altman analysis showed comparable Agatston scores between the scans (*Figure 4*). The intraclass correlation coefficient was 1.0 at 27% and 82% dose reduction and 0.9 at routine dose and 55% reduced dose. The median interscan difference was 24 Agatston units (1.7%) for calcium score, 14 mg (4.6%) for calcium mass and 18 mm<sup>3</sup> (2.5%) for calcium volume.

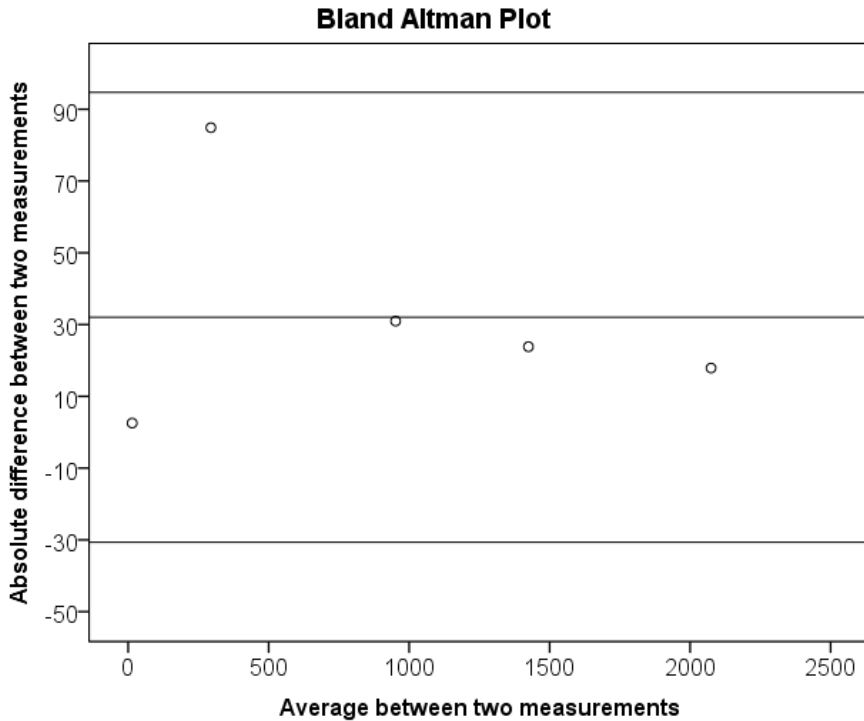


Figure 4 – Bland Altman plot for the difference in Agatston score between the two scans at the FBP reconstruction (at routine dose). The upper and lower lines represent the lines of agreement and the central line represents the mean difference between the two measurements.

## Discussion

This study showed that radiation dose reduction up to 82% did not affect calcium scores with standard FBP reconstructions and low iDose<sup>4</sup> levels, while Agatston scores significantly decreased with IMR and the highest iDose<sup>4</sup> level. Furthermore, coronary mass values remained unaffected by dose reduction for all reconstruction methods and coronary volume decreased with IMR at 82% dose reduction. Objective image quality significantly improved with iterative reconstruction, in particular with IMR.

Iterative reconstruction has been mainly investigated in (contrast-enhanced) coronary CT angiography where improved image quality and increased diagnostic accuracy has been reported [10,18-22]. Coronary calcium scores are assessed on unenhanced cardiac CT. To our best knowledge only four other

published studies investigated the effect of IR on coronary calcifications [23-26]. *Kurata et al.* [23] investigated the influence of different levels of a hybrid IR algorithm from a single vendor, sinogram-affirmed iterative reconstruction (SAFIRE), on the coronary calcium score at normal dose levels in 70 patients. They also found decreased Agatston scores, calcium mass and volumes with increased IR levels. *Murazaki et al.* [25] used a cardiac phantom with known calcium content and found the same Agatston score, calcification mass and volume compared to FBP at normal and reduced dose levels up to 70% using different iDose<sup>4</sup> levels. Only one phantom was used for this in vitro study. *Takx et al.* [26] investigated the use of iDose<sup>4</sup> in 63 patients at normal dose levels and analysed plaque composition and objective image noise. While objective image noise decreased significantly using iDose<sup>4</sup>, there was no effect of iterative reconstruction on plaque composition. *Gebhard et al.* [24] performed an *in-vivo* study with 50 patients using 20-100% ASIR at unenhanced cardiac CT scans at normal dose levels. The maximum decrease in Agatston scores was 128.5 Agatston units (15.3%) with 100% ASIR compared to FBP while mass scores remained unchanged. The maximum difference in mass score was 1.9% with 40% ASIR.

In the current study both a hybrid and a model-based IR technique were used at normal and reduced dose levels. The current study showed that radiation dose reductions up to 82% did not significantly influence Agatston scores, calcification mass and volume with standard FBP reconstructions. Agatston score differences with IR were relatively small and remained within 5.3% and only two patients changed risk classification category. Therefore the effect of IR on calcium scores is presumably not clinically relevant. This study confirms the results of *Kurata et al.* [23] and *Gebhard et al.* [24] that IR leads to lower Agatston scores.

The current study not only investigated hybrid iterative reconstruction, as the previous mentioned studies, but also model-based iterative reconstruction. Objective image noise decreased even further using model-based iterative reconstruction compared to hybrid iterative reconstruction. However, the diagnostic value of model-based IR algorithms should be further evaluated on diagnostic CT protocols. A preliminary report of a study investigating the objective and subjective image noise using IMR found no improvement in overall image quality, likely due to the more 'plastic' appearance using IMR [14]. In the current study objective image quality increased with IR, especially with IMR. However, the subjective image quality of IMR should be further investigated.

In the current study calcification mass remained unchanged, which is comparable to the findings of *Gebhard et al.* [24]. A possible explanation for the fact that coronary mass remains unchanged is that with IR the borders of the calcified area are smoothed and the central area appears denser. Therefore calcium mass remains unchanged while the Agatston score and volume decreases. Moreover previous studies demonstrated that calcium mass is better reproducible than the Agatston score [27-29]. Because the calcium score could also be used for follow-up, a low variability is important [27]. Also calcification mass and volume are not influenced by tube voltage variations unlike the Agatston score [30,31]. Therefore the coronary calcification mass might be a better quantification method than the Agatston score.

Our study has limitations. It concerns an *ex-vivo* study with relatively high Agatston scores (median 397). With high Agatston scores, the change of reclassification in a different risk group due to IR is likely to be small. Because this is an *ex-vivo* study, the effect of IR on motion artefacts could not be measured. Potentially IMR may have an effect on image artefacts which in turn may influence calcium scores, However this need to be evaluated in future research. Furthermore, because all major vendors developed their own IR technique, the applicability of the findings of this study to CT-scans from different vendors may be limited. However, besides IMR there are currently no other commercially available model-based algorithms that are compatible with prospectively triggered cardiac CT. Also the calcium scores were measured by a single observer in a standard order. This could have led to falsely improved assessment on the lower dose scans. However, this method ensures the detection of the same calcifications on all reconstructions.

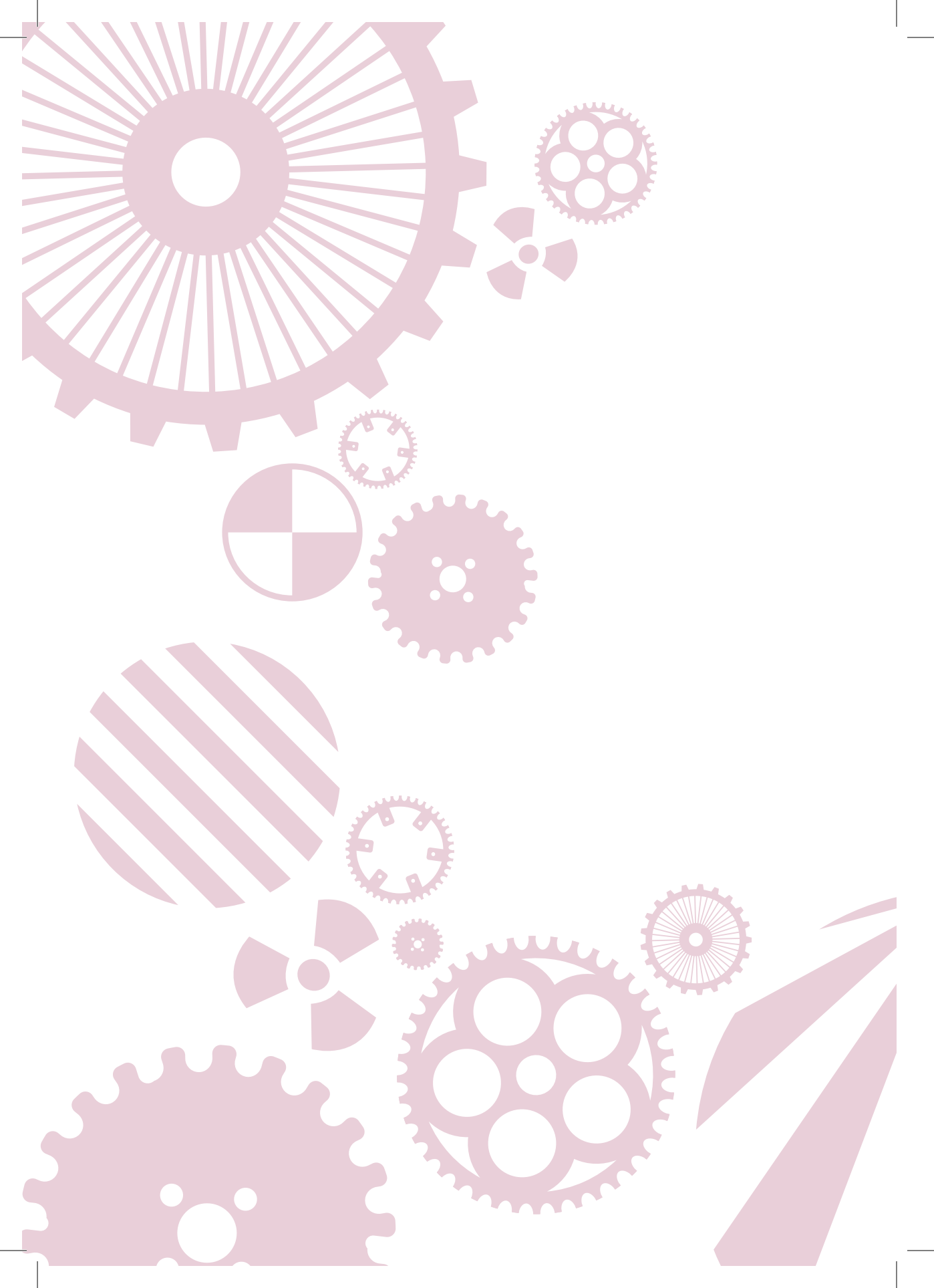
While IMR has a significant influence on calcium scores, low level *iDose<sup>4</sup>* does not affect calcium scores. Therefore low level *iDose<sup>4</sup>* was preferred over IMR in the current study. Objective image quality increased significantly using both hybrid and model-based IR. Therefore for coronary calcium scoring radiation dose can be reduced up to 82% whereby a low *iDose<sup>4</sup>* level is preferable over FBP.

## References

- [1] World Health Organization, Cardiovascular diseases. Fact sheet No 317. 2013;2013(May).
- [2] Mohlenkamp S, Lehmann N, Greenland P, et al., Coronary artery calcium score improves cardiovascular risk prediction in persons without indication for statin therapy. *Atherosclerosis* 2011;215(1):229-36.
- [3] Brenner DJ, Hall EJ, Computed tomography--an increasing source of radiation exposure. *N Engl J Med* 2007;357(22):2277-84.
- [4] Greenland P, Alpert JS, Beller GA, et al., 2010 ACCF/AHA guideline for assessment of cardiovascular risk in asymptomatic adults: a report of the American College of Cardiology Foundation/American Heart Association Task Force on Practice Guidelines. *J Am Coll Cardiol* 2010;56(25):e50-103.
- [5] Lee TY, Chhem RK, Impact of new technologies on dose reduction in CT. *Eur J Radiol* 2010;76(1):28-35.
- [6] Yu L LS, Image reconstruction techniques. American College of Radiology 2010.
- [7] Nelson RC, Feuerlein S, Boll DT, New iterative reconstruction techniques for cardiovascular computed tomography: how do they work, and what are the advantages and disadvantages? *J Cardiovasc Comput Tomogr* 2011;5(5):286-92.
- [8] Willemink MJ, de Jong PA, Leiner T, et al., Iterative reconstruction techniques for computed tomography Part 1: Technical principles. *Eur Radiol* 2013;23(6):1623-31.
- [9] Zeng GL, Image reconstruction--a tutorial. *Comput Med Imaging Graph* 2001;25(2):97-103.
- [10] Willemink MJ, Leiner T, de Jong PA, et al., Iterative reconstruction techniques for computed tomography part 2: initial results in dose reduction and image quality. *Eur Radiol* 2013;23(6):1632-42.
- [11] Scibelli A, iDose<sup>4</sup> iterative reconstruction technique. Philips Healthcare Whitepaper. 2011; Available via [https://www.healthcare.philips.com/pwc\\_hc/main/shared/Assets Documents/ct/idose\\_white\\_paper\\_452296267841.pdf](https://www.healthcare.philips.com/pwc_hc/main/shared/Assets Documents/ct/idose_white_paper_452296267841.pdf) (Accessed 30 September 2013).
- [12] Funama Y, Taguchi K, Utsunomiya D, et al., Combination of a low-tube-voltage technique with hybrid iterative reconstruction (iDose) algorithm at coronary computed tomographic angiography. *J Comput Assist Tomogr* 2011;35(4):480-5.
- [13] Mehta D, Thompson R, Morton T, Dhanantwari A, Shefer E, Iterative Model Reconstruction: simultaneously lowered computed tomography radiation dose and improved image quality. *Med Phys* 2013;1(2):147-155.
- [14] Kligerman S, Read K, Dhanantwari A, et al., Iterative model reconstruction (IMR) a novel method of noise reduction to improve diagnostic confidence in obese patients undergoing CT pulmonary angiography (CTPA). Radiological Society of North America 2012. Scientific assembly and annual meeting 2011. (07/25).

- [15] Quality Assurance in Radiology and Medicine (QRM) GmbH, Anthropomorphic cardio phantom; <http://www.qrm.de/content/pdf/QRM-Cardio-Phantom.pdf>. 2008;2013(May).
- [16] Agatston AS, Janowitz WR, Hildner FJ, Zusmer NR, Viamonte M, Jr, Detrano R, Quantification of coronary artery calcium using ultrafast computed tomography. *J Am Coll Cardiol* 1990;15(4):827-32.
- [17] Schoepf JU, CT of the heart: principles and applications. 2005.
- [18] Fuchs TA, Fiechter M, Gebhard C, et al., CT coronary angiography: impact of adapted statistical iterative reconstruction (ASIR) on coronary stenosis and plaque composition analysis. *Int J Cardiovasc Imaging* 2013;29(3):719-24.
- [19] Moscariello A, Takx RA, Schoepf UJ, et al., Coronary CT angiography: image quality, diagnostic accuracy, and potential for radiation dose reduction using a novel iterative image reconstruction technique-comparison with traditional filtered back projection. *Eur Radiol* 2011;21(10):2130-8.
- [20] Renker M, Nance JW, Jr, Schoepf UJ, et al., Evaluation of heavily calcified vessels with coronary CT angiography: comparison of iterative and filtered back projection image reconstruction. *Radiology* 2011;260(2):390-9.
- [21] Stolzmann P, Schlett CL, Maurovich-Horvat P, et al., Variability and accuracy of coronary CT angiography including use of iterative reconstruction algorithms for plaque burden assessment as compared with intravascular ultrasound-an ex vivo study. *Eur Radiol* 2012;22(10):2067-75.
- [22] Pontana F, Pagniez J, Duhamel A, et al., Reduced-dose low-voltage chest CT angiography with Sinogram-affirmed iterative reconstruction versus standard-dose filtered back projection. *Radiology* 2013;267(2):609-18.
- [23] Kurata A, Dharampal A, Dedic A, et al., Impact of iterative reconstruction on CT coronary calcium quantification. *Eur Radiol* 2013;23(12):3246-52.
- [24] Gebhard C, Fiechter M, Fuchs TA, et al., Coronary artery calcium scoring: Influence of adaptive statistical iterative reconstruction using 64-MDCT. *Int J Cardiol* 2012.
- [25] Murazaki H, Funama Y, Hatemura M, Fujioka C, Tomiguchi S, Quantitative evaluation of calcium (content) in the coronary artery using hybrid iterative reconstruction (iDose) algorithm on low-dose 64-detector CT: comparison of iDose and filtered back projection. *Nihon Hoshasen Gijutsu Gakkai Zasshi* 2011;67(4):360-6.
- [26] Takx RA, Willemink MJ, Nathoe HM, et al., The effect of iterative reconstruction on quantitative computed tomography assessment of coronary plaque composition. *Int J Cardiovasc Imaging* 2013.
- [27] Ohnesorge B, Flohr T, Fischbach R, et al., Reproducibility of coronary calcium quantification in repeat examinations with retrospectively ECG-gated multisection spiral CT. *Eur Radiol* 2002;12(6):1532-40.

- [28] Ulzheimer S, Kalender WA, Assessment of calcium scoring performance in cardiac computed tomography. *Eur Radiol* 2003;13(3):484-97.
- [29] Rutten A, Isgum I, Prokop M, Coronary calcification: effect of small variation of scan starting position on Agatston, volume, and mass scores. *Radiology* 2008;246(1):90-8.
- [30] Deprez FC, Vlassenbroek A, Ghaye B, Raaijmakers R, Coche E, Controversies about effects of low-kilovoltage MDCT acquisition on Agatston calcium scoring. *J Cardiovasc Comput Tomogr* 2013;7(1):58-61.
- [31] Marwan M, Mettin C, Pflederer T, et al., Very low-dose coronary artery calcium scanning with high-pitch spiral acquisition mode: comparison between 120-kV and 100-kV tube voltage protocols. *J Cardiovasc Comput Tomogr* 2013;7(1):32-8.



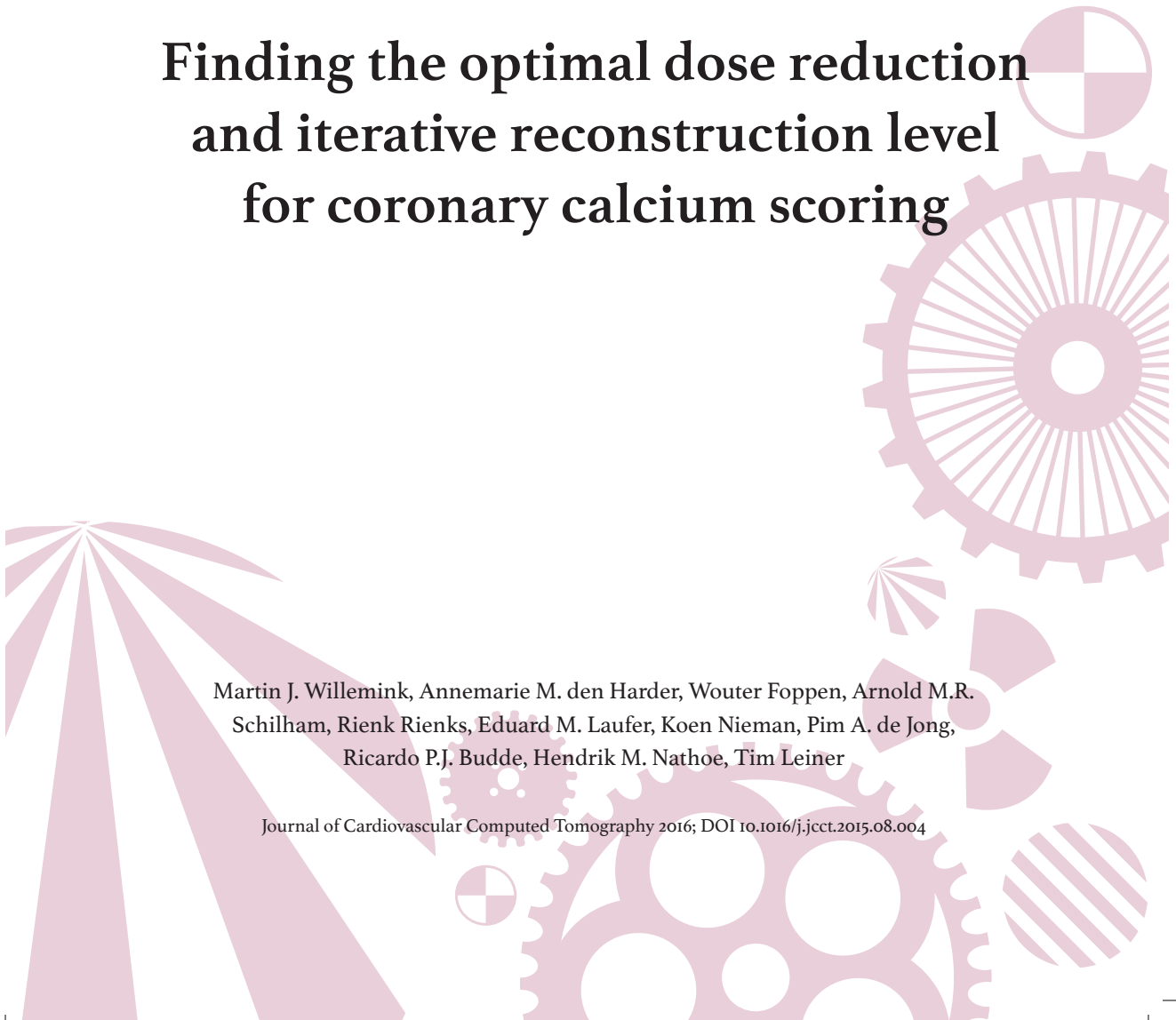
# Chapter 1.3

## *Part I Cardiac*

### Finding the optimal dose reduction and iterative reconstruction level for coronary calcium scoring

Martin J. Willemink, Annemarie M. den Harder, Wouter Foppen, Arnold M.R. Schilham, Rienk Rienks, Eduard M. Laufer, Koen Nieman, Pim A. de Jong, Ricardo P.J. Budde, Hendrik M. Nathoe, Tim Leiner

Journal of Cardiovascular Computed Tomography 2016; DOI 10.1016/j.jcct.2015.08.004



## Abstract

### *Objective*

To assess the maximally achievable computed tomography (CT) dose reduction for coronary artery calcium (CAC) scoring with iterative reconstruction (IR) by using phantom-experiments and a systematical within-patient study.

### *Methods*

Our local institutional review-board approved this study and informed consent was obtained from all participants. A phantom and patient study were conducted with 30 patients (23 men, median age 55.0 (52.0-56.0) years) who underwent 256-slice electrocardiogram-triggered CAC-scoring at four dose levels (routine, 60%, 40%, and 20%-dose) in a single session. Tube-voltage was 120 kVp, tube-current was lowered to achieve stated dose levels. Data were reconstructed with filtered back-projection (FBP) and three IR levels. Agatston, volume and mass scores were determined with validated software and compared using Wilcoxon signed ranks-tests. Subsequently, patient reclassification was analyzed.

### *Results*

The phantom study showed that Agatston scores remained nearly stable with FBP between routine-dose and 40%-dose and increased substantially at lower dose. Twenty-three patients (77%) had coronary calcifications. For Agatston scoring, one 40%-dose and six 20%-dose FBP reconstructions were not interpretable due to noise. In contrast, with IR all reconstructions were interpretable. Median Agatston scores increased with FBP from 26.1 (5.2-192.2) at routine-dose to 60.5 (11.6-251.7) at 20% dose. However, IR lowered Agatston scores to 22.9 (5.9-195.5) at 20%-dose and strong IR (level 7) with Agatston reclassifications in 15%.

### *Conclusion*

IR allows for CAC-scoring radiation dose reductions of up to 80% resulting in effective doses between 0.15 and 0.18 mSv. At these dose-levels, reclassification-rates remain within 15% if the highest IR-level is applied.

## Introduction

Coronary artery calcium (CAC), as measured by non-contrast cardiac computed tomography (CT), is a strong predictor for future cardiovascular events and mortality [1-4]. Although the presence of CAC does not necessarily imply the presence of flow-limiting coronary artery obstruction, current international guidelines recommend the use of CAC scoring for risk re-stratification of asymptomatic individuals at low-to-intermediate and intermediate risk of cardiovascular disease based on traditional risk factors. In 2007, 600,000 CAC scans were performed in the United States alone, a number expected to increase with the recent guideline support [1,5]. The radiation dose of approximately 1 mSv for CAC scans may be considered relatively low [6], but in the context of screening growing numbers of healthy individuals, exposure will become considerable on a population level [7].

Traditionally, CAC scans were reconstructed with an image reconstruction algorithm called filtered back projection (FBP). With more powerful computer processing now widely available, iterative reconstruction techniques are being used clinically for CT image reconstruction. Although these iterative reconstruction algorithms are more computationally intensive they have the potential to provide better image quality and indirectly create opportunities for radiation dose reductions [8-13]. However, the optimal combination of radiation dose reduction and iterative reconstruction setting has not yet been evaluated for CAC scoring. Therefore, the aim of the current study was to assess the maximally achievable dose reduction with iterative reconstruction by using a phantom study and subsequently a systematical within-patient study design using CAC scoring at multiple radiation dose levels.

## Methods

### *Phantom study*

Prior to the patient study, a phantom study was performed to evaluate the potential radiation dose reduction and make a more informed choice regarding acquisition protocols in the patient study. A commercially available anthropomorphic calcium scoring phantom (QRM GmbH, Moehrendorf, Germany) was scanned with a 256-slice CT system (iCT, Philips Healthcare, Best, The Netherlands). The phantom was surrounded by an external ring (medium size) in order to simulate the thoracic attenuation of an average size patient [14]. An electrocardiogram (ECG) simulator was used at 60 beats per minute to trigger

the image acquisition. CT parameters were 120 kVp and 55 mAs (reference level) and the tube-current was decreased with steps of 5 mAs down to 10 mAs. Data were reconstructed with FBP and hybrid iterative reconstruction (iDose<sup>4</sup>, Philips Healthcare, Best, The Netherlands) at increasing levels from 3 to 7. Agatston scores of 6 inserts (3 cylindrical inserts of 5 mm diameter and 3 cylindrical inserts of 3 mm diameter) containing hydroxyapatite at different concentrations (800 mg/cm<sup>3</sup>, 400 mg/cm<sup>3</sup> and 200 mg/cm<sup>3</sup>) were quantified with commercially available software (Heartbeat CS, Philips Healthcare, Best, The Netherlands).

#### *Patients*

Our local institutional review board approved this prospective study and written informed consent was obtained from all participants. Thirty patients with a clinical indication for a cardiac CT successively underwent 4 calcium scoring CT scans in a single session. Patients were scanned between January 2014 and August 2014. Only patients of 50 years or older were selected since the effects of the additional radiation exposure was considered less potentially harmful in these patients compared to younger patients. The routine dose level for CAC scoring of patients  $\geq 80$  kg at our institution is approximately 0.9 mSv. Additional scans at 60%, 40% and 20% of the routine radiation dose would cumulatively result in a maximal additional dose of 1.1 mSv, for a total of approximately 2 mSv.

#### *CT Protocol and Analysis*

Image acquisition was performed with a 256-slice CT system (iCT, Philips Healthcare, Best, The Netherlands). If the patient had a resting heart rate above 60 beats per minute at the Cardiology outpatient clinic, the patient was instructed to take 50 mg Metoprolol orally two hours prior to the CT examination. Patients were placed in the supine position and an ECG-trace was recorded during the procedure. If the heart rate was higher than approximately 70 beats per minute, 20 mg of Metoprolol was administered intravenously. First, a locator image was made to select the acquisition region, ranging from the carina of the trachea to the inferior surface of the heart. Second, if the heart rate was regular, acquisition was performed during the mid-diastolic phase with a prospectively ECG-triggered axial scan protocol. In case of an irregular heart rate, acquisition was performed during the systolic phase, also with a prospectively ECG-triggered axial scan protocol. Image acquisition was performed at routine, 40%-reduced, 60%-reduced and 80%-reduced doses for each patient. To make sure patients' heart rates were similar and patients would not move between acquisitions, the

technician planned the four acquisitions beforehand. Therefore, the scans were acquired consecutively within a matter of seconds. The following parameters were used: slice thickness, 3 mm; matrix size 512 x 512 pixels. Tube voltage was kept constant at 120 kVp and tube current-time products depended on body size. Tube current-time products were 50, 30, 20, and 10 mAs for patients with a body weight < 80 kg and 60, 36, 24, and 12 mAs for patients with a body weight  $\geq$  80 kg, respectively. Dose was reduced by decreasing tube current since CAC acquisition protocols are validated at a tube voltage of 120 kVp. Volumetric CT dose index (CTDIvol), dose-length product (DLP) and mean heart rates were recorded for each scan. Effective doses were estimated by multiplying DLP with the effective dose estimate of 0.0145 mSv/(mGy $\times$ cm) for the chest [15].

Raw data were reconstructed with standard FBP and three hybrid iterative reconstruction levels (iDose<sup>4</sup> levels 1, 4 and 7, Philips Healthcare, Best, The Netherlands). Iterative reconstruction algorithms allow for radiation dose reduction due to less noisy images [13]. iDose<sup>4</sup> offers seven levels of noise reduction. Higher iDose<sup>4</sup> levels result in less noise compared to lower levels.

CAC was quantified as Agatston scores, volume scores and mass scores with commercially available validated software (Heartbeat CS, Philips Healthcare, Best, The Netherlands). Signal densities above 130 Hounsfield units (HU) were identified by the software package as potential calcifications. Two observers independently selected the semi-automatically identified regions that were located within the coronary arteries. Subsequently Agatston scores, volume scores and mass scores were quantified by the software package.

#### *Data analysis*

BMI values and heart rates were compared between interpretable and not-interpretable scans using the Mann-Whitney U test. Within-patient CAC scores assessed at different dose levels with different reconstruction algorithms were compared to the reference score (routine radiation dose reconstructed with FBP). Inter-observer agreement was evaluated with two-way random single measures intra-class correlation coefficients (ICCs). ICC values above 0.7 were interpreted as good and ICC values above 0.8 were considered excellent [16]. Statistical differences of CAC scores were analyzed with the Friedman test for paired non-parametric continuous data and subsequently post-hoc analyses were performed with the Wilcoxon signed ranks test. Patients were classified based on reference Agatston scores (routine radiation dose reconstructed with FBP): very low risk (score = 0), low risk ( $0 < \text{score} < 10$ ), moderate risk ( $10 \leq \text{score}$

< 100), moderately high risk ( $100 \leq \text{score} < 400$ ) and high risk ( $\text{score} \geq 400$ ) [13,17,18]. Subsequently, the effect of radiation dose reduction and reconstruction settings on reclassification of Agatston scores was evaluated. The risk categories based on reference Agatston scores (routine radiation dose reconstructed with FBP) were used as the reference risk category. Reclassification was defined as a change in risk category for the same patient at a low-dose protocol compared to the reference risk category. Finally recommended CAC scoring protocols were derived based on Agatston results from the phantom study and the patient study. Protocols with the lowest reclassification rates and Agatston scores similar to the reference scores were selected. A P-value < 0.05 was considered significant and for the post-hoc analyses a Bonferroni corrected P-value of < 0.0033 was used. Data are presented as medians with interquartiles, unless otherwise stated. Statistical analyses were performed with MedCalc version 13.2.2.0 (Mariakerke, Belgium) and IBM SPSS version 20.0 (SPSS Inc, Chicago, Illinois, USA).

## Results

### *Phantom study*

The total Agatston score of the phantom data reconstructed with FBP at 55 mAs was 712.3, and increased with lower mAs-values up to 951.1 at 10 mAs (*Figure 1*).

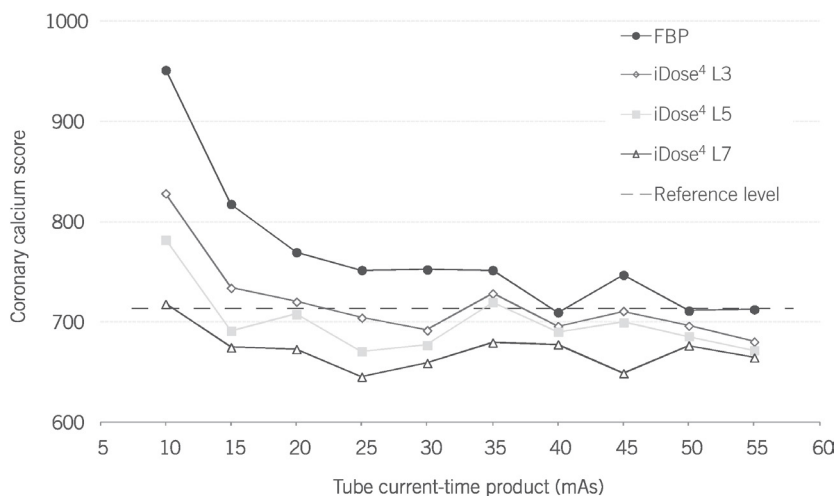


**Figure 1** – Coronary artery calcium scores of the phantom at different tube currents and reconstruction algorithms. FBP Filtered back projection; L3, L5 and L7 Level 3, 5 and 7, respectively; Reference level Coronary calcium score derived from routine dose filtered back projection scan.

Iterative reconstruction led to lower Agatston scores of 679.9 and 664.0 at 55 mAs, and increased to 827.9 and 717.6 at 10 mAs (iDose<sup>4</sup> levels 3 and 7, respectively). The Agatston score was nearly stable between 55 mAs and 20 mAs and increased substantially at lower mAs-values, especially with FBP reconstructed data.

### Patient study

Demographic characteristics of the study population are listed in *Table 1* and radiation doses are listed in *Table 2*. Low dose / reference dose ratios were 0.6, 0.4 and 0.2, respectively for all dose measures. All routine dose reconstructions were interpretable. However, for Agatston scoring one 40% dose and six 20% dose FBP reconstructions were not interpretable due to the presence of extensive noise artifacts with densities above 130 HU (*Figure 2*).

**Table 1** – Patient characteristics. Results are presented as medians with interquartiles.

Variable	Value
Number of Patients (n)	30
Gender (M = male, F = female)	23 M / 7 F
Age (years)	55.0 (52.0-56.0)
Distribution over weight category (<80 kg / ≥80 kg)	11 / 19
Weight (kg)	87.5 (77.5-97.3)
Body mass index (kg/m <sup>2</sup> )	27.1 (25.1-30.0)
Heart rate (/min)	59.0 (52.5-63.0)

**Table 2** – Radiation dose. Results are presented as medians with interquartiles.

	Routine dose		60% dose		40% dose		20% dose	
	< 80 kg	≥ 80 kg	< 80 kg	≥ 80 kg	< 80 kg	≥ 80 kg	< 80 kg	≥ 80 kg
Tube current-time product (mAs)	50	60	30	36	20	24	10	12
CTDIvol (mGy)	4.1	4.9	2.5	3.0	1.7	2.0	0.8	1.0
DLP (mGy×cm)	51.2	61.5	30.9	36.9	20.6	24.0	10.3	12.0
Effective dose (mSv)	0.7	0.9	0.5	0.5	0.3	0.4	0.2	0.2

CTDIvol Volume CT dose index; DLP Dose-length product

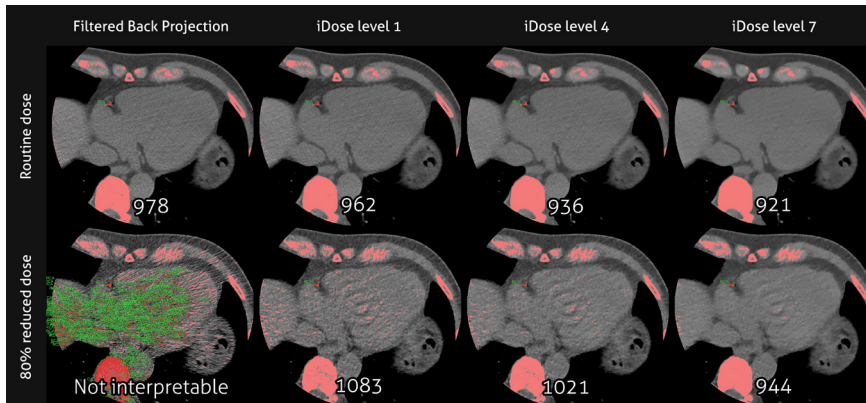


**Figure 2** – Effect of dose reduction and iterative reconstruction on evaluation of coronary calcium. Images of a patient with a reference Agatston score of 978, reconstructed at routine dose (upper row) and 80% reduced dose (lower row) with filtered back projection and iDose4 levels 1, 4 and 7. The 80% reduced dose filtered back projection reconstruction is not interpretable, whereas all levels of iterative reconstruction scans are interpretable.

In contrast, with iterative reconstruction all reconstructions were interpretable. The median body mass index (BMI) and heart rate of patients with non-interpretable reconstructions were 30.9 (29.4-33.0) kg/m<sup>2</sup> and 61 (59-64) beats per minute. For patients with interpretable reconstructions these values were 25.8 (24.8-28.2) kg/m<sup>2</sup> and 58 (51-61) beats per minute, respectively. BMI values for the individuals with non-interpretable reconstructions were significantly higher compared to individuals with interpretable reconstructions ( $P < 0.01$ ). Heart rate differed not significantly between both groups ( $P = 0.1$ ). The non-interpretable low dose reconstructions were excluded for statistical analyses.

#### *Inter-observer agreement*

Agatston score ICC values for the assessment of inter-observer agreement varied between 0.996 and 1.000. For volume scores the ICC values varied between 0.942 and 1.000, and for the mass scores ICC values varied between 0.935 and 1.000, respectively. Therefore, inter-observer agreement was considered excellent.

#### *Agatston scores*

Seven patients (23%) had a reference Agatston score of zero. Both radiation dose reduction and iterative reconstruction did not result in false positive

Agatston scores, except for one case. This patient had a score of 6.9 at 20% dose reconstructed with FBP and 2.4 at 20% dose reconstructed with iDose<sup>4</sup> level 1, higher iDose<sup>4</sup> levels resulted in zero scores in this patient. False positive Agatston scores were caused by noise within the coronary arteries simulating small calcifications.

Twenty-three patients (77%) had a reference Agatston score larger than zero. Median Agatston scores of the patients with interpretable reconstructions (N=18) are listed in *Table 3*, and increased with FBP from 26.1 (5.2-192.2) at routine dose to 60.5 (11.6-251.7) at 20% dose. Iterative reconstruction resulted in lower Agatston scores. The Friedman test showed that overall differences were present ( $P < 0.001$ ). Post-hoc analyses showed that differences were only significant between reference dose FBP and routine dose iDose<sup>4</sup> levels 4 and 7 ( $P = 0.002$  and  $P = 0.001$ , respectively).

The clinical relevance of Agatston score differences was evaluated in terms of risk reclassification compared to routine dose FBP Agatston scores (*Figure 3*). Reducing the radiation dose with FBP resulted in increased risk classifications (N=4 at 60% dose, N=5 at 40% dose and N=6 at 20% dose, respectively), which decreased with higher levels of iterative reconstruction (to N=3 at 60% dose and N=1 at 40% and 20% dose, respectively). However, increased levels of iterative reconstruction resulted in more patients being reclassified to a lower risk category (N=1 at 60% dose, N=5 at 40% dose and N=3 at 20% dose). The minimal number of patients that were reclassified to another risk category compared to the routine dose FBP classification was 4/30 (13%, for all reconstructions) at 60% dose, 4/30 (13%, for iDose<sup>4</sup> levels 1 and 4) at 40% dose, and 4/30 (13%, for iDose<sup>4</sup> level 7) at 20% dose. The maximum number of patients that were reclassified to another risk category compared to the routine dose FBP classification was 4/30 (13%, for all reconstructions) at 60% dose, 7/30 (23%, for FBP) at 40% dose, and 13/30 (43%, for FBP) at 20% dose. Maximum of reclassification category shift was 1 category for all reclassifications. *Figure 4* demonstrates the reclassifications between reference scores and 20% dose iDose<sup>4</sup> level 7 scores.

**Table 3** – Median coronary artery calcium scores of patients with non-zero scores and interpretable reconstructions.

	Agatston score (N=18)	Volume score (mm <sup>3</sup> ) (N=15)	Mass score (mg) (N=15)
<b>Routine dose</b>			
FBP	26.1 (5.2-192.2)	21.1 (7.3-87.6)	4.5 (1.0-17.4)
iDose4 level 1	25.1 (5.2-192.1)	21.1 (6.5-86.5)	4.4 (1.0-17.3)
iDose4 level 4	24.6 (5.0-189.1)	20.5 (7.0-86.5)	4.4 (1.0-17.2)
iDose4 level 7	23.2 (5.0-186.9)	18.7 (6.8-84.5)	4.2 (1.0-17.1)
<b>60% dose</b>			
FBP	25.6 (13.6-166.6)	19.9 (13.8-94.0)	4.2 (2.2-18.3)
iDose4 level 1	24.6 (13.4-164.0)	19.9 (13.3-91.7)	4.0 (2.0-18.0)
iDose4 level 4	22.8 (13.1-160.1)	19.9 (12.8-91.8)	4.0 (2.0-18.0)
iDose4 level 7	22.3 (13.1-158.3)	19.2 (11.0-87.9)	3.8 (1.8-17.5)
<b>40% dose</b>			
FBP	30.3 (9.7-191.2)	21.4 (11.4-148.4)	4.8 (1.9-28.7)
iDose4 level 1	28.4 (8.1-188.2)	20.3 (11.1-137.3)	4.6 (1.8-23.9)
iDose4 level 4	28.7 (7.6-184.8)	20.8 (10.4-130.3)	4.7 (1.7-22.9)
iDose4 level 7	27.6 (7.3-182.6)	19.8 (9.6-128.0)	4.6 (1.6-22.4)
<b>20% dose</b>			
FBP	60.5 (11.6-251.7)	21.4 (14.5-215.3)	3.3 (2.6-33.1)
iDose4 level 1	29.4 (6.8-206.4)	17.6 (9.2-127.0)	3.0 (1.4-22.8)
iDose4 level 4	26.4 (6.6-199.9)	17.1 (8.4-118.1)	2.9 (1.2-21.4)
iDose4 level 7	22.9 (5.9-195.5)	16.6 (5.4-108.7)	2.8 (0.9-20.1)

Results are presented as medians with interquartiles. *FBP Filtered back projection*

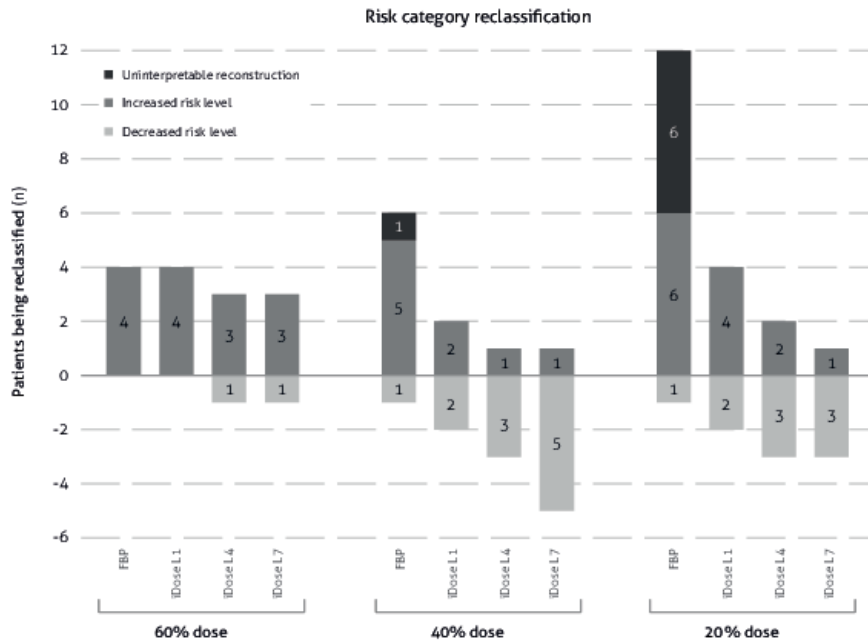


Figure 3 – Reclassification of coronary artery calcium score risk categories (N = 30). *FBP* Filtered back projection; *L1*, *L4* and *L7* Levels 1, 4 and 7, respectively.

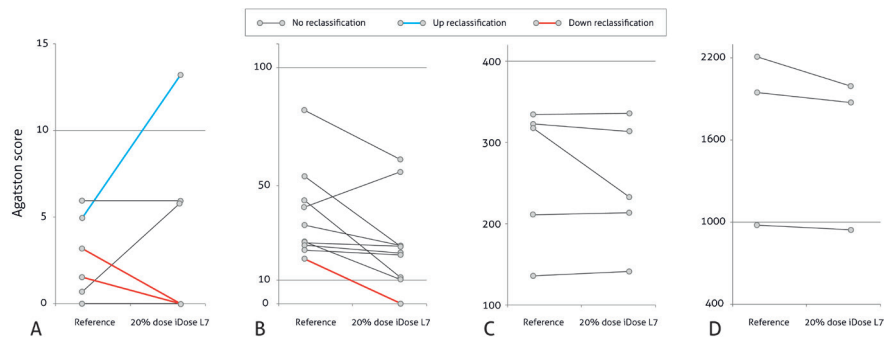


Figure 4 – Reclassification of coronary artery calcium score risk categories, reference scores versus 20% dose iDose level 7

### *Volume and Mass scores*

Since thresholds for Agatston scoring and mass/volume scoring differ, some patients had interpretable scans for Agatston scoring but not for volume and mass scoring. At 60% dose 1 patient had a FBP reconstructed scan that was not interpretable for volume and mass scoring. This number increased at 40% dose to 4 non-interpretable FBP and 1 non-interpretable iDose<sup>4</sup> level 1 reconstructions, and at 20% dose to 8 non-interpretable FBP and 1 non-interpretable iDose<sup>4</sup> level 1 reconstructions. The effect of radiation dose reduction on volume and mass scores in patients with non-zero calcium scores and with interpretable reconstructions was less prominent as compared to Agatston scores (*Table 3*).

The median reference volume score was 21.1 (7.3-87.6) mm<sup>3</sup> and remained approximately the same at FBP reconstructed lower dose scans with median scores of 19.9 (13.8-94.0) mm<sup>3</sup> at 60% dose, 21.4 (11.4-148.4) mm<sup>3</sup> at 40% dose and 21.4 (14.5-215.3) mm<sup>3</sup> at 20% dose. Volume scores also decreased with increasing levels of iterative reconstruction. None of the volume scores differed significantly from the reference volume score ( $P > 0.0033$ ).

The median reference mass score was 4.5 (1.0-17.4) mg and remained also approximately the same at FBP reconstructed lower levels with median scores of 4.2 (1.0-17.1) mg at 60% dose, 4.8 (1.9-28.7) mg at 40% dose and 3.3 (2.6-33.1) mg at 20% dose. Similar to Agatston scores and volume scores, mass scores also decreased with increasing levels of iterative reconstruction. None of the mass scores differed significantly from the reference mass score ( $P > 0.0033$ ).

### *Recommended calcium scoring protocol*

An overview of recommended protocols is composed based on the Agatston data from both the phantom and the patient studies (*Table 4*). Only protocols were selected with less than 15% reclassifications.

**Table 4** – Recommended Agatston scoring protocols. For all protocols: 120 kVp, slice thickness and increment 3.0 mm, matrix size 512 x 512 pixels

	< 80 kg		≥ 80 kg		Reconstruction algorithm	Reclassification rate	
	Tube current (mAs)	Effective dose (mSv)	Tube current (mAs)	Effective dose (mSv)		Up	Down
60% dose	30	0.45	36	0.54	iDose4 level 4	10.0% (3/30)	3.3% (1/30)
					iDose4 level 7	10.0% (3/30)	3.3% (1/30)
40% dose	20	0.30	24	0.36	iDose4 level 1	6.7% (2/30)	6.7% (2/30)
					iDose4 level 4	3.3% (1/30)	10.0% (3/30)
20% dose	10	0.15	12	0.18	iDose4 level 7	3.3% (1/30)	10.0% (3/30)

## Discussion

This study shows that iterative reconstruction allows for CAC scoring radiation dose reduction of up to 80%, resulting in effective doses between 0.15 and 0.18 mSv. At these dose levels, reclassification rates remain within 15% if the highest iterative reconstruction level is applied. Up to our knowledge, this is the first study that aimed at finding the optimal vendor specific combination of dose reduction and iterative reconstruction settings using a systematic within-patient analysis.

Coronary calcium deposition, as measured by non-enhanced CT, correlates with atherosclerotic plaque burden and predicts future adverse cardiovascular events, with incremental predictive value over traditional risk factors [19]. Current guidelines support the use of CAC scoring in asymptomatic adults at intermediate and low to intermediate risk based on traditional risk factors, which represents approximately 40% of the adult population in the United States [1,19]. Particularly in the context of screening healthy asymptomatic populations the radiation exposure is of concern and all efforts should be taken to minimize dose.

Our phantom study showed that Agatston scores remained unchanged between 55 mAs and 20 mAs (approximately 40% of the reference dose), in line with phantom studies performed by Murazaki and colleagues [20]. Doses below 20 mAs increased Agatston scores, especially with FBP reconstructed images.

Based on these data, a prospective patient study was designed. To find the maximally achievable radiation dose reduction, three additional dose levels were selected: 60%, 40% and 20% of the routine dose. The phantom study indicated that the effect of iterative reconstruction would be most obvious at 20% dose. This was confirmed by the patient study: at 20% dose both the absolute Agatston scores as well as the number of reclassifications decreased substantially with higher iterative reconstruction levels. Previous studies have shown that normal variation by changing only the scan starting position of the scan results in reclassification in 10% to 11% [17,21]. These reclassification rates are comparable to the 13% we found in the current study.

#### *Low-dose calcium imaging*

In contrast to other studies we found that a lower radiation dose affected the CAC score. Dey et al.[22] reported no effect of lowering the tube current-time product on CAC scores. However, they compared 120 kVp and 150, 120, or 85 mAs values which resulted in substantially higher doses (CTDIvol: 8.5 mGy versus 5.1 mGy) compared to the dose parameters used in the current study (CTDIvol: 4.8, 2.9, 1.9 and 1.0 mGy). Furthermore, Nakazato and colleagues [23] reported that lowering tube voltage (routine protocol: 120 kVp and 150 mAs; low dose protocol: 100 kVp and 180 mAs) did not affect CAC scoring. They also used substantially higher doses (CTDIvol: 8.6 mGy versus 5.9 mGy) compared to the present study. In neither study iterative reconstruction was used. A more recent study by Hecht et al.[24] found similar results as our current study. They found that CAC scores were not influenced by tube current reductions of 50%, with high iDose<sup>4</sup> levels. Their standard protocol was similar to ours, however they only evaluated a single iterative reconstruction level for the reduced dose protocol (CTDIvol: 4.2 mGy versus 2.0 mGy).

#### *Iterative reconstruction*

Several in vitro and in vivo studies have evaluated the effect of iterative reconstruction on calcium scores and generally demonstrated that calcium scores decreased in comparison to standard FBP reconstructions [8,10-12,23]. Lowering tube current to reduce radiation dose increases image noise and artifacts, which results in larger calcification areas and false positive identification of calcifications by semi-automatic software packages. Because the Agatston score is strongly affected by the highest measurable attenuation (HU) within a lesion, and image noise widens the range of attenuation values,

it is expected that low-dose FBP images result in higher calcium scores [13]. Iterative reconstruction reduces image noise and artifacts [25,26], which is likely to be reflected by lower Agatston scores. These effects are indeed found in our phantom study. One 40% dose and six 20% dose FBP reconstructions were not interpretable for Agatston scoring due to extensive noise artifacts. However, iterative reconstruction preserved Agatston score interpretability in all cases. In comparison, patients with non-interpretable reconstructions had a higher BMI ( $>5 \text{ kg/m}^2$ ,  $P < 0.01$ ) but comparable heart rate, which suggests that body size was more important for interpretability than heart rate associated motion artifacts. Iterative reconstruction resulted in false negative Agatston scores in three patients. At reference dose, these individuals had Agatston scores higher than 0. Levels 4 and 7 of iDose<sup>4</sup> at different low dose protocols resulted in a score of 0. It should be noted that these individuals all had reference scores only slightly above 0. The consequences of this would be relevant in younger patients since lower scores translate to higher percentile scores in these individuals. Furthermore, missing calcification could be clinically relevant if the test were to be performed in low-probability, symptomatic patients to rule out coronary artery disease, as recommended by the NICE guidelines [27]. One individual had a false positive Agatston score at 20% dose with FBP and iDose<sup>4</sup> level 1, caused by image noise. The noise was corrected with higher iterative reconstruction levels, since the Agatston score was 0 with iDose<sup>4</sup> levels 4 and 7 at 20% dose. In the current study, reclassification rates were 13% or lower. For clinical decision making only reclassifications with Agatston scores of around 0 and 400 are of importance. Therefore, the actual number of patients that will be treated differently based on the low-dose protocols in this study will be lower than 13%.

Inter-observer agreement was excellent, but ICCs were smallest using iterative reconstruction. Higher noise levels increase the number of regions with attenuation values above 130 HU, which may be difficult to differentiate from true calcification, thereby reducing the reproducibility between readers.

Recommended Agatston scoring protocols (*Table 4*) were selected based on both the phantom study and the patient study. Absolute Agatston numbers were similar to reference scores and reclassification rates were below 15% for these recommended protocols. It should be noted that these recommendations can only be applied to one vendor. CT systems from different vendors use different iterative reconstruction techniques and calcium quantification algorithms and result in different Agatston scores [28], therefore optimal protocols may be

different for other vendors. Another limitation is the sample size of 30 patients. For ethical reasons the sample size was kept as small as possible. However, we feel the power is sufficient since this study concerns a within-patient analysis with four scans per patient. We reduced radiation doses by only lowering tube currents and keeping tube voltages constant at 120 kVp. Similar to Dey and colleagues [22], we chose to do this for feasibility reasons. Recalibration of the standard calcification threshold of 130 Hounsfield units is needed when tube voltages are lowered, whereas no recalibration is needed with reduced tube currents.

### **Conclusion**

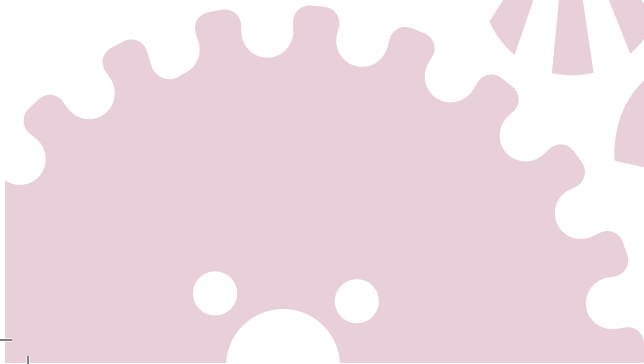
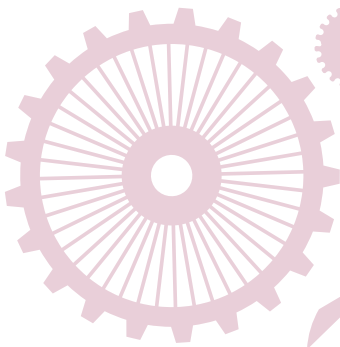
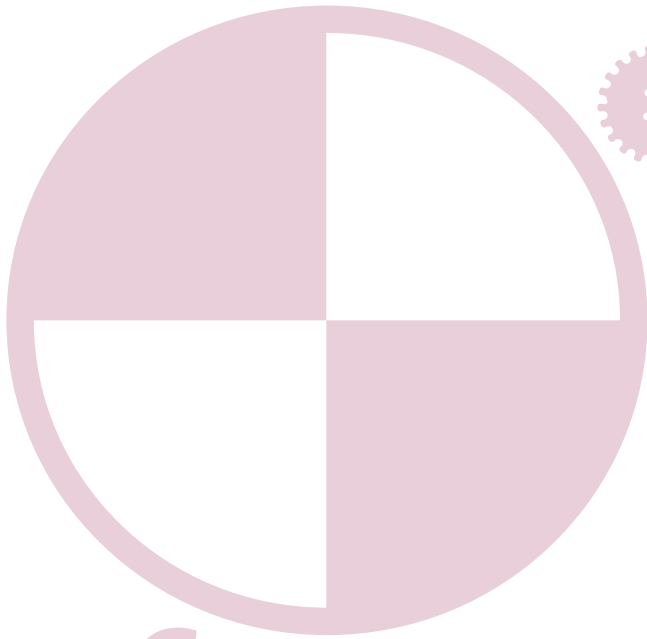
This study shows that iterative reconstruction allows for CAC scoring radiation dose reductions of up to 80% resulting in effective doses between 0.15 and 0.18 mSv. At these dose levels, reclassification rates remain within 15% if the highest iterative reconstruction level is applied.

## References

- [1] Greenland P, Alpert JS, Beller GA, et al., 2010 ACCF/AHA guideline for assessment of cardiovascular risk in asymptomatic adults: a report of the American College of Cardiology Foundation/American Heart Association Task Force on Practice Guidelines. *J Am Coll Cardiol* 2010;56(25):e50-103.
- [2] Budoff MJ, Shaw LJ, Liu ST, et al., Long-term prognosis associated with coronary calcification: observations from a registry of 25,253 patients. *J Am Coll Cardiol* 2007;49(18):1860-70.
- [3] Detrano R, Guerci AD, Carr JJ, et al., Coronary calcium as a predictor of coronary events in four racial or ethnic groups. *N Engl J Med* 2008;358(13):1336-45.
- [4] Wong ND, Hsu JC, Detrano RC, Diamond G, Eisenberg H, Gardin JM, Coronary artery calcium evaluation by electron beam computed tomography and its relation to new cardiovascular events. *Am J Cardiol* 2000;86(5):495-8.
- [5] Berrington de Gonzalez A, Mahesh M, Kim KP, et al., Projected cancer risks from computed tomographic scans performed in the United States in 2007. *Arch Intern Med* 2009;169(22):2071-7.
- [6] Youssef G, Kalia N, Darabian S, Budoff MJ, Coronary calcium: new insights, recent data, and clinical role. *Curr Cardiol Rep* 2013;15(1):325,012-0325-3.
- [7] Kim KP, Einstein AJ, Berrington de Gonzalez A, Coronary artery calcification screening: estimated radiation dose and cancer risk. *Arch Intern Med* 2009;169(13):1188-94.
- [8] den Harder AM, Willeminck MJ, Bleys RL, et al., Dose reduction for coronary calcium scoring with hybrid and model-based iterative reconstruction: an ex vivo study. *Int J Cardiovasc Imaging* 2014;30(6):1125-33.
- [9] Gebhard C., Fiechter M., Fuchs T.A., et al., Coronary artery calcium scoring: Influence of adaptive statistical iterative reconstruction using 64-MDCT. *Eur Heart J* 2012;33:90.
- [10] Kurata A, Dharampala A, Dedic A, et al., Impact of iterative reconstruction on CT coronary calcium quantification. *Eur Radiol* 2013;23(12):3246-52.
- [11] Schindler A, Vliegenthart R, Schoepf UJ, et al., Iterative image reconstruction techniques for CT coronary artery calcium quantification: comparison with traditional filtered back projection in vitro and in vivo. *Radiology* 2014;270(2):387-93.
- [12] van Osch JA, Mouden M, van Dalen JA, et al., Influence of iterative image reconstruction on CT-based calcium score measurements. *Int J Cardiovasc Imaging* 2014.
- [13] Willeminck MJ, Takx RA, de Jong PA, et al., The impact of CT radiation dose reduction and iterative reconstruction algorithms from four different vendors on coronary calcium scoring. *Eur Radiol* 2014;24(9):2201-12.
- [14] McCollough CH, Ulzheimer S, Halliburton SS, Shanneik K, White RD, Kalender WA, Coronary artery calcium: a multi-institutional, multimanufacturer international standard for quantification at cardiac CT. *Radiology* 2007;243(2):527-38.

- [15] Deak PD, Smal Y, Kalender WA, Multisection CT protocols: sex- and age-specific conversion factors used to determine effective dose from dose-length product. *Radiology* 2010;257(1):158-66.
- [16] van Hamersvelt RW, Willemink MJ, Takx RA, et al., Cardiac valve calcifications on low-dose unenhanced ungated chest computed tomography: inter-observer and inter-examination reliability, agreement and variability. *Eur Radiol* 2014;24(7):1557-64.
- [17] Rutten A, Isgum I, Prokop M, Coronary calcification: effect of small variation of scan starting position on Agatston, volume, and mass scores. *Radiology* 2008;246(1):90-8.
- [18] Rumberger JA, Brundage BH, Rader DJ, Kondos G, Electron beam computed tomographic coronary calcium scanning: a review and guidelines for use in asymptomatic persons. *Mayo Clin Proc* 1999;74(3):243-52.
- [19] Oudkerk M, Stillman AE, Halliburton SS, et al., Coronary artery calcium screening: current status and recommendations from the European Society of Cardiac Radiology and North American Society for Cardiovascular Imaging. *Int J Cardiovasc Imaging* 2008;24(6):645-71.
- [20] Murazaki H, Funama Y, Hatemura M, Fujioka C, Tomiguchi S, Quantitative evaluation of calcium (content) in the coronary artery using hybrid iterative reconstruction (iDose) algorithm on low-dose 64-detector CT: comparison of iDose and filtered back projection. *Nihon Hoshasen Gijutsu Gakkai Zasshi* 2011;67(4):360-6.
- [21] Devries S, Wolfkiel C, Shah V, Chomka E, Rich S, Reproducibility of the measurement of coronary calcium with ultrafast computed tomography. *Am J Cardiol* 1995;75(14):973-5.
- [22] Dey D, Nakazato R, Pimentel R, et al., Low radiation coronary calcium scoring by dual-source CT with tube current optimization based on patient body size. *J Cardiovasc Comput Tomogr* 2012;6(2):113-20.
- [23] Nakazato R, Dey D, Gutstein A, et al., Coronary artery calcium scoring using a reduced tube voltage and radiation dose protocol with dual-source computed tomography. *J Cardiovasc Comput Tomogr* 2009;3(6):394-400.
- [24] Hecht HS, de Siqueira ME, Cham M, et al., Low- vs. standard-dose coronary artery calcium scanning. *Eur Heart J Cardiovasc Imaging* 2015;16(4):358-63.
- [25] Willemink MJ, de Jong PA, Leiner T, et al., Iterative reconstruction techniques for computed tomography Part 1: technical principles. *Eur Radiol* 2013;23(6):1623-31.
- [26] Willemink MJ, Leiner T, de Jong PA, et al., Iterative reconstruction techniques for computed tomography part 2: initial results in dose reduction and image quality. *Eur Radiol* 2013;23(6):1632-42.
- [27] Skinner JS, Smeeth L, Kendall JM, Adams PC, Timmis A, Chest Pain Guideline Development Group, NICE guidance. Chest pain of recent onset: assessment and diagnosis of recent onset chest pain or discomfort of suspected cardiac origin. *Heart* 2010;96(12):974-8.
- [28] Willemink MJ, Vliegenthart R, Takx RA, et al., Coronary artery calcification scoring with state-of-the-art CT scanners from different vendors has substantial effect on risk classification. *Radiology* 2014;273(3):695-702.





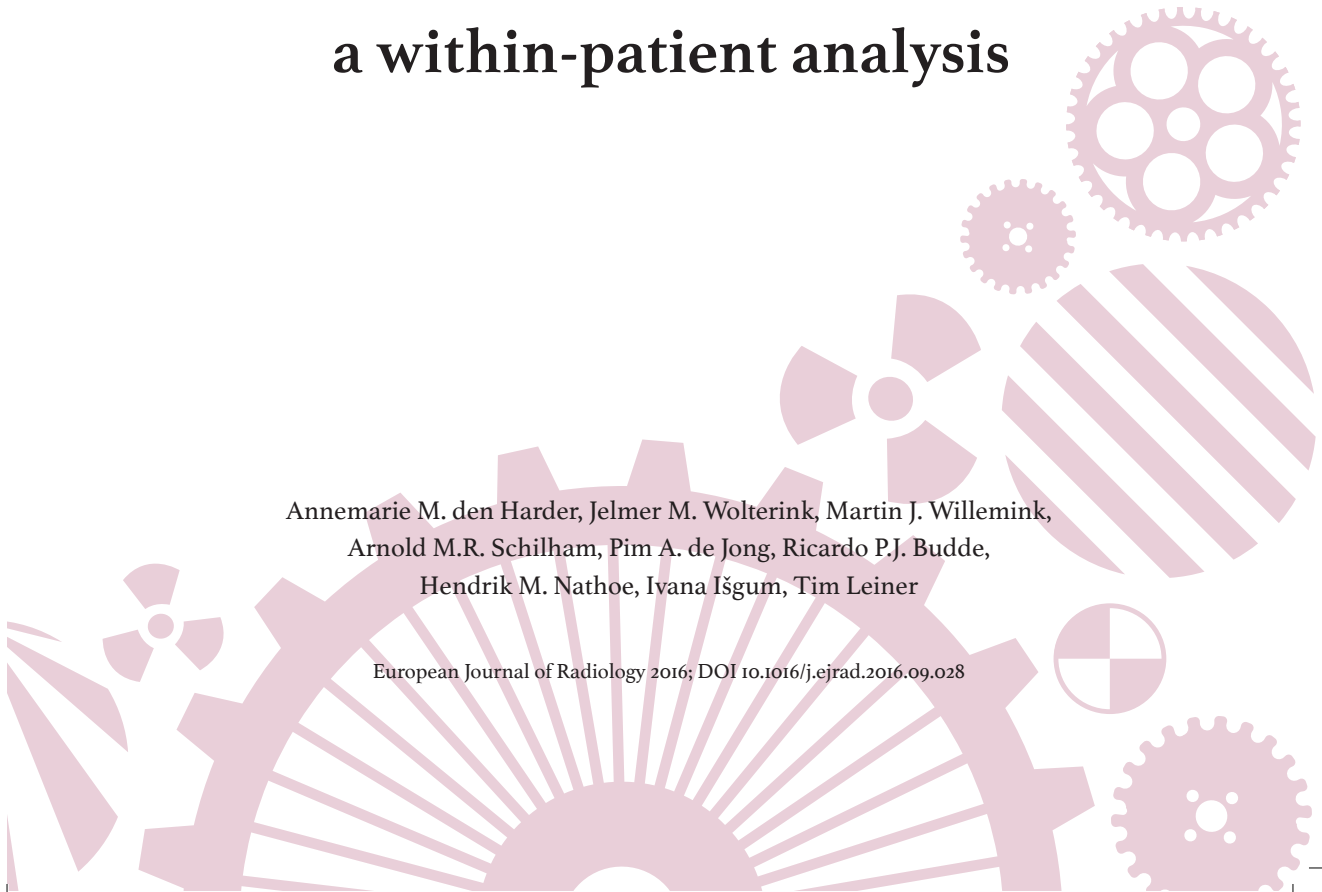
# Chapter 1.4

## *Part I Cardiac*

### **Submillisievert coronary calcium quantification using model-based iterative reconstruction: a within-patient analysis**

Annemarie M. den Harder, Jelmer M. Wolterink, Martin J. Willemink,  
Arnold M.R. Schilham, Pim A. de Jong, Ricardo P.J. Budde,  
Hendrik M. Nathoe, Ivana Išgum, Tim Leiner

European Journal of Radiology 2016; DOI 10.1016/j.ejrad.2016.09.028



## Abstract

### *Purpose*

To determine the effect of model-based iterative reconstruction (IR) on coronary calcium quantification using different submillisievert CT acquisition protocols.

### *Methods*

Twenty-eight patients received a clinically indicated non contrast-enhanced cardiac CT. After the routine dose acquisition, low-dose acquisitions were performed with 60%, 40% and 20% of the routine dose mAs. Images were reconstructed with filtered back projection (FBP), hybrid IR (HIR) and model-based IR (MIR) and Agatston scores, calcium volumes and calcium mass scores were determined.

### *Results*

Effective dose was 0.9, 0.5, 0.4 and 0.2 mSv, respectively. At 0.5 and 0.4 mSv, differences in Agatston scores with both HIR and MIR compared to FBP at routine dose were small (-0.1 to -2.9%), while at 0.2 mSv, differences in Agatston scores of -12.6 to -14.6% occurred. Reclassification of risk category at reduced dose levels was more frequent with MIR (21 – 25%) than with HIR (18%).

### *Conclusions*

Radiation dose for coronary calcium scoring can be safely reduced to 0.4 mSv using both HIR and MIR, while FBP is not feasible at these dose levels due to excessive noise. Further dose reduction can lead to an underestimation in Agatston score and subsequent reclassification to lower risk categories. Mass scores were unaffected by dose reductions.

## Introduction

Recent guidelines recommend coronary calcium scoring even for asymptomatic adults at intermediate risk [1]. It is expected that this will lead to an increase in the number of acquired non contrast-enhanced coronary CT exams for calcium scoring. Consequently, radiation dose reduction will gain importance since there are growing concerns about radiation-induced malignancies [2]. To reduce radiation exposure, several techniques have been developed including iterative reconstruction (IR) [3]. IR is an alternative to the commonly used reconstruction technique filtered back projection (FBP). IR reduces noise thereby making scanning at reduced dose possible. IR was first described in the 1970s, however due to heavy computational requirements it was only used in nuclear medicine. Recently, IR has been reintroduced and dose reductions up to 76% have been reported using IR in coronary CT exams [3]. There are two distinct types of IR algorithms, namely hybrid and model-based algorithms. Most clinically available IR algorithms are hybrid, which means that they are not fully iterative reconstructions, but FBP reconstructions combined with advanced noise reduction in the image domain. In contrast, model-based IR algorithms are fully iterative and are expected to allow even greater reductions in radiation dose. However, since only two model-based IR algorithms are currently commercially available, the achievable dose reduction and effect of model-based IR on coronary artery calcium scoring is still unclear. To the best of our best knowledge only two studies were performed investigating this effect, namely an ex vivo study [4] and a patient study [5]. Both studies reported a decrease in noise, but also a decrease in calcium scores compared to hybrid IR. Several dose levels were investigated in the ex vivo study [4] while the patient study [5] only used one dose level. In the current study we present the results of the first patient study investigating the effect of various dose reduction levels and model-based IR on coronary calcium scoring using a within-patient analysis.

## Materials and methods

This prospective monocenter study was approved by our local institutional review board and written informed consent was obtained from all participants. The CT protocol has previously been described in detail by Willeminck et al. [6]. Twenty-eight patients aged 50 years or older and scheduled for a clinically indicated cardiac CT were included. No additional exclusion criteria were applied besides age. Patients were included between January 2014 and August 2014.

*CT protocol and image reconstruction*

A 256-slice CT system (Brilliance iCT, software version 4.1, Philips Healthcare, Best, The Netherlands) was used for all image acquisitions. For each patient the mean heart rate, weight and length were recorded. A scout image was made, after which routine image acquisition was followed by three acquisitions at reduced radiation dose levels. All acquisitions were performed with the same scan length, which ranged from the tracheal bifurcation to the inferior surface of the heart. Patients with a heart rate > 70 beats per minute received beta-blockers prior to imaging. If the heart rate was regular, prospective ECG-triggering with the step-and-shoot technique was used with image acquisition during the mid-diastolic phase. If the heart rate was irregular the image acquisition was performed during the systolic phase with the step-and-shoot technique. No contrast was administered.

Tube voltage was 120 kV for all acquisitions. Tube current was 50, 30, 20 and 10 mAs for patients < 80 kilogram and 60, 36, 24 and 12 mAs for patients ≥ 80 kilogram, respectively. Thereby, the radiation dose was reduced with 40, 60 and 80% compared to the dose of the routine protocol. Dose-length-product (DLP) and volumetric CT dose index (CTDI<sub>vol</sub>) were recorded for each scan. The effective dose was defined as the DLP times the conversion factor for the chest (0.0145 mSv/(mGy\*cm)) [7]. A matrix size of 512 x 512 pixels was used and images were reconstructed with a slice thickness of 3 mm and a reconstruction increment of 1.5 mm.

We have previously investigated the effect of hybrid IR (iDose<sup>4</sup> level 1, 4 and 7, Philips Healthcare, Best, The Netherlands) using on-site reconstructed data [6]. In the current study the effect of model-based IR (IMR level 1, 2 and 3, Philips Healthcare, Best, The Netherlands) was investigated. For FBP and iDose the routinely used kernel XCA was selected while for IMR the cardiac routine kernel was chosen. The IMR reconstructions, as well as a FBP and an iDose<sup>4</sup> level 4 reconstruction for reference, were made off-site which enabled us to use the most recent software version (R11b) and settings. This software version is currently commercially available. In both iDose<sup>4</sup> and IMR, a higher level implies more noise reduction. iDose<sup>4</sup> has seven levels of noise reduction, while IMR has three levels.

### *Calcium score*

Coronary calcium scores were obtained semi-automatically using in-house-developed validated software (iX Viewer, Image Sciences Institute, Utrecht, The Netherlands) [8]. The software applied a threshold of 130 Hounsfield units for calcium and the user selected 3D-connected voxels above this threshold representing coronary artery calcifications with a single mouse click. Subsequently, the Agatston score, calcification volume score, calcification mass equivalent score and the number of calcifications were quantified by the software. The mass equivalent score was computed as the product of the mean attenuation in the lesion and the volume of the lesion [9]. Patients were classified to a risk group based on the Agatston score, namely normal (0), low (1–10), low-intermediate (11–100), intermediate (101–400) or high (> 400) risk [10].

### *Statistical analysis*

SPSS (version 20.0, IBM, Chicago, USA) was used for statistical analysis. Calcium scores in the FBP reconstruction at routine dose were considered the reference standard. The Friedman test was used to compare data to this reference standard, with a significance level set at a p-value below 0.05. Post-hoc analyses were performed using the Wilcoxon signed rank test with a Bonferroni corrected p-value of 0.003 (0.05 divided by 16 comparisons). In cases where excessive noise hampered the interpretability of the images, the reconstructions were excluded from further analysis. The difference in Agatston score, volume and mass score compared to the reference standard was also investigated using Bland-Altman plots and by calculating the percentage difference compared to the reference standard. Data are presented as medians with interquartiles unless stated otherwise.

## **Results**

### *Patients*

In total 28 patients (7 females) were included. Median age was 55 (52 – 56) years. In 10 patients the < 80 kg protocol was used and in 18 patients the ≥ 80 kg protocol. Median heart rate was 59 (53 – 63) beats per minute. Body mass index was 27 (25 – 30) kg/m<sup>2</sup>. Dose characteristics are provided in *Table 1*. The effective dose with the routine protocol was 0.9 mSv and decreased to 0.5, 0.4 and 0.2 mSv, respectively at reduced dose levels.

**Table 1** – Dose characteristics. Values are presented as median (interquartiles).

	Routine dose	60% dose	40% dose	20% dose
CTDIvol (mGy)	4.8 (4.1 – 4.9)	2.9 (2.5 – 3.0)	1.9 (1.7 – 2.0)	1.0 (0.8 – 1.0)
DLP (mGy*cm)	61.5 (51.2 – 61.5)	36.8 (32.2 – 36.9)	24.6 (21.5 – 24.7)	12.3 (10.7 – 12.3)
Effective dose (mSv)	0.9 (0.7 – 0.9)	0.5 (0.5 – 0.5)	0.4 (0.3 – 0.4)	0.2 (0.2 – 0.2)

CTDIvol Volume computed tomography dose index; DLP Dose length product

### Agatston score

An overview of the Agatston scores, number of calcifications, calcium volume and calcium mass score is provided in *Table 2*. Excessive noise reduced the interpretability of reconstructions. Hence, five FBP reconstructions at 40% dose, and eight FBP and one iDose<sup>4</sup> level 4 reconstruction at 20% dose were not interpretable. These reconstructions were excluded from further analysis. The median reference Agatston score at routine dose reconstructed with FBP for all patients was 28.0 (2.1 – 193.0). Six patients had a reference Agatston score of zero. An example of the difference in image appearance among FBP, iDose<sup>4</sup> and IMR is shown in *Figure 1*.

At 60% dose, there were no significant differences in Agatston scores between the reference standard and both iDose<sup>4</sup> and IMR. The relative differences varied from -1.6 to -2.9% for the different reconstructions (*Figure 2*). However, at 40% dose IMR level 2 yielded a significant reduction in Agatston scores. Furthermore, at 20% the Agatston score was significantly lower ( $p=0.001$ ) at all IMR levels compared to the reference score, with relative differences up to -14.6% (*Figure 3*). Bland-Altman plots are provided online [11]. The mean difference between measurements is relatively small at routine dose and 60% dose, while differences increase with IMR at the two lowest dose levels. Three patients had an Agatston score between 1 and 10 at reference dose while a zero score was found with iterative reconstruction which resulted in differences of 100%. The largest percentages of difference were found in patients with low Agatston scores, since a small difference in Agatston score in these patients result in a large percentage difference at low scores.

Risk reclassification in comparison with FBP at routine dose was analyzed (*Table 3, Figure 4*). Dose reduction resulted in reclassification of 18% patients with iDose<sup>4</sup> at all reduced dose levels, while with IMR 21% of the patients were reclassified at all reduced dose levels except for IMR level 1 at the lowest dose

**Table 2** – Agatston score, number of calcifications, calcium volume and calcium mass score at different dose levels. Values are provided as median (interquartiles).

	FBP	iDose <sup>4</sup> level 4	IMR level 1	IMR level 2	IMR level 3
<b>Routine dose</b>					
Agatston score	28.0 (2.1 – 193.0)	26.6 (2.6 – 190.6)*	27.5 (1.3 – 193.5)	27.1 (1.2 – 192.9)	26.0 (1.2 – 192.1)
Number of calcifications	2.5 (1.0 – 8.8)	2.0 (0.7 – 7.8)	2.0 (0.3 – 7.8)	2.0 (0.3 – 7.8)	2.0 (0.3 – 7.8)
Volume (mm <sup>3</sup> )	27.2 (4.6 – 161.0)	23.0 (1.8 – 159.2)*	25.3 (1.8 – 164.3)	23.7 (1.8 – 163.6)	22.2 (1.8 – 163.3)
Mass score	7.1 (0.7 – 60.2)	6.3 (1.2 – 60.1)*	8.2 (0.4 – 69.9)	8.0 (0.4 – 70.0)	7.9 (0.4 – 70.1)
<b>60% dose</b>					
Agatston score	23.7 (0.4 – 197.5)	24.4 (1.0 – 193.8)	22.7 (1.2 – 188.4)	22.6 (0.5 – 186.5)	23.6 (0.5 – 186.7)
Number of calcifications	2.0 (1.0 – 8.8)	2.5 (0.3 – 8.0)	1.5 (0.3 – 7.0)	1.5 (0.3 – 7.0)	2.0 (0.3 – 7.0)
Volume (mm <sup>3</sup> )	22.3 (1.3 – 160.6)	21.4 (1.5 – 157.3)	18.7 (1.8 – 154.1)	18.6 (1.6 – 153.8)	18.8 (1.5 – 153.7)
Mass score	5.5 (0.5 – 61.5)	5.8 (0.3 – 61.0)	6.5 (0.4 – 69.7)	6.6 (0.2 – 69.8)	6.7 (0.2 – 70.0)
<b>40% dose</b>					
Agatston score		26.9 (0.0 – 230.1)	24.0 (0.0 – 198.1)	22.2 (0.0 – 199.1)*	21.4 (0.0 – 197.0)
Number of calcifications	5 reconstructions	2.0 (0.0 – 7.8)	2.0 (0.0 – 8.0)	2.0 (0.0 – 7.0)	2.0 (0.0 – 7.0)
Volume (mm <sup>3</sup> )	not interpretable	26.2 (0.0 – 291.2)	20.2 (0.0 – 164.7)*	14.7 (0.0 – 164.2)*	19.7 (0.0 – 162.2)*
Mass score		6.5 (0.0 – 70.8)	7.3 (0.0 – 87.0)	4.9 (0.0 – 72.1)	6.5 (0.0 – 72.0)
<b>20% dose</b>					
Agatston score			17.1 (0.0 – 183.3)*	16.0 (0.0 – 181.6)*	16.9 (0.0 – 177.6)*
Number of calcifications	8 reconstructions not interpretable	1 reconstruction	2.0 (0.0 – 6.8)*	1.0 (0.0 – 6.8)*	1.5 (0.0 – 5.5)*
Volume (mm <sup>3</sup> )	interpretable	not interpretable	17.3 (0.0 – 161.6)*	16.8 (0.0 – 158.6)*	16.8 (0.0 – 154.7)*
Mass score			4.8 (0.0 – 66.5)	4.1 (0.0 – 64.5)	4.0 (0.0 – 62.3)

\*Statistical significant difference compared to FBP at routine dose with a Bonferroni-corrected p-value of 0.003. FBP Filtered Back Projection, IMR Iterative Model Reconstruction

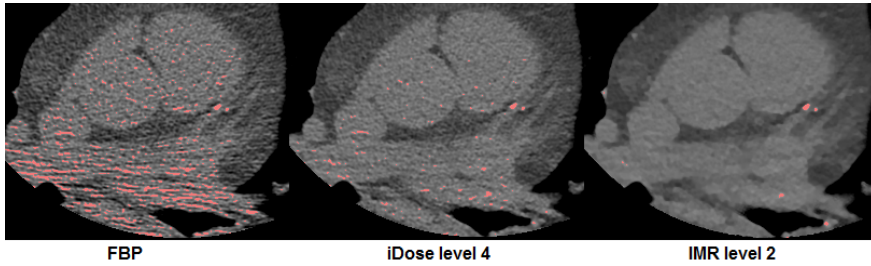


Figure 1 – Fifty-year-old male patient (heart rate 64 beats/minute) with two calcifications in the left anterior descending coronary artery. CT-acquisition at routine dose reconstructed with FBP, iDose<sup>4</sup> level 4 and IMR level 2. Note the decrease in noise with iDose<sup>4</sup> and especially with IMR compared to FBP. The calcium score was 26, 23 and 23 with FBP, iDose<sup>4</sup> and IMR, respectively.

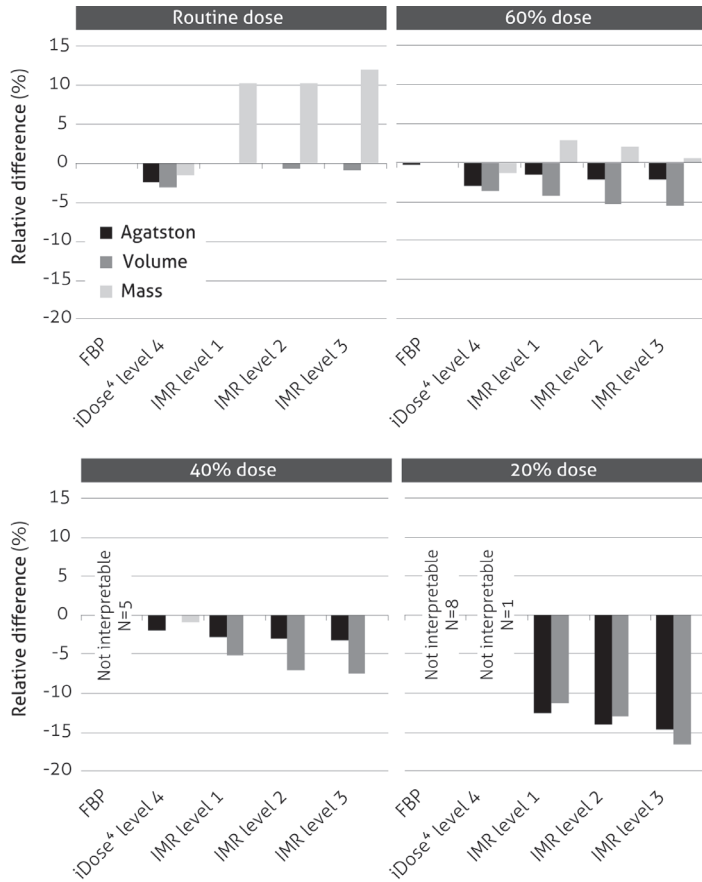
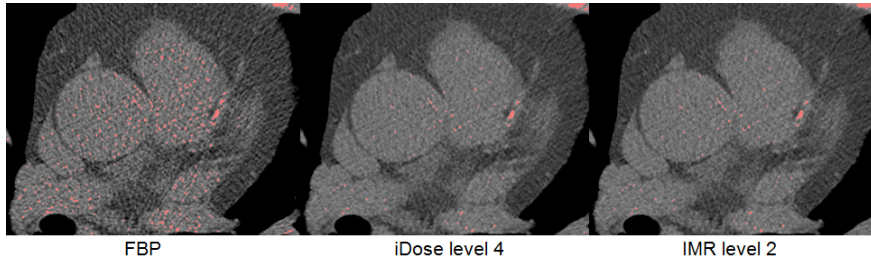
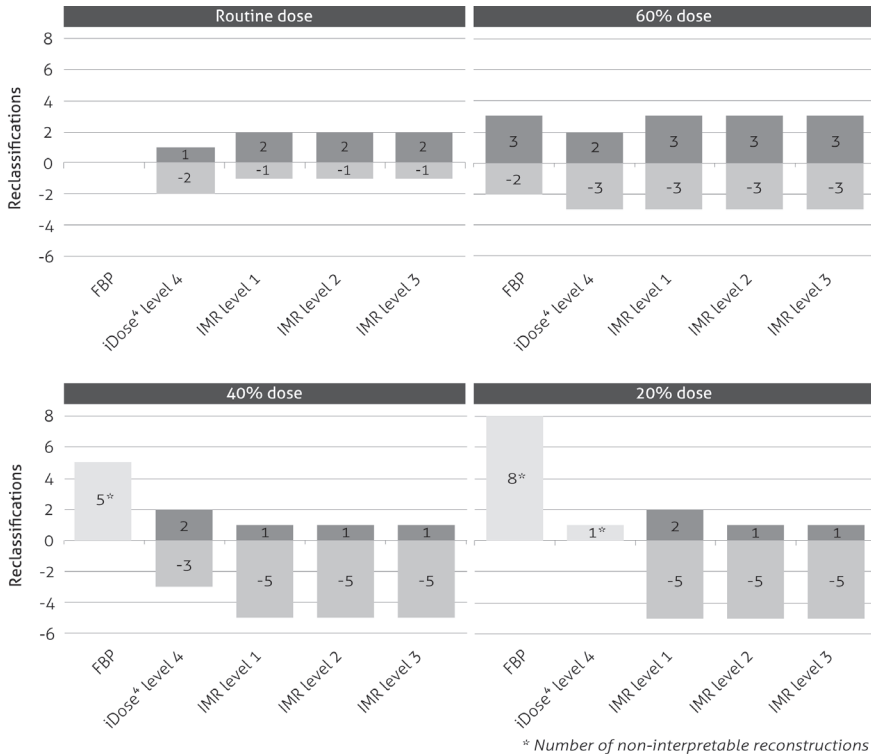


Figure 2 – Relative difference in Agatston score, volume and mass score compared to FBP at routine dose.



**Figure 3** – Fifty-five year old male (heart rate 62 beats/minute). Example of an acquisition acquired at routine dose reconstructed with FBP, iDose<sup>4</sup> level 4 and IMR level 2. The routine dose reconstructed with FBP results in a lot of noise leading to an overestimation of the calcium score. The calcium score was 48, 36 and 37 with FBP, iDose<sup>4</sup> and IMR, respectively.



**Figure 4** – Number of patients reclassified for each reconstruction at different dose levels. A positive number means reclassification to a higher risk category while a negative number means reclassification to a lower risk category.

Table 3 – Distribution of patients over the different risk categories

	Normal (0)	Low (1 – 10)	Low – Intermediate (11 – 100)	Intermediate (101 – 400)	High (>400)
<b>Routine dose</b>					
FBP	6	4	10	4	4
iDose <sup>4</sup> level 4	6	4	10	5	3
IMR level 1	7	3	9	4	5
IMR level 2	7	3	9	4	5
IMR level 3	7	3	9	4	5
<b>60% dose</b>					
FBP	6	5	8	4	5
iDose <sup>4</sup> level 4	7	3	9	6	3
IMR level 1	7	3	9	5	4
IMR level 2	7	3	9	5	4
IMR level 3	7	3	9	5	4
<b>40% dose</b>					
iDose <sup>4</sup> level 4	8	2	9	5	4
IMR level 1	9	2	8	6	3
IMR level 2	9	2	8	6	3
IMR level 3	9	2	8	6	3
<b>20% dose</b>					
IMR level 1	8	4	6	7	3
IMR level 2	8	4	7	6	3
IMR level 3	8	4	7	6	3

(20%) which resulted in a reclassification rate of 25%. Although there was a trend towards lower Agatston scores with iDose<sup>4</sup>, patients were both reclassified to higher and lower risk categories with iDose<sup>4</sup>. With IMR patients were mainly reclassified to a lower risk category. One patient had a score of zero at routine dose (all reconstructions) while at 60% reduced dose calcifications were visible (all reconstructions). This was most likely due to interscan variation. Three patients had an Agatston score between 1 and 10 at reference dose while iterative reconstruction resulted in zero scores leading to false negatives (*Figure 5*). No patients were reclassified more than one risk category.

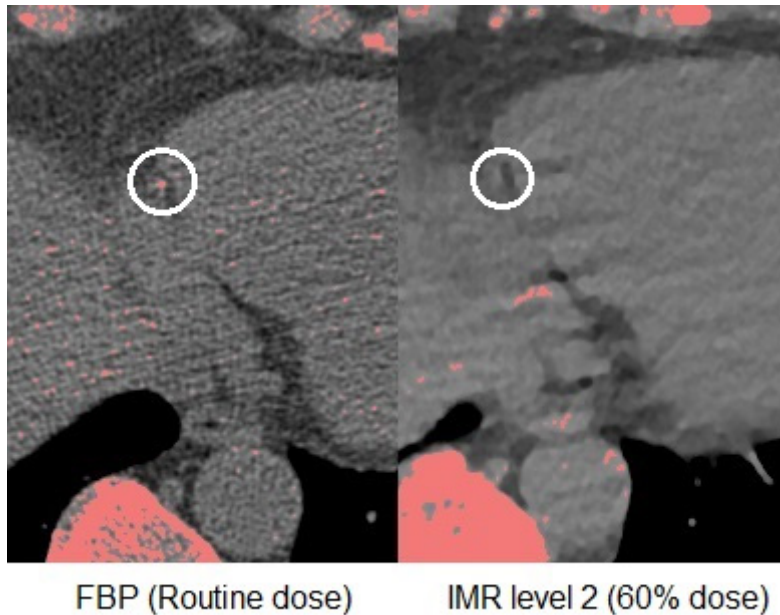


Figure 5 – Example of patient with a calcification in the right coronary artery on routine dose, which was not visible on all reduced dose acquisitions, possibly due to interscan variation, leading to a false negative score.

#### *Calcification volume, mass score and number of calcifications*

Median calcification volume was 27.2 (4.6 – 161.0) mm<sup>3</sup> at routine dose reconstructed with FBP. At 60% dose, IR did not affect volume measurements while at 40% and 20% dose the volume was significantly lower with IMR. Differences of -5.1% to -7.4% occurred at 40% dose while 20% resulted in larger differences of -11.2% to -16.5%. Median calcification mass score was 7.1 (0.7 – 60.2) at the reference scan. There were no significant differences in mass score at reduced dose levels (Bonferroni corrected p-value of 0.003). Bland-Altman plots are provided online [11]. In agreement with the Bland-Altman plots for Agatston scores, large percentages of difference were found in patients with low volume and mass scores while the higher volume and mass scores were less affected by dose reduction and image reconstruction.

The median number of calcifications was 2.5 (1.0 – 8.8) with FBP at routine dose. There were no significant differences in the number of calcifications at 60% and 40% dose compared to FBP at routine dose. At the lowest dose level (20% of

routine dose) the number of calcifications was significantly lower namely 2.0 (0.0 – 6.8,  $p=0.001$ ), 1.0 (0.0 – 6.8,  $p=0.001$ ) and 1.5 (0.0 – 5.5,  $p=0.001$ ) for IMR levels 1, 2 and 3, respectively.

## Discussion

This study showed that coronary calcium scoring at dose levels reduced to 0.4 mSv does not lead to significant differences in Agatston scores when using hybrid IR and model-based IR. Although differences in Agatston scores were small and non-significant, reclassifications were frequent with both hybrid and model-based IR.

According to guidelines of the American College of Cardiology and the American Heart Association, coronary calcium scoring should be considered in asymptomatic adults at intermediate risk of cardiovascular disease as well as patients with atypical cardiac symptoms [1]. This concerns over 40 million Americans, potentially leading to a tremendous increase in the number of acquired cardiac CTs and a subsequent increase in radiation exposure [12]. The potential increase in the number of cardiac CTs has led to concerns about the associated increase in radiation dose, and hence, dose reduction techniques are being explored. Iterative reconstruction is a promising technique that has enabled a decrease of radiation dose of up to 76% for different body parts [3]. Several studies have investigated the effects of dose reduction and IR on coronary calcium scoring, with mixed results (*Table 4*). While a number of studies reported no effect of dose reduction and IR on coronary calcium scoring [13-18], most studies reported a significant decrease in the Agatston score while using IR [4,5,12,15,19-23]. This decrease was not limited to an IR algorithm of a single vendor, but was observed with IR algorithms of all four major CT vendors. This is important since differences between CT scanners lead to substantial differences in calcium scores which can result in reclassifications in up to 6.5% of patients [24]. Differences in calcium scores caused by reconstruction algorithms can possibly be solved with calibration factors, in order to get similar scores as in the original protocol on which risk classification is based. However, those factors are not currently available and determination of such calibration factors would likely require prospective studies with larger sample sizes than in studies performed thus far. Furthermore, the decrease in calcium score is not always clinically relevant. Hecht et al. [12] performed one of the largest patient studies using dose levels of 0.8 and 0.4 mSv and reported a significant decrease

in Agatston scores but also found an excellent agreement in risk classification between FBP and IR and therefore concluded that the significant differences in Agatston scores were not clinically relevant. However, Gebhard and colleagues [21] reported a decrease in cardiovascular risk based on IR calcium measurements using a single dose level of 0.8 mSv, and studies performed by Kurata et al. [22] and Van Osch and colleagues [20] using 0.9 and 0.6 mSv respectively reported several false negative scores with IR.

The current study is the first within-patient study investigating the effect of model-based IR on coronary calcium scoring at multiple reduced dose levels. A recent study by Szilveszter et al. [5] investigated the effect of both iDose<sup>4</sup> and IMR on coronary artery calcification in 63 patients at a single dose level of 0.5 mSv. A significant decrease in calcium score of -7.3% was reported using model-based IR, resulting in reclassifications in 10% of patients. These patients were all reclassified to a lower risk group. This percentage is comparable to our study where 11% of the patients were reclassified at routine dose with model-based IR. However, in our study reclassifications to a higher risk group also occurred. This might be explained by the higher median Agatston score in the study by Szilveszter and colleagues (Agatston score 148) compared to the current study (Agatston score 28). Patients with lower Agatston scores are more likely to be reclassified, as the cutoff points between low risk categories are closer to each other. In a previous *ex vivo* study where we investigated the effect of hybrid and model-based IR on calcium scoring, we found a significant decrease in Agatston scores with model-based IR [4]. However, the effect on risk reclassifications was small. In that study, like in the study by Szilveszter and colleagues, the median Agatston score was relatively high (397 Agatston units). In our study, the number of reclassifications increased at reduced dose levels. These differences can be partly explained by inter-scan variation, which has been reported to be approximately 20% [25]. Relative variability increases with low calcium scores, as was the case in the current study. Furthermore, motion artifacts might have resulted in variation between acquisitions. However, several studies investigating the effect of IR on a single dose acquisition also reported a decrease in Agatston scores, which cannot be explained by inter-scan variation [19-22]. Furthermore, Dey et al. [26] investigated the effect of radiation dose reduction without the use of IR and found no effect of dose reduction on coronary calcium scores. However, in that study higher dose levels were used of 1.7 and 1.0 mSv. In our study we used FBP at routine dose as a reference standard since this is currently used

Table 4 – Overview of studies investigating the effect of IR on coronary calcium scoring. In studies investigating multiple dose levels, routine dose reconstructed with FBP was compared with reduced dose reconstructed with IR.

Author	Study	No	IR	mAs	DLP (mGy*cm)	ED (mSv)
Tatsugami [13]	Phantom (static)	NA	AIDR 3D	150, 100, 70, 50, 40 mAs	Not reported	Not reported
	Patients	54	AIDR 3D	315, 104 mAs	157, 50	2.2, 0.7
Obmann[19]	Patients	68	iDose	64 mAs	74	1.0
Van Osch [20]	Patients	112	ASIR	125 mAs	41	0.6
Funabashi [14]	Phantom (moving)	NA	AIDR 3D	500, 100, 50 mAs	Not reported	Not reported
Gebhard [21]	Patients	50	ASIR	200 mAs	58	0.8
Willemink [15]	Ex vivo	15	iDose	259, 189, 118, 47 mAs	Not reported	Not reported
		15	AIDR 3D	160, 120, 70, 30 mAs	Not reported	Not reported
		15	ASIR	220, 160, 105, 45 mAs	Not reported	Not reported
		15	SAFIRE	252, 184, 116, 48 mAs	Not reported	Not reported
Schindler [16]	Phantom (moving)	NA	IRIS, SAFIRE	80 mAs	Not reported	Not reported
	Patients	110	IRIS, SAFIRE	80 mAs	73	1.0
Kurata [22]	Patients	70	SAFIRE	80 mAs	61	0.9
Murazaki [17]	Phantom (static)	NA	iDose	50, 25, 20, 15 mAs	Not reported	Not reported
Den Harder [4]	Ex vivo	15	iDose, IMR	259, 189, 118, 47 mAs	Not reported	Not reported
Blobel [23]	Phantom (static)	NA	AIDR 3D	80, 40 mAs	Not reported	1.1, 0.2
Matsuura [18]	Patients	77	iDose	364, 73 mAs	86, 17	1.2, 0.2
Hecht [12]	Patients	102	iDose	30-80, 15-40 mAs	54, 27	0.8, 0.4
Szilveszter [5]	Patients	63	iDose, IMR	30 mAs	32	0.5

NA not assessed, NR not reported

CTDIvol (mGy)	Agatston	Mass	Volume
Not reported	No significant differences.	No significant differences.	No significant differences.
Not reported	No significant differences, absolute difference 16%.	No significant differences, absolute difference 12%.	No significant differences, absolute difference 13%.
5.3	Significant decrease with IR of 3 – 13%.	Not assessed.	Not assessed.
Not reported	Significant decrease with IR.	Decrease with IR.	Decrease with IR.
Not reported	No significant differences.	Not assessed.	Not assessed.
Not reported	Significant decrease with IR of 6 – 22%.	No significant differences.	Significant decrease with IR of 4 – 19%.
4.1, 3.0, 1.9, 0.8	No significant differences.	No significant differences.	No significant differences.
4.2, 3.1, 1.8, 0.8	No significant differences.	Significant decrease at reduced dose with IR.	No significant differences.
4.1, 3.0, 1.9, 0.8	Significant decrease at reduced dose with IR.	No significant differences.	Significant decrease at reduced dose with IR.
4.1, 3.0, 1.9, 0.8	No significant differences.	No significant differences.	No significant differences.
Not reported	No significant differences.	Not assessed.	Not assessed.
4.5	No significant differences.	Not assessed.	Not assessed.
Not reported	Significant decrease with IR.	Significant decrease with IR.	Significant decrease with IR.
3.5, 1.8, 1.4, 1.1	No significant differences.	No significant differences.	Not assessed.
4.1, 3.0, 1.9, 0.8	Significant decrease at reduced dose with IR.	No significant differences.	Significant decrease at reduced dose with IR.
14.5/7.5, 2.6/1.5	Significant decrease with IR.	Not assessed.	Not assessed.
6.1, 0.3	No significant differences.	No significant differences.	No significant differences.
Not reported	Significant decrease at reduced dose with IR.	No significant differences.	Significant decrease at reduced dose with IR.
Not reported	Significant decrease at reduced dose with IR.	Not assessed	Significant decrease at reduced dose with IR.

in clinical practice. However, image noise and artefact superimposition could have led to an overestimation of the true calcium load on the reference scan [19]. Model-based IR algorithms lead to a reduction in image noise, which results in a change of pixel HU-values. Since the HU-values determine whether pixels are considered as calcium, noise can subsequently affect calcium scores. Noise reduction can in this way lead to lower calcium scores [22]. Therefore, Blobel and colleagues [23] proposed a correction factor to correct for the systematical underestimation in calcium scores with IR.

In the current study a tube voltage of 120 kV was used. Lowering the tube voltage can lead to a substantial lower radiation dose, however most literature regarding coronary risk stratification is based on 120 kV acquisitions. A substantial overestimation of the coronary calcium score has been reported at lower kV levels, therefore only the tube current was lowered in the current study [27].

Coronary calcium scoring is performed using a non-contrast acquisition. Dual-energy CT offers the possibility to derive virtually non-contrast images from contrast-enhanced acquisition. First results have shown good correlation between the calcium score from virtually non-contrast images and true non-contrast images. This offers the opportunity to further reduce radiation dose by abandoning the non-contrast acquisition [28,29].

In our study the calcification mass score remained constant at all dose levels with all reconstructions. This is in line with previous studies reporting a decrease in Agatston scores with unaffected mass scores [4,12,21]. We also investigated the number of calcifications that decreased at the lowest dose level with IR. Williams et al. [30] investigated the prognostic value of the number of calcifications and reported that mortality rates increase proportionally with the number of calcifications, although its added value to the Agatston score was minimal.

This study has several limitations. First, a small number of patients were included because the patients were exposed to higher radiation doses due to multiple CT acquisitions. Since this concerned a pilot study, no sample size calculation was performed. However, we feel that the current study is not lacking power due to the within-patient design in which every patient underwent four acquisitions at different dose levels. Second, the results of this study may not extend to IR algorithms from other vendors since studies have shown differences between vendors. Third, calcium scores were measured by a single observer. However, observer agreement for coronary calcium scoring has shown to be excellent [31]. Fourth, the observer was not blinded to the reconstruction technique, but since

IR images have a different image appearance observers cannot be completely blinded.

In conclusion, radiation dose for coronary calcium scoring can be safely reduced to 0.4 mSv using both hybrid and model-based iterative reconstruction. A further decrease in dose can lead to an underestimation in Agatston scores and subsequent reclassification to lower risk categories.

## References

- [1] Greenland P, Alpert JS, Beller GA, et al., 2010 ACCF/AHA guideline for assessment of cardiovascular risk in asymptomatic adults: a report of the American College of Cardiology Foundation/American Heart Association Task Force on Practice Guidelines. *J Am Coll Cardiol* 2010;56(25):e50-103.
- [2] Brenner DJ, Hall EJ, Computed tomography--an increasing source of radiation exposure. *N Engl J Med* 2007;357(22):2277-84.
- [3] Willemink MJ, Leiner T, de Jong PA, et al., Iterative reconstruction techniques for computed tomography part 2: initial results in dose reduction and image quality. *Eur Radiol* 2013;23(6):1632-42.
- [4] den Harder AM, Willemink MJ, Bleys RL, et al., Dose reduction for coronary calcium scoring with hybrid and model-based iterative reconstruction: an ex vivo study. *Int J Cardiovasc Imaging* 2014;30(6):1125-33.
- [5] Szilveszter B, Elzomor H, Karolyi M, et al., The effect of iterative model reconstruction on coronary artery calcium quantification. *Int J Cardiovasc Imaging* 2015.
- [6] Willemink MJ, den Harder AM, Foppen W, et al., Finding the optimal dose reduction and iterative reconstruction level for coronary calcium scoring. *Journal of cardiovascular computed tomography* 2015.
- [7] Deak PD, Smal Y, Kalender WA, Multisection CT protocols: sex- and age-specific conversion factors used to determine effective dose from dose-length product. *Radiology* 2010;257(1):158-66.
- [8] van Hamersvelt RW, Willemink MJ, Takx RA, et al., Cardiac valve calcifications on low-dose unenhanced ungated chest computed tomography: inter-observer and inter-examination reliability, agreement and variability. *Eur Radiol* 2014;24(7):1557-64.
- [9] Hoffmann U, Kwait DC, Handwerker J, Chan R, Lamuraglia G, Brady TJ, Vascular calcification in ex vivo carotid specimens: precision and accuracy of measurements with multi-detector row CT. *Radiology* 2003;229(2):375-81.
- [10] Rumberger JA, Brundage BH, Rader DJ, Kondos G, Electron beam computed tomographic coronary calcium scanning: a review and guidelines for use in asymptomatic persons. *Mayo Clin Proc* 1999;74(3):243-52.
- [11] den Harder AM, Wolterink JM, Willemink MJ, et al., Submillisievert coronary calcium quantification using model-based iterative reconstruction: A within-patient analysis. *Eur J Radiol* 2016;85(11):2152-9.
- [12] Hecht HS, de Siqueira ME, Cham M, et al., Low- vs. standard-dose coronary artery calcium scanning. *Eur Heart J Cardiovasc Imaging* 2015;16(4):358-63.

- [13] Tatsugami F, Higaki T, Fukumoto W, et al., Radiation dose reduction for coronary artery calcium scoring at 320-detector CT with adaptive iterative dose reduction 3D. *Int J Cardiovasc Imaging* 2015;31(5):1045-52.
- [14] Funabashi N, Irie R, Aiba M, et al., Adaptive-Iterative-Dose-Reduction 3D with multisector-reconstruction method in 320-slice CT may maintain accurate-measurement of the Agatston-calcium-score of severe-calcification even at higher pulsating-beats and low tube-current in vitro. *Int J Cardiol* 2013;168(1):601-3.
- [15] Willemink MJ, Takx RA, de Jong PA, et al., The impact of CT radiation dose reduction and iterative reconstruction algorithms from four different vendors on coronary calcium scoring. *Eur Radiol* 2014;24(9):2201-12.
- [16] Schindler A, Vliegenthart R, Schoepf UJ, et al., Iterative image reconstruction techniques for CT coronary artery calcium quantification: comparison with traditional filtered back projection in vitro and in vivo. *Radiology* 2014;270(2):387-93.
- [17] Murazaki H, Funama Y, Hatemura M, Fujioka C, Tomiguchi S, Quantitative evaluation of calcium (content) in the coronary artery using hybrid iterative reconstruction (iDose) algorithm on low-dose 64-detector CT: comparison of iDose and filtered back projection. *Nihon Hoshasen Gijutsu Gakkai Zasshi* 2011;67(4):360-6.
- [18] Matsuura N, Urashima M, Fukumoto W, et al., Radiation dose reduction at coronary artery calcium scoring by using a low tube current technique and hybrid iterative reconstruction. *J Comput Assist Tomogr* 2015;39(1):119-24.
- [19] Obmann VC, Klink T, Heverhagen JT, et al., Impact of Hybrid Iterative Reconstruction on Agatston Coronary Artery Calcium Scores in Comparison to Filtered Back Projection in Native Cardiac CT. *Rofo* 2015;187(5):372-9.
- [20] van Osch JA, Mouden M, van Dalen JA, et al., Influence of iterative image reconstruction on CT-based calcium score measurements. *Int J Cardiovasc Imaging* 2014;30(5):961-7.
- [21] Gebhard C, Fiechter M, Fuchs TA, et al., Coronary artery calcium scoring: Influence of adaptive statistical iterative reconstruction using 64-MDCT. *Int J Cardiol* 2012.
- [22] Kurata A, Dharampal A, Dedic A, et al., Impact of iterative reconstruction on CT coronary calcium quantification. *Eur Radiol* 2013;23(12):3246-52.
- [23] Blobel J, Mews J, Schuijff JD, Overlaet W, Determining the radiation dose reduction potential for coronary calcium scanning with computed tomography: an anthropomorphic phantom study comparing filtered backprojection and the adaptive iterative dose reduction algorithm for image reconstruction. *Invest Radiol* 2013;48(12):857-62.
- [24] Willemink MJ, Vliegenthart R, Takx RA, et al., Coronary artery calcification scoring with state-of-the-art CT scanners from different vendors has substantial effect on risk classification. *Radiology* 2014;273(3):695-702.

- [25] Lu B, Budoff MJ, Zhuang N, et al., Causes of interscan variability of coronary artery calcium measurements at electron-beam CT. *Acad Radiol* 2002;9(6):654-61.
- [26] Dey D, Nakazato R, Pimentel R, et al., Low radiation coronary calcium scoring by dual-source CT with tube current optimization based on patient body size. *J Cardiovasc Comput Tomogr* 2012;6(2):113-20.
- [27] Marwan M, Mettin C, Pflederer T, et al., Very low-dose coronary artery calcium scanning with high-pitch spiral acquisition mode: comparison between 120-kV and 100-kV tube voltage protocols. *J Cardiovasc Comput Tomogr* 2013;7(1):32-8.
- [28] Yamada Y, Jinzaki M, Okamura T, et al., Feasibility of coronary artery calcium scoring on virtual unenhanced images derived from single-source fast kVp-switching dual-energy coronary CT angiography. *J Cardiovasc Comput Tomogr* 2014;8(5):391-400.
- [29] Song I, Yi JG, Park JH, Kim SM, Lee KS, Chung MJ, Virtual Non-Contrast CT Using Dual-Energy Spectral CT: Feasibility of Coronary Artery Calcium Scoring. *Korean J Radiol* 2016;17(3):321-9.
- [30] Williams M, Shaw LJ, Raggi P, et al., Prognostic value of number and site of calcified coronary lesions compared with the total score. *JACC Cardiovasc Imaging* 2008;1(1):61-9.
- [31] Williams MC, Golay SK, Hunter A, et al., Observer variability in the assessment of CT coronary angiography and coronary artery calcium score: substudy of the Scottish COmputed Tomography of the HEART (SCOT-HEART) trial. *Open Heart* 2015;2(1):e000234,2014-000234. eCollection 2015.





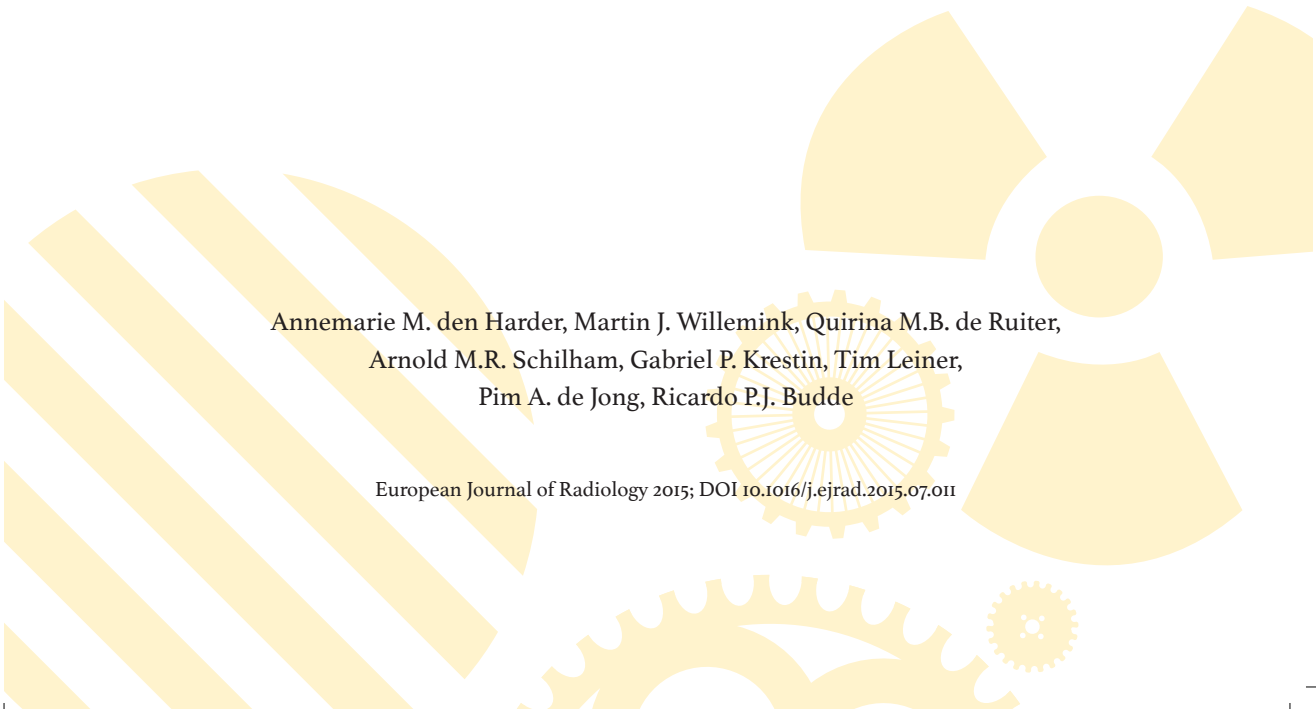
# Chapter 2.1

## *Part II Thoraco-abdominal*

### **Achievable dose reduction using iterative reconstruction for chest computed tomography: a systematic review**

Annemarie M. den Harder, Martin J. Willeminck, Quirina M.B. de Ruiter,  
Arnold M.R. Schilham, Gabriel P. Krestin, Tim Leiner,  
Pim A. de Jong, Ricardo P.J. Budde

European Journal of Radiology 2015; DOI 10.1016/j.ejrad.2015.07.011



## Abstract

### *Objectives*

Iterative reconstruction (IR) allows for dose reduction with maintained image quality in CT imaging. In this systematic review the reported effective dose reductions for chest CT and the effects on image quality are investigated.

### *Methods*

A systematic search in PubMed and EMBASE was performed. Primary outcome was the reported local reference and reduced effective dose and secondary outcome was the image quality with IR. Both non contrast-enhanced and enhanced studies comparing reference dose with reduced dose were included.

### *Results*

24 studies were included. The median number of patients per study was 66 (range 23–200) with in total 1,806 patients. The median reported local reference dose of contrast-enhanced chest CT with FBP was 2.6 (range 1.5 – 21.8) mSv. This decreased to 1.4 (range 0.4 – 7.3) mSv at reduced dose levels using IR. With non contrast-enhanced chest CT the dose decreased from 3.4 (range 0.7 – 7.8) mSv to 0.9 (range 0.1 – 4.5) mSv. Objective image quality and diagnostic confidence and acceptability remained the same or improved with IR compared to FBP in most studies while data on diagnostic accuracy was limited.

### *Conclusion*

Radiation dose can be reduced to less than 2 mSv for contrast-enhanced chest CT and non contrast-enhanced chest CT is possible at a submillisievert dose using IR algorithms.

## Introduction

The rapid increase in the number of computed tomography (CT) scans has raised concerns about the safety of CT examinations and the associated radiation exposure [1]. As lung cancer screening with chest CT is now implemented in the USA a further increase in the number of chest CT scans is anticipated [2]. To reduce radiation dose several options are available including automatic tube current and potential selection and, more recently, iterative reconstruction (IR) [3,4].

Although the concept of IR has been around for decades these techniques were not widely used due to a lack of computational power. These limitations have been overcome and all major CT vendors now have IR algorithms available for clinical use. The traditionally used CT reconstruction method, filtered back projection (FBP), is fast but leads to image deterioration when radiation dose is lowered. IR involves multiple iterations leading to improved image quality even at a reduced dose. Most IR algorithms are not fully iterative but use a combination of IR and FBP, also called hybrid IR. Two vendors developed more advanced algorithms approaching true IR, also known as model-based IR. Previously the technical principles of IR have been explained in detail [5]. A brief overview of the different available IR techniques is presented in *Table 1*. The potential of IR for dose reduction in chest CT has been investigated in a substantial number of studies. Interestingly, even chest CT examinations at a radiation dose approaching conventional chest x-rays have been reported using IR [6,7]. This may open the possibility to replace radiography with low dose CT for certain indications [8]. However, it is not clear yet to which extent the radiation dose can be reduced routinely by using IR for chest CT.

**Table 1** – Overview of different available iterative reconstruction techniques.

Abbreviation	Vendor	Full name	Type
ASIR	GE	Adaptive Statistical Iterative Reconstruction	Hybrid
MBIR-Veo	GE	Model-Based Iterative Reconstruction	Model-based
iDose	Philips	iDose	Hybrid
IMR	Philips	Iterative Model Reconstruction	Model-based
ADMIRE	Siemens	Advanced Modeled Iterative Reconstruction	Hybrid
IRIS	Siemens	Iterative Reconstruction in Image Space	Hybrid
SAFIRE	Siemens	Sinogram-Affirmed Iterative Reconstruction	Hybrid
AIDR	Toshiba	Adaptive Iterative Dose Reduction	Hybrid
AIDR 3D	Toshiba	Adaptive Iterative Dose Reduction 3D	Hybrid

Therefore the reported achievable dose reductions of studies using IR in chest CT were evaluated. Furthermore, the reported effects of dose reduction and IR on image quality were assessed.

## Material and methods

### *Search*

MEDLINE and EMBASE were systematically searched by combining synonyms for 'IR techniques' and 'CT' with English language restriction. The full search syntax is provided in the *Appendix*. Duplicates were removed and reference lists of included articles and review articles were searched for additional articles.

### *Inclusion and exclusion criteria*

Two authors screened all articles (AH and MW). In case of discrepancy consensus was reached between authors. Original research articles concerning chest CT with IR in adults investigating routine and reduced dose levels were included. All indications for chest CT were included. Ex-vivo, in-vitro, animal and pediatric studies were excluded. Studies combining chest CT with abdominal CT were excluded, because the primary outcome was the effective dose of chest CT alone. Reviews as well as case reports (<5 patients) were excluded.

### *Data extraction*

Data, including first author, journal, publication date, title, study design, participant characteristics, scan indication, reconstruction technique, type of scan, type of CT system, and reported dose and image quality measurements were extracted to a standardized sheet.

Primary outcome was the effective dose, which was defined as the dose-length product (DLP) times the conversion factor for chest CT (0.014 mSv/(mGy\*cm)) [9,10]. In case the effective dose was not provided and not computable the corresponding author was contacted. If a different conversion factor was used, the effective dose was recalculated. Secondary outcome was the influence of IR on objective and subjective image quality. This was specified as lower (i.e. deteriorated) image quality, no change in image quality or improved image quality compared to FBP. The most favorable outcome was used in case different IR levels were studied. Objective image quality is measured using signal-to-noise ratio, contrast-to-noise ratio or noise. Different methods can be used to measure subjective image quality. If the study reported that the difference in objective and/or image quality was significant between FBP and IR, this was defined as deteriorated or improved.

### Statistical analysis

SPSS (version 20.0 for Microsoft Windows) was used for statistical analyses. Correlations between effective dose and publication year were tested by Pearson's correlation test. A p-value below 0.05 was considered statistically significant.

## Results

### Study selection

In total 2,556 articles were identified. After removal of duplicates 1,616 articles were screened on title and abstract. Fifteen-hundred-eighty-six articles were excluded because the articles did not investigate IR for CT (n=1,338), did not evaluate chest CT (n=194), were not based on in-vivo data (n=16), concerned pediatric studies (n=2), studied combined chest CT with abdominal CT (n=21) or investigated only a single dose level (n=15). A flowchart is provided in *Figure 1*. Corresponding authors of seven articles were contacted because reported information about radiation dose was insufficient [11-17]. One author provided the requested dose information [17] and the remaining six articles were excluded due to insufficient information about radiation dose. Therefore ultimately 24 studies were included.

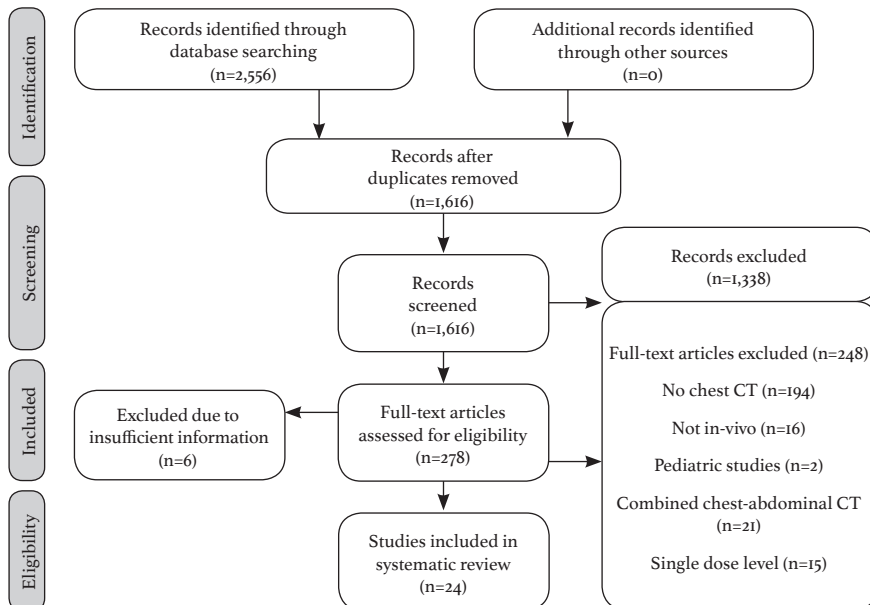


Figure 1: Flowchart

*Baseline characteristics*

Baseline characteristics are provided in *Table 2*. Patients in the included articles had a median age of 62 years (not reported in 3 studies), median BMI of 24 kg/m<sup>2</sup> (not reported in 9 studies) and 46% was female (not reported in 1 study). The median number of patients per study was 66 (range 23–200) with in total 1,806 patients. Studies were published in 2010 (n=1), 2011, (n=3), 2012 (n=6), 2013 (n=10) and 2014 (n=4). Different IR techniques were used: ASIR (n=11), SAFIRE (n=5), iDose<sup>4</sup> (n=1), IRIS (n=5), MBIR (n=6), AIDR (n=1) and AIDR 3D (n=1). Six studies used two different IR techniques namely AIDR and AIDR 3D [18] and ASIR and MBIR [6,19–22].

Fifteen studies (63%) compared imaging at a local reference dose with reduced dose imaging in the same patient. Comparison of different dose levels in the same patient was achieved by using data from only one detector of a dual source CT scanner (n=2) [23,24], using a previously made scan (n=2) [17,25], comparing the scan non contrast-enhanced scan with the contrast-enhanced scan (n=1) [26] or by making one (n=7) [6,18,19,22,27–29] two (n=2) [20,21] or four (n=1) [30] additional scans for research purposes. The indication for chest CT varied widely. Two studies solely investigated lung nodule follow-up scans and lung cancer screening scans [28,29]. Most studies included patients with different indications for chest CT like suspected pulmonary infection, oncology staging and surveillance or an abnormality on chest x-ray.

Nine studies reported the dose of contrast-enhanced CT, 13 studies of non contrast-enhanced CT and two studies [17,23] investigated both contrast-enhanced and non contrast-enhanced CT.

*Radiation dose*

The median reported local reference dose of contrast-enhanced chest CT with FBP was 2.6 (range 1.5 – 21.8) mSv. This decreased to 1.4 (range 0.4 – 7.3) mSv at reduced dose levels using IR. The median percentage of dose reduction achieved with IR was 50 (range 13 – 76)%. The relatively high local reference dose was partly caused by the study of Li et al. [31] who reported a local reference dose of 21.8 mSv. Patients included in this study had an average BMI (22 ± 1.4 kg/m<sup>2</sup>), however a relatively high tube current and voltage were used of 200 mAs and 120 kVp, respectively.

The median reported local reference dose of non contrast-enhanced chest CT with FBP was 3.4 (range 0.7 – 7.8) mSv. This decreased to 0.9 (range 0.1 – 4.5) mSv at reduced dose levels using IR. The median percentage of dose reduction

Table 2 – Baseline characteristics. \* non contrast-enhanced / contrast-enhanced.

Author	Year of publication	Number of patients	IR algorithm	Slice thickness (mm)	Indications						Image quality				Effective dose			
					Lung cancer screening / lung nodule evaluation	Pulmonary infections	Oncology (staging/surveillance)	Abnormality chest x-ray	Other indications	Contrast enhanced	Noise	CNR	SNR	Subjective image quality	Mean effective dose (mSv)	Mean effective reduced dose (mSv)	Decrease in effective dose (%)	
Baumüller S[39]	2012	60	SAFIRE	2	Y	Y	U	U	Y	N	Y	N	+	-	+	0.70	0.50	29
Chen JH[32]	2014	200	ASIR	5	Y	Y	N	N	N	N	N	N	+	-	+	2.71	0.36	87
Co S[40]	2013	100	SAFIRE	1	N	N	N	N	Y	Y	Y	Y	-	+	+	2.13	1.10	48
Gorycki T[41]	2014	125	ASIR	5	U	U	U	U	U	N	U	N	-	-	-	5.49	4.45	19
Hwang H[23]	2012	100	IRIS	1 and 5	U	U	U	U	U	B	U	B	+	-	+	1.78/2.84*	0.89/1.42*	50/50
Ichikawa Y[22]	2013	55	ASIR + MBIR	0.625	N	N	N	Y	N	N	N	N	+	-	+	5.70	1.60	72
Kalra MK[27]	2013	24	SAFIRE	2	U	U	Y	U	U	N	U	N	+	-	+	3.60	0.46	87
Katsura M[19]	2012	100	ASIR+MBIR	0.625	U	U	U	U	U	N	U	N	+	-	+	4.04	0.85	95
Katsura M[21]	2013	59	ASIR+MBIR	0.625	U	U	U	U	U	N	U	N	-	-	+	4.31	0.20	79
Li Q[31]	2013	80	iDose	1	U	Y	Y	Y	Y	Y	Y	Y	-	+	+	21.78	6.24	71
Liu W[42]	2014	72	ASIR	5	U	U	U	Y	Y	N	Y	N	-	+	+	3.03	1.18	61
May MS[24]	2014	52	IRIS	1 and 5	U	Y	Y	U	Y	Y	Y	Y	+	-	+	3.40	1.70	50
Neroladaki A[6]	2013	42	ASIR+MBIR	0.625	Y	N	N	Y	Y	N	Y	N	+	-	+	7.84	0.11	99
Pontana F[25]	2013	80	SAFIRE	1	U	U	U	U	U	Y	U	Y	-	+	+	2.29	1.08	38
Pontana F[17]	2011	80	IRIS	0.6	Y	Y	Y	N	Y	B	Y	B	+	+	+	1.94/2.48*	1.33/1.55*	31/38
Pontana F[43]	2011	32	IRIS	1	U	U	U	U	U	N	U	N	+	-	+	1.75	1.08	53



Table 2 – Baseline characteristics. \* non contrast-enhanced / contrast-enhanced.

Author	Year of publication	Number of patients	IR algorithm	Slice thickness (mm)	Indications							Image quality				Effective dose		
					Lung cancer screening / Lung nodule evaluation	Pulmonary infections	Oncology (staging/surveillance)	Abnormality chest x-ray	Other indications	Contrast enhanced	Noise	CNR	SNR	Subjective image quality	Mean effective dose (mSv)	Mean effective reduced dose (mSv)	Decrease in effective dose (%)	
Prakash P[44]	2010	152	ASIR	2.5	Y	U	Y	U	U	Y	Y	U	Y	Y	10.05	7.33	27	
Singh S[30]	2011	23	ASIR	2.5	Y	Y	Y	U	U	Y	Y	U	Y	Y	1.51	0.43	72	
Vardhanabhuti V[20]	2013	30	ASIR+MBIR	1.25	N	N	Y	N	N	Y	Y	N	Y	Y	3.70	0.90	76	
Wang H[45]	2013	87	SAFIRE	5	Y	N	Y	N	Y	Y	Y	N	Y	Y	2.57	1.28	50	
Yamada Y[18]	2012	50	AIDR+AIDR 3D	2	Y	Y	Y	Y	Y	N	Y	N	Y	Y	3.43	1.23	92	
Yamada Y[28]	2012	52	MBIR	0.625	Y	N	N	N	N	N	N	N	N	Y	2.10	0.17	64	
Yanagawa M[29]	2012	35	ASIR	0.625	Y	N	N	N	N	N	N	N	N	Y	7.18	1.78	75	
Zizka J[46]	2013	116	IRIS	1	N	N	N	N	Y	Y	Y	Y	Y	1.87	1.62	13		

Abbreviations: Y=yes, N=no, U=unknown, B=both, +=investigated, -=not investigated

achieved with IR was 72 (range 19 – 99)%. The relationship between local reference dose and reduced dose for both contrast-enhanced and non contrast-enhanced studies is shown in *Figure 2*.

There was no correlation between publication date and lowest reported dose ( $p=0.733$ , Pearson correlation  $-0.073$ ).

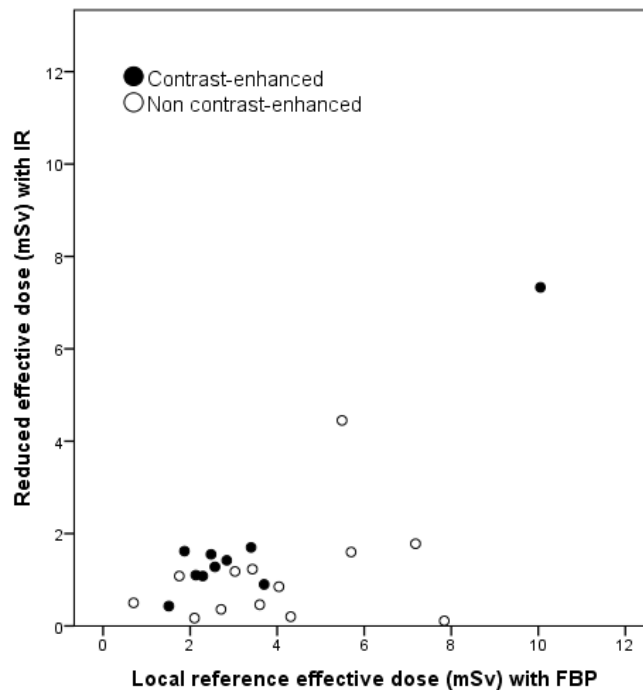


**Figure 2** – The relationship between local reference effective dose with FBP and reduced effective dose with IR. One outlier (*Li et al.*[31], local reference effective dose 21.8mSv) is left out of the figure in order to make the figure more clear.

### *Image quality*

Twenty-one studies investigated subjective image quality, mainly by reporting on diagnostic confidence and acceptability. Six studies investigated image artifacts, mostly using 4-point Likert scales. One study investigated diagnostic accuracy. Objective image quality was scored based on noise (15 studies), contrast-to-noise ratio (5 studies) and/or signal-to-noise ratio (9 studies).

At local reference dose levels IR achieved improved (5 studies, 83%) or the same (1 study, 17%) objective image quality as FBP (*Table 3*). IR at reduced dose compared to FBP at local reference dose led to worse image quality in two studies (11%), whereas image quality remained the same (5 studies, 26%) or improved in most studies (12 studies, 63%). The study of Chen et al. [32] and Li et al. [31] reported a decrease in objective image quality which both used a relatively large dose reduction of 87% and 71% respectively. At reduced dose level, objective image quality improved in all fourteen studies with IR compared to FBP. [13,20,30].

**Table 3** – Subjective and objective image quality of IR compared to FBP. Improved means that IR achieved better image quality compared to FBP.

		Local reference dose (FBP)		Low dose (FBP)	
		Subjective image quality	Objective image quality	Subjective image quality	Objective image quality
Local reference dose (IR)	Subjective image quality	Improved n=5 Equal n=2 Worse n=0			
	Objective image quality		Improved n=5 Equal n=1 Worse n=0		
Low dose (IR)	Subjective image quality	Improved n=1 Equal n=14 Worse n=3		Improved n=10 Equal n=2 Worse n=0	
	Objective image quality		Improved n=12 Equal n=5 Worse n=2		Improved n=14 Equal n=0 Worse n=0

*n=number of studies, FBP=filtered back projection, IR=iterative reconstruction.*

Subjective image quality at local reference dose improved (5 studies, 71%) or remained the same (2 studies, 29%) with IR. IR at reduced dose compared to FBP at local reference dose resulted in improved (1 study, 6%), the same (14 studies, 78%) or worse (3 studies, 17%) image quality. Two studies reporting a decrease in subjective image quality used a very low dose namely 0.36 [32] and 0.11 mSv [6]. The third study investigated radiologists' preference and reported that radiologists preferred local reference dose images reconstructed with FBP over reduced dose images reconstructed with IR [23]. At reduced dose, IR resulted in

the same (2 studies, 17%) or improved image quality (10 studies, 83%) compared to FBP. Artifacts were reported in six studies and mainly concerned pixilated and blotchy appearances with high level IR. However, IR also resulted in reduced streak artifacts. There was no difference in diagnostic accuracy between local reference dose reconstructed with FBP and IR at reduced dose levels. However, this was investigated in only one study [6].

## Discussion

This systematic review found that iterative reconstruction allows for chest CT with substantially decreased radiation dose. Mean effective dose using IR decreased by 50% to 1.4 mSv for contrast-enhanced chest CT and to submillisievert dose for non contrast-enhanced CT using IR. In almost all cases dose reduction was possible without loss of objective and subjective image quality.

Increased concerns about radiation dose have led to the development of several radiation dose reduction tools in the past years [33,34]. The most important developments were the introduction of automatic tube current and potential selection, and IR algorithms compatible with short, clinically acceptable reconstruction times.

IR is associated with several advantages and disadvantages. The most important advantage is the achievable reduction in radiation dose, which can be decreased by more than half as shown by the current systematic review. Furthermore, some algorithms can also improve low-contrast detectability and reduce streak artifacts [35]. One of the concerns of IR is the increased demand on computational power, which may lead to prolonged reconstruction times [36]. However, this does not result in a clinically important delay in image reconstruction for one of the hybrid IR algorithms [37]. Another concern is the somewhat different appearance of the images, since noise and artifacts characteristics are different with IR leading to a different image appearance [36]. This may partly be explained by the fact that radiologists are used to FBP image appearance and have to get used to the new image appearance. Despite this limitation, subjective image quality was rated as similar or improved in most studies included in this systematic review.

In this review a thorough and systematic search was performed and the effective dose was calculated in a uniform way by using the same conversion factor for each study. However, there are several limitations. First of all, the indication for a chest CT is important, since a lung cancer screening CT is typically performed at lower radiation dose compared to an oncology surveillance CT. Most articles

evaluated patients with different indications for a chest CT and did not provide the effective dose separately per indication thereby making it impossible to calculate the dose per indication. Differences in scan length, CT-system, dose optimization and BMI might explain differences in effective dose between studies. For example the study of Kligerman et al. [38] found a relatively high local reference dose of 11.50 mSv but only included obese patients.

The true capability of IR to reduce dose without loss of image quality and diagnostic accuracy is ideally studied by comparing different dose levels of a different additional acquisition in the same patient. However, this was only done in ten studies, because problems with contrast enhancement can occur and approval of the ethical committee has to be obtained due to increased radiation exposure for participating patients. Two studies performed multiple contrast-enhanced scans in the same patient. Vardhanabhuti et al. [20] made the first scan in the caudocranial direction and saved time by performing the next scan in the craniocaudal direction to avoid contrast enhancement problems. Singh et al. [30] used a shorter scan length for the additional scans to save time, which explains the low radiation dose (0.4 mSv).

This study provides the first detailed overview to which extent radiation dose can be lowered for chest CT. It is important to note that patients with interstitial lung disease have not been widely studied using chest CT with IR. Future studies should address this population, especially in light of the relative high frequency with which they undergo CT of the chest. A limitation of the current studies is that the impact of IR on diagnostic accuracy remains largely unknown. Although the majority of studies reported on diagnostic confidence and acceptability using a Likert scale, only one study investigated diagnostic accuracy and found no difference between FBP and IR [6]. This study investigated the diagnostic accuracy of pulmonary nodule detection. A further limitation of this systematic review is the large heterogeneity between studies. Therefore, we decided not to perform a meta-analysis. Most included studies investigated hybrid IR while six studies investigated more advanced model-based IR (MBIR) algorithms. MBIR is expected to decrease the radiation dose even further and the included studies investigating MBIR found that a radiation dose below 1 mSv is possible for both contrast-enhanced and non contrast-enhanced chest CT. Future research should determine the exact dose reduction with MBIR algorithms. In conclusion, a radiation dose reduction to less than 1.4 mSv is possible for contrast-enhanced CT while the dose of non contrast-enhanced chest CT can be reduced below 1 mSv. Future research should address the effect of dose reduction and IR on diagnostic accuracy.

## Appendix

### *Search syntax PubMed*

(((((iterative[Title/Abstract]) AND reconstruction[Title/Abstract])) OR (((iterative[Title/Abstract]) AND dose[Title/Abstract]) AND reduction[Title/Abstract])) OR (((((((ASIR[Title/Abstract]) OR iDose[Title/Abstract]) OR IRIS[Title/Abstract]) OR AIDR[Title/Abstract]) OR IMR[Title/Abstract]) OR MBIR[Title/Abstract]) OR Veo[Title/Abstract]) OR SAFIRE[Title/Abstract]) OR ADMIRE[Title/Abstract]))) AND (((CT [Title/Abstract] OR “Tomography, X-Ray Computed” [Mesh] OR “Cone-Beam Computed Tomography” [Mesh] OR “Four-Dimensional Computed Tomography” [Mesh] OR “Spiral Cone-Beam Computed Tomography” [Mesh] OR “Tomography Scanners, X-Ray Computed” [Mesh] OR “Tomography, Spiral Computed” [Mesh]))) OR ((computed[Title/Abstract]) AND tomography[Title/Abstract])) Filters: English

### *Search syntax EMBASE*

((((iterative:ab,ti AND reconstruction:ab, ti) OR (iterative:ab,ti AND dose:ab,ti AND reduction:ab,ti) OR (ASIR:ab,ti OR iDose:ab,ti OR IRIS:ab,ti OR AIDR:ab,ti OR IMR:ab,ti OR MBIR:ab,ti OR Veo:ab,ti OR SAFIRE:ab,ti OR ADMIRE:ab,ti)) AND ((computed:ab,ti AND tomography:ab,ti) OR (CT:ab,ti OR ‘tomography, x-ray computed’:ab,ti OR ‘cone-beam computed tomography’:ab,ti OR ‘four-dimensional computed tomography’:ab,ti OR ‘spiral cone-beam computed tomography’:ab,ti OR ‘tomography scanners, x-ray computed’:ab, ti OR ‘tomography, spiral computed’:ab,ti))) AND [english]/lim

## References

- [1] Brenner DJ, Hall EJ, Computed tomography--an increasing source of radiation exposure. *N Engl J Med* 2007;357(22):2277-84.
- [2] Field JK, Hansell DM, Duffy SW, Baldwin DR, CT screening for lung cancer: countdown to implementation. *Lancet Oncol* 2013;14(13):e591-600.
- [3] Kubo T, Ohno Y, Kauczor HU, Hatabu H, Radiation dose reduction in chest CT-Review of available options. *Eur J Radiol* 2014.
- [4] Singh S, Kalra MK, Ali Khawaja RD, et al., Radiation dose optimization and thoracic computed tomography. *Radiol Clin North Am* 2014;52(1):1-15.
- [5] Willemink MJ, de Jong PA, Leiner T, et al., Iterative reconstruction techniques for computed tomography Part 1: technical principles. *Eur Radiol* 2013;23(6):1623-31.
- [6] Neroladaki A, Botsikas D, Boudabbous S, Becker CD, Montet X, Computed tomography of the chest with model-based iterative reconstruction using a radiation exposure similar to chest X-ray examination: preliminary observations. *Eur Radiol* 2013;23(2):360-6.
- [7] Willemink MJ, de Jong PA, Pediatric chest computed tomography at a radiation dose approaching a chest radiograph. *Am J Respir Crit Care Med* 2013;188(5):626-7.
- [8] Willemink MJ, den Harder AM, de Jong PA, Leiner T, The future of the CT scan; will CT replace conventional radiography? *Ned Tijdschr Geneesk* 2014;158:A7438.
- [9] American Association of Physicists in Medicine, The measurement, reporting and management of radiation dose in CT: report of AAPM Task Group 23 of the Diagnostic Imaging Council CT Committee. 2008(Accessed June 2014).
- [10] Deak PD, Smal Y, Kalender WA, Multisection CT protocols: sex- and age-specific conversion factors used to determine effective dose from dose-length product. *Radiology* 2010;257(1):158-66.
- [11] Mueck FG, Michael L, Deak Z, et al., Upgrade to iterative image reconstruction (IR) in MDCT imaging: a clinical study for detailed parameter optimization beyond vendor recommendations using the adaptive statistical iterative reconstruction environment (ASIR) Part2: The chest. *Rofo* 2013;185(7):644-54.
- [12] Nishio M, Matsumoto S, Ohno Y, et al., Emphysema quantification by low-dose CT: potential impact of adaptive iterative dose reduction using 3D processing. *AJR Am J Roentgenol* 2012;199(3):595-601.
- [13] Khawaja RD, Singh S, Gilman M, et al., Computed Tomography (CT) of the Chest at Less Than 1 mSv: An Ongoing Prospective Clinical Trial of Chest CT at Submillisievert Radiation Doses with Iterative Model Image Reconstruction and iDose<sup>4</sup> Technique. *J Comput Assist Tomogr* 2014;38(4):613-619.
- [14] Leipsic J, Nguyen G, Brown J, Sin D, Mayo J.R., A prospective evaluation of dose reduction and image quality in chest CT using adaptive statistical iterative reconstruction. *Am J Roentgenol* 2010;195(5):1095-9.

- [15] Ohno Y, Takenaka D, Kanda T, et al., Adaptive iterative dose reduction using 3D processing for reduced- and low-dose pulmonary CT: comparison with standard-dose CT for image noise reduction and radiological findings. *AJR Am J Roentgenol* 2012;199(4):W477-85.
- [16] Qi LP, Li Y, Tang L, et al., Evaluation of dose reduction and image quality in chest CT using adaptive statistical iterative reconstruction with the same group of patients. *Br J Radiol* 2012;85(1018):e906-11.
- [17] Pontana F, Duhamel A, Pagniez J, et al., Chest computed tomography using iterative reconstruction vs filtered back projection (Part 2): Image quality of low-dose CT examinations in 80 patients. *Eur Radiol* 2011;21(3):636-43.
- [18] Yamada Y, Jinzaki M, Hosokawa T, et al., Dose reduction in chest CT: comparison of the adaptive iterative dose reduction 3D, adaptive iterative dose reduction, and filtered back projection reconstruction techniques. *Eur J Radiol* 2012;81(12):4185-95.
- [19] Katsura M, Matsuda I, Akahane M, et al., Model-based iterative reconstruction technique for radiation dose reduction in chest CT: comparison with the adaptive statistical iterative reconstruction technique. *Eur Radiol* 2012;22(8):1613-23.
- [20] Vardhanabhuti V, Loader RJ, Mitchell GR, Riordan RD, Roobottom CA, Image quality assessment of standard- and low-dose chest CT using filtered back projection, adaptive statistical iterative reconstruction, and novel model-based iterative reconstruction algorithms. *AJR Am J Roentgenol* 2013;200(3):545-52.
- [21] Katsura M, Matsuda I, Akahane M, et al., Model-based iterative reconstruction technique for ultralow-dose chest CT: comparison of pulmonary nodule detectability with the adaptive statistical iterative reconstruction technique. *Invest Radiol* 2013;48(4):206-12.
- [22] Ichikawa Y, Kitagawa K, Nagasawa N, Murashima S, Sakuma H, CT of the chest with model-based, fully iterative reconstruction: comparison with adaptive statistical iterative reconstruction. *BMC Med Imaging* 2013;13:27,2342-13-27.
- [23] Hwang HJ, Seo JB, Lee JS, et al., Radiation dose reduction of chest CT with iterative reconstruction in image space - Part II: assessment of radiologists' preferences using dual source CT. *Korean J Radiol* 2012;13(6):720-7.
- [24] May MS, Eller A, Stahl C, et al., Dose Reduction in Computed Tomography of the Chest: Image Quality of Iterative Reconstructions at a 50% Radiation Dose Compared to Filtered Back Projection at a 100% Radiation Dose. *RofO* 2014.
- [25] Pontana F, Pagniez J, Duhamel A, et al., Reduced-dose low-voltage chest CT angiography with Sinogram-affirmed iterative reconstruction versus standard-dose filtered back projection. *Radiology* 2013;267(2):609-18.
- [26] Lee SW, Kim Y, Shim SS, et al., Image quality assessment of ultra low-dose chest CT using sinogram-affirmed iterative reconstruction. *Eur Radiol* 2014;24(4):817-26.

- [27] Kalra MK, Woisetschlager M, Dahlstrom N, et al., Sinogram-affirmed iterative reconstruction of low-dose chest CT: effect on image quality and radiation dose. *AJR Am J Roentgenol* 2013;201(2):W235-44.
- [28] Yamada Y, Jinzaki M, Tanami Y, et al., Model-based iterative reconstruction technique for ultralow-dose computed tomography of the lung: a pilot study. *Invest Radiol* 2012;47(8):482-9.
- [29] Yanagawa M, Honda O, Kikuyama A, et al., Pulmonary nodules: effect of adaptive statistical iterative reconstruction (ASIR) technique on performance of a computer-aided detection (CAD) system-comparison of performance between different-dose CT scans. *Eur J Radiol* 2012;81(10):2877-86.
- [30] Singh S., Kalra M.K., Gilman M.D., et al., Adaptive statistical iterative reconstruction technique for radiation dose reduction in chest CT: A pilot study. *Radiology* 2011;259(2):565-73.
- [31] Li Q, Yu H, Zhang L, Fan L, Liu SY, Combining low tube voltage and iterative reconstruction for contrast-enhanced CT imaging of the chest-initial clinical experience. *Clin Radiol* 2013;68(5):e249-53.
- [32] Chen JH, Jin EH, He W, Zhao LQ, Combining Automatic Tube Current Modulation with Adaptive Statistical Iterative Reconstruction for Low-Dose Chest CT Screening. *PLoS One* 2014;9(4):e92414.
- [33] Raman SP, Johnson PT, Deshmukh S, Mahesh M, Grant KL, Fishman EK, CT dose reduction applications: available tools on the latest generation of CT scanners. *J Am Coll Radiol* 2013;10(1):37-41.
- [34] Flohr T.G., Klotz E., Allmendinger T., Raupach R., Bruder H., Schmidt B., Pushing the envelope: New computed tomography techniques for cardiothoracic imaging. *J Thorac Imaging* 2010;25(2):100-11.
- [35] Nelson R.C., Feuerlein S., Boll D.T., New iterative reconstruction techniques for cardiovascular computed tomography: How do they work, and what are the advantages and disadvantages? *J Cardiovasc Comput Tomogr* 2011;5(5):286-92.
- [36] Xu J, Mahesh M, Tsui BM, Is iterative reconstruction ready for MDCT? *J Am Coll Radiol* 2009;6(4):274-6.
- [37] Willemink MJ, Schilham AM, Leiner T, Mali WP, de Jong PA, Budde RP, Iterative reconstruction does not substantially delay CT imaging in an emergency setting. *Insights Imaging* 2013;4(3):391-7.
- [38] Kligerman S, Mehta D, Farnadesh M, Jeudy J, Olsen K, White C, Use of a hybrid iterative reconstruction technique to reduce image noise and improve image quality in obese patients undergoing computed tomographic pulmonary angiography. *J Thorac Imaging* 2013;28(1):49-59.
- [39] Baumuellner S, Winklehner A, Karlo C, et al., Low-dose CT of the lung: potential value of iterative reconstructions. *Eur Radiol* 2012;22(12):2597-606.

- [40] Co SJ, Mayo J, Liang T, Krzemyk K, Yousefi M, Nicolaou S, Iterative reconstructed ultra high pitch CT pulmonary angiography with cardiac bowtie-shaped filter in the acute setting: effect on dose and image quality. *Eur J Radiol* 2013;82(9):1571-6.
- [41] Gorycki T, Lasek I, Kaminski K, Studniarek M, Evaluation of radiation doses delivered in different chest CT protocols. *Pol J Radiol* 2014;79:1-5.
- [42] Liu W, Ding X, Kong B, Fan B, Chen L, Reducing the radiation dose with the adaptive statistical iterative reconstruction technique for chest CT in adults: a parameter study. *Chin Med J (Engl)* 2014;127(7):1284-8.
- [43] Pontana F., Pagniez J., Flohr T., et al., Chest computed tomography using iterative reconstruction vs filtered back projection (Part 1): Evaluation of image noise reduction in 32 patients. *Eur Radiol* 2011;21(3):627-35.
- [44] Prakash P, Kalra M.K., Digumarthy S.R., et al., Radiation dose reduction with chest computed tomography using adaptive statistical iterative reconstruction technique: Initial experience. *J Comput Assisted Tomogr* 2010;34(1):40-5.
- [45] Wang H, Tan B, Zhao B, Liang C, Xu Z, Raw-data-based iterative reconstruction versus filtered back projection: image quality of low-dose chest computed tomography examinations in 87 patients. *Clin Imaging* 2013;37(6):1024-32.
- [46] Zizka J, Ryska P, Stepanovska J, et al., Iterative reconstruction of pulmonary MDCT angiography: Effects on image quality, effective dose and estimated organ dose to the breast. *Biomed Pap Med Fac Univ Palacky Olomouc Czech Repub* 2013.



## Chapter 2.2

*Part II Thoraco-abdominal*

# **Pulmonary nodule volumetry at different low CT radiation dose levels with hybrid and model-based iterative reconstruction: a within patient analysis**

Annemarie M. Den Harder, Martin J. Willemink, Robbert W. van Hamersvelt,  
Evertjan P.A. Vonken, Arnold M.R. Schilham, Jan-Willem J. Lammers,  
Bart Luijk, Ricardo P.J. Budde, Tim Leiner, Pim A. de Jong

Journal of Computer Assisted Tomography 2016; DOI 10.1097/RCT.000000000000408

## **Abstract**

### *Objective*

To determine the effects of dose reduction and iterative reconstruction (IR) on pulmonary nodule volumetry.

### *Methods*

In this prospective study 25 patients scheduled for follow-up of pulmonary nodules were included. Computed tomography (CT) acquisitions were acquired at four dose levels with a median of 2.1, 1.2, 0.8 and 0.6mSv. Data were reconstructed with filtered back projection (FBP), hybrid IR and model-based IR. Volumetry was performed using semi-automatic software.

### *Results*

At the highest dose level >91% (34/37) of the nodules could be segmented and at the lowest dose level this was >83%. Thirty-three nodules were included for further analysis. FBP and hybrid IR did not lead to significant differences while model-based IR resulted in an lower volume measurements with a maximum difference of -11% compared to FBP at routine dose.

### *Conclusions*

Pulmonary nodule volumetry can be accurately performed at a submillisievert dose with both FBP and hybrid IR.

## Introduction

Pulmonary nodules are a common incidental finding on chest computed tomography (CT). The number of chest CT acquisitions has rapidly increased in the past decade and is expected to further increase due to rising numbers of lung cancer screening [1]. The volume of pulmonary nodules is an important characteristic to guide clinical management and it is more accurate than diameter measurements to detect growth [2,3].

Substantial growth in the number of CT acquisitions will lead to an undesirable increase in radiation exposure if acquisition parameters are kept identical. One of the most promising radiation dose reduction methods is iterative reconstruction (IR). IR allows for image acquisition at decreased radiation dose levels by reducing image noise [4]. There are two basic forms of IR. The simplest version of the technique is a blend of conventionally used filtered back projection (FBP) and IR, also known as hybrid IR. This is opposed to the more advanced family of model-based IR techniques. Radiation dose reductions up to 50% have been reported for chest CT using IR [5]. Chest CT for pulmonary nodules has been reported at submillisievert doses using IR [5]. Phantom studies showed that pulmonary nodule volumetry is accurate with IR at submillisievert dose levels [6-9]. However, none of these studies investigated the effect of different IR techniques on pulmonary nodule volumetry at submillisievert dose levels in patients. We hypothesize that IR and dose reduction will not affect pulmonary nodule volumetry in patients. In this study we investigate the effect of radiation dose reduction and application of different forms of IR on pulmonary nodule volumetry using hybrid and model-based IR at 4 different radiation dose levels.

## Material and methods

### *Patients*

This prospective study was approved by our local institutional review board and informed consent was obtained from all patients. Patients 50 years or older with one or more pulmonary nodules scheduled for a follow-up chest CT were eligible for inclusion. Patients participating in other studies with x-ray exposure were excluded. Previously we investigated the influence of computer-aided detection of pulmonary nodules in the same patient population [10].

*CT protocol*

A 256-slice CT system (Brilliance iCT, Philips Healthcare, Best, The Netherlands) was used for image acquisition. Patients were asked to hold their breath at deep inspiration during each acquisition. A scout image was made after which image acquisition was performed at our routine protocol, followed by three acquisitions at reduced radiation dose levels. All acquisitions within a patient were performed with the same length (Z-coverage). Images were reconstructed with a slice thickness of 1mm and an increment of 0.7mm. Tube current-time products of 60 (reference dose), 33 (45% reduction), 24 (60% reduction) and 15mAs (75% reduction) were used in combination with a tube voltage of 100kV for patients with a weight below 80kg and a tube voltage of 120kV for patients with a weight above 80kg. Gantry rotation time was 0.33 seconds with a pitch of 0.758. No contrast medium was injected. Dose-length product (DLP) and volumetric CT dose index (CTDI<sub>vol</sub>) were recorded for each acquisition and the effective dose was determined by multiplying the DLP with the conversion factor for the chest (0.0145 mSv/(mGxcm)) [11].

All images were reconstructed with FBP, a hybrid IR algorithm (iDose<sup>4</sup>, Philips Healthcare, Best, The Netherlands) and a prototype version of an iterative model-based algorithm (IMR, Philips Healthcare, Best, The Netherlands). For iDose<sup>4</sup> levels 1, 4 and 6 (kernel filter C) were used and for IMR levels 1, 2 and 3 (kernel filter Body Routine). It is not possible to use kernel filter C for IMR, therefore we used vendor recommended kernel filter Body Routine.

*Pulmonary nodule volumetry*

Two experienced radiologists (PJ and EV) independently identified solid pulmonary nodules with diameters  $\geq 3$ mm on routine dose FBP reconstructions to be sure no pulmonary nodules were missed. Discordant cases were discussed to reach consensus. Subsequently, pulmonary nodule volume was measured by one observer using semi-automatic software (IntelliSpace Portal, V6.0.1.20250, Lung Nodule Assessment, Philips Healthcare, Best, The Netherlands). Clicking on the pulmonary nodule resulted in automatic delineation and volume quantification. Correctness of the lesion segmentation was visually inspected. If incorrect, segmentation was attempted again to a maximum of ten times by clicking at different positions in the nodule. No manual correction of segmentation was performed. For correctly segmented pulmonary nodules the volume (mm<sup>3</sup>) was recorded. Volumes were compared to the reference volume (routine dose acquisitions reconstructed with FBP) and the relative percentage

difference compared to the reference volume was calculated.

#### *Objective image quality assessment*

Contrast-to-noise ratio (CNR) and signal-to-noise ratio (SNR) were calculated by drawing a homogeneous region of interest (ROI) to measure the mean Hounsfield Units (HU) and the standard deviation (SD). One ROI was drawn in the descending aorta directly below the aortic arch. The other ROI was drawn in the subcutaneous fat within the anterior chest wall. The CNR was determined using the following formula [12]:

$$\text{CNR} = \frac{\text{Density (aorta)} - \text{Density (fat)}}{\sqrt{\frac{1}{2} * (\text{SD (aorta)}^2 + \text{SD (fat)}^2)}}$$

The SNR was defined as the ratio between the mean HU and the SD of the ROI in the aorta.

#### *Statistical analysis*

Statistical analysis was performed using SPSS (version 20.0, IBM). Pulmonary nodules with a missing reference volume (FBP at routine dose) or with more than 25% missing values due to incorrect or failed segmentations were excluded from further analysis. Pulmonary nodules with 25% or less missing values were imputed using multiple imputations with 10 imputations [13]. Hereby 10 datasets are simulated and the results are combined to produce estimates. The Friedman test was used to compare data with regard to the reference standard (FBP at routine dose) and post hoc analyses were performed with the Wilcoxon signed rank test. A p-value below 0.05 was considered statistically significant for the Friedman test and a Bonferroni correction was made for the post hoc Wilcoxon test resulting in a p-value of 0.007. Values are given as medians with interquartile ranges (IQR) unless otherwise stated.

## **Results**

In total 25 patients were included with a median age of 66 years (IQR 60 – 72). Baseline characteristics are provided in *Table 1*. One patient participated in a lung cancer screening study while the other patients had incidentally discovered pulmonary nodules. Thirteen patients were female and the median body mass index was 28.6kg/m<sup>2</sup>. Twelve patients were scanned with the <80kg protocol and 13 patients with the ≥80kg protocol. Median weight was 82kg (IQR 71 – 91). Radiation dose characteristics are provided in *Table 2*. The median effective dose

**Table 1** – Baseline characteristics.

Variable	Value
Number of patients	25
Age (years)	66 (60 – 72)
Gender	13 F / 12 M
Weight (kg)	82 (71 – 91)
Distribution over weight category (<80 kg / ≥80 kg)	12 / 13
Height (cm)	169 (164 – 176)
BMI (kg/m <sup>2</sup> )	28.6 (24.6 – 30.6)

Values are presented as median (interquartile range).

was 2.1mSv at routine dose and 1.2, 0.8 and 0.6mSv at reduced dose levels. In one patient the lowest dose acquisition was erroneously omitted.

**Table 2** – Radiation dose. Results are presented as medians (interquartile range).

	Routine dose	45% reduced mAs	60% reduced mAs	75% reduced mAs
CTDIvol (mGy)	4.1 (2.4 – 4.1)	2.2 (1.3 – 2.2)	1.6 (1.0 – 1.6)	1.0 (0.6 – 1.0)*
DLP (mGy×cm)	144.9 (95.5 – 169.1)	79.7 (52.5 – 93.0)	56.9 (37.8 – 66.5)	38.1 (23.8 – 42.3)*
Effective dose (mSv)	2.1 (1.4 – 2.5)	1.2 (0.8 – 1.6)	0.8 (0.5 – 1.0)	0.6 (0.4 – 0.6)*

\*n=24, one patient did not receive the lowest dose scan CTDIvol Volume CT dose index; DLP Dose-length product.

### *Lesion segmentation*

An example of pulmonary nodule volumetry at different dose levels and reconstructed with different IR algorithms is provided in *Figure 1*. Nine patients did not have pulmonary nodules ≥3 mm and were therefore excluded from pulmonary nodule volumetry analysis. In the remaining (n=16) patients in total 37 pulmonary nodules were present. At maximum 7 nodules were present in a patient. In two nodules lesion segmentation failed in one or more reconstructions, while in thirteen nodules incorrect segmentations occurred when adjacent blood vessels were included in the segmentation or when the nodule was only partly segmented.

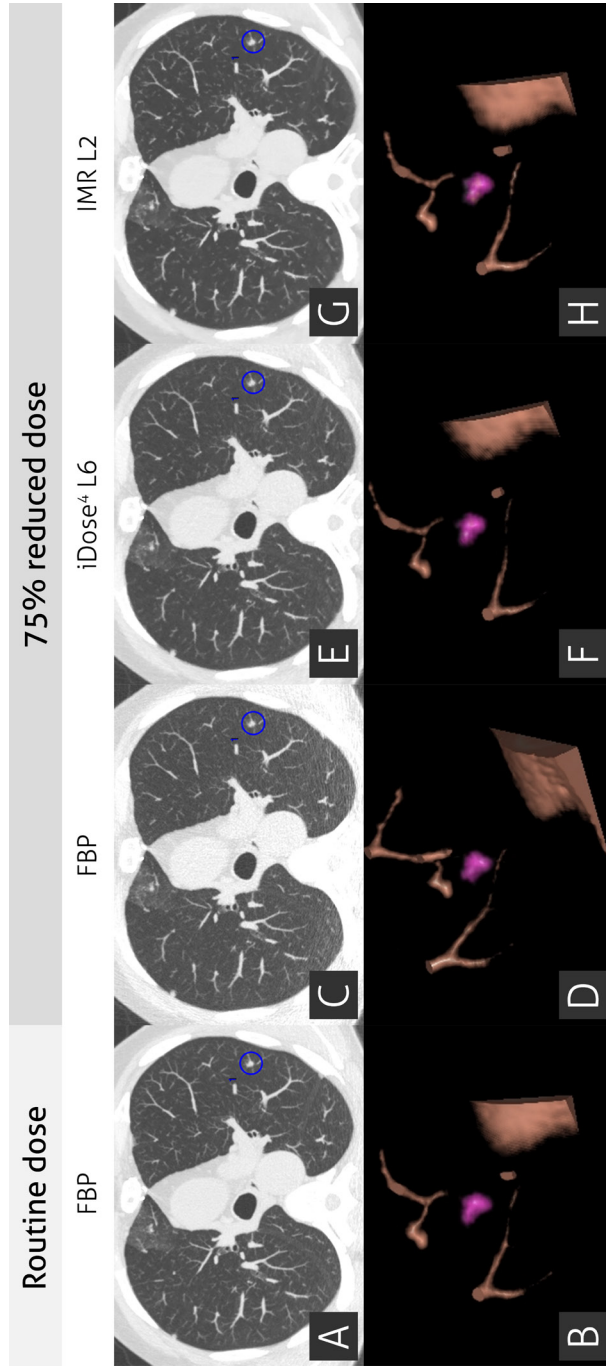


Figure 1 – Semi-automatic pulmonary nodule volumetry at routine dose with FBP and at the lowest dose level with FBP, iDose<sup>4</sup> level 6 and IMR level 2.

At routine dose, at least 34 out of 37 nodules (92%) were correctly segmented for FBP, iDose<sup>4</sup> and IMR. Two nodules that were incorrectly segmented with FBP at routine dose, were correctly segmented with IMR. At reduced dose levels, the number of correct segmentations remained high with a minimum of 32 out of 37 nodules (87%) correctly segmented nodules with FBP and 31 out of 37 nodules (84%) with iDose<sup>4</sup> and IMR (Table 3). Three nodules were excluded due to failed or incorrect segmentation on the reference reconstruction (routine dose reconstructed with FBP) and one nodule was excluded because on more than 25% of the reconstructions resulted in incorrect segmentations. Ultimately, 33 pulmonary nodules with a median diameter of 6.4mm (IQR 4.4 – 8.7mm) could be included for further analysis. In total 52 missing values (5.6%) were imputed out of 924 (33 nodules x 28 reconstructions) data points.

Table 3 – Percentage of correctly segmented pulmonary nodules per reconstruction method at the different dose levels.

	Routine dose	45% reduced mAs	60% reduced mAs	75% reduced mAs
FBP	91.9% (34/37)	94.6% (35/37)	86.5% (32/37)	91.9% (34/37)
iDose <sup>4</sup> level 1	91.9% (34/37)	91.9% (34/37)	97.3% (36/37)	89.2% (33/37)
iDose <sup>4</sup> level 4	91.9% (34/37)	91.9% (34/37)	97.3% (36/37)	83.8% (31/37)
iDose <sup>4</sup> level 6	94.6% (35/37)	94.6% (35/37)	91.9% (34/37)	89.2% (33/37)
IMR level 1	91.9% (34/37)	89.2% (33/37)	86.5% (32/37)	83.8% (31/37)
IMR level 2	91.9% (34/37)	83.8% (31/37)	89.2% (33/37)	83.8% (31/37)
IMR level 3	91.9% (34/37)	89.2% (33/37)	89.2% (33/37)	83.8% (31/37)

### Volumetry

There were no statistically significant differences in pulmonary nodule volume between FBP, iDose<sup>4</sup> and IMR at routine dose (Table 4). At 45% and 60% reduced mAs, IMR resulted in a lower pulmonary nodule volume while at 75% reduced mAs there were no differences. iDose did not affect pulmonary nodule volumes at all dose levels. The relative percentage difference in pulmonary nodule volume with iDose<sup>4</sup> and IMR at routine dose compared to FBP at routine dose ranged from -5.6 – 0.4%. At reduced dose levels the relative percentage difference with FBP at routine dose was larger to a maximum of -4.4% with FBP (60% reduced mAs), -4.5% with iDose<sup>4</sup> level 6 (45% reduced mAs) and -11.3% with IMR level 3 (60% reduced mAs).

**Table 4 – Mean Pulmonary Nodule Volume and relative difference as a function of radiation dose and iterative reconstruction algorithm used. This table presents the relative differences in volume compared to FBP at routine dose and the volume of the pulmonary nodules.**

	Routine dose			45% reduced mAs			60% reduced mAs			75% reduced mAs		
	Volume (mm <sup>3</sup> )	Difference (%)		Volume (mm <sup>3</sup> )	Difference (%)		Volume (mm <sup>3</sup> )	Difference (%)		Volume (mm <sup>3</sup> )	Difference (%)	
FBP	134 (45 – 308)	NA		101 (51 – 258)	-1.1 (-19.3 – 8.7)		101 (54 – 294)	-4.4 (-12.0 – 10.4)		94 (54 – 273)	-0.9 (-23.2 – 7.1)	
iDose <sup>4</sup> level 1	119 (46 – 292)	-0.8 (-8.7 – 0.6)		105 (51 – 264)	2.4 (-15.4 – 8.0)		94 (53 – 288)	-4.7 (-13.6 – 7.6)		109 (53 – 270)	-3.5 (-12.9 – 6.1)	
iDose <sup>4</sup> level 4	104 (45 – 290)	-0.4 (-7.9 – 7.7)		111 (52 – 287)	-2.8 (-13.5 – 6.1)		114 (42 – 289)	-1.1 (-10.7 – 8.6)		101 (56 – 262)	-3.7 (-14.3 – 6.8)	
iDose <sup>4</sup> level 6	103 (43 – 298)	-4.4 (-10.9 – 3.5)		97 (49 – 271)	-4.5 (-11.5 – 3.5)		109 (46 – 285)	-1.8 (-12.0 – 4.9)		100 (58 – 267)	-0.5 (-12.3 – 15.0)	
IMR level 1	122 (45 – 276)	-5.6 (-16.1 – 4.4)		105 (55 – 237)*	-13.3 (-22.0 – -0.3)	p=0.002	110 (54 – 248)	-8.8 (-22.1 – 6.5)		103 (46 – 277)	-8.5 (-18.3 – 3.3)	
IMR level 2	94 (43 – 285)	-6.2 (-15.6 – 3.1)		97 (55 – 266)*	-8.9 (-19.2 – 0.0)	p=0.003	111 (44 – 254)*	-10.7 (-24.7 – 2.6)		79 (47 – 273)	-9.4 (-20.5 – 7.3)	
IMR level 3	93 (43 – 273)	-4.5 (-14.7 – 5.1)		101 (52 – 256)*	-10.0 (-22.0 – -2.6)	p=0.001	103 (49 – 256)*	-11.3 (-22.2 – 0.5)		120 (57 – 261)	-9.0 (-20.7 – 12.7)	

Values are presented as median (interquartile range). \*Significant different (p-value below 0.007) compared to FBP at routine dose. N=14, 33 pulmonary nodules

Table 5 – Objective image quality. Values are presented as median (interquartile range).

	Routine dose			45% reduced mAs			60% reduced mAs			75% reduced mAs		
	SNR	CNR		SNR	CNR		SNR	CNR		SNR	CNR	
FBP	1.1 (0.9 – 1.5)	3.5 (2.9 – 4.4)		0.8 (0.6 – 1.0)*	2.6 (2.2 – 3.0)*		0.7 (0.5 – 0.8)*	2.4 (1.8 – 2.9)*		0.5 (0.4 – 0.6)*	1.6 (1.4 – 2.1)*	
iDose <sup>4</sup> level 1	1.4 (1.1 – 1.7)*	4.4 (3.4 – 5.0)*		1.1 (0.8 – 1.2)	3.3 (3.0 – 3.7)		0.9 (0.8 – 1.1)*	3.2 (2.8 – 3.6)*		0.8 (0.7 – 0.9)*	2.7 (2.4 – 3.1)*	
iDose <sup>4</sup> level 4	1.8 (1.4 – 2.2)*	5.1 (4.0 – 6.0)*		1.3 (1.1 – 1.6)	4.1 (3.8 – 4.7)		1.2 (1.0 – 1.3)*	4.0 (3.5 – 4.4)		1.0 (0.8 – 1.1)*	3.2 (2.9 – 3.8)	
iDose <sup>4</sup> level 6	2.3 (1.7 – 2.8)*	5.9 (4.8 – 7.5)*		1.7 (1.4 – 2.0)*	5.1 (4.6 – 5.9)*		1.5 (1.3 – 1.7)*	4.9 (4.3 – 5.5)*		1.2 (1.0 – 1.4)	3.9 (3.5 – 4.8)	
IMR level 1	4.1 (3.4 – 4.7)*	9.3 (6.2 – 12.3)*		3.5 (2.9 – 4.1)*	8.3 (6.7 – 9.9)*		3.1 (2.6 – 3.5)*	8.5 (6.3 – 10.8)*		2.6 (2.1 – 2.9)*	6.5 (5.1 – 8.5)*	
IMR level 2	5.8 (5.0 – 6.6)*	9.4 (7.1 – 16.9)*		5.0 (4.1 – 5.7)*	10.6 (7.4 – 15.2)*		4.3 (3.7 – 5.0)*	10.6 (8.2 – 14.2)*		3.5 (3.0 – 4.0)*	8.4 (6.3 – 11.0)*	
IMR level 3	8.4 (7.6 – 9.4)*	10.5 (7.5 – 23.0)*		7.7 (6.8 – 10.0)*	13.5 (7.6 – 19.0)*		6.5 (5.3 – 8.1)*	13.4 (9.9 – 21.8)*		5.0 (4.1 – 6.0)*	9.4 (6.2 – 14.3)*	

\*Significant different (p-value below 0.007) compared to FBP at routine dose. SNR signal-to-noise ratio CNR contrast-to-noise ratio

### *Objective image quality*

CNR and SNR values are listed in *Table 5*. The Friedman test was significant ( $p < 0.05$ ) and post hoc analyses were performed. Measured values were compared to the reference value derived with FBP at routine dose.

FBP led to a significant decrease in both CNR and SNR at all three reduced dose levels (*Table 5*). Objective image quality decreased with iDose<sup>4</sup> level 1 at the lowest two dose levels while iDose<sup>4</sup> level 4 and 6 resulted in comparable or improved CNR and SNR. All IMR levels led to an increase in both CNR and SNR at all reduced dose levels.

### **Discussion**

The main finding of this study is that pulmonary nodule volumetry can be accurately performed in >83% of relatively small pulmonary nodules at a submillisievert dose with FBP and hybrid IR. Furthermore, hybrid IR and especially model-based IR leads to a significant improvement in objective image quality. Based on these findings it seems reasonable to conclude that radiation dose levels for pulmonary nodule follow-up can be reduced substantially and conversion from FBP to IR will improve image quality while nodule volumetry remains accurate. This is important because the number of chest CT acquisitions is expected to increase further due to implementation of lung cancer screening. The National Lung Screening Trial (NLST) using low dose CT has shown to reduce mortality [14]. In the United States lung cancer screening is advised in high risk individuals while recently the European Society of Radiology and the European Respiratory Society also recommended to implement lung cancer screening with low dose CT in routine clinical practice [15,16]. In the NLST, pulmonary nodules ( $\geq 4$ mm) were reported in 24% of the participants at baseline. This large number of pulmonary nodules requires follow-up, which can lead to a high cumulative radiation dose [14]. The aim is to reduce radiation dose while at the same time maintaining image quality and accurate and consistent pulmonary nodule volumetry.

Pulmonary nodule volume is dependent of several factors such as image-acquisition and reconstruction parameters, software performance for nodule quantification and nodule characteristics [17]. For instance different software packages can lead to differences in volume of up to 25% [18]. Twelve studies have investigated radiation dose reduction for chest CT using IR by making multiple chest CT acquisitions in the same patient at the same time [19-30]. Four of these

studies included acquisitions with a radiation dose below 1mSv [19,27,28,30], but did not investigate the effect on pulmonary nodule volumetry and only focused on image quality and lesion nodule detection. Those studies found that pulmonary nodule detection rate was identical for IR at low dose compared to FBP at routine dose. Several phantom studies have shown that IR can accurately determine pulmonary nodule volume even at submillisievert dose, but this had not been confirmed in humans [6-9,31]. A patient study investigating the effect of hybrid IR on pulmonary nodule volumetry at routine dose levels also found comparable results between FBP and IR [31]. However, a relatively high effective dose (3.1mSv) was used.

To our best knowledge this is the first in vivo study investigating the effect of radiation dose reduction and different types of IR on pulmonary nodule volume at extremely low dose levels. We found significant differences in pulmonary nodule volume using model-based IR. When looking at volume differences compared to FBP at routine dose differences up to 11.3% occurred. This can be caused by interscan variation because multiple acquisitions were performed. The effect of interscan variation on volumetry at similar radiation dose levels can lead to differences up to 24% [32,33]. Based on these studies, a change in volume of 25% between acquisitions is regarded as nodule growth. The volume differences found at reduced dose levels in the present study are below this cut-off and within the normal interscan variation. Model-based IR resulted in a significant lower pulmonary nodule volume but the differences were below 25% and therefore most likely not clinically relevant. However, caution should be taken with changing to model-based IR within one patient.

In this study we used multiple imputations to estimate and replace missing values. Imputation is a well-established theory for handling missing data and there is substantial support for the validity of multiple imputations in simulations [13]. The results without multiple imputation, e.g. with complete case analysis, were in the same effect size as the results presented in this study. We chose for this approach since with general missing data, bias tends to be smaller with multiple imputations compared to complete case analysis [34].

The present study has several limitations. The sample size was kept small, because participants were exposed to increased radiation doses due to multiple acquisitions. Furthermore, nine patients turned out to have pulmonary nodules smaller than 3mm or non-solid although we only included patients that received a follow-up chest CT for known pulmonary nodules. We excluded

four pulmonary nodules in which lesion segmentation failed in the reference reconstruction or more than 25% of the reconstructions to allow a fair nodule-by-nodule comparison. There were small differences between reconstructions and dose levels in the number of failed or incorrect lesion segmentations. At the lowest dose level there was an increase in the number of failed or incorrect lesion segmentations whereby IMR performed slightly worse. However, the percentage of failed or incorrect lesion segmentations in our study was relatively small compared to other studies [18,33]. We used a nodule size threshold of 3mm in our study. However, recent guidelines of the British Thoracic Society advise to offer CT surveillance follow-up only for nodules  $\geq 5$ mm [35] and in lung cancer screening programs even higher thresholds are considered [36]. The lesion segmentation was done by one operator. We did not investigate operator dependency, however, we expect this to be neglectable since the operator only has to click on the pulmonary nodule to instruct the software to calculate the volume. Another limitation is that we used IR algorithms from a single vendor. Future research with IR algorithms from other vendors is recommended and should focus on submillisievert radiation dose levels. Further radiation dose reduction can potentially be reached by lowering kVp-values. Despite these limitations, this study is the first patient study assessing the effect of pulmonary nodule volumetry at very low dose levels. This study shows that the dose used in lung cancer screening trials (1.6mSv for men and 2.1mSv for women) can be further reduced without affecting pulmonary nodule volumetry or image quality [14], and that it is safe to convert FBP protocols to either hybrid IR and model-based IR.

In conclusion, pulmonary nodule volumetry was not affected by both FBP and hybrid IR. Caution should be taken with model-based IR, which resulted in lower volumes, however differences were within the normal interscan variation. Dose reduction to submillisievert dose levels is therefore possible while maintaining accurate pulmonary nodule volumetry and image quality.

## References

- [1] Field JK, Hansell DM, Duffy SW, Baldwin DR, CT screening for lung cancer: countdown to implementation. *Lancet Oncol* 2013;14(13):e591-600.
- [2] Horeweg N, van Rosmalen J, Heuvelmans MA, et al., Lung cancer probability in patients with CT-detected pulmonary nodules: a prespecified analysis of data from the NELSON trial of low-dose CT screening. *Lancet Oncol* 2014;15(12):1332-41.
- [3] Truong MT, Ko JP, Rossi SE, et al., Update in the evaluation of the solitary pulmonary nodule. *Radiographics* 2014;34(6):1658-79.
- [4] Willemink MJ, de Jong PA, Leiner T, et al., Iterative reconstruction techniques for computed tomography Part 1: technical principles. *Eur Radiol* 2013;23(6):1623-31.
- [5] den Harder AM, Willemink MJ, de Ruiter QM, et al., Achievable dose reduction using iterative reconstruction for chest computed tomography: A systematic review. *Eur J Radiol* 2015;84(11):2307-13.
- [6] Kim H, Park CM, Song YS, Lee SM, Goo JM, Influence of radiation dose and iterative reconstruction algorithms for measurement accuracy and reproducibility of pulmonary nodule volumetry: A phantom study. *Eur J Radiol* 2014;83(5):848-57.
- [7] Coenen A, Honda O, van der Jagt E, Tomiyama N, Computer-assisted solid lung nodule 3D volumetry on CT: influence of scan mode and iterative reconstruction: a CT phantom study. *Jpn J Radiol* 2013;31(10):677-84.
- [8] Willemink MJ, Leiner T, Budde RP, et al., Systematic error in lung nodule volumetry: effect of iterative reconstruction versus filtered back projection at different CT parameters. *AJR Am J Roentgenol* 2012;199(6):1241-6.
- [9] Wielputz MO, Lederlin M, Wroblewski J, et al., CT volumetry of artificial pulmonary nodules using an ex vivo lung phantom: influence of exposure parameters and iterative reconstruction on reproducibility. *Eur J Radiol* 2013;82(9):1577-83.
- [10] den Harder AM, Willemink MJ, van Hamersvelt RW, et al., Effect of radiation dose reduction and iterative reconstruction on computer-aided detection of pulmonary nodules: Intra-individual comparison. *European Journal of Radiology* 2016;85:346-351.
- [11] Deak PD, Smal Y, Kalender WA, Multisection CT protocols: sex- and age-specific conversion factors used to determine effective dose from dose-length product. *Radiology* 2010;257(1):158-66.
- [12] den Harder AM, Willemink MJ, Bleys RL, et al., Dose reduction for coronary calcium scoring with hybrid and model-based iterative reconstruction: an ex vivo study. *Int J Cardiovasc Imaging* 2014;30(6):1125-33.
- [13] Li P, Stuart EA, Allison DB, Multiple Imputation: A Flexible Tool for Handling Missing Data. *JAMA* 2015;314(18):1966-7.

- [14] Prosch H, Implementation of lung cancer screening: promises and hurdles. *Transl Lung Cancer Res* 2014;3(5):286-90.
- [15] Kauczor HU, Bonomo L, Gaga M, et al., ESR/ERS white paper on lung cancer screening. *Eur Radiol* 2015.
- [16] Moyer VA, U.S. Preventive Services Task Force, Screening for lung cancer: U.S. Preventive Services Task Force recommendation statement. *Ann Intern Med* 2014;160(5):330-8.
- [17] Hochegger B, Marchiori E, Alves GR, Guimaraes MD, Irion K, Influences in CT scan lung nodule volumetry. *Chest* 2014;146(2):e69-70.
- [18] de Hoop B, Gietema H, van Ginneken B, Zanen P, Groenewegen G, Prokop M, A comparison of six software packages for evaluation of solid lung nodules using semi-automated volumetry: what is the minimum increase in size to detect growth in repeated CT examinations. *Eur Radiol* 2009;19(4):800-8.
- [19] Neroladaki A, Botsikas D, Boudabbous S, Becker CD, Montet X, Computed tomography of the chest with model-based iterative reconstruction using a radiation exposure similar to chest X-ray examination: preliminary observations. *Eur Radiol* 2013;23(2):360-6.
- [20] Yamada Y, Jinzaki M, Hosokawa T, et al., Dose reduction in chest CT: comparison of the adaptive iterative dose reduction 3D, adaptive iterative dose reduction, and filtered back projection reconstruction techniques. *Eur J Radiol* 2012;81(12):4185-95.
- [21] Katsura M, Matsuda I, Akahane M, et al., Model-based iterative reconstruction technique for radiation dose reduction in chest CT: comparison with the adaptive statistical iterative reconstruction technique. *Eur Radiol* 2012;22(8):1613-23.
- [22] Ohno Y, Takenaka D, Kanda T, et al., Adaptive iterative dose reduction using 3D processing for reduced- and low-dose pulmonary CT: comparison with standard-dose CT for image noise reduction and radiological findings. *AJR Am J Roentgenol* 2012;199(4):W477-85.
- [23] Vardhanabhuti V, Loader RJ, Mitchell GR, Riordan RD, Roobottom CA, Image quality assessment of standard- and low-dose chest CT using filtered back projection, adaptive statistical iterative reconstruction, and novel model-based iterative reconstruction algorithms. *AJR Am J Roentgenol* 2013;200(3):545-52.
- [24] Katsura M, Matsuda I, Akahane M, et al., Model-based iterative reconstruction technique for ultralow-dose chest CT: comparison of pulmonary nodule detectability with the adaptive statistical iterative reconstruction technique. *Invest Radiol* 2013;48(4):206-12.
- [25] Ichikawa Y, Kitagawa K, Nagasawa N, Murashima S, Sakuma H, CT of the chest with model-based, fully iterative reconstruction: comparison with adaptive statistical iterative reconstruction. *BMC Med Imaging* 2013;13:27,2342-13-27.

- [26] Kalra MK, Woisetschlager M, Dahlstrom N, et al., Sinogram-affirmed iterative reconstruction of low-dose chest CT: effect on image quality and radiation dose. *AJR Am J Roentgenol* 2013;201(2):W235-44.
- [27] Khawaja RD, Singh S, Gilman M, et al., Computed Tomography (CT) of the Chest at Less Than 1 mSv: An Ongoing Prospective Clinical Trial of Chest CT at Submillisievert Radiation Doses with Iterative Model Image Reconstruction and iDose<sup>4</sup> Technique. *J Comput Assist Tomogr* 2014;38(4):613-619.
- [28] Yamada Y, Jinzaki M, Tanami Y, et al., Model-based iterative reconstruction technique for ultralow-dose computed tomography of the lung: a pilot study. *Invest Radiol* 2012;47(8):482-9.
- [29] Yanagawa M, Honda O, Kikuyama A, et al., Pulmonary nodules: effect of adaptive statistical iterative reconstruction (ASIR) technique on performance of a computer-aided detection (CAD) system-comparison of performance between different-dose CT scans. *Eur J Radiol* 2012;81(10):2877-86.
- [30] Singh S., Kalra M.K., Gilman M.D., et al., Adaptive statistical iterative reconstruction technique for radiation dose reduction in chest CT: A pilot study. *Radiology* 2011;259(2):565-73.
- [31] Willemink MJ, Borstlap J, Takx RA, et al., The effects of computed tomography with iterative reconstruction on solid pulmonary nodule volume quantification. *PLoS One* 2013;8(2):e58053.
- [32] de Jong PA, Leiner T, Lammers JW, Gietema HA, Can low-dose unenhanced chest CT be used for follow-up of lung nodules? *AJR Am J Roentgenol* 2012;199(4):777-80.
- [33] Gietema HA, Schaefer-Prokop CM, Mali WP, Groenewegen G, Prokop M, Pulmonary nodules: Interscan variability of semiautomated volume measurements with multisection CT-- influence of inspiration level, nodule size, and segmentation performance. *Radiology* 2007;245(3):888-94.
- [34] White IR, Carlin JB, Bias and efficiency of multiple imputation compared with complete-case analysis for missing covariate values. *Stat Med* 2010;29(28):2920-31.
- [35] Baldwin DR, Callister ME, Guideline Development Group, The British Thoracic Society guidelines on the investigation and management of pulmonary nodules. *Thorax* 2015;70(8):794-8.
- [36] Yip R, Henschke CI, Yankelevitz DF, Smith JP, CT screening for lung cancer: alternative definitions of positive test result based on the national lung screening trial and international early lung cancer action program databases. *Radiology* 2014;273(2):591-6.

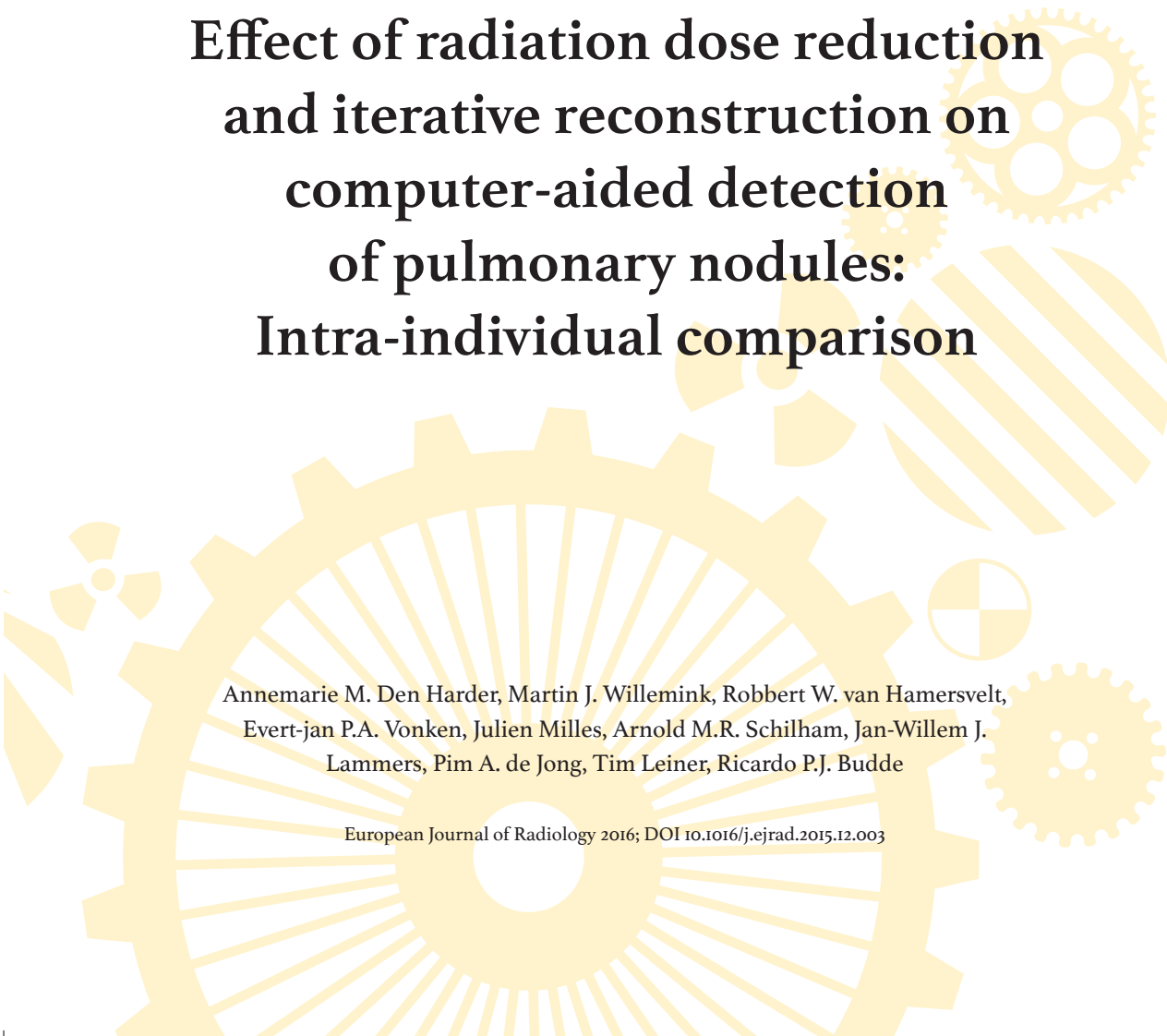




## Chapter 2.3

### *Part II Thoraco-abdominal*

# Effect of radiation dose reduction and iterative reconstruction on computer-aided detection of pulmonary nodules: Intra-individual comparison



Annemarie M. Den Harder, Martin J. Willeminck, Robbert W. van Hamersvelt,  
Evert-jan P.A. Vonken, Julien Milles, Arnold M.R. Schilham, Jan-Willem J.  
Lammers, Pim A. de Jong, Tim Leiner, Ricardo P.J. Budde

European Journal of Radiology 2016; DOI 10.1016/j.ejrad.2015.12.003

## Abstract

### *Objective*

To evaluate the effect of radiation dose reduction and iterative reconstruction (IR) on the performance of computer-aided detection (CAD) for pulmonary nodules.

### *Methods*

In this prospective study twenty-five patients were included who were scanned for pulmonary nodule follow-up. Image acquisition was performed at routine dose and three reduced dose levels in a single session by decreasing mAs-values with 45%, 60% and 75%. Tube voltage was fixed at 120 kVp for patients  $\geq 80$  kg and 100 kVp for patients  $< 80$  kg. Data were reconstructed with filtered back projection (FBP), iDose<sup>4</sup> (levels 1,4,6) and IMR (levels 1,2,3). All noncalcified solid pulmonary nodules  $\geq 4$ mm identified by two radiologists in consensus served as the reference standard. Subsequently, nodule volume was measured with CAD software and compared to the reference consensus. The numbers of true-positives, false-positives and missed pulmonary nodules were evaluated as well as the sensitivity.

### *Results*

Median effective radiation dose was 2.2 mSv at routine dose and 1.2, 0.9 and 0.6 mSv at respectively 45%, 60% and 75% reduced dose. A total of 28 pulmonary nodules were included. With FBP at routine dose, 89% (25/28) of the nodules were correctly identified by CAD. This was similar at reduced dose levels with FBP, iDose<sup>4</sup> and IMR. CAD resulted in a median number of false-positives findings of 11 per scan with FBP at routine dose (93% of the CAD marks) increasing to 15 per scan with iDose<sup>4</sup> (95% of the CAD marks) and 26 per scan (96% of the CAD marks) with IMR at the lowest dose level.

### *Conclusion*

CAD can identify pulmonary nodules at submillisievert dose levels with FBP, hybrid and model-based IR. However, the number of false-positive findings increased using hybrid and especially model-based IR at submillisievert dose while dose reduction did not affect the number of false-positives with FBP.

## Introduction

Lung cancer screening in high-risk individuals reduces mortality [1]. Therefore, both European and American guidelines recommend lung cancer screening implementation [2,3]. Since 23-53% of patients in lung cancer screening trials have pulmonary nodules at baseline which require follow-up, this will lead to an increased workload for radiologists [4,5]. Also in routine practice incidental pulmonary nodules and pulmonary metastases are a common finding. Computer-aided detection (CAD) can assist radiologists in the identification of pulmonary nodules in screening as well as routine care in patients with and without a known malignancy. Dedicated software tools are available that automatically identify and annotate potential nodules [6]. CAD combined with assessment by a radiologist improves the sensitivity for pulmonary nodule detection compared to assessment by a radiologist alone [6-8]. However, CAD can also lead to an increased number of false positive findings [9].

Increased awareness of the harmful effects of radiation exposure has led to technical innovations to reduce the radiation dose associated with CT examinations [10]. Iterative reconstruction (IR) computationally decreases image noise compared to the conventional reconstruction technique filtered back projection (FBP) making radiation dose reduction possible. A phantom study investigated the effect of application of a hybrid IR technique on CAD and concluded that IR did not affect CAD performance [6]. However, results may be different in patients and for more advanced model-based IR techniques because these are associated with a smoother appearance of anatomical structures in which details can be missed [11]. It is unknown if the use of these advanced IR techniques also affects the performance of CAD for pulmonary nodules, because current CAD is trained with FBP images. Therefore, in this patient study we investigated the effect of dose reduction and hybrid and model-based IR on the performance of CAD for pulmonary nodules.

## Methods

Our local institutional review board approved this prospective study (NL46146.041.13). Inclusion criteria were an age of 50 years or older (1) and scheduled for a follow-up chest CT for known pulmonary nodules (2). Exclusion criterion was concomitant participation in another study with x-ray exposure.

### *Computed tomography*

All CT acquisitions were performed on a 256-slice Brilliance iCT system (*Philips Healthcare, Best, The Netherlands*). CT data were acquired in full inspiration and without contrast injection. After a scout image, the routine dose scan was acquired, followed by three reduced dose scans. Every scan was acquired during a different breath hold and all scans within a patient were performed with the same scan length. Exposure settings were 60, 33, 24 and 15 mAs combined with a tube voltage of 100 kV for patients with a weight below 80 kg and 120 kV for patients with a weight above 80 kg. Reconstructed slice thickness was 1 mm. All images were reconstructed with FBP, a hybrid IR algorithm (iDose<sup>4</sup>, Philips Healthcare, Best, The Netherlands) and a prototype version of an iterative model-based algorithm (IMR, Philips Healthcare, Best, The Netherlands). For iDose<sup>4</sup> levels 1, 4 and 6 (kernel filter C) were used and for IMR levels 1, 2 and 3 (kernel filter Body Routine). It is not possible to use kernel filter C for IMR, therefore we used vendor recommended kernel filter Body Routine.

For each scan the volumetric CT dose index ( $CTDI_{vol}$ ) and the dose-length product (DLP) were recorded. Effective dose was determined by multiplying the DLP with the conversion factor for the chest (0.0145 mSv/(mG×cm) for 120 kV and 0.0144 mSv/(mG×cm) for 100 kV) [12].

### *Computer-aided detection*

As a reference, solid non-calcified pulmonary nodules with a diameter of 4 mm or more were identified on routine dose FBP reconstructions by two radiologists independently. In case of discrepancy the case was discussed to reach consensus. Commercially available software (*IntelliSpace Portal, V6.0.I.20250, Lung Nodule Assessment, Philips Healthcare, Best, The Netherlands*) was used for CAD of pulmonary nodules. CAD automatically identified pulmonary nodules with a size of 4 – 30mm. These were subsequently inspected by one observer and compared with the reference nodules detected by the two radiologists. The numbers of true-positives, false-positives and missed (false-negative) pulmonary nodules were determined. Sensitivity was calculated for each reconstruction technique at each dose level by dividing the total number of true pulmonary nodules detected by CAD by the total number of true nodules present.

### *Statistical analysis*

SPSS (*version 20.0, IBM, New York, United States*) was used for statistical analysis. All measurements were compared to the reference standard namely FBP at

routine dose. Data were compared using the Friedman test and the Wilcoxon signed rank test was used for post hoc analyses. A p-value below 0.05 was considered statistically significant for the Friedman test and a Bonferroni correction was made for the post hoc Wilcoxon test resulting in a p-value of 0.007. Values are given as medians with interquartile ranges (IQR) unless otherwise stated.

## Results

Twenty-five patients were included. In two patients IMR data were accidentally deleted before the IMR reconstructions were made and in one patient the lowest dose scan was not performed. These three patients were excluded from further analysis. Therefore, data of 22 patients was analyzed.

The median age was 66 (IQR 60 – 72) years and half of the patients were female. Median BMI was 28.6 (IQR 26.0 – 31.4) kg/m<sup>2</sup> and in twelve patients the ≥80 kg protocol was used. Radiation dose characteristics are provided in *Table 1*. Effective dose was 2.2 (1.4 – 2.4) mSv at routine dose and 1.2 (0.8 – 1.3), 0.9 (0.5 – 1.0) and 0.6 (0.3 – 0.6) mSv at reduced dose levels respectively.

**Table 1** – Radiation dose characteristics. Results are presented as medians (interquartiles).

	Routine dose	45% reduced dose	60% reduced dose	75% reduced dose
CTDI <sub>vol</sub> (mGy)	4.1 (2.4 – 4.1)	2.2 (1.3 – 2.2)	1.6 (1.0 – 1.6)	1.0 (0.6 – 1.0)
DLP (mGy×cm)	150.2 (95.9 – 168.8)	83.8 (52.9 – 92.9)	60.4 (37.9 – 66.3)	38.1 (23.9 – 42.2)
Effective dose (mSv)	2.2 (1.4 – 2.4)	1.2 (0.8 – 1.3)	0.9 (0.5 – 1.0)	0.6 (0.3 – 0.6)

CTDI<sub>vol</sub> Volume CT dose index; DLP Dose-length product.

### *Pulmonary nodules*

Nine patients did not have pulmonary nodules. The remaining patients had 1 nodule (5 patients), 2 nodules (5 patients), 3 nodules (1 patient) or 5 nodules (2 patients). In total 28 nodules were included with a median diameter of 7.0 (5.1 – 8.7) mm and median volume of 177 (70 – 346) mm<sup>3</sup> as measured on the reference dose scan reconstructed with FBP.

### Computer-aided detection

The CAD system read and analyzed all datasets successfully. *Figure 1* shows the user interface of the CAD system while *Figure 2* shows an example of a nodule detected at different dose levels with FBP, iDose<sup>4</sup> and IMR. The total number of true-positive, false-negative and false-positive nodules is provided in *Table 2*. Sensitivity with FBP at routine dose was 89% (25/28) while 93% (353/381) of the CAD marks were incorrect. The sensitivity was the same with iDose<sup>4</sup> level 1 and 4 and all IMR levels while iDose<sup>4</sup> level 6 resulted in a slightly higher sensitivity of 93% (26/28) at routine dose. At 45% and 60% reduced dose FBP and iDose<sup>4</sup> and IMR level 3 yielded the same or increased sensitivity while sensitivity slightly decreased with IMR level 1 and 2 to 82% (23/28). At the lowest dose level, sensitivity increased to 93% (26/28) for all reconstructions except iDose<sup>4</sup> level 1.

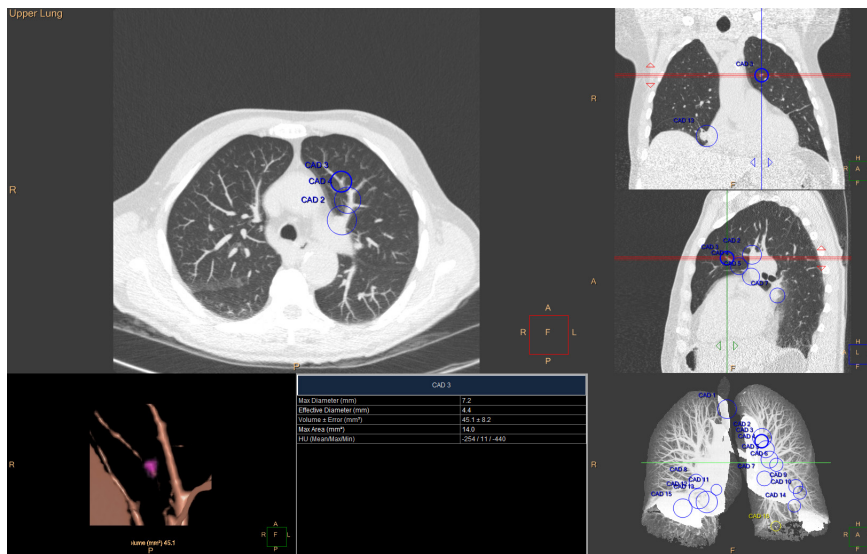


Figure 1 – CAD system output. Each suspected site is marked with a circle.

None of the differences in sensitivity were significant. Six pulmonary nodules were missed on one or more reconstructions (*Figure 3*). These nodules had a median diameter of 7.2 (range 4.5 – 21.0) mm and a volume of 195.2 (range 48.3 – 4874.9) mm<sup>3</sup>. Three of the missed pulmonary nodules were localized adjacent

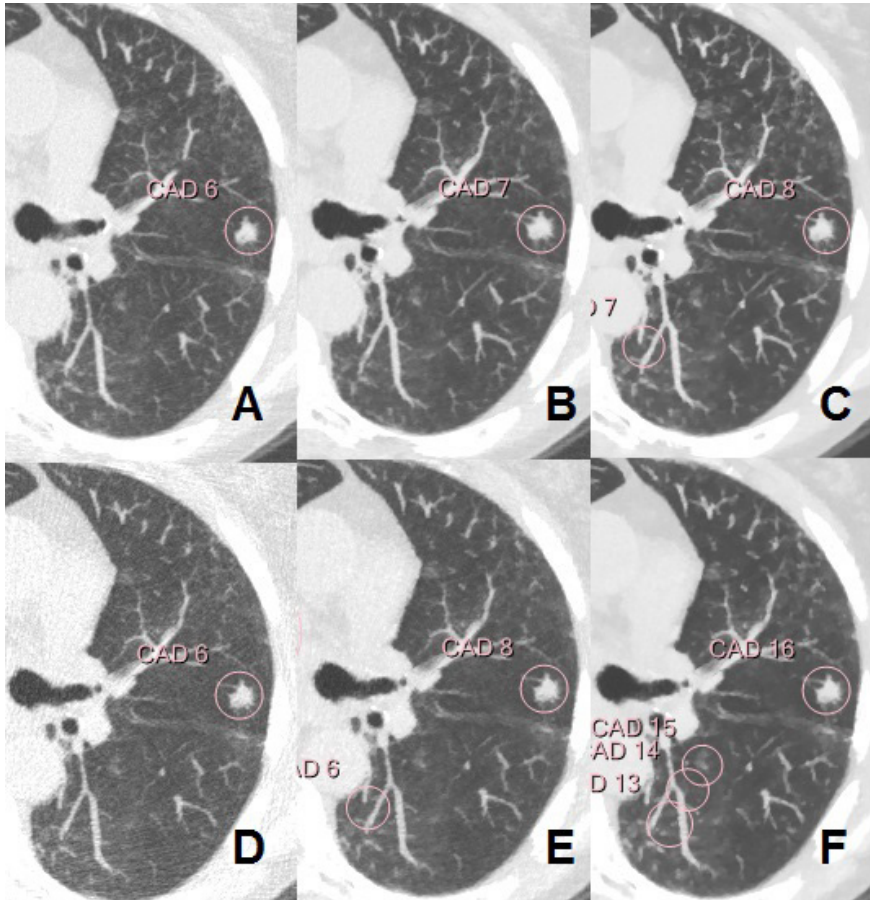


Figure 2 – Example of a pulmonary nodule marked by CAD at routine dose (A – C) and 75% reduced dose (D – F) with FBP (A, D), iDose<sup>+</sup> level 6 (B, E) and IMR level 2 (C, F)

to blood vessels or the pleural wall. Two missed pulmonary nodules were very small (5 mm) while one missed pulmonary nodule was extremely large (21 mm), although the CAD software should be able to detect pulmonary nodules up to 30 mm.

The number of false-positive nodules identified with CAD was high: at routine dose reconstructed with FBP, 93% (353/378) of the CAD marks were incorrect. At reduced dose levels this remained 93% with FBP, 92 – 95% with iDose<sup>+</sup> and 94 – 96% with IMR.

**Table 2** – Performance of CAD. Values represent the total number of true-positives, false-negatives and false-positives of all patients. The percentage values for the true-positives and false-negatives were calculated in relation to the total number of 28 true pulmonary nodules. The percentage values for false positives are calculated in relation to the total number of lesions detected with CAD.

	Routine dose	45% reduced dose	60% reduced dose	75% reduced dose
<b>FBP</b>				
True-positives	25/28 (89%)	27/28 (96%)	27/28 (96%)	26/28 (93%)
False-negatives	3/28 (11%)	1/28 (4%)	1/28 (4%)	2/28 (7%)
False-positives	353/378 (93%)	349/376 (93%)	364/391 (93%)	363/389 (93%)
<b>iDose<sup>+</sup> level 1</b>				
True-positives	25/28 (89%)	25/28 (89%)	25/28 (89%)	25/28 (89%)
False-negatives	3/28 (11%)	3/28 (11%)	3/28 (11%)	3/28 (11%)
False-positives	355/380 (93%)	340/365 (93%)	395/420 (94%)	390/415 (94%)
<b>iDose<sup>+</sup> level 4</b>				
True-positives	25/28 (89%)	26/28 (93%)	25/28 (89%)	26/28 (93%)
False-negatives	3/28 (11%)	2/28 (7%)	3/28 (11%)	2/28 (7%)
False-positives	372/397 (94%)	371/397 (93%)	422/447 (94%) * <i>p</i> =0.003	442/468 (94%)
<b>iDose<sup>+</sup> level 6</b>				
True-positives	26/28 (93%)	26/28 (93%)	25/28 (89%)	26/28 (93%)
False-negatives	2/28 (7%)	2/28 (7%)	3/28 (11%)	2/28 (7%)
False-positives	380/406 (94%)	403/429 (94%)	433/458 (95%)* <i>p</i> =0.002	472/498 (95%)* <i>p</i> =0.001
<b>IMR level 1</b>				
True-positives	25/28 (89%)	23/28 (82%)	25/28 (89%)	26/28 (93%)
False-negatives	3/28 (11%)	5/28 (18%)	3/28 (11%)	2/28 (7%)
False-positives	418/443 (94%)	493/516 (96%)* <i>p</i> =0.001	581/606 (96%)* <i>p</i> <0.001	630/656 (96%)* <i>p</i> <0.001
<b>IMR level 2</b>				
True-positives	25/28 (89%)	23/28 (82%)	23/28 (82%)	26/28 (93%)
False-negatives	3/28 (11%)	5/28 (18%)	5/28 (18%)	2/28 (7%)
False-positives	431/456 (95%)	531/554 (96%)* <i>p</i> <0.001	587/610 (96%)* <i>p</i> <0.001	684/710 (96%)* <i>p</i> <0.001
<b>IMR level 3</b>				
True-positives	25/28 (89%)	25/28 (89%)	25/28 (89%)	26/28 (93%)
False-negatives	3/28 (11%)	3/28 (11%)	3/28 (11%)	2/28 (7%)
False-positives	475/500 (95%)* <i>p</i> =0.003	579/604(96%)* <i>p</i> <0.001	598/623 (96%)* <i>p</i> <0.001	675/701 (96%)* <i>p</i> <0.001

\*Statistical significant difference compared to FBP at routine dose. FBP filtered back projection; IMR iterative model-based reconstruction

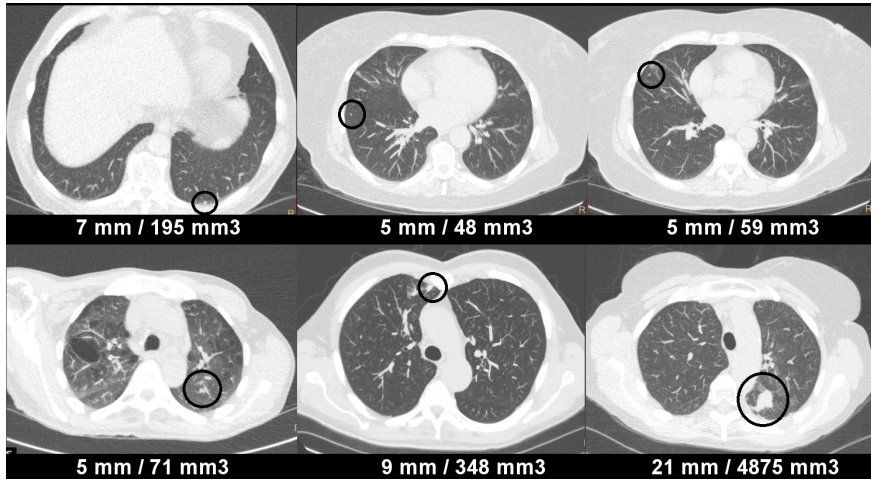


Figure 3 – Overview of the pulmonary nodules that were missed on one or more reconstructions.

Dose reduction and IR had no significant effect on the number of true-positives and false-negatives. However, the number of false-positive nodules increased significantly with IMR at all reduced dose levels up to a median of 26 pulmonary nodules with IMR level 2 at the lowest dose level (*Figure 4*). Furthermore, iDose<sup>4</sup> resulted in a significant increase at 60% reduced dose (iDose<sup>4</sup> level 4 and 6) and 75% reduced dose (iDose<sup>4</sup> level 6). Most false positive nodules were perihilar or structures in the mediastinum or intrapulmonary blood vessels.

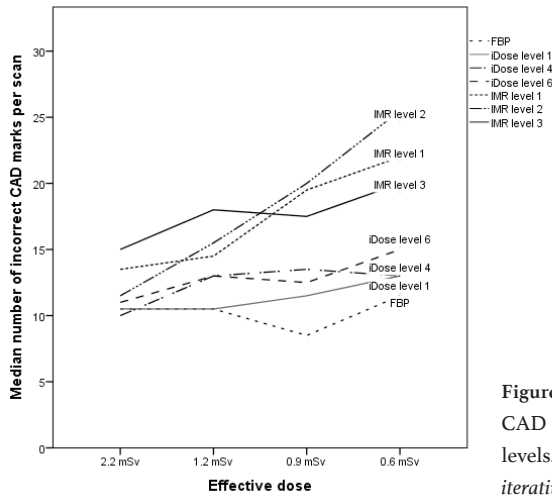


Figure 4 – Median number of incorrect CAD marks per scan at different dose levels. *FBP* filtered back projection; *IMR* iterative model-based reconstruction

## Discussion

CAD is able to identify pulmonary nodules at submillisievert dose levels and the detection rate does not deteriorate with hybrid and model-based IR. However, when scanning at reduced dose levels, IR results in an increase in the number of false-positives findings, especially with model-based IR.

Despite the fact that CAD of pulmonary nodules has been available for over ten years it is rarely used in clinical practice because it is time consuming [13]. With the expected rise in the number of chest CT acquisitions due to lung cancer screening implementation, computer assistance becomes more important [2,3]. It is essential that CAD has a high detection rate with a limited number of false positive findings to use it efficiently in clinical practice. The performance of CAD varies highly among studies and is dependent on several factors such as the type of CAD software, nodule characteristics and acquisition parameters [14]. A review article by Saba et al. [15] described an overall sensitivity of 79% for CAD alone, without assessment by a radiologist, which is in line with our findings. The sensitivity further increased to 92% when radiologists had access to CAD results [15]. The rate of false-positive findings varies widely with some studies reporting rates below 5 per patient [9,16-19] while this increased to more than 10 pulmonary nodules per patient in other studies [15,20,21]. However, low false-positive rates were often accompanied by a lower sensitivity compared to the studies reporting higher false-positive rates. Several studies investigated the effect of dose reduction on CAD. While some studies found similar sensitivity between normal and low dose scans [20,22,23], other studies found impaired sensitivity at low dose levels [14,17]. Some studies describe an increase in the number of false positive marks [22,23] at reduced dose levels while other studies describe no differences [17] or lower rates of false positives [14,20]. In our study we found a high sensitivity (89%) with FBP at routine dose compared to the literature. Furthermore, the sensitivity was not affected by dose reduction. The number of false-positives however increased at reduced dose levels but was still similar to previous reported rates [15,20,21].

To our best knowledge, only two studies investigated the effect of IR on CAD. In a phantom study performed by Wielputz and colleagues [6] both FBP and a hybrid algorithm (SAFIRE, Siemens, level 1 – 5) were used with CTDI<sub>s</sub> ranging from 8.07 to 0.25 mGy. Sensitivity remained the same up till a dose of 0.59 mGy while at 0.25 mGy a significant decrease was seen for both FBP and IR. The number of false positives was low (2 – 8 per lung) and tended to be slightly

higher with IR. The other study was performed by Yanagawa et al. [14] who used both FBP and hybrid IR (ASIR, GE, 50 and 100%) in 35 patients scanned at two dose levels. CTDIs were approximately 14.6 mGy at routine dose and decreased to 3.5 mGy at low dose. IR resulted in improved rate at both normal and reduced dose. Sensitivity decreased at reduced dose from 70% to 50% with FBP while IR resulted in a sensitivity of 67% at reduced dose. The number of false positive findings increased with IR, especially at reduced dose which is comparable to the findings in our study.

The current study indicates that radiation doses can be reduced to 0.6 mSv (1 mGy) without affecting CAD detection rates. IR did not substantially affect sensitivity, however, IR resulted in increased numbers of false-positives. This is in line with the studies of Wielputz [6] and Yanagawa [14] who also reported an increase in false-positives findings with IR. Current CAD software is trained on FBP images, however hybrid and especially model-based IR images have a different image appearance, which can lead to higher rates of false-positive CAD findings. False positives however are easily differentiated from true pulmonary nodules by a radiologist and therefore the sensitivity of CAD is more important. Furthermore, CAD software can be further improved using IR datasets.

This study has several limitations. First, the sample size was kept small because the included patients were exposed to an increased radiation dose. The small sample size might have been the reason that no significant differences in sensitivity were found. Second, we only used one CAD software package, but this is the system we use in our hospital and represents routine practice. The purpose of this study was to detect differences between FBP and IR at different dose levels and not to evaluate software performance. However, future research should evaluate the performance of different software packages at low dose IR images. Third, we only used IR algorithms from one vendor. Therefore, our results may not apply to other IR algorithms. Previous studies investigating IR algorithms from other vendors found comparable results.

The current study is the first study with an intra-individual comparison of CAD at four dose levels using IR. Also the effect of model-based IR on CAD of pulmonary nodules has not been described before. Future research should determine the effect of other IR algorithms and CAD software programs on sensitivity and false positive rates.

In conclusion, sensitivity of CAD does not decrease both with FBP and IR at submillisievert dose levels. The use of IR did result in an increased number of false-positive findings at reduced dose levels.

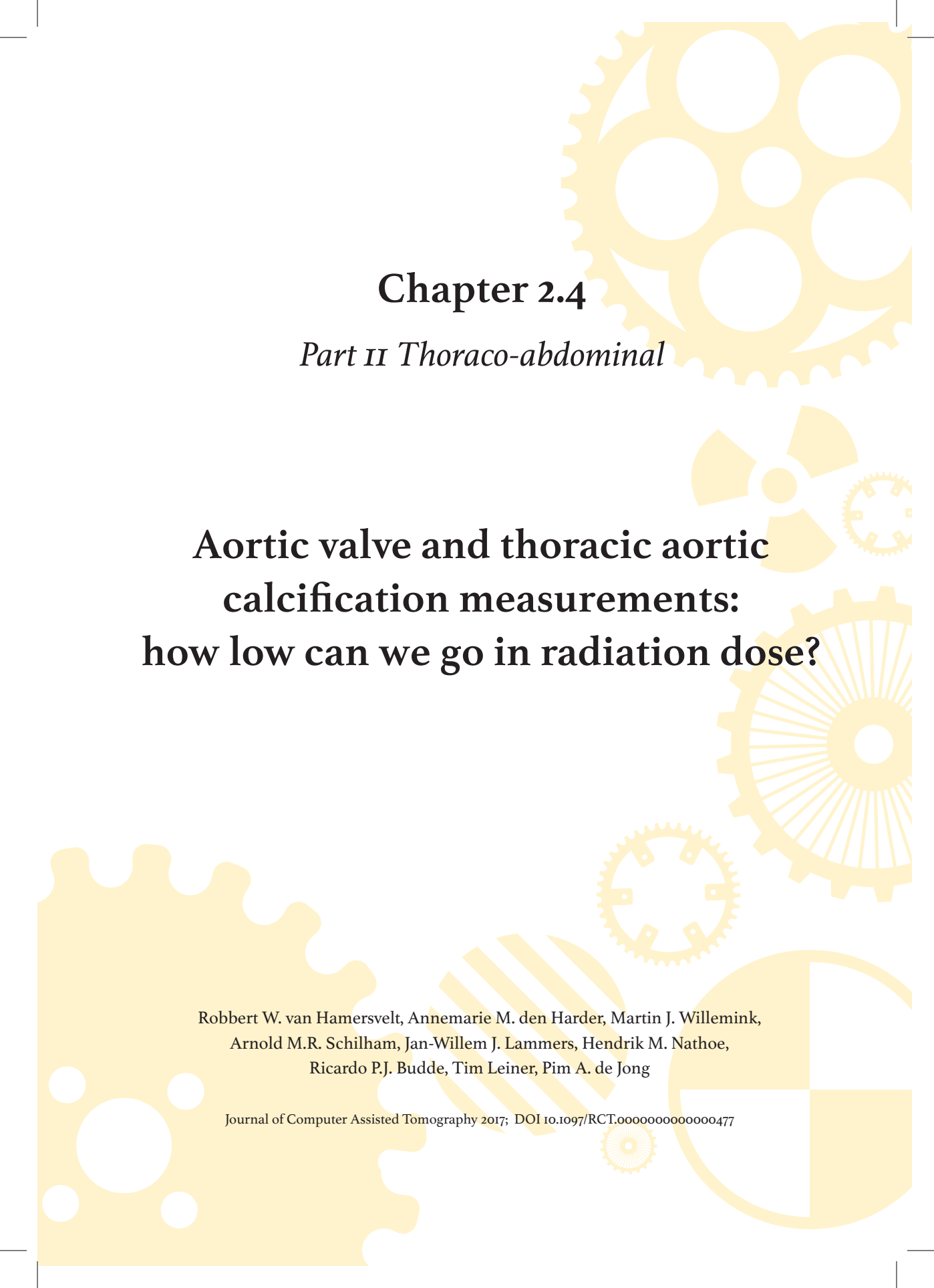
## References

- [1] Chudgar NP, Bucciarelli PR, Jeffries EM, et al., Results of the National Lung Cancer Screening Trial: Where Are We Now? *Thorac Surg Clin* 2015;25(2):145-53.
- [2] Kauczor HU, Bonomo L, Gaga M, et al., ESR/ERS white paper on lung cancer screening. *Eur Radiol* 2015.
- [3] Moyer VA, U.S. Preventive Services Task Force, Screening for lung cancer: U.S. Preventive Services Task Force recommendation statement. *Ann Intern Med* 2014;160(5):330-8.
- [4] Henschke CI, McCauley DI, Yankelevitz DF, et al., Early lung cancer action project: a summary of the findings on baseline screening. *Oncologist* 2001;6(2):147-52.
- [5] Veronesi G, Bellomi M, Mulshine JL, et al., Lung cancer screening with low-dose computed tomography: a non-invasive diagnostic protocol for baseline lung nodules. *Lung Cancer* 2008;61(3):340-9.
- [6] Wielputz MO, Wroblewski J, Lederlin M, et al., Computer-aided detection of artificial pulmonary nodules using an ex vivo lung phantom: Influence of exposure parameters and iterative reconstruction. *Eur J Radiol* 2015;84(5):1005-11.
- [7] Jeon KN, Goo JM, Lee CH, et al., Computer-aided nodule detection and volumetry to reduce variability between radiologists in the interpretation of lung nodules at low-dose screening computed tomography. *Invest Radiol* 2012;47(8):457-61.
- [8] Christe A, Leidolt L, Huber A, et al., Lung cancer screening with CT: evaluation of radiologists and different computer assisted detection software (CAD) as first and second readers for lung nodule detection at different dose levels. *Eur J Radiol* 2013;82(12):e873-8.
- [9] Brown MS, Lo P, Goldin JG, et al., Toward clinically usable CAD for lung cancer screening with computed tomography. *Eur Radiol* 2014;24(11):2719-28.
- [10] McCollough CH, Primak AN, Braun N, Kofler J, Yu L, Christner J, Strategies for reducing radiation dose in CT. *Radiol Clin North Am* 2009;47(1):27-40.
- [11] den Harder AM, Willeminck MJ, Budde RP, Schilham AM, Leiner T, de Jong PA, Hybrid and model-based iterative reconstruction techniques for pediatric CT. *AJR Am J Roentgenol* 2015;204(3):645-53.
- [12] Deak PD, Smal Y, Kalender WA, Multisection CT protocols: sex- and age-specific conversion factors used to determine effective dose from dose-length product. *Radiology* 2010;257(1):158-66.
- [13] Rubin GD, Lung nodule and cancer detection in computed tomography screening. *J Thorac Imaging* 2015;30(2):130-8.
- [14] Yanagawa M, Honda O, Kikuyama A, et al., Pulmonary nodules: effect of adaptive statistical iterative reconstruction (ASIR) technique on performance of a computer-aided detection (CAD) system-comparison of performance between different-dose CT scans. *Eur J Radiol* 2012;81(10):2877-86.

- [15] Saba L, Caddeo G, Mallarini G, Computer-aided detection of pulmonary nodules in computed tomography: analysis and review of the literature. *J Comput Assist Tomogr* 2007;31(4):611-9.
- [16] Armato SG, 3rd, Roy AS, Macmahon H, et al., Evaluation of automated lung nodule detection on low-dose computed tomography scans from a lung cancer screening program(1). *Acad Radiol* 2005;12(3):337-46.
- [17] Lee JY, Chung MJ, Yi CA, Lee KS, Ultra-low-dose MDCT of the chest: influence on automated lung nodule detection. *Korean J Radiol* 2008;9(2):95-101.
- [18] Goo JM, Kim HY, Lee JW, et al., Is the computer-aided detection scheme for lung nodule also useful in detecting lung cancer? *J Comput Assist Tomogr* 2008;32(4):570-5.
- [19] Yuan R, Vos PM, Cooperberg PL, Computer-aided detection in screening CT for pulmonary nodules. *AJR Am J Roentgenol* 2006;186(5):1280-7.
- [20] Christe A, Szucs-Farkas Z, Huber A, et al., Optimal dose levels in screening chest CT for unimpaired detection and volumetry of lung nodules, with and without computer assisted detection at minimal patient radiation. *PLoS One* 2013;8(12):e82919.
- [21] Retico A, Delogu P, Fantacci ME, Gori I, Preite Martinez A, Lung nodule detection in low-dose and thin-slice computed tomography. *Comput Biol Med* 2008;38(4):525-34.
- [22] Bodelle B, Klement D, Kerl JM, et al., 70 kV computed tomography of the thorax: valence for computer-assisted nodule evaluation and radiation dose - first clinical results. *Acta Radiol* 2014;55(9):1056-62.
- [23] Hein PA, Rogalla P, Klessen C, Lembcke A, Romano VC, Computer-aided pulmonary nodule detection - performance of two CAD systems at different CT dose levels. *Rofo* 2009;181(11):1056-64.







## Chapter 2.4

*Part II Thoraco-abdominal*

# Aortic valve and thoracic aortic calcification measurements: how low can we go in radiation dose?

Robbert W. van Hamersvelt, Annemarie M. den Harder, Martin J. Willemink,  
Arnold M.R. Schilham, Jan-Willem J. Lammers, Hendrik M. Nathoe,  
Ricardo P.J. Budde, Tim Leiner, Pim A. de Jong

Journal of Computer Assisted Tomography 2017; DOI 10.1097/RCT.0000000000000477

## Abstract

### *Objective*

To determine the lowest radiation dose and iterative reconstruction (IR) level(s) at which computed tomography (CT) based quantification of aortic valve calcification (AVC) and thoracic aortic calcification (TAC) is still feasible.

### *Methods*

Twenty-eight patients underwent a cardiac CT and 20 patients a chest CT at four different dose levels (routine dose and approximately 40%, 60% and 80% reduced dose). Data were reconstructed with filtered back projection (FBP), three iDose<sup>4</sup> levels and three iterative model-based reconstruction (IMR) levels. Two observers scored subjective image quality. AVC and TAC were quantified using mass and compared to the reference scan (routine dose reconstructed with FBP).

### *Results*

In cardiac CT at 0.35 mSv (60% reduced) all scans reconstructed with iDose<sup>4</sup> (all levels) were diagnostic, calcification detection errors occurred in only 1 patient and there were no significant differences in mass scores compared to the reference scan. Similar results were found for chest CT at 0.48 mSv (75% reduced) with iDose<sup>4</sup> levels 4 and 6 and IMR levels 1 and 2.

### *Conclusion*

IR enables AVC and TAC quantification on CT at sub-milliSievert dose.

## Introduction

Thoracic aortic calcification (TAC) and aortic valve calcification (AVC) are associated with coronary heart disease, stroke and mortality [1-5]. AVC is an independent predictor of adverse cardiovascular outcomes [6,7]. Furthermore, quantification of AVC provides prognostic information in patients with aortic valve stenosis [8]. In addition TAC is recently found to be an independent predictor for future development of coronary artery calcifications (CAC) [9,10], which is a strong predictor of adverse cardiovascular outcomes [11,12].

Cardiac and chest computed tomography (CT) are commonly performed for a wide range of indications, including chest pain, trauma and lung cancer screening. AVC and TAC can be reliably quantified on ECG-triggered unenhanced cardiac CT as well as on unenhanced untriggered chest CT [13,14]. However, radiation exposure is thought to be associated with an increased risk of developing cancer. It is estimated that about 0.4% of all cancers in the United States of America are caused by CT examinations [15]. Dose optimisation is therefore important.

When using standard filtered back projection (FBP), dose reduction is associated with more image noise and thereby reduced image quality. Image quality and noise are important for the assessment of calcifications. Image noise can be mistaken for calcifications and can, if severe, even render an examination non diagnostic [16]. To allow image acquisition at reduced dose levels iterative reconstruction (IR) techniques have been developed. IR reduces image noise and thus improves image quality and accuracy of calcium scoring on low dose CT scans [17]. Some studies suggest that radiation dose can be substantially reduced to 0.85 millisieverts (mSv) for unenhanced chest CT and 0.37 mSv for unenhanced cardiac CT while maintaining acceptable image quality [18-21]. However, it is unclear if dose reduction and IR have an effect on AVC and TAC quantification.

The aim of the current study was to find the optimal dose reduction and IR level(s) for AVC and TAC quantification on CT.

## Materials and Methods

### *Study population*

Our local institutional review board approved this prospective study (NL46146.041.13). Forty-eight patients were included between January 2014 and February 2015, written informed consent was obtained from all participants.

Patients with suspected cardiovascular disease (cardiac CT, n=28) or follow-up of pulmonary nodule(s) (chest CT, n=20) were eligible for inclusion. To reduce the risk of carcinogenesis to a minimum only patients of 50 years or older were included and patients who were pregnant or concomitantly participated in another study with X-rays were excluded. All participants were informed about the added radiation risk and provided written informed consent.

### *Image acquisition*

Each patient underwent 4 CT-scans (cardiac or chest) in a single session at four different dose levels. For the cardiac protocol this consisted of a scan at routine dose and scans at 40%, 60% and 80% reduced dose. For the chest protocol this concerned a scan at routine dose and scans at 45%, 60% and 75% reduced dose. Dose reduction was achieved by lowering the tube current (*Table 1*). The 4 different scans per patient were performed with the same scan length and same starting position. Cardiac scans were prospectively ECG-triggered and used a tube voltage of 120 kV. For patients with a weight  $\geq 80$ kg, mAs was increased by 20%. Chest scans were untriggered and 100 kV was used for patients  $< 80$ kg and 120 kV for patients  $\geq 80$ kg. All CT examinations were performed with the same 256-slice CT scanner (Brilliance iCT, Philips Healthcare, Best, The Netherlands) and no contrast agent was injected for both cardiac and chest scans. A matrix size of 512 x 512 pixels and collimation of 128 x 0.625 mm was used. For cardiac scans both slice thickness and increment were 3 mm, while for chest scans slice thickness was 1 mm and increment 0.7 mm. Volumetric CT dose index (CTDI<sub>vol</sub>) and dose-length product (DLP) were automatically recorded for each scan. The effective dose was calculated by multiplying the DLP by a conversion coefficient of 0.0145 mSv/[mGy·cm] for 120 kV acquisitions and 0.0144 mSv/[mGy·cm] for 100 kV acquisitions [22].

### *Image reconstruction*

Routine dose CT scans were reconstructed using standard FBP. Low-dose CT scans were reconstructed using FBP, three levels (1, 4 and 7 for cardiac CT and 1, 4 and 6 for chest CT) of a hybrid IR technique (iDose<sup>4</sup>, Philips Healthcare, Best, The Netherlands) and three levels (1, 2 and 3) of a prototype model-based IR technique (IMR, Philips Healthcare, Best, The Netherlands). A higher IR level implies more noise reduction. Filter CB was used for cardiac acquisitions and filter B for chest acquisitions. IMR uses different filters, therefore vendor recommended kernels were used, namely “cardiac routine” for cardiac CT and “body routine” for chest CT.

### *Subjective image quality*

The subjective image quality of each reconstruction was rated on a five-point Likert scale regarding the diagnostic value with respect to calcifications: 1=poor quality, no distinction can be made between noise and (small) calcification, non-diagnostic; 2=insufficient quality, little distinction can be made between noise and (small) calcifications, limited diagnostic value; 3=moderate quality, small chance of missing small calcifications, just diagnostic; 4=proper quality, unlikely that calcifications are missed, good diagnostic value; 5=excellent quality, certainly no calcifications are missed, excellent diagnostic value.

The rating was done by two independent blinded observers and the mean diagnostic score of each reconstruction was calculated. Reconstructions with a mean score  $\leq 2$  were excluded from further analyses. If  $>20\%$  of the scans of a reconstruction level at a certain dose reduction level were non-diagnostic, this entire reconstruction level was considered non-diagnostic and was therefore excluded from analysis.

### *Calcium quantification*

The amount of AVC and TAC was quantified using mass score (mg). The calcification scoring was performed manually by a single observer using commercially available semi-automatic software (Heartbeat CS, Philips Healthcare, Best, The Netherlands). All reconstructions per patient were assessed consecutively in a random order to minimize intra-observer variability. After clicking on a calcification, the observer instructed the software program to automatically select the calcification across multiple slices and quantified the calcification in terms of mass. The observer visually checked and if needed manually corrected the selection. In case of substantial noise and/or if noise was connected to the calcification, the selection was manually adjusted per slice to prevent overestimation of calcification measurements. A standard threshold for calcification detection was set to 130 HU in scans with a tube voltage of 120 kV. The threshold was adapted to 147 HU in acquisitions with a tube voltage of 100 kV as previously proposed [23].

If a calcium score of zero was found on the reference scan and a score  $>0$  was found on a reduced dose reconstruction, this reconstruction was considered false positive. If a calcium score  $>0$  was found on the reference scan and a calcium score of zero on a reduced dose reconstruction, this reconstruction was considered false negative.

*Statistical analysis*

The scan at routine dose reconstructed with FBP served as reference standard. All reconstructions at reduced dose were compared to the reference standard. Statistical differences of calcium scores and diagnostic image quality scores were analysed with the Friedman test ( $P < 0.05$ ) and subsequently post hoc analyses with the Wilcoxon signed rank test. For the post hoc analyses a Bonferroni corrected  $P < 0.007$  ( $0.05/\text{number of reconstruction levels used}$ ) was considered significant, unless stated otherwise. Values are listed as medians with interquartiles, unless stated otherwise. Inter-observer agreement was assessed using quadratic weighted kappa statistics ( $\kappa$ ) for the five-point Likert scale[24], interpreted as: 0=absence of agreement;  $<0.20$ =poor agreement;  $0.21-0.40$ =fair agreement;  $0.41-0.60$ =moderate agreement;  $0.61-0.80$ =good agreement;  $>0.80$ =excellent agreement [14]. Statistical analyses were performed with IBM SPSS version 20.0.0 (IBM corp., Armonk, New York, USA) and MedCalc version 13.2.2.0 (MedCalc Software, Ostend, Belgium).

**Results***Study characteristics*

Patient and dose characteristics are listed in *Table 1*. Forty-eight patients (31 males) were included which had a mean $\pm$ SD age of  $60\pm 8.8$  years and a BMI of  $28.4\pm 5.1$  kg/m<sup>2</sup>. Twenty-eight patients underwent cardiac CT and twenty patients underwent chest CT.

Mean effective radiation dose of the cardiac CT-scans were 0.86 (reference dose), 0.51 (40% reduced), 0.35 (60% reduced) and 0.17 (80% reduced) mSv. For the chest CT-scans the effective dose was 1.93 (reference dose), 1.06 (45% reduced), 0.77 (60% reduced) and 0.48 (75% reduced) mSv.

*Subjective Image quality*

The results of the diagnostic image quality assessment are provided in *Table 2*. Inter-observer agreement for visual grading was good for cardiac scans (weighted  $\kappa$ -value=0.7) and moderate for chest scans (weighted  $\kappa$ -value=0.5). At reduced dose image quality decreased significantly in all reconstructions of cardiac and chest CT, except for chest CT with iDose<sup>4</sup> level 6 and IMR level 1 and 2 at 45% reduced dose and IMR level 1 at 60% reduced dose. At lower dose IR improved image quality more compared to FBP and with improving image quality, less scans were rendered non-diagnostic (*Table 2, Figure 1*). For the cardiac scans at

Table 1. Patient and study characteristics

Group	Weight protocol	N	Age <sup>§</sup>	Male, N (%)	BMI (kg/m <sup>2</sup> ) <sup>§</sup>	kV	Dose level	mAs	CTDIvol (mGy) <sup>§</sup>	DLP (mGy·cm) <sup>§</sup>	ED (mSv) <sup>§</sup>
Cardiac	<80kg	10	56.8 (7.3)	7 (70)	24.5 (2.0)	120	Standard	50	4.17 (0.14)	53.85 (4.24)	0.78 (0.06)
							40% reduced	30	2.45 (0.09)	32.42 (2.56)	0.47 (0.04)
							60% reduced	20	1.64 (0.06)	21.65 (1.69)	0.31 (0.02)
Cardiac	≥80kg	18	54.7 (4.0)	14 (78)	30.0 (5.2)	120	Standard	60	4.89 (0.09)	62.67 (3.42)	0.91 (0.05)
							40% reduced	36	2.93 (0.06)	37.62 (2.20)	0.55 (0.03)
							60% reduced	24	1.96 (0.04)	25.16 (1.45)	0.36 (0.02)
Chest	<80kg	9	67.7 (9.5)	4 (45)	25.3 (3.3)	100	Standard	60	2.43 (0.01)	95.57 (6.13)	1.37 (0.09)
							45% reduced	33	1.33 (0.01)	52.51 (3.45)	0.75 (0.05)
							60% reduced	24	0.96 (0.01)	38.00 (2.12)	0.55 (0.03)
Chest	≥80kg	11	65.4 (8.2)	6 (55)	32.0 (4.8)	120	Standard	60	4.06 (0.00)	164.97 (9.63)	2.39 (0.14)
							45% reduced	33	2.22 (0.02)	90.75 (4.90)	1.32 (0.07)
							60% reduced	24	1.61 (0.02)	65.79 (3.65)	0.95 (0.05)
							75% reduced	15	1.02 (0.00)	41.45 (2.28)	0.60 (0.03)

<sup>§</sup>Data depicted as mean (standard deviation). BMI=body mass index; CTDIvol=CT volume dose index; DLP=dose-length product; ED=effective radiation dose, estimated as DLP·k (k=0.0144 for 100 kV and k=0.0145 for 120 kV); N=number of patients

Table 2. Image quality and diagnostic value. Image quality is depicted as median (IQ). FP and FN values are defined for diagnostic scans only

Recon-structure	Cardiac						Chest							
	Image quality (N=28)		AVC		TAC		Image quality (N=20)		N. Diagnostic		AVC		TAC	
	FP	FN	FP	FN	FP	FN	FP	FN	FP	FN	FP	FN	FP	FN
<b>Routine dose</b>														
FBP	5.0 (4.5-5.0)	28	0	0	3	0	4.0 (3.9-4.0)	20	0	1	0	1	0	
<b>40% / 45% reduced dose</b>														
FBP	4.5 (3.5-4.6)*	28	0	0	3	0	3.5 (3.0-3.5)*	20	0	0	0	1	0	
iDose <sup>4</sup> I1	4.5 (4.0-4.6)*	28	0	0	0	0	3.5 (3.5-3.6)*	20	0	0	0	0	0	
iDose <sup>4</sup> L4	4.5 (4.0-4.5)*	28	0	0	0	0	3.5 (3.5-4.0)*	20	0	0	0	0	0	
iDose <sup>4</sup> I7/6	4.0 (4.0-4.0)*	28	0	0	0	1	4.0 (4.0-4.0)	20	0	0	0	0	0	
IMR I1	4.0 (4.0-4.0)*	28	0	1	8	0	4.0 (4.0-4.0)	20	0	1	0	0	0	
IMR I2	4.0 (4.0-4.0)*	28	0	1	8	0	4.0 (4.0-4.0)	20	0	1	0	0	0	
IMR I3	3.5 (3.0-3.5)*	28	0	1	9	0	3.5 (3.4-3.5)*	20	0	1	1	0	0	
<b>60% / 60% reduced dose</b>														
FBP	3.5 (3.0-4.1)*	25	0	0	4	0	3.0 (2.5-3.0)*	13	0	1	1	0	0	
iDose <sup>4</sup> I1	4.0 (3.8-4.5)*	28	0	0	1	0	3.5 (3.0-3.5)*	20	0	1	0	0	0	
iDose <sup>4</sup> L4	4.0 (4.0-4.5)*	28	0	0	0	1	3.5 (3.5-3.6)*	20	0	1	0	0	0	
iDose <sup>4</sup> I7/6	4.0 (3.5-4.0)*	28	0	1	0	1	3.5 (3.5-4.0)*	20	0	1	0	0	0	
IMR I1	4.0 (4.0-4.0)*	28	0	0	9	1	4.0 (3.5-4.0)	20	0	1	1	0	0	
IMR I2	4.0 (3.5-4.1)*	28	0	0	9	2	3.5 (3.5-4.0)*	20	0	2	1	0	0	
IMR I3	3.0 (3.0-3.5)*	27	0	1	8	2	3.0 (3.0-3.0)*	20	0	2	1	0	0	
<b>80% / 75% reduced dose</b>														
FBP	2.5 (2.0-3.0)*	15	0	1	9	0	2.0 (1.9-2.1)*	2	0	0	1	0	0	
iDose <sup>4</sup> I1	3.5 (3.0-4.0)*	27	0	0	5	0	2.5 (2.5-3.0)*	18	0	1	1	0	0	
iDose <sup>4</sup> L4	3.5 (3.0-4.0)*	27	0	0	7	0	3.0 (3.0-3.5)*	20	0	1	1	0	0	
iDose <sup>4</sup> I7/6	3.5 (3.0-3.6)*	25	0	2	5	1	3.0 (3.0-3.5)*	20	0	1	1	0	0	
IMR I1	3.5 (3.0-4.0)*	28	0	1	8	2	3.5 (3.0-4.0)*	20	0	1	0	0	0	
IMR I2	3.0 (3.0-3.5)*	26	0	1	9	2	3.0 (3.0-3.5)*	20	0	1	0	0	0	
IMR I3	3.0 (2.5-3.0)*	19	0	1	7	2	3.0 (2.5-3.0)*	18	0	1	0	0	0	

\*= significant difference compared to FBP at routine dose (Bonferroni  $P < 0.007$ ). AVC= Aortic valve calcification, FN= False negative, FP= False positive, I= level, N. Diagnostic= number of patients with a diagnostic scan (diagnostic score  $\geq 2$  or agreed after discussion when one observer scored 2 and the other 3), TAC= Thoracic aortic calcification

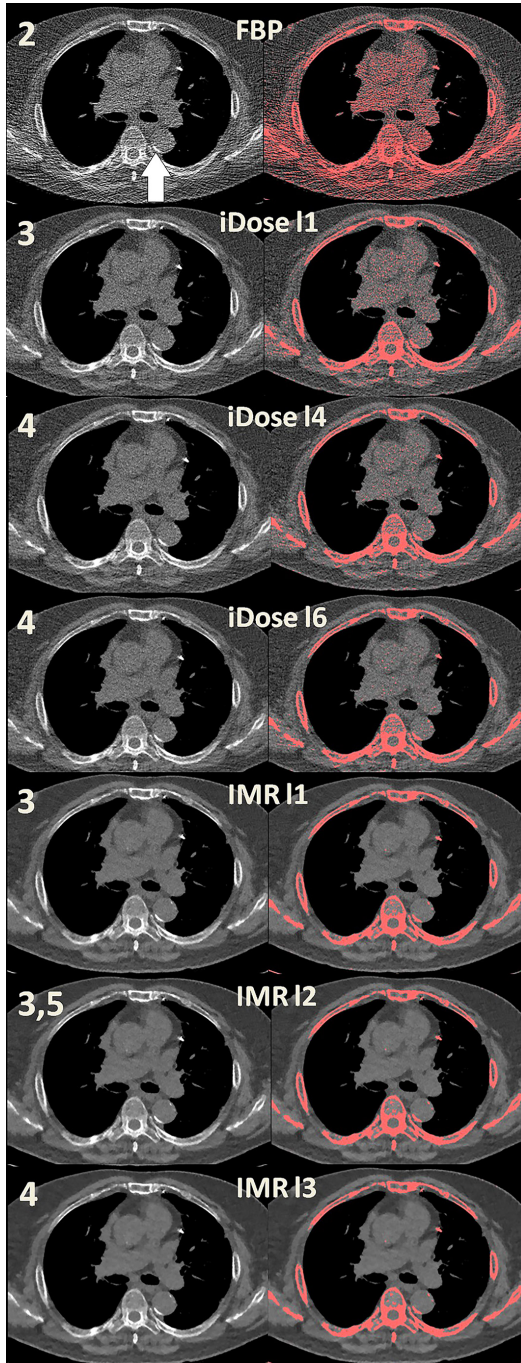


Figure 1 – Chest CT at 75% reduced dose of one single patient with TAC (white arrow). All images are taken at the same slice position. In the right series values >130HU are highlighted pink, indicating the effect of different iterative reconstruction levels on image noise. Diagnostic score of these scans are depicted in the left upper corner as mean of the two observers. FBP= Filtered back projection, IMR= iterative model reconstruction, l= level

Part II

80% reduced dose FBP and IMR level 3 were in more than 20% of the patients of insufficient quality and hence rated as non-diagnostic. For chest scans with FBP the same was found at 45% and 75% reduced dose, while IR reconstructions resulted in sufficient image quality in >80% of the patients at all dose levels.

#### *Calcium quantification - Cardiac CT*

Six patients (21%) had AVC and ten patients (36%) TAC scores higher than zero on the reference scan (routine dose reconstructed with FBP). A high false positive (FP) rate (3-9 patients) for TAC was observed for FBP and all IMR reconstruction levels at all dose reduction levels. A high FP rate for TAC was also seen for all iDose<sup>4</sup> levels at maximum reduced dose, while at 40% and 60% reduced dose a maximum of one FP or false negative (FN) was observed for iDose<sup>4</sup> (Table 2). No FP for AVC was found at any reduced dose level. Overall the FN rate of TAC and AVC were low with a maximum of two.

Calcification mass of patients with a calcium score higher than zero are listed in Table 3. When compared to FBP at routine dose, AVC and TAC mass scores did not change significantly at reduced dose with application of IR (Table 3).

Absolute differences in TAC mass were overall lower with iDose<sup>4</sup> than with IMR (Figure 2). Absolute differences in AVC mass declined with increasing IMR levels and increased with increasing iDose<sup>4</sup> levels.

#### *Calcium quantification - Chest CT*

Eight patients (40%) had AVC and seventeen patients (85%) TAC scores higher than zero on the reference scan. A maximum of one FP and zero FN for TAC and zero FP and two FN for AVC were found for all reconstructions at all dose reduction levels (Table 2).

Post hoc analyses showed no significant difference for AVC mass scores at any reduced dose level when compared to FBP at routine dose (Table 3). However, a significant difference for TAC mass was found with FBP at 45% reduced dose, iDose<sup>4</sup> level 1 at 75% reduced dose and iDose<sup>4</sup> level 6 at 45% and 60% reduced dose (Table 3). No significant differences were found with IMR (all levels) at any reduced dose level.

Absolute differences of TAC mass were overall lower with IMR than with iDose<sup>4</sup> reconstructions (Figure 2). Absolute differences of AVC mass remained the same with increasing IMR levels and increased with increasing iDose<sup>4</sup> levels.

Table 3. Calcification mass scores of patients with non-zero scores, depicted as median with interquartiles.

	FBP	iDose <sup>1</sup> I <sub>1</sub>	iDose <sup>1</sup> I <sub>4</sub>	iDose <sup>1</sup> I <sub>6/7</sub>	IMR I <sub>r</sub>	IMR I <sub>2</sub>	IMR I <sub>3</sub>
<b>AVC in cardiac group (N=6)</b>							
Routine	12.0(1.4-24.0)						
40% reduced <sup>o</sup>	11.6(2.2-21.1)	11.4(0.9-18.7)	10.8(1.1-18.8)	10.4(0.8-17.5)	14.2(1.5-28.7)	13.8(1.6-28.1)	13.6(1.6-27.6)
60% reduced <sup>o</sup>	9.6(1.3-30.7) <sup>*</sup>	10.8(1.2-22.4)	9.8(0.8-20.3)	8.4(0.6-18.2)	10.9(2.6-27.6)	10.6(2.4-26.2)	10.3(2.0-25.6)
80% reduced <sup>ooo</sup>	ND	12.6(2.3-23.3)	11.2(1.2-21.0)	5.6(0.0-21.8) <sup>*</sup>	9.6(1.6-26.2)	7.9(0.8-24.4)	ND
<b>TAC in cardiac group (N=10)</b>							
Routine	2.7(1.1-15.8)						
40% reduced <sup>o</sup>	3.9(1.5-42.3)	3.0(1.9-19.4)	2.6(1.4-17.1)	2.1(1.3-17.6)	4.6(3.0-17.4)	4.2(2.6-18.0)	5.5(2.2-17.9)
60% reduced <sup>o</sup>	5.2(3.5-29.7)	2.8(1.7-16.2)	2.7(0.9-16.0)	2.1(0.6-15.9)	4.2(1.8-18.9)	5.7(1.3-18.3)	4.7(1.2-18.1)
80% reduced <sup>ooo</sup>	ND	5.8(2.6-21.6)	4.3(2.1-14.7)	2.4(0.7-19.6) <sup>*</sup>	5.8(1.2-15.3)	5.1(0.4-19.2) <sup>*</sup>	ND
<b>AVC in chest group (N=8)</b>							
Routine	17.0(4.9-50.2)						
45% reduced <sup>o</sup>	22.8(4.2-46.8)	18.2(2.5-44.4)	15.4(2.0-42.8)	15.3(0.9-41.5)	14.8(0.5-46.8)	15.8(0.4-47.1)	14.5(0.3-47.1)
60% reduced <sup>oo</sup>	ND	17.5(4.8-47.0)	14.2(3.5-45.5)	11.1(2.6-42.7)	12.1(0.5-46.2)	12.1(0.4-45.9)	11.1(0.2-45.4)
75% reduced <sup>ooo</sup>	ND	19.1(6.0-47.1)	12.9(5.1-44.8)	10.6(3.6-44.0)	8.2(2.1-44.5)	8.8(1.6-44.0)	10.9(1.0-47.1) <sup>*</sup>
<b>TAC in chest group (N=17)</b>							
Routine	455.6(132.6-1796.9)						
45% reduced <sup>o</sup>	499.1(146.6-1875.4) <sup>*</sup>	478.7(129.5-1823.8)	453.4(131.2-1778.0)	440.7(123.6-1748.6) <sup>*</sup>	466.8(129.9-1850.8)	464.6(123.0-1864.1)	464.8(129.0-1855.0)
60% reduced <sup>oo</sup>	ND	472.8(125.7-1835.6)	451.3(123.5-1783.8)	438.5(120.9-1717.5) <sup>*</sup>	454.2(126.9-1811.3)	453.0(124.5-1813.9)	453.4(123.7-1801.0)
75% reduced <sup>ooo</sup>	ND	538.7(176.6-2222.2) <sup>**</sup>	487.1(132.7-1867.8)	462.8(129.6-1797.0)	478.6(127.5-1836.7)	476.6(129.4-1837.7)	575.8(160.9-2362.6) <sup>**</sup>

<sup>\*</sup>= Total number of diagnostic scans is one less due to one non-interpretable reconstruction, <sup>\*\*</sup>= total number of diagnostic scans is two less due to two non-interpretable reconstruction, <sup>o</sup>= significant difference compared to FBP at routine dose, <sup>oo</sup>= Bonferroni correction of (0.05/7)= P<0.007 was considered significant, <sup>ooo</sup>= Bonferroni correction of (0.05/6)= P<0.008 was considered significant, <sup>oooo</sup>= Bonferroni correction of (0.05/5)= P<0.01 was considered significant. AVC= aortic valve calcification, FBP= filtered back projection, IMR= iterative model reconstruction, I= level, N= number of patients, ND= non-diagnostic (>20% of the scans were of insufficient quality), TAC= thoracic aortic calcification



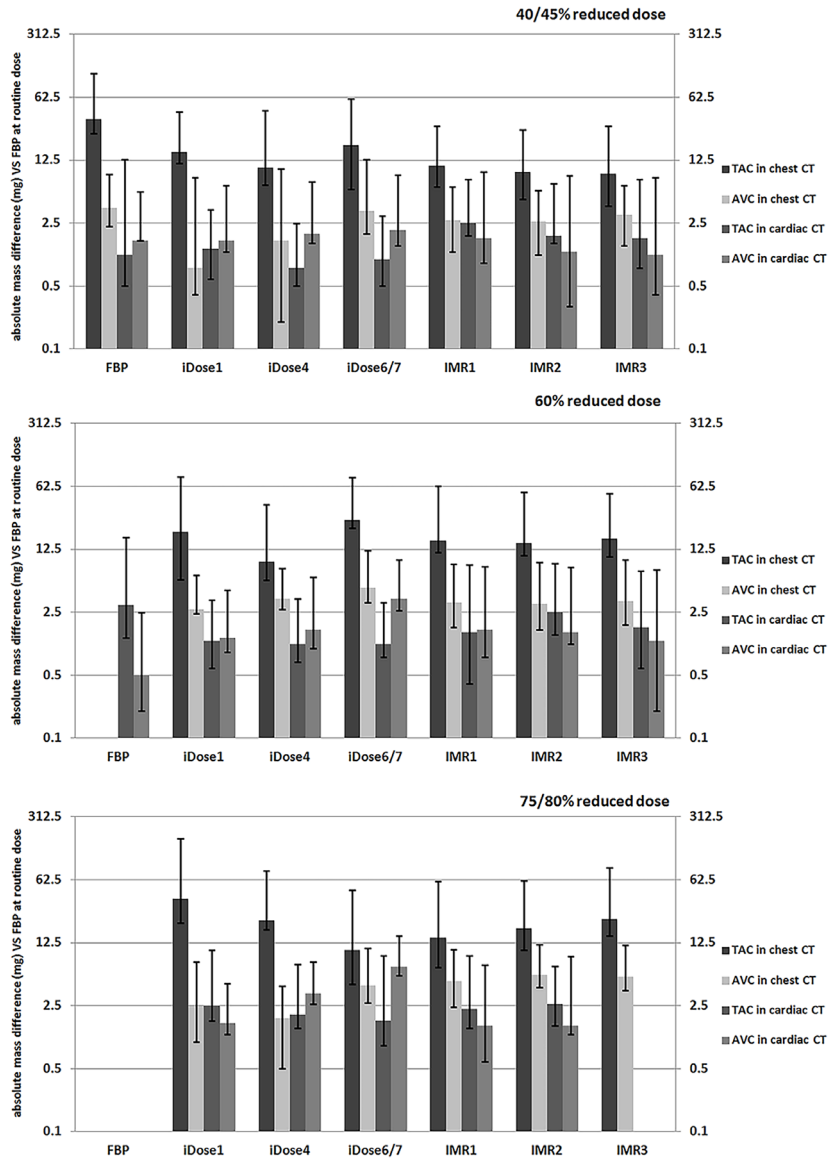


Figure 2 – Absolute difference in mass between reconstruction methods in patients with non-zero calcification. Differences are depicted as median absolute difference compared to the reference scan (FBP at routine dose). Error bars indicate interquartiles. AVC= aortic valve calcification, CT= computed tomography, FBP= filtered back projection, iDose1= iDose level 1 (etc.), IMR1= IMR level 1 (etc.), IMR= iterative model reconstruction, TAC= thoracic aortic calcification

## Discussion

In this study we found that when reducing radiation dose, down to an effective radiation dose of 0.35 mSv for cardiac CT and 0.48 mSv for chest CT, IR allows for AVC and TAC scoring on CT scans acquired for coronary calcium scoring and pulmonary nodule volumetry. We also found that at lower dose rating of TAC on cardiac scans becomes more problematic in terms of false positives.

We evaluated several aspects of the images to reach our conclusion. Firstly, the number of diagnostic scans was investigated, because if image quality is too low, no conclusions can be made on the presence or severity of calcifications. Secondly, false positives and negatives were deemed relevant as this can cause over- or under prediction and possibly influence treatment. Thirdly, calcium scores were compared to routine dose scores because deviating calcium scores could also affect predictive value. The same holds true for our fourth parameter, the absolute difference in calcium score. A weighted assessment of these aspects would enable us to identify the optimal dose and IR level.

For cardiac CT, we have observed the lower limit of what is possible with our system and current IR techniques. In our 80% dose reduction protocol many non-diagnostic scans were found as well as a high false positive rate for calcifications that were not visible on the routine dose scan. We think that, with application of iDose<sup>4</sup> levels 1, 4 or 7, 60% reduced dose (0.35 mSv) is the lowest dose achievable for AVC and TAC scoring on unenhanced ECG-triggered cardiac CT. At this dose level only these IR levels showed a low acceptable FP and FN rate, we did not have to excluded scans and we did not observe significant differences in mass scores. For unenhanced untriggered chest CT, we think that the optimal dose is 0.48 mSv (our 75% dose reduction protocol) if reconstructed with IMR levels 1 and 2 or iDose<sup>4</sup> levels 4 and 6. For these IR levels FP and FN rates were low and mass scores were of insignificant difference compared to FBP at routine dose. Since 0.48 mSv was the lowest dose we tested maybe even more dose reduction could be achieved for AVC and TAC scoring.

Multiple studies on subjective and objective image quality have suggested the feasibility of dose reduction with IR in unenhanced cardiac and chest CT [18-21,25,26]. In line with these studies we found that the application of IR at low dose scans improved image quality compared to FBP at the same dose level. However, improved image quality does not necessarily mean good diagnostic value. The optimal dose reduction and IR level is therefore in particular determined by diagnostic value. It can be assumed that low dose CT with IR can safely replace the standard dose CT if the diagnostic value is equal or better.

Previous work by colleagues den Harder et al. [25,27,28] and Willemink et al.[29] showed the feasibility of pulmonary nodule volumetry and CAC scoring on low dose unenhanced chest and cardiac CT scans using IR. However, the feasibility of dose reduction and IR for other indications, such as infections, interstitial lung disease and skeletal assessment is currently uncertain. Den Harder et al.[27,28] showed that for the detection of pulmonary nodules, unenhanced chest CT can be reduced to submillisievert dose when using IR. Willemink et al.[29] evaluated CAC on low dose unenhanced cardiac CT using IR. CAC is the main indication for unenhanced cardiac CT and is the most widely used calcium scoring in clinical use. Willemink et al.[29] showed that with the use of IR at 80% reduced dose (0.15-0.18 mSv) CAC scoring is possible with reclassification rates below 15%. However, no AVC and/or TAC was taken into account. Since AVC and TAC are associated with coronary heart disease, stroke and mortality [1-5] and are found to be independent predictors for adverse cardiovascular outcomes [6,7,9,10], we seek to find the optimal dose reduction and IR level(s) for AVC and TAC quantification on CT. To our best knowledge this is the first study that aimed to find the optimal dose reduction and IR level for quantifying AVC and TAC separately in patients who underwent CT for cardiac and pulmonary indications.

Previously, Hecht et al.[18] investigated the accuracy of scoring coronary artery calcification and in addition TAC combined with AVC (called “aortic calcification”) in 102 patients at two dose levels using hybrid IR. Images acquired with iDose<sup>4</sup> level 7 at low dose ECG-triggered cardiac CT (0.37±0.16 mSv) were compared to standard dose (0.76±0.34 mSv) images reconstructed with iDose<sup>4</sup> level 3. Dose reduction was achieved by lowering mAs with 50%. For “aortic calcification” they found no significant difference in Agatston or mass scores between these dose levels. However, they found a significant difference (p=0.03) for volume with a mean of 88.8±204.0 mm<sup>3</sup> at low dose (iDose<sup>4</sup> level 7) and 93.7±207.3 mm<sup>3</sup> at standard dose (iDose<sup>4</sup> level 3). The dose reductions investigated are comparable to cardiac CT routine dose and 60% reduced dose in our study. In contrast to this study we did not find a significant difference in mass score for AVC and TAC, neither separately nor combined, with the application IR.

In the current study, the amount of calcium was quantified using mass. Although the Agatston score is more widely used, mass is suggested to be a more robust quantification method than Agatston score [30] and was found to be less influenced by IR at low dose scans [25,31]. In addition previous studies have

shown that mass is less influenced by tube voltage and is better reproducible than Agatston [32,33].

Findings of the current study indicate that clinical implementation of AVC and TAC scoring on low dose CT using IR could possibly be achievable in low dose lung and cardiac scans with a range of indications, such as lung cancer screening CT. Previous research already showed an excellent inter-scan and inter-observer agreement for AVC scoring in unenhanced untriggered lung cancer screening chest CT (<0.9 mSv for <80kg and <1.6 mSv for ≥80kg) [14]. In the current study, at the same amount of effective radiation dose and even lower dose down to 0.35 mSv for cardiac CT and 0.48 mSv for chest CT, we found reliable AVC and TAC scoring when using IR. This implies that AVC and TAC could be quantified at unenhanced untriggered lung cancer screening chest CT.

The strength of our study is the fact that we not only evaluated image quality but primarily investigated diagnostic value to find the optimal dose reduction and IR level for measuring aortic and aortic valve calcifications. In addition we compared four different dose levels per patient, three levels of a hybrid and three levels of a model based IR algorithm, which enabled us to make a good comparison and a stronger recommendation. Our study also has some limitations. For ethical reasons the sample size was kept low. Since calcifications were not present in every patient, the sample size of our subgroups was even smaller. Nevertheless we think the power is sufficient since our study has a within-patient analysis of four scans and twenty-two reconstructions per patient. A larger-scale study with two dose levels may be required to confirm our findings. Another limitation is the consecutive scoring of all twenty-two reconstructions per patients by one observer. This could introduce recall bias of the location of calcifications for lower dose scans. However, the advantage is that intra-observer variation is hereby kept low. Finally, application of our recommendations may be limited to the vendor used in our study since all vendors developed their own IR techniques.

In conclusion this study shows that IR allows for reliable AVC and TAC scoring when reducing dose down to 0.35 mSv on unenhanced ECG-triggered cardiac CT and down to 0.48 mSv on unenhanced untriggered chest CT. At these dose reduction levels, iDose<sup>4</sup> levels 1, 4 and 7 for cardiac CT and iDose<sup>4</sup> levels 4 and 6 and IMR levels 1 and 2 for chest CT could be considered the optimal iterative reconstruction level.

## References

- [1] Santos RD, Rumberger JA, Budoff MJ, et al., Thoracic aorta calcification detected by electron beam tomography predicts all-cause mortality. *Atherosclerosis* 2010;209(1):131-5.
- [2] Jacobs PC, Prokop M, van der Graaf Y, et al., Comparing coronary artery calcium and thoracic aorta calcium for prediction of all-cause mortality and cardiovascular events on low-dose non-gated computed tomography in a high-risk population of heavy smokers. *Atherosclerosis* 2010;209(2):455-62.
- [3] Hermann DM, Lehmann N, Gronewold J, et al., Thoracic aortic calcification is associated with incident stroke in the general population in addition to established risk factors. *Eur Heart J Cardiovasc Imaging* 2015;16(6):684-90.
- [4] Otto CM, Lind BK, Kitzman DW, Gersh BJ, Siscovick DS, Association of aortic-valve sclerosis with cardiovascular mortality and morbidity in the elderly. *N Engl J Med* 1999;341(3):142-7.
- [5] Clavel MA, Pibarot P, Messika-Zeitoun D, et al., Impact of aortic valve calcification, as measured by MDCT, on survival in patients with aortic stenosis: results of an international registry study. *J Am Coll Cardiol* 2014;64(12):1202-13.
- [6] Owens DS, Budoff MJ, Katz R, et al., Aortic valve calcium independently predicts coronary and cardiovascular events in a primary prevention population. *JACC Cardiovasc Imaging* 2012;5(6):619-25.
- [7] Mets OM, Vliegenthart R, Gondrie MJ, et al., Lung cancer screening CT-based prediction of cardiovascular events. *JACC Cardiovasc Imaging* 2013;6(8):899-907.
- [8] Utsunomiya H, Yamamoto H, Kitagawa T, et al., Incremental prognostic value of cardiac computed tomography angiography in asymptomatic aortic stenosis: significance of aortic valve calcium score. *Int J Cardiol* 2013;168(6):5205-11.
- [9] Brodov Y, Gransar H, Rozanski A, et al., Extensive thoracic aortic calcification is an independent predictor of development of coronary artery calcium among individuals with coronary artery calcium score of zero. *Atherosclerosis* 2015;238(1):4-8.
- [10] Rivera JJ, Nasir K, Katz R, et al., Relationship of thoracic aortic calcium to coronary calcium and its progression (from the Multi-Ethnic Study of Atherosclerosis [MESA]). *Am J Cardiol* 2009;103(11):1562-7.
- [11] Detrano R, Guerci AD, Carr JJ, et al., Coronary calcium as a predictor of coronary events in four racial or ethnic groups. *N Engl J Med* 2008;358(13):1336-45.
- [12] Greenland P, LaBree L, Azen SP, Doherty TM, Detrano RC, Coronary artery calcium score combined with Framingham score for risk prediction in asymptomatic individuals. *JAMA* 2004;291(2):210-5.
- [13] Budoff MJ, Nasir K, Kinney GL, et al., Coronary artery and thoracic calcium on noncontrast thoracic CT scans: comparison of ungated and gated examinations in patients from the COPD Gene cohort. *J Cardiovasc Comput Tomogr* 2011;5(2):113-8.

- [14] van Hamersvelt RW, Willeminck MJ, Takx RA, et al., Cardiac valve calcifications on low-dose unenhanced ungated chest computed tomography: inter-observer and inter-examination reliability, agreement and variability. *Eur Radiol* 2014;24(7):1557-64.
- [15] Brenner DJ, Hall EJ, Computed tomography--an increasing source of radiation exposure. *N Engl J Med* 2007;357(22):2277-84.
- [16] Bittencourt M.S., Schmidt B., Seltmann M., et al., Iterative reconstruction in image space (IRIS) in cardiac computed tomography: Initial experience. *Int J Card Imaging* 2011;27(7):1081-7.
- [17] Brooks R.A., Di CG, Theory of image reconstruction in computed tomography. *Radiology* 1975;117(3):561-72.
- [18] Hecht HS, de Siqueira ME, Cham M, et al., Low- vs. standard-dose coronary artery calcium scanning. *Eur Heart J Cardiovasc Imaging* 2015;16(4):358-63.
- [19] Hu X.H., Ding X.F., Wu R.Z., Zhang M.M., Radiation dose of non-enhanced chest CT can be reduced 40% by using iterative reconstruction in image space. *Clin Radiol* 2011;66(11):1023-9.
- [20] Willeminck MJ, Leiner T, de Jong PA, et al., Iterative reconstruction techniques for computed tomography part 2: initial results in dose reduction and image quality. *Eur Radiol* 2013;23(6):1632-42.
- [21] Katsura M, Matsuda I, Akahane M, et al., Model-based iterative reconstruction technique for radiation dose reduction in chest CT: comparison with the adaptive statistical iterative reconstruction technique. *Eur Radiol* 2012;22(8):1613-23.
- [22] Deak PD, Smal Y, Kalender WA, Multisection CT protocols: sex- and age-specific conversion factors used to determine effective dose from dose-length product. *Radiology* 2010;257(1):158-66.
- [23] Marwan M, Mettin C, Pflederer T, et al., Very low-dose coronary artery calcium scanning with high-pitch spiral acquisition mode: comparison between 120-kV and 100-kV tube voltage protocols. *J Cardiovasc Comput Tomogr* 2013;7(1):32-8.
- [24] Norman G, Likert scales, levels of measurement and the "laws" of statistics. *Adv Health Sci Educ Theory Pract* 2010;15(5):625-32.
- [25] den Harder AM, Willeminck MJ, Bleys RL, et al., Dose reduction for coronary calcium scoring with hybrid and model-based iterative reconstruction: an ex vivo study. *Int J Cardiovasc Imaging* 2014;30(6):1125-33.
- [26] Yamada Y, Jinzaki M, Hosokawa T, et al., Dose reduction in chest CT: comparison of the adaptive iterative dose reduction 3D, adaptive iterative dose reduction, and filtered back projection reconstruction techniques. *Eur J Radiol* 2012;81(12):4185-95.
- [27] den Harder AM, Willeminck MJ, de Ruyter QM, et al., Achievable dose reduction using iterative reconstruction for chest computed tomography: A systematic review. *Eur J Radiol* 2015;84(11):2307-13.

- [28] den Harder AM, Willemink MJ, van Hamersvelt RW, et al., Pulmonary Nodule Volumetry at Different Low Computed Tomography Radiation Dose Levels With Hybrid and Model-Based Iterative Reconstruction: A Within Patient Analysis. *J Comput Assist Tomogr* 2016;40(4):578-83.
- [29] Willemink MJ, den Harder AM, Foppen W, et al., Finding the optimal dose reduction and iterative reconstruction level for coronary calcium scoring. *J Cardiovasc Comput Tomogr* 2016;10(1):69-75.
- [30] Hoffmann U, Siebert U, Bull-Stewart A, et al., Evidence for lower variability of coronary artery calcium mineral mass measurements by multi-detector computed tomography in a community-based cohort--consequences for progression studies. *Eur J Radiol* 2006;57(3):396-402.
- [31] Willemink MJ, Takx RA, de Jong PA, et al., The impact of CT radiation dose reduction and iterative reconstruction algorithms from four different vendors on coronary calcium scoring. *Eur Radiol* 2014;24(9):2201-12.
- [32] Deprez FC, Vlassenbroek A, Ghaye B, Raaijmakers R, Coche E, Controversies about effects of low-kilovoltage MDCT acquisition on Agatston calcium scoring. *J Cardiovasc Comput Tomogr* 2013;7(1):58-61.
- [33] Rutten A, Isgum I, Prokop M, Coronary calcification: effect of small variation of scan starting position on Agatston, volume, and mass scores. *Radiology* 2008;246(1):90-8.





# Chapter 2.5

*Part II Thoraco-abdominal*

## **Radiation dose reduction for CT assessment of urolithiasis using iterative reconstruction: a prospective intra-individual study**

Annemarie M. den Harder, Martin J. Willemink, Pieter J. van Doormaal,  
Frank J. Wessels, M.T.W.T. (Tycho) Lock, Arnold M.R. Schilham,  
Ricardo P.J. Budde, Tim Leiner, Pim A. de Jong

European Radiology 2017; DOI 10.1007/s00330-017-4929-2

## Abstract

### *Objectives*

To assess the performance of hybrid (HIR) and model-based iterative reconstruction (MIR) in patients with urolithiasis at reduced dose computed tomography (CT).

### *Methods*

Twenty patients scheduled for unenhanced abdominal CT for follow-up of urolithiasis were prospectively included. Routine dose acquisition was followed by three low dose acquisitions at 40%, 60% and 80% reduced doses. All images were reconstructed with filtered back projection (FBP), HIR and MIR. Urolithiasis detection rates, gall bladder, appendix and rectosigmoid evaluation and overall subjective image quality were evaluated by two observers.

### *Results*

In total 74 stones were present in 17 patients. Half of the stones were not detected on FBP at the lowest dose level, but this improved with MIR to a sensitivity of 100%. HIR resulted in a slight decrease in sensitivity at the lowest dose to 72%, but outperformed FBP. Evaluation of other structures with HIR at 40% and with MIR at 60% dose reductions was comparable to FBP at routine dose, but 80% dose reduction resulted in non-evaluable images.

### *Conclusions*

The CT radiation dose for urolithiasis detection can be safely reduced with 40% (HIR) to 60% (MIR) without affecting assessment of urolithiasis, possible extra-urinary tract pathology or overall image quality.

## Introduction

The most frequent cause of acute flank pain is urolithiasis, which affects 3-5% of the population [1]. The risk of recurrence of urolithiasis is high with 50% after 5 years and more than 72% after 20 years [2]. In the USA, the total estimated annual cost for stone disease was over US\$ 10.3 billion in 2006, an almost five-fold increase in six years [3]. This rise is still present today. Unenhanced computed tomography (CT) is often used for the diagnosis of urolithiasis. Compared to ultrasonography CT offers the possibility to detect extra-urinary causes of flank pain [1], and has a higher specificity and sensitivity. The guidelines of the European Association of Urology [4] as well as the American College of Radiology [5] advise to use low dose CT in patients with acute disease and suspicion of urolithiasis, while the American Urological Association provides no clear recommendation [6]. However, CT suffers from several disadvantages such as higher costs compared to ultrasonography, limited availability in developing countries and the associated exposure to ionizing radiation. Technical advancements like iterative reconstruction (IR) algorithms have resulted in substantial radiation dose reductions. IR results in reduced noise, allowing to acquire images at reduced radiation dose levels without intrinsically hampering image quality. Several studies have investigated the potential of IR for unenhanced abdominal CT, with most studies focusing on urinary stone detection and image quality [7-10]. The purpose of this study was to assess the performance of hybrid IR (HIR) and model-based IR (MIR) in patients with urolithiasis at reduced dose CT.

## Materials and methods

This prospective study was approved by our local institutional review board (NL46146.041.13). Inclusion criteria were: patient age of  $\geq 40$  years and a scheduled unenhanced abdominal CT for follow-up of urolithiasis. Patients with concomitant participation in another study with x-ray exposure were excluded. All patients were informed about the additional radiation exposure and provided written informed consent. Gender, age, height and weight of all patients were recorded. Twenty patients were included between April 2014 and October 2015.

### *CT acquisition*

All acquisitions were performed on a 256-slice CT system (Brilliance iCT, Philips Healthcare, Best, The Netherlands). The routine dose acquisition was followed by three low dose acquisitions with the same scan length during the same session. A tube voltage of 120 kVp was used for all acquisitions. To create different dose levels, the tube current was lowered. All patients were imaged with automatic exposure control using a reference of 100 mAs (routine dose) and 60, 40 and 20 mAs (reduced dose levels), respectively. The pitch was 0.915 with a rotation time of 0.4 seconds. Slices were reconstructed with a thickness of 0.9 mm and increment of 0.7 mm for all measurements. All acquisitions were reconstructed with filtered back projection (FBP), HIR (iDose<sup>4</sup> level 4, Philips Healthcare, Best, The Netherlands) and MIR (IMR level 2, Philips Healthcare, Best, The Netherlands). The routinely used kernel B was used for FBP and iDose<sup>4</sup> reconstructions. IMR has three groups of kernels, namely Body Soft Tissue, Body Routine and Body SharpPlus [11]. Both Body Soft Tissue and Body Routine are recommended by the vendor for soft tissue evaluation, and were therefore both used. Dose length product (DLP) and volumetric CT dose index ( $CTDI_{vol}$ ) were recorded for each scan. The effective dose was calculated by multiplying the DLP with the conversion factor for 120 kV abdominal acquisitions (0.0153 mSv/(mGy×cm)) [12].

### *Image Evaluation*

All FBP acquisitions at routine dose were assessed to set the reference for the number and location of the stones. Urolithiasis was classified as stones (both kidney, ureter or bladder), papillary calcifications or parenchymal calcifications. The reference evaluation was done by a certified board radiologist with over 10 years of experience in abdominal radiology. This radiologist was not an observer in the current study. The maximal size of all stones was measured in three planes (transversal, coronal and sagittal) using the routine dose acquisition reconstructed with FBP and the average maximal diameter was calculated [13]. Subsequently, two observers (FW and PD) with more than 5 years of experience in abdominal radiology assessed the number of stones on all acquisitions and reconstructions.

Subjective image quality was assessed by the same two observers who were blinded for patient characteristics, acquisition and reconstruction information and images were evaluated in randomized order. Overall image quality was scored using a 4-point Likert scale:

Score 1: poor image quality—not diagnostically acceptable for interpretation;  
Score 2: suboptimal image quality—partially non-diagnostic;  
Score 3: acceptable image quality—diagnostic interpretation possible;  
Score 4: excellent image quality.

A score of 1-2 was considered unacceptable. One patient was used as a test case and used for training in a consensus meeting. Because it is important to be able to diagnose extra-urinary tract pathology, several other aspects were scored as well. Observers were asked to assess if there was a prior cholecystectomy, or, in case the gall bladder was still present, it was assessed for the presence of stones or wall thickening, or whether these could have been visualized if present. The maximal infrarenal diameter of the aorta was assessed in the anterior-posterior direction for abdominal aneurysm evaluation. The sigmoid and appendix were evaluated to see if there were signs of diverticulitis or appendicitis, or whether these could have been visualized if present. The maximal width of the body of the adrenal gland was assessed on the transversal plane, and the average Hounsfield unit (HU) was derived by drawing a circular region of interest (ROI) as large as possible.

Objective image quality was measured by drawing a circular ROI in the renal cortex (both left and right), aorta, retroperitoneal fat and air in the bowel. Noise was defined as the standard deviation (SD) of the HU measurement in the ROI.

### *Statistical analysis*

Statistical analyses were performed using SPSS (version 20.0, IBM, New York, United States). The test case was excluded from further analysis. FBP at routine dose was used as a reference standard, and all data were compared to the reference standard. To assess the subjective overall image quality the scores of the two observers were averaged. Also, the number of unacceptable scans (score 1 or 2) was calculated per observer. Sensitivity for the detection of stones was calculated by dividing the number of correctly identified stones by the total number of stones and multiplying this number with 100%. The sensitivity as well as the number of false positives was calculated both on a patient level and overall. In the per patient level analysis, the number of false positives and the sensitivity was calculated for each patient separately. Therefore, missing a stone in a patient with only 1 stone will weights more heavy than missing a stone in a patient with multiple stones. In the overall analysis the total number of false positives for all patients combined was calculated per observer, as well as the

overall sensitivity. In this analysis, each stone has an equal weight.

Data were compared using the Friedman test and post hoc analyses were performed using the Wilcoxon signed rank test. A p-value below 0.05 was considered significant. For the post hoc tests a Bonferroni corrected p-value of 0.0125 was used. Values are presented as medians (interquartile range, IQR) unless stated otherwise.

Inter-observer agreement was measured using Cohen's kappa coefficient and the percentage of agreement for categorical variables. The kappa was interpreted as poor ( $0.00 \leq k \leq 0.20$ ), fair ( $0.21 \leq k \leq 0.40$ ), moderate ( $0.41 \leq k \leq 0.60$ ), good ( $0.61 \leq k \leq 0.80$ ) or excellent ( $0.81 \leq k \leq 1.00$ ). For categorical variables with more than two categories a weighted kappa was used. A two-way random intraclass correlation coefficient (ICC) was used for continuous parameters, as well as the difference (in mm or HU).

## Results

A total of 20 patients were included, of which 1 patient was used as a test case for the consensus meeting. Therefore, ultimately 19 patients were investigated: sixteen males (16/19, 84%) and three females (3/19, 16%). The median age was 61 (IQR 52 – 67) years. Mean height was 181 (172 – 189) cm with a weight of 86 (75 – 100) kg resulting in a body mass index of 25.6 (25.0 – 32.4) kg/m<sup>2</sup>.

Effective dose was 4.8 (4.1 – 7.8) mSv at routine dose and 2.8 (2.5 – 4.7), 1.9 (1.6 – 3.1) and 0.9 (0.8 – 1.5) mSv at reduced dose levels, respectively. CTDI<sub>vol</sub> was 6.6 (5.5 – 10.5), 3.9 (3.3 – 6.3), 2.6 (2.2 – 4.2) and 1.3 (1.1 – 2.1) mGy, respectively while the DLP was 312 (270 – 508) mGy\*cm at routine dose and 184 (162 – 304), 123 (106 – 204) and 60 (51 – 99) mGy\*cm at reduced dose levels, respectively.

### *Diagnostic performance for stones and calcifications*

In total 74 stones were present in 17 patients, including 63 stones, 7 papillary calcifications and 4 parenchymal calcifications (*Table 1*). Of the 63 stones, 62 were in the kidney and 1 in the ureter. The size of the stones was smaller than 3 mm (19/74, 26%), 3-5 mm (26/74, 35%), 5-10 mm (21/74, 28%) or larger than 10 mm (8/74, 11%).

The accuracy of stone detection is shown in *Table 2*. The sensitivity at routine dose was 94% with FBP, because some stones were missed by a single observer. The sensitivity at routine dose with IR was 100%. At reduced dose, the sensitivity with FBP decreased to 89%, 88% and 50% respectively. While with HIR the

Table 1 – Stone and calcification characteristics.

	Diameter								Total
	<3 mm		3 – 5 mm		5 – 10 mm		>10 mm		
	n	Density (HU)	n	Density (HU)	n	Density (HU)	n	Density (HU)	
Stone	16	307 (251 – 371)	23	365 (323 – 531)	16	720 (541 – 897)	8	822 (665 – 982)	63
Papillary calcification	2	333 (257 – 333)	1	335	4	837 (645 – 1237)	0	NA	7
Parenchymal calcification	1	481	2	312 (258 – 312)	1	694	0	NA	4
Total	19		26		21		8		74

**Table 2 – Diagnostic performance.** The sensitivity for stone detection was calculated on a patient level and stones, papillary calcifications and parenchymal calcifications were combined. Two patients did not have any stones. The sensitivity is presented as median (interquartiles). For the assessment of extra-urinary tract pathology the number [percentage] of not assessable reconstructions is displayed per observer.

	Sensitivity	Cholecystectomy		Gall bladder stones		Gall bladder wall thickening		Sigmoid diverticulitis		Appendix visible		Appendicitis	
		Obs.1	Obs.2	Obs.1	Obs.2	Obs.1	Obs.2	Obs.1	Obs.2	Obs.1	Obs.2	Obs.1	Obs.2
<b>Routine dose</b>													
FBP	94.4 (80.0 – 100.0)	0 [0]	1 [5]	1 [5]	1 [5]	8 [42]	0 [0]	0 [0]	0 [0]	0 [0]	1 [5]	0 [0]	2 [11]
HIR	100.0 (80.0 – 100.0)	0 [0]	1 [5]	1 [5]	2 [11]	2 [11]	0 [0]	0 [0]	0 [0]	0 [0]	1 [5]	0 [0]	1 [5]
MIR (BR)	100.0 (92.9 – 100.0)	0 [0]	0 [0]	1 [5]	0 [0]	3 [16]	0 [0]	0 [0]	0 [0]	1 [5]	1 [5]	1 [5]	1 [5]
MIR (ST)	100.0 (77.8 – 100.0)	0 [0]	1 [5]	1 [5]	1 [5]	2 [11]	0 [0]	0 [0]	0 [0]	2 [11]	1 [5]	1 [5]	2 [11]
<b>40% reduced dose</b>													
FBP	88.9 (50.0 – 100.0)	0 [0]	1 [5]	2 [11]	4 [21]	16 [84]	0 [0]	0 [0]	0 [0]	0 [0]	2 [11]	0 [0]	3 [16]
HIR	100.0 (80.0 – 100.0)	0 [0]	1 [5]	1 [5]	4 [21]	8 [42]	0 [0]	0 [0]	0 [0]	1 [5]	1 [5]	1 [5]	2 [11]
MIR (BR)	100.0 (92.9 – 100.0)	0 [0]	1 [5]	1 [5]	1 [5]	4 [21]	0 [0]	0 [0]	0 [0]	0 [0]	1 [5]	0 [0]	2 [11]
MIR (ST)	100.0 (92.9 – 100.0)	0 [0]	1 [5]	1 [5]	1 [5]	5 [26]	0 [0]	0 [0]	0 [0]	1 [5]	0 [0]	2 [5]	2 [11]
<b>60% reduced dose</b>													
FBP	87.5 (50.0 – 100.0)	0 [0]	2 [11]	5 [26]	7 [37]	19 [100]	0 [0]	0 [0]	0 [0]	2 [11]	4 [21]	4 [21]	5 [26]
HIR	88.9 (75.0 – 100.0)	0 [0]	1 [5]	2 [11]	5 [26]	13 [68]	0 [0]	0 [0]	0 [0]	1 [5]	1 [5]	0 [0]	5 [26]
MIR (BR)	100.0 (81.3 – 100.0)	0 [0]	1 [5]	1 [5]	2 [11]	8 [42]	0 [0]	0 [0]	0 [0]	0 [0]	1 [5]	0 [0]	1 [5]
MIR (ST)	100.0 (80.0 – 100.0)	0 [0]	1 [5]	1 [5]	3 [16]	4 [21]	1 [5]	0 [0]	1 [5]	1 [5]	1 [5]	1 [5]	1 [5]
<b>80% reduced dose</b>													
FBP	50.0 (16.7 – 100.0)	1 [5]	3 [15]	14 [74]	18 [95]	10 [100]	17 [90]	8 [42]	16 [84]	18 [95]	16 [84]	18 [95]	16 [84]
HIR	72.2 (62.5 – 100.0)	0 [0]	0 [0]	4 [21]	6 [32]	11 [58]	1 [5]	0 [0]	0 [0]	6 [32]	3 [16]	4 [21]	6 [32]
MIR (BR)	100.0 (68.8 – 100.0)	0 [0]	0 [0]	2 [11]	3 [16]	4 [21]	1 [5]	0 [0]	0 [0]	1 [5]	1 [5]	1 [5]	4 [21]
MIR (ST)	78.6 (50.0 – 100.0)	0 [0]	0 [0]	1 [5]	1 [5]	4 [21]	11 [58]	0 [0]	0 [0]	0 [0]	2 [11]	2 [11]	2 [11]

FBP Filtered Back Projection, HIR Hybrid Iterative Reconstruction, MIR Model-based Iterative Reconstruction, BR Body Routine, ST Soft Tissue, Obs Observer

sensitivity was 100%, 89% and 72%, respectively. MIR Body Routine resulted in a sensitivity of 100% at all dose levels while the sensitivity with MIR Soft Tissue reduced to 79% at the lowest dose level. An example of decreased sensitivity is provided in *Figure 1*. All missed stones concerned stones with a size below 3 mm. The number of false-positives was low at all dose levels with a median number between 0 and 1. The overall sensitivity is presented in *Table 3*.

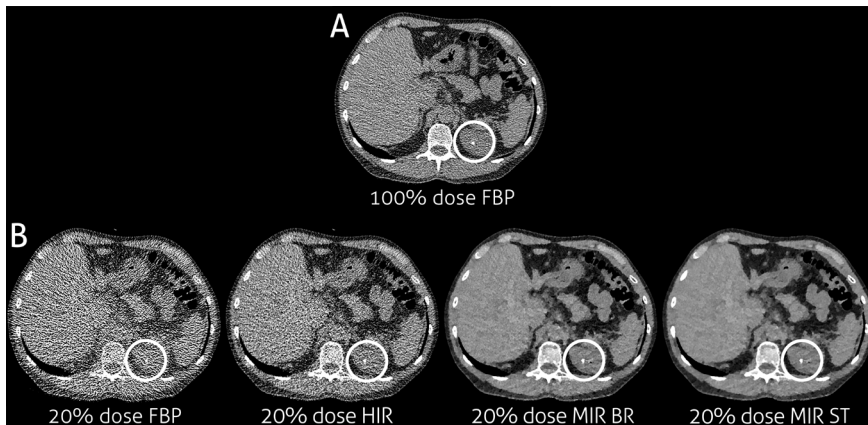


**Figure 1** – Example of decreased sensitivity for stone detection. The reference image at routine dose reconstructed with FBP (A), FBP reconstruction at the lowest dose level on which the stone was missed (B) and the IR reconstructions (HIR, MIR Body Routine and MIR Soft Tissue) at the same dose level on which the stone is clearly visible

#### *Extra-urinary tract pathology*

Results of the assessment of extra-urinary tract pathology are displayed in *Table 2*. At routine dose reconstructed with FBP, the assessment of prior cholecystectomy and sigmoid diverticulitis was possible in all patients. Gall bladder assessment for stones and for wall thickening was hampered in 1 patient (5%) and 1 or 8 patients (5 or 42%), respectively, depending on the observer. One observer also scored the appendix as not assessable (1 patient, 5%) or as inflammatory signs not assessable (2 patients, 11%). The assessment of prior cholecystectomy and sigmoid diverticulitis was possible up to 60% reduced dose with FBP, while with HIR and MIR the dose could be decreased with 80%. Gall bladder stones were still assessable at 60% reduced dose with both MIR kernels, and at 80%

**Table 3** – Overall sensitivity for stone detection and the number of false positives. The sensitivity was calculated per observer and stones, papillary calcifications and parenchymal calcifications were combined.

	Sensitivity		False positives	
	Obs. 1	Obs. 2	Obs. 1	Obs. 2
<b>Routine dose</b>				
FBP	89%	86%	18	8
HIR	88%	86%	10	26
MIR BR	95%	95%	25	32
MIR ST	92%	89%	23	23
<b>40% reduced dose</b>				
FBP	86%	76%	6	15
HIR	91%	85%	6	23
MIR BR	91%	92%	17	40
MIR ST	91%	93%	15	15
<b>60% reduced dose</b>				
FBP	76%	64%	19	6
HIR	83%	80%	11	12
MIR BR	88%	88%	19	27
MIR ST	89%	88%	6	19
<b>80% reduced dose</b>				
FBP	42%	46%	5	5
HIR	70%	73%	5	9
MIR BR	78%	76%	5	15
MIR ST	73%	81%	4	7

FBP Filtered Back Projection, HIR Hybrid Iterative Reconstruction, MIR Model-based Iterative Reconstruction, BR Body Routine, ST Soft Tissue, Obs Observer

dose using MIR Soft Tissue. The assessment of gall bladder wall thickening was similar to the reference at 40% reduced dose using MIR (both kernels). While for the assessment of the appendix the dose could be reduced with 40% for HIR and with 60% using MIR (both kernels). Overall, 40% dose reduction with HIR and 60% dose reduction with MIR yielded similar results as the reference (routine dose with FBP). The aorta and adrenal gland measurements did not show any significant differences at reduced dose (*Table 4*). However, with FBP the adrenal glands were not always assessable at all reduced dose levels, while at 60% dose reduced dose HIR resulted in not assessable reconstructions as well. At the lowest dose level, the adrenal gland was not assessable in several patients on all reconstruction methods (*Table 4*).

Table 4 – Aorta and adrenal gland measurements. The average value of both observers is used. There were no significant differences, however several reconstructions were not assessable due to excessive noise.

	Aorta diameter	Left adrenal gland – size (mm)	Left adrenal gland – density (HU)	Right adrenal gland – size (mm)	Right adrenal gland – density (HU)
<b>Routine dose</b>					
FBP	22.0 [20.7 – 25.0]	6.9 [5.7 – 8.1]	17.0 [6.5 – 26.8]	5.9 [5.3 – 6.8]	25.8 [8.0 – 30.7]
HIR	21.3 [20.1 – 24.7]	7.1 [4.8 – 7.8]	28.7 [11.9 – 37.2]	6.2 [4.9 – 6.9] 1 NA	27.8 [17.6 – 33.4] 1 NA
MIR (BR)	21.6 [20.0 – 25.0]	6.5 [5.4 – 8.3]	25.1 [21.3 – 30.1]	5.5 [5.0 – 6.3]	25.8 [16.6 – 37.5]
MIR (ST)	21.1 [19.6 – 25.8]	6.1 [5.4 – 7.4]	22.2 [16.3 – 31.0]	5.8 [5.3 – 6.7]	24.3 [15.8 – 32.4]
<b>40% reduced dose</b>					
FBP	21.5 [19.7 – 25.1]	6.2 [5.6 – 6.9] 3 NA	23.8 [15.9 – 33.9] 3 NA	5.5 [5.2-5.9] 3 NA	29.8 [16.4 – 47.6] 3 NA
HIR	22.0 [20.2 – 25.7]	6.8 [5.8 – 7.1]	20.6 [14.8 – 26.1]	5.6 [5.4-6.4]	29.9 [12.0 – 34.3]
MIR (BR)	21.1 [20.2 – 25.6]	5.8 [5.1 – 7.6]	27.3 [18.2 – 34.7]	5.6 [4.8-6.6]	22.2 [20.4 – 30.8]
MIR (ST)	21.4 [20.3 – 25.4]	6.7 [5.5 – 7.0]	18.9 [14.3 – 29.7]	5.9 [5.2-6.5]	21.1 [10.0 – 25.2]
<b>60% reduced dose</b>					
FBP	21.6 [19.7 – 25.1]	7.2 [6.7 – 7.9] 13 NA	23.5 [17.6-41.9] 13 NA	6.3 [6.2 – 6.8] 14 NA	27.5 [25.0 – 38.1] 14 NA
HIR	21.7 [20.1 – 25.2]	6.6 [6.0 – 7.7] 1 NA	21.1 [9.8 – 37.2] 1 NA	5.7 [5.3 – 6.2] 1 NA	23.2 [14.2 – 37.9] 1 NA
MIR (BR)	21.2 [20.5 – 25.0]	6.6 [5.7 – 7.4]	24.2 [11.8 – 32.2]	5.7 [5.2 – 6.8]	25.4 [17.5 – 34.8]
MIR (ST)	21.4 [20.4 – 24.5]	6.4 [5.7 – 6.9]	19.9 [14.0 – 32.8]	5.6 [5.2 – 6.3]	25.4 [13.0 – 31.2]
<b>80% reduced dose</b>					
FBP	21.3 [19.8 – 24.8] 2 NA	19 NA	19 NA	19 NA	19 NA
HIR	22.6 [20.3 – 24.9]	7.0 [6.1 – 7.8] 7 NA	29.1 [18.2 – 52.6] 7 NA	5.7 [5.5 – 6.4] 10 NA	46.5 [23.7 – 48.2] 10 NA
MIR (BR)	22.0 [20.5 – 24.3] 1 NA	6.2 [5.7 – 7.1] 1 NA	20.4 [8.7 – 30.6] 1 NA	5.6 [5.1 – 6.3] 3 NA	30.7 [22.9 – 42.7] 3 NA
MIR (ST)	22.0 [19.7 – 24.7]	6.3 [5.7 – 6.9] 1 NA	22.1 [15.6 – 32.3] 1 NA	5.8 [4.8 – 6.3] 3 NA	27.2 [14.9 – 37.6] 3 NA

FBP Filtered Back Projection, HIR Hybrid Iterative Reconstruction, MIR Model-based Iterative Reconstruction, BR Body Routine, ST Soft Tissue, NA Not Assessable

Observer agreement for subjective parameters was moderate to excellent, except for gallbladder wall thickening with a kappa of 0.31. The ICC was excellent for measuring the diameter of the aorta (ICC 0.95), and poor to fair for the adrenal gland measurements. Differences between observers were low with a mean difference of 1.2 and 0.2 mm and 3.9 and 7.5 HU for the left and right adrenal gland respectively. Results are also shown in the *Table 5*.

Table 5 - Agreement between observers for subjective measurements.

	Kappa	Total agreement (%)
Subjective image quality	0.59*	46.7
Prior cholecystectomy	0.91	99.0
Gall bladder stones	0.87	94.4
Gall bladder wall thickening	0.31	64.1
Sigmoid diverticulitis	0.53	95.7
Appendix visible	0.66	79.9
Appendicitis	0.44	85.9
	<b>ICC</b>	<b>Difference</b>
Aorta diameter	0.95	-0.42
Left adrenal gland – size (mm)	0.18	-1.23
Left adrenal gland – density (HU)	0.00	3.91
Right adrenal gland – size (mm)	0.27	-0.18
Right adrenal gland – density (HU)	0.39	7.53

\*A weighted kappa was used for the subjective image quality score

### Image Quality

An example of the different subjective image quality scores is provided in *Figures 2 and 3*. The image quality scores are provided in *Table 6*. The median image quality score at routine dose reconstructed with FBP was 3 (acceptable image quality). One observer scored all scans at routine dose as acceptable image quality, while the other observer scored 9 patients (47%) as unacceptable image quality. Both HIR, MIR Body Routine and MIR Soft Tissue resulted in significantly higher subjective image quality scores of 4 [4 – 4] routine dose. In addition, the number of patients with unacceptable image quality decreased to 1 (5%) with HIR and to zero with both MIR kernels. With FBP the image quality significantly decreased at the two lowest dose levels. At the lowest dose level,

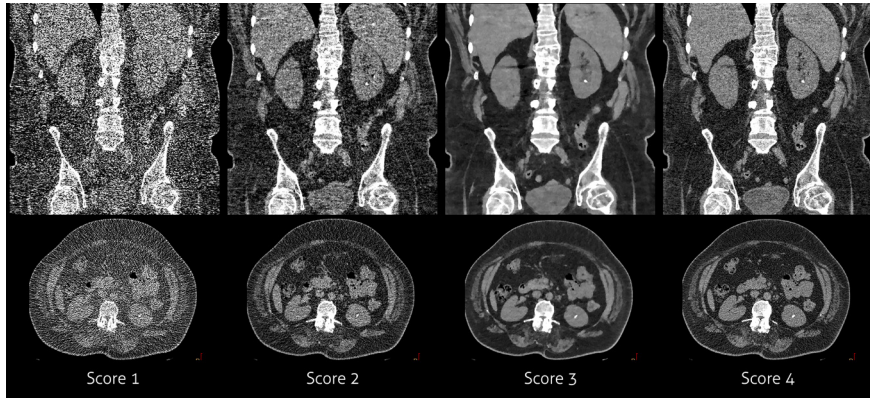


**Figure 2** – Example of the subjective image quality score. From left to right the different scores: score 1 with FBP at 80% reduced dose, score 2 with HIR at 80% reduced dose, score 3 with MIR Soft Tissue at 60% reduced dose and score 4 with HIR at the routine dose level. Note that the kidney stone can be seen in all images. Score 1 was mainly because of excessive noise. Score 2 was also due to substantial noise. Score 3 was given because of smoothing by IR. Score 4 contains some noise, but radiologists are used to some noise and tend to prefer this to extensive smoothing and noise reduction.

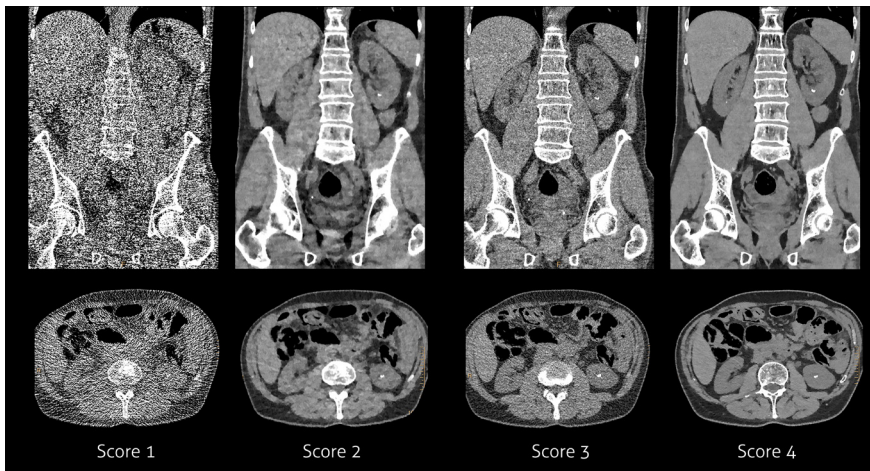


**Figure 3** – Additional example of the subjective image quality score. From left to right the different scores: score 1 with FBP at 80% reduced dose, score 2 with MIR Soft Tissue at 80% reduced dose, score 3 with HIR at 60% reduced dose and score 4 with MIR Body Routine at the routine dose level.

Table 6 – Subjective image quality and noise per reconstruction method and per dose level. For the image quality, the average score of the two observers was used. Those data are presented as mean [SD]. Also, the number of examinations [%] with unacceptable image quality (score 1 or 2) is shown per observer. The noise is presented as medians (interquartiles).

	Subjective image quality	Unacceptable image quality	Renal cortex (right)	Renal cortex (left)	Aorta	Retroperitoneal fat	Air
		Obs. 1	Obs. 2				
<b>Routine dose</b>							
FBP	3 [3–3]	0 [0]	53.3 (48.6–61.2)	51.8 (42.8–60.0)	56.5 (50.3–68.8)	54.7 (45.7–61.4)	23.5 (22.4–26.3)
			Reference	Reference	Reference	Reference	Reference
HIR	4 [4–4]*	0 [0]	32.2 (29.0–37.1)*	32.4 (28.5–36.1)*	37.4 (30.8–42.0)*	35.6 (29.6–37.3)*	17.7 (16.9–17.7)*
MIR (BR)	4 [4–4]*	0 [0]	10.2 (9.5–11.6)*	11.5 (10.0–12.3)*	11.7 (10.0–13.6)*	13.0 (11.4–14.8)*	6.6 (5.7–7.3)*
MIR (ST)	4 [4–4]*	0 [0]	7.2 (6.2–8.2)*	7.5 (7.0–8.0)*	7.7 (6.0–9.5)*	9.1 (7.6–10.9)*	4.2 (4.0–7.3)*
<b>40% reduced dose</b>							
FBP	3 [3–3]	3 [16]	70.0 (62.8–83.5)*	72.2 (63.5–79.3)*	77.3 (69.6–97.0)*	74.8 (55.6–83.8)*	31.7 (25.9–37.7)*
HIR	3 [3–4]	0 [0]	37.8 (34.6–39.7)*	38.0 (34.2–42.4)*	44.0 (37.7–45.7)*	39.4 (36.2–44.2)*	23.6 (20.0–28.6)
MIR (BR)	4 [3–4]*	0 [0]	12.4 (10.2–12.8)*	11.6 (9.8–14.4)*	13.6 (11.4–15.7)*	13.5 (11.2–17.6)*	7.5 (5.9–8.6)*
MIR (ST)	4 [3–4]*	0 [0]	8.4 (7.3–9.8)*	9.3 (7.3–10.7)*	10.2 (9.4–11.3)*	10.5 (8.9–14.3)*	5.6 (4.9–7.9)*
<b>60% reduced dose</b>							
FBP	2 [2–3]*	13 [68]	97.5 (84.1–106.7)*	88.7 (77.4–120.8)*	103.1 (89.8–115.0)*	103.7 (85.6–111.1)*	42.2 (33.0–49.8)*
HIR	3 [3–3]	0 [0]	40.6 (38.9–45.1)*	39.3 (35.8–48.1)*	46.2 (40.2–52.5)*	45.6 (38.3–49.5)*	27.4 (24.5–37.2)*
MIR (BR)	4 [3–4]	1 [5]	13.7 (11.2–15.6)*	12.9 (10.8–14.6)*	15.2 (13.1–17.4)*	14.2 (12.5–16.4)*	8.5 (7.3–11.7)*
MIR level 2 (ST)	3 [3–4]*	0 [0]	10.1 (8.3–12.0)*	9.2 (8.6–10.7)*	11.6 (10.1–13.3)*	10.2 (9.2–12.3)*	7.2 (5.3–10.5)*
<b>80% reduced dose</b>							
FBP	1 [1–1]*	19 [100]	160.9 (136.0–187.6)*	168.7 (131.0–192.9)*	184.7 (152.8–203.3)*	165.6 (146.9–187.5)*	57.2 (36.8–63.2)*
HIR	2 [2–3]*	11 [58]	47.4 (45.3–64.7)	51.0 (45.4–59.0)	50.6 (44.3–63.6)	51.8 (48.0–64.7)	33.4 (26.8–41.7)*
MIR (BR)	3 [3–3]*	4 [21]	15.9 (12.9–17.2)*	14.6 (12.3–17.8)*	17.1 (15.6–19.4)*	15.2 (13.9–19.1)*	9.8 (8.8–15.4)*
MIR (ST)	3 [2–3]*	6 [32]	12.4 (9.9–13.9)*	11.8 (10.3–14.7)*	14.4 (11.8–16.0)*	12.5 (10.5–15.7)*	9.2 (6.4–15.1)*

Subjective image quality and noise per reconstruction method and per dose level. Image quality is presented as median [interquartiles]. Also, the number of examinations [%] with unacceptable image quality (score 1 or 2) is shown per observer. The noise is presented as medians (interquartiles).

the image quality was unacceptable in all patients with FBP. At 40% and 60% reduced dose, IR resulted in similar or improved image quality compared to the reference acquisition (FBP at routine dose). While at the lowest dose level, the image quality significantly decreased with all reconstruction techniques, however the image quality was still better with HIR (2) and MIR (3) compared to FBP (1).

Overall agreement for subjective image quality was moderate with a weighted kappa of 0.59. The percentage of total agreement was 47%. In 4.3% of comparisons there was more than one point difference in the subjective image quality score between observers.

Noise and attenuation are presented in *Table 6 and 7*. At routine dose, both HIR and MIR resulted in a reduction in noise. Reducing the radiation dose led to a significant increase in noise with FBP, while MIR resulted in a decrease in noise compared to FBP at routine dose, even at 80% reduced dose. With a 40% or 60% reduction in dose, HIR resulted in less noise compared to FBP at routine dose, while at 80% reduced dose the amount of noise was comparable to FBP at routine dose.

Mean densities were not affected by dose reduction, except for the lowest dose level and the density of air. This resulted in a slightly higher attenuation.

Table 7 – Organ attenuation as a function of reconstruction method and dose level. Variables are presented as medians (interquartiles). \*Significant difference compared to the reference ( $p < 0.0125$ )

	Renal cortex (right)	Renal cortex (left)	Aorta	Retroperitoneal fat	Air
<b>Routine dose</b>					
FBP	36.3 (33.0 – 40.3) Reference	35.7 (32.1 – 39.0) Reference	50.7 (48.4 – 55.3) Reference	-105.0 (-109.9 – -99.3) Reference	-996.3 (-998.1 – -994.4) Reference
HIR	35.9 (33.5 – 39.6)	36.3 (33.9 – 38.3)	50.1 (47.9 – 54.6)	-105.4 (-109.5 – -99.8)	-997.5 (-1000.9 – -992.5)
MIR (BR)	36.2 (33.3 – 39.3)	36.0 (33.0 – 37.1)	53.1 (46.0 – 56.6)	-103.3 (-107.9 – -95.7)	-991.6 (-993.9 – -990.5)*
MIR (ST)	37.6 (34.7 – 40.4)	37.1 (34.7 – 38.9)	54.1 (48.0 – 56.4)	-103.2 (-107.0 – -97.1)	-995.9 (-997.3 – -993.0)
<b>40% reduced dose</b>					
FBP	37.3 (33.7 – 41.1)	36.3 (33.4 – 39.9)	52.5 (48.7 – 55.7)	-105.8 (-112.8 – -100.7)	-991.9 (-994.5 – -989.3)
HIR	36.1 (31.2 – 39.7)	33.6 (32.4 – 37.8)	50.8 (47.6 – 55.1)	-106.3 (-110.6 – -99.0)	-993.6 (-996.8 – -992.3)
MIR (BR)	36.8 (32.3 – 40.3)	35.4 (33.3 – 39.3)	53.2 (49.8 – 56.3)	-105.9 (-108.7 – -97.6)	-987.7 (-994.0 – -983.1)*
MIR (ST)	37.3 (33.6 – 40.9)	36.9 (34.6 – 40.6)	54.2 (50.4 – 56.8)	-105.4 (-108.2 – -96.8)	-991.0 (-994.0 – -987.5)*
<b>60% reduced dose</b>					
FBP	40.7 (34.4 – 48.6)*	39.4 (35.9 – 42.1)	52.9 (43.5 – 56.8)	-104.5 (-108.4 – -96.0)	-998.4 (-993.4 – -982.3)*
HIR	36.5 (29.5 – 39.8)	34.5 (30.3 – 39.9)	49.6 (42.9 – 51.9)	-107.0 (-110.2 – -95.0)	-994.3 (-996.1 – -981.7)
MIR (BR)	37.8 (32.5 – 38.9)	37.8 (34.7 – 40.9)	49.6 (45.5 – 55.8)	-105.7 (-109.7 – -96.8)	-983.0 (-988.4 – -977.3)*
MIR (ST)	39.2 (33.7 – 40.1)	39.2 (35.8 – 41.7)	50.5 (46.2 – 56.6)	-105.4 (-108.9 – -95.7)	-988.1 (-993.2 – -984.2)*
<b>80% reduced dose</b>					
FBP	49.2 (40.1 – 57.0)*	46.9 (42.0 – 54.1)*	63.6 (54.1 – 78.5)*	-101.4 (-109.7 – -89.6)	-984.5 (-996.3 – -979.6)*
HIR	39.6 (32.6 – 45.2)	36.7 (33.7 – 44.0)	47.0 (40.6 – 55.5)	-104.6 (-110.8 – -95.3)	-992.1 (-996.4 – -985.7)
MIR (BR)	39.9 (32.7 – 42.3)	38.0 (34.2 – 41.6)	52.9 (47.1 – 58.3)	-102.6 (-105.6 – -97.8)	-984.9 (-990.1 – -979.0)*
MIR (ST)	41.1 (34.4 – 43.2)*	39.0 (35.4 – 42.9)	54.9 (48.7 – 59.1)	-102.0 (-104.4 – -97.0)	-988.1 (-994.4 – -982.0)*

FBP filtered back projection, HIR Hybrid Iterative Reconstruction, MIR Model-based Iterative Reconstruction, BR Body Routine, ST Soft Tissue

## Discussion

This prospective within-patient study showed that radiation dose can be reduced with 40% (to median 3.8 mGy) using HIR and with 60% (to median 2.6 mGy) using MIR in CT scans for urolithiasis evaluation in patients with a median weight of 86 kg and a range in BMI from 20 to 39 kg/m<sup>2</sup>. Sensitivity for stones remained excellent at 60% reduced dose with IR while sensitivity decreased with low dose FBP. At these low dose levels, extra-urinary tract pathology was still assessable with IR, while objective and subjective image quality improved compared to FBP at routine dose. Further dose reduction hampered the diagnosis of extra-urinary tract pathology and is therefore not advised with current reconstruction methods.

Current guidelines recommend the use of low dose CT in patients suspected of urolithiasis [4,6]. The definition of low dose is not unambiguous, but a dose below 3 mSv is usually considered low dose for native abdominal CT for follow-up of urolithiasis [14]. A large survey study performed in 93 hospitals in the United States between 2011-2013 including 49,903 renal colic CT examinations reported a mean radiation dose of 11.2 mSv (14.3 mGy) in clinical practice [15]. Only two percent of those examinations was performed at a low dose (<3 mSv) and 0.2% at a dose below 2 mSv. The high contrast between stones and the surrounding soft tissue should make it possible to substantially reduce the radiation dose without affecting diagnostic accuracy, and various studies have shown that the radiation dose for urinary stone CT acquisitions can be safely reduced below 3 mSv without affecting the diagnostic accuracy of stone detection [16]. One of the largest studies (201 patients) was performed by Moore and colleagues [8]. Patients suspected of ureteral stones received both a routine and low dose CT acquisition with a radiation dose of 12.7 mSv and 1.6 mSv, respectively. The sensitivity at low dose was 90% with a specificity of 99%. There were 102 stones present, of which 75% was smaller than 5 mm. No IR was used. Fontarensky et al. [9] compared routine dose acquisitions with hybrid IR (ASIR, GE Healthcare) to low dose acquisitions with model based IR (MBIR, GE Healthcare) at a radiation dose level of 8.8 mSv (10.9 mGy) and 1.4 mSv (1.7 mGy), respectively. Both acquisitions were made successively in the same patients. The diagnostic accuracy at low dose was excellent and objective and subjective image quality were comparable. Also the detection of alternative diagnoses was not hampered at reduced dose. To our best knowledge, only two studies investigated ultra-low dose acquisitions at submillisievert dose levels [10,17]. In a study by Glazer et al. [10] a split-dose design

was used in which 52 patients received both a 80% dose scan and a 20% dose scan. Radiation dose was 3.9 mSv (4.8 mGy) and 1.0 mSv (1.2 mGy) respectively, and MBIR was used for reconstruction. Subjective and objective image quality were significantly lower at reduced dose, and the diagnostic accuracy decreased to a sensitivity of 74% and a specificity of 77% for stones smaller than 3 mm. In a similar study by McLaughlin and colleagues [17] patients received a routine dose (4.4 mSv) and low dose (0.5 mSv) acquisition. The sensitivity decreased to 72% at low dose, which was mainly caused by missed small stones. In addition, several extra-urinary findings like gall stones and appendicitis were missed at low dose. The current study corroborates those results and underscores that excessive radiation dose reduction to submillisievert dose levels is not feasible in an average adult due to a decrease in diagnostic accuracy. This study also found that the decrease in sensitivity is caused by small stones (<3 mm) that are missed, while larger stones remain visible.

One of the disadvantages of IR often mentioned, is the longer reconstruction time compared to FBP [18]. This is mainly a problem of MIR algorithms, while HIR results in less than a minute delay compared to FBP [19]. The MIR algorithm used in the current study, IMR, takes less than 5 minutes for the majority of the protocols according to the vendor [20]. A more recent study by Yuki et al. investigating chest CT reported a reconstruction time within 3 minutes for all cases [21]. This delay is clinically acceptable for CT scans for urolithiasis. However longer reconstruction times up to an hour have been reported for other MIR algorithms [22-24].

The main strength of the current study is the within-patient design using four different dose levels to investigate the achievable radiation dose reduction. Not only the accuracy for stone detection was researched, but also the possibility to diagnose extra-urinary tract pathology which is important in clinical practice. Furthermore, both hybrid and more advanced model-based IR was investigated and, to our best knowledge, this is the first study using IMR for this purpose. This study has several limitations. First, a relatively small sample size was used because the study participants were exposed to 4 CT scans. However, compared to other studies a large number of stones was present. Second, the IR algorithms of only one vendor were investigated. Lastly, the effect of dose reduction and IR on the stone size was not investigated. A previous study showed that MIR might overestimate the stone density and size compared to HIR [25]. It was however not clear if this was truly an overestimation, or if HIR underestimated the stone size.

Future studies using a phantom with stones with known density and size should be performed to demonstrate this.

In conclusion, the radiation dose for the assessment of urolithiasis can be reduced with 40% (HIR) to 60% (MIR) without affecting diagnostic performance or image quality. Further dose reduction leads to decreased sensitivity for small stones and hampers the assessment of extra-urinary tract pathology.

## References

- [1] Heidenreich A, Desgrandschamps F, Terrier F, Modern approach of diagnosis and management of acute flank pain: review of all imaging modalities. *Eur Urol* 2002;41(4):351-62.
- [2] Bartoletti R, Cai T, Mondaini N, et al., Epidemiology and risk factors in urolithiasis. *Urol Int* 2007;79 Suppl 1:3-7.
- [3] Campschroer T, Zhu Y, Duijvesz D, Grobbee DE, Lock MT, Alpha-blockers as medical expulsive therapy for ureteral stones. *Cochrane Database Syst Rev* 2014;(4):CD008509. doi(4):CD008509.
- [4] Turk C, Petrik A, Sarica K, et al., EAU Guidelines on Diagnosis and Conservative Management of Urolithiasis. *Eur Urol* 2016;69(3):468-74.
- [5] Coursey CA, Casalino DD, Remer EM, et al., ACR Appropriateness Criteria(R) acute onset flank pain--suspicion of stone disease. *Ultrasound Q* 2012;28(3):227-33.
- [6] Pearle MS, Goldfarb DS, Assimos DG, et al., Medical management of kidney stones: AUA guideline. *J Urol* 2014;192(2):316-24.
- [7] Veldhoen S, Laqmani A, Derlin T, et al., 256-MDCT for evaluation of urolithiasis: Iterative reconstruction allows for a significant reduction of the applied radiation dose while maintaining high subjective and objective image quality. *J Med Imaging Radiat Oncol* 2014.
- [8] Moore CL, Daniels B, Ghita M, et al., Accuracy of reduced-dose computed tomography for ureteral stones in emergency department patients. *Ann Emerg Med* 2015;65(2):189,98.e2.
- [9] Fontarensky M, Alfidja A, Perignon R, et al., Reduced Radiation Dose with Model-based Iterative Reconstruction versus Standard Dose with Adaptive Statistical Iterative Reconstruction in Abdominal CT for Diagnosis of Acute Renal Colic. *Radiology* 2015;276(1):156-66.
- [10] Glazer DI, Maturen KE, Cohan RH, et al., Assessment of 1 mSv urinary tract stone CT with model-based iterative reconstruction. *AJR Am J Roentgenol* 2014;203(6):1230-5.
- [11] Khawaja RD, Singh S, Blake M, et al., Ultra-low dose abdominal MDCT: using a knowledge-based Iterative Model Reconstruction technique for substantial dose reduction in a prospective clinical study. *Eur J Radiol* 2015;84(1):2-10.
- [12] Deak PD, Smal Y, Kalender WA, Multisection CT protocols: sex- and age-specific conversion factors used to determine effective dose from dose-length product. *Radiology* 2010;257(1):158-66.
- [13] Merigot de Treigny O, Bou Nasr E, Almont T, et al., The Cumulated Stone Diameter: A Limited Tool for Stone Burden Estimation. *Urology* 2015;86(3):477-81.
- [14] Gervaise A, Gervaise-Henry C, Pernin M, Naulet P, Junca-Laplace C, Lapierre-Combes M, How to perform low-dose computed tomography for renal colic in clinical practice. *Diagn Interv Imaging* 2016;97(4):393-400.
- [15] Lukasiewicz A, Bhargavan-Chatfield M, Coombs L, et al., Radiation dose index of renal colic protocol CT studies in the United States: a report from the American College of Radiology National Radiology Data Registry. *Radiology* 2014;271(2):445-51.

- [16] Niemann T, Kollmann T, Bongartz G, Diagnostic performance of low-dose CT for the detection of urolithiasis: a meta-analysis. *AJR Am J Roentgenol* 2008;191(2):396-401.
- [17] McLaughlin PD, Murphy KP, Hayes SA, et al., Non-contrast CT at comparable dose to an abdominal radiograph in patients with acute renal colic; impact of iterative reconstruction on image quality and diagnostic performance. *Insights Imaging* 2014;5(2):217-30.
- [18] den Harder AM, Willemink MJ, Budde RP, Schilham AM, Leiner T, de Jong PA, Hybrid and model-based iterative reconstruction techniques for pediatric CT. *AJR Am J Roentgenol* 2015;204(3):645-53.
- [19] Willemink MJ, Schilham AM, Leiner T, Mali WP, de Jong PA, Budde RP, Iterative reconstruction does not substantially delay CT imaging in an emergency setting. *Insights Imaging* 2013;4(3):391-7.
- [20] Mehta D, Thompson R, Morton T, Dhanantwari A., Shefer E, Iterative model reconstruction: simultaneously lowered computed tomography radiation dose and improved image quality. *Medical Physics International* 2013;1(2):147-155.
- [21] Yuki H, Oda S, Utsunomiya D, et al., Clinical impact of model-based type iterative reconstruction with fast reconstruction time on image quality of low-dose screening chest CT. *Acta Radiol* 2016;57(3):295-302.
- [22] Ichikawa Y, Kitagawa K, Nagasawa N, Murashima S, Sakuma H, CT of the chest with model-based, fully iterative reconstruction: comparison with adaptive statistical iterative reconstruction. *BMC Med Imaging* 2013;13:27,2342-13-27.
- [23] Pickhardt PJ, Lubner MG, Kim DH, et al., Abdominal CT with model-based iterative reconstruction (MBIR): initial results of a prospective trial comparing ultralow-dose with standard-dose imaging. *AJR Am J Roentgenol* 2012;199(6):1266-74.
- [24] Shen J, Du X, Guo D, et al., Prospective ECG-triggered coronary CT angiography: clinical value of noise-based tube current reduction method with iterative reconstruction. *PLoS One* 2013;8(5):e65025.
- [25] Botsikas D, Stefanelli S, Boudabbous S, Toso S, Becker CD, Montet X, Model-based iterative reconstruction versus adaptive statistical iterative reconstruction in low-dose abdominal CT for urolithiasis. *AJR Am J Roentgenol* 2014;203(2):336-40.



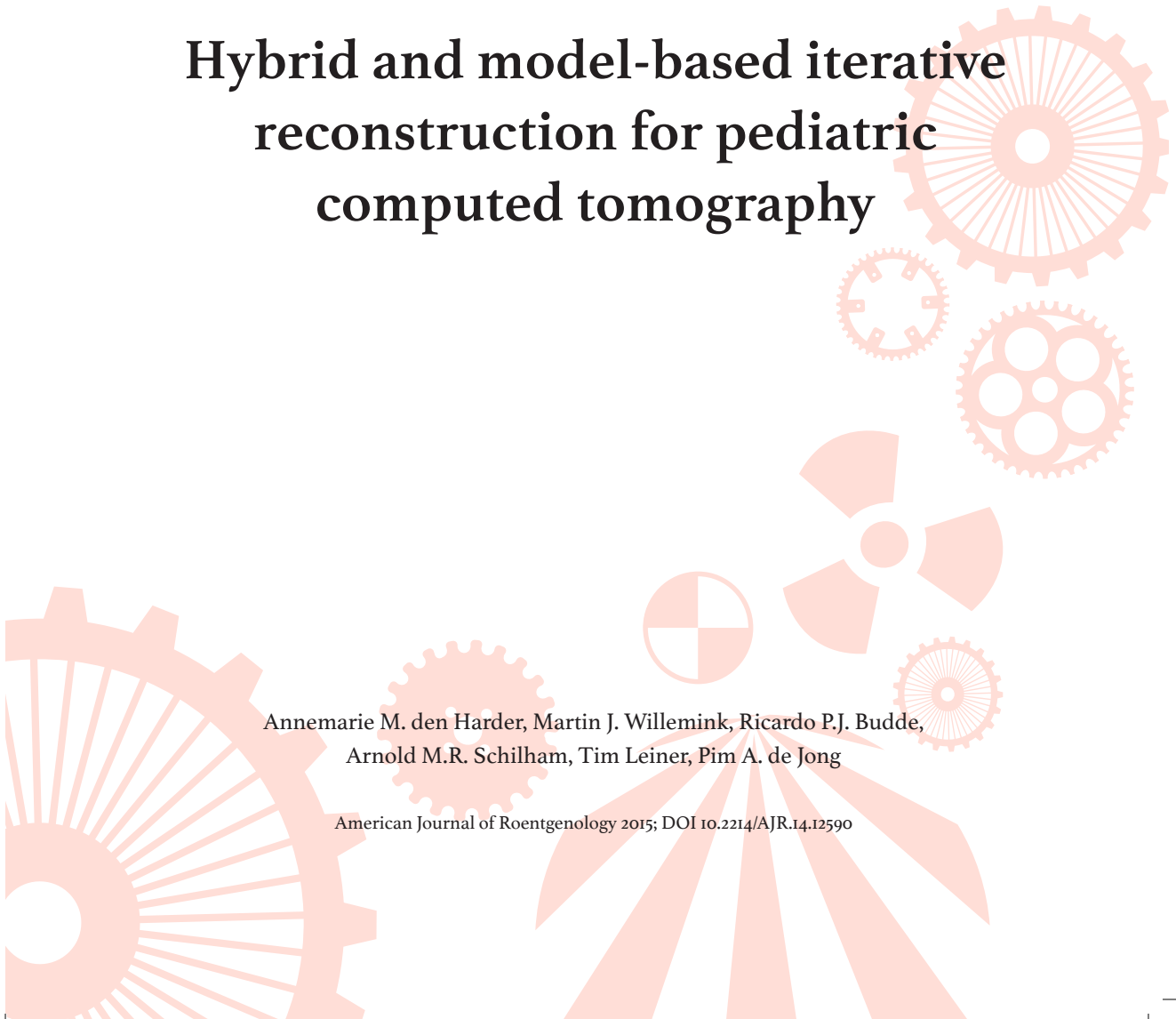
# Chapter 3.1

*Part III Pediatric*

## Hybrid and model-based iterative reconstruction for pediatric computed tomography

Annemarie M. den Harder, Martin J. Willeminck, Ricardo P.J. Budde,  
Arnold M.R. Schilham, Tim Leiner, Pim A. de Jong

American Journal of Roentgenology 2015; DOI 10.2214/AJR.14.12590



### **Abstract**

Radiation exposure in children should be reduced to a minimum. Iterative reconstruction is a method to reduce image noise that can be used to improve CT image quality, thereby allowing for radiation dose reduction. This article reviews the use of iterative reconstruction in pediatric CT. After completion, the reader should be familiar with the possibilities, advantages and disadvantages of iterative reconstruction in pediatric CT and the importance of radiation dose reduction for CT in children.

## Introduction

The number of computed tomography (CT) examinations is increasing rapidly. This has raised concerns about the possible risk of carcinogenesis after low radiation exposure in the context of medical imaging. Approximately 6% to 11% of all CT examinations in the United States are performed in children [1]. This number is worrisome since children are ten times more sensitive to the effects of ionizing radiation compared to middle-aged adults due to the radiosensitivity of rapidly dividing cells [1,2]. Children also have a longer expected lifetime to develop harmful radiation effects [3].

Awareness that CT scans may induce cancer in children has increased over the past decade [4-6]. This awareness stimulated the development of guidelines for pediatric CT examinations, which resulted in a slightly decreased number of CT scans performed in children over the last years [7]. Nevertheless, due to its strong diagnostic performance CT remains a commonly used technique and therefore dose optimisation is important. Simply reducing tube voltage and tube current can often decrease radiation dose. However, excessive dose reduction substantially affects image quality and diagnostic value.

The concept of iterative reconstruction (IR) was first described in the early 1970s [8]. However, at that time IR was not used for clinical CT imaging due to limited computational power of CT reconstruction workstations [9]. In clinical practice a fast and simple computational reconstruction technique called filtered back projection (FBP) was used instead. The downside of FBP is increased image noise when images are acquired at low radiation dose. Therefore, FBP is not well suited for low radiation dose CT imaging. Noise reducing reconstruction algorithms such as IR can ameliorate this problem. Advances in computing hardware performance have enabled the commercial introduction of IR for clinical CT imaging. IR algorithms reduce noise and improve image quality [10] and have been introduced by all major CT vendors. Therefore, IR allows for either improving image quality at routine radiation dose levels, or for a reduction in radiation dose without compromising image quality [10]. The latter is especially important for pediatric CT imaging. Another advantage of model-based IR is a reduction of artifacts [11]. Here we provide an overview of the literature and describe our experiences with hybrid and model-based IR in pediatric CT.

*Iterative reconstruction*

IR algorithms reduce image noise, which results in the possibility to lower CT radiation dose without affecting image quality. Full IR works with both forward and backward projection steps. With backward projection steps images are created based on the projection data [12]. Conversely, with forward projection steps, projection data are created based on image data. With forward projection an assumption is made about the attenuation distribution in the scanned area, based on characteristics of the CT system. The assumed attenuation distribution is then compared to the measured attenuation distribution and based on this comparison a more accurate assumption is made. The forward and backward projections are repeated until they do not change in subsequent iterations or the maximum number of iterations is reached. Subsequently a final optimised image is reconstructed. Due to these iterations, IR is a computationally demanding technique, which results in longer reconstruction times. However, this does not result in a clinically significant delay [13].

All major CT vendors have developed their own IR techniques. Most commercially available IR algorithms are not fully iterative but use a combination of IR and FBP (also known as ‘hybrid’ reconstruction techniques) [14,15]. Currently available hybrid iterative reconstruction techniques are Adaptive Statistical Iterative Reconstruction (ASIR, *GE Healthcare*), Adaptive Iterative Dose Reduction 3D (AIDR 3D, *Toshiba Medical Systems*), Iterative Reconstruction in Image Space (IRIS, *Siemens Healthcare*), Sinogram-Affirmed Iterative Reconstruction (SAFIRE, *Siemens Healthcare*), Advanced Modeled Iterative Reconstruction (ADMIRE, *Siemens Healthcare*) and iDose<sup>4</sup> (*Philips Healthcare*). Three vendors developed more advanced model-based IR (MBIR) algorithms that approach true IR, Veo (MBIR-Veo, *GE Healthcare*) and Iterative Model-based Reconstruction (IMR, *Philips Healthcare*). Hybrid IR algorithms mostly use only one backward projection step, whereas model-based IR techniques are based on both forward and backward projection steps [14]. The exact number of iterations for each vendor is unknown, proprietary information.

The examples shown in this article were reconstructed with a hybrid IR algorithm (iDose<sup>4</sup>, *Philips Healthcare, Best, The Netherlands*) and a prototype version of a model-based IR algorithm (IMR, *Philips Healthcare, Best, The Netherlands*) and data were acquired with a 256-slice CT scanner (*Brilliance iCT, Philips Healthcare, Best, The Netherlands*) [16].

The hybrid IR technique, iDose<sup>4</sup>, filters noise iteratively in both the projection domain and the image domain [17]. Dose reductions of up to 76% have been reported without loss of image quality [18]. A reconstruction speed of 18 slices per second can be reached using iDose<sup>4</sup>, which is slightly slower than 26 slices per second with FBP but this is not clinically significant [13].

The model-based IR technique, IMR, uses forward and backward reconstruction steps. More detailed information about the IMR algorithm is published elsewhere [16]. An initial study showed significant noise reduction and contrast-to-noise improvements with IMR in comparison to FBP [19]. A case report demonstrated that it was possible to perform a pediatric chest CT with IMR at a radiation dose approaching chest radiography with diagnostic image quality [20]. In addition, a phantom study showed that dose reductions of 60% to 80% were possible, with 70% to 83% less image noise and an improved low-contrast detectability at the same time compared to FBP [16].

The strength of iDose<sup>4</sup> and IMR is defined in different levels of noise reduction in which a higher level implicates a stronger noise reduction. Seven levels of noise reduction are available for iDose<sup>4</sup> and three levels for IMR.

The maximum dose reduction achievable using IR depends on the scanned body area. Therefore in this article the use of IR in pediatrics will be discussed per body area. *Table 1* provides an overview of studies investigating IR in pediatric CT and the associated radiation dose. IR in pediatrics has been mainly investigated using ASIR and reported dose reduction varied from 24-92% depending on the scanned body area. Effective dose calculations are based on age- and sex specific conversion factors from the International Commission on Radiological Protection publication 103 [21]. To measure the noise in each figure, two homogenous regions of interest (ROI) were drawn. Noise was defined as the standard deviation in Hounsfield Units of the mean density in a homogenous ROI. The contrast-to-noise ratio (CNR) was computed using the following equation:

$$\text{CNR} = \frac{\text{Density (ROI 1)} - \text{Density (ROI 2)}}{\sqrt{\frac{1}{2} \times (\text{SD (ROI 1)}^2 + \text{SD (ROI 2)}^2)}}$$

Table 1 – Overview of published studies investigating iterative reconstruction in pediatrics.

Protocol	Publication	Year of publication	In/ex vivo	Subjects (n)	Iterative reconstruction technique (level)	Objective quality			Subjective quality			
						Noise	CNR	SNR	Quality	Noise	Diagnostic utility	Artifacts
Head CT	Kilic [22]	2013	In vivo	305	ASIR (30%)	+	+	+	+	+	+	+
	Vorona [23]	2013	In vivo + ex vivo	24	ASIR (20%)*	+	-	-	+	+	+	+
	Ho [24]	2013	In vivo	44	iDose (1-4)	+	-	-	+	+	+	-
Chest CT	Lee [29]	2012	In vivo	26	ASIR (50%)	+	-	-	+	+	+	+
	Lee [30]	2012	In vivo	43	iDose <sup>4</sup> (1-7)	+	-	+	+	-	-	+
	Mieville [31]	2013	In vivo	22	MBIR (VEO)	+	-	+	+	-	-	-
Cardiac CT	Mieville [26]	2011	In vivo + ex vivo	10	ASIR (20%, 30%, 40%, 50%, 60%, 80%, 100%)	-	-	-	+	-	-	-
	Han [43]	2012	In vivo	74	SAFIRE	+	+	+	+	+	+	-
	Tricarico [44]	2013	In vivo	40	IRIS & SAFIRE	+	+	+	+	-	+	+
	Nie [45]	2014	In vivo	28	SAFIRE	+	+	+	+	-	+	-
Chest + abdominal CT	Singh [33]	2012	In vivo	234	ASIR (30%) ASIR (10%, 20%, 30%, 40%, 50%, 60%, 70%, 80%, 90%, 100%) ASIR (100%)	+	-	-	+	+	+	+
	Brady [28]	2012	Ex vivo	NA	ASIR (100%)	+	+	-	-	-	-	-
	Mieville [32]	2013	Ex vivo	NA	MBIR (VEO), iDose <sup>4</sup> (6)	+	+	-	-	-	-	-
	Gay [35]	2014	In vivo + ex vivo	26	ASIR (40%)*	-	-	+	+	+	-	+
	Brady [27]	2014	In vivo	183	ASIR (40%)	+	+	-	-	-	-	-
	Koc [36]	2014	In vivo	17	MBIR (VEO) + ASIR (30%)	+	-	-	+	-	+	-
	Karmazyn [37]	2014	In vivo	88	iDose <sup>4</sup> (2-6)	+	-	-	+	-	+	-
	Smith [34]	2014	In vivo	25	MBIR (VEO) + ASIR (100%)	+	-	-	+	-	-	-
Abdominal CT	Vorona [38]	2011	In vivo	11	ASIR (40%)	+	-	-	+	+	+	-

+ Reported, -not reported, NA not available, NP not provided, CNR contrast-to-noise ratio, CTDI Computed tomography dose index, DLP dose length product, SNR signal-to-noise ratio, CCTA coronary computed tomographic angiography, IRIS Iterative Reconstruction in Image Space, Siemens Medical Solutions, ASIR Adaptive Statistical

Maximal dose reduction (%)	CTDI <sub>vol</sub> (mGy)	CTDI <sub>vol</sub> at reduced dose (mGy)	DLP (mGy x cm)	DLP at reduced dose level (mGy x cm)	Effective dose (mSv)	Effective dose at reduced level (mSv)
32%	28.95	20.16	466.48	329.21	2.16	1.47
24%	28.8	22.4	444.5	338.4	NP	NP
NA	28.0	NA	514.4	NA	NP	NA
60%	18.73	7.43	307.42	134.51	4.12	1.84
NA	NA	NA	NA	NA	NA	NA
92%	1.84	0.14	63.5	4.57	NP	NP
38%	6.7	3.7	112	NP	NP	NP
NA	NA	NA	NA	NA	NA	NA
50%	4	NP	63	NP	1.36	0.68
NA	0.47	NA	6.11	NA	0.30	NA
46%	8.1	5.0	327.9	216.8	NP	NP
82%	NP	NP	NP	NP	NP	NP
86%	7.1	0.2	NP	NP	NP	NP
31%	4.2 (chest) / 4.1 (abdominal)	3.1 (chest) / 3.05 (abdominal)	141 (chest) / 193 (abdominal)	93 (chest) / 112 (abdominal)	NP	NP
72%	19.9 (chest) / 21.2 (abdominal)	5.2 (chest) / 18.8 (abdominal)	NP	NP	NP	NP
NA	3.05	NA	67.18	NA	NP	NP
NA	NP	NP	NP	NP	NP	NP
46%	5.6	3.1	NP	NP	NP	NP
37%	6.75	4.25	275.79	185.04	NP	NP

Iterative Reconstruction, GE Healthcare, iDose<sup>+</sup> Philips Healthcare, SAFIRE Sinogram-Affirmed Iterative Reconstruction, Siemens Medical Solutions, MBIR (Veo) Model-Based Iterative Reconstruction, GE Healthcare  
 \*in vivo while in the phantom study ASIR 10%, 20%, 30%, 40%, 50%, 60%, 70%, 80%, 90% and 100% was used.

### Neuroimaging

The use of IR in pediatric head CT has been previously studied. *Kilic et al* [22] investigated a blend of 30% adaptive statistical iterative reconstruction (ASIR, GE Healthcare) in pediatric head CT and found that a dose reduction of 29% was possible while maintaining diagnostic acceptability. ASIR is one of the first IR techniques that became commercially available. Therefore ASIR is the most widely investigated IR technique in pediatric CT. With ASIR it is possible to adjust the amount of blending between ASIR and FBP.

*Vorona et al* [23] evaluated the use of ASIR in pediatric head phantoms. In this phantom study similar noise was found at normal dose FBP images compared to 20% dose reduced images with a blend of 20% ASIR. After the phantom study was performed, pediatric head CT scans were made with 20% dose reduction and reconstructed with ASIR 20%. These head CT scans were compared to previous head CT examinations in the same patients. This study demonstrated that diagnostic acceptability and noise were comparable between 20% reduced dose ASIR images and normal dose FBP images.

*Ho et al* [24] investigated the use of different iDose<sup>4</sup> levels in pediatric head CT in 44 children at normal dose levels. Improved image quality and a reduction in noise were found.

A head CT from an 8-year old boy is shown in *Figure 1*. This figure shows that model-based IR allows for more detailed images and better discrimination between gray and white matter. These findings are supported by the study of *Ho et al* [24] who described a subjective improvement in gray-white discrimination with IR compared to FBP. With most IR algorithms different noise reduction levels can be selected. Higher IR levels result in lower noise levels.

One of the disadvantages of IR is the smoother appearance of images, in which details sometimes have a blurred appearance. This is especially the case with higher IR levels [25,26]. An example of a head CT in an 8-year old boy is shown in *Figure 2*. To reduce IMR image blurring, different kernels can be selected. Analogous to FBP, different kernels can be selected with FBP to make images appear less blurred. It is important to note that different tissues may necessitate the use of different reconstruction filters for optimal evaluation. For instance, with the sharpest filter bony structures are better visualized, whereas for assessment of soft tissues a softer kernel might be more appropriate. Therefore it is important to select the right combination of kernel and IR level to achieve optimal diagnostic acceptability. Despite the noise reduction of IR

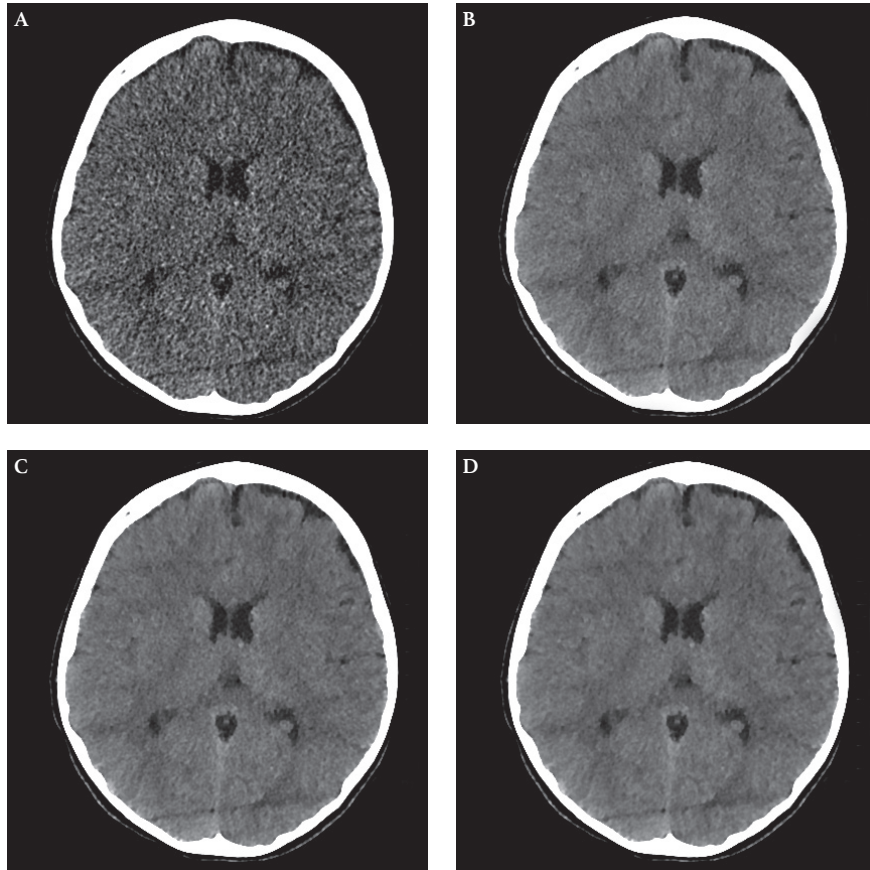


**Figure 1** – Head CT in an 8-year old boy reconstructed with FBP (a), IMR level 1 (b), IMR level 2 (c) and IMR level 3 (d). Model-based IR allows for more detailed images and better discrimination between gray and white matter.

120 kVp, 198 mAs, CTDIvol 27.0 mGy, DLP: 528.7 mGy\*cm, ED: 1.4 mSv  
 Noise 7.7 (a) – 3.2 (b) – 2.8 (c) – 2.4 (d); CNR 0.3 (a) – 3.4 (b) – 3.9 (c) – 4.5 (d)

algorithms, *Figure 3* demonstrates that the optimal combination of IR level and a sharp reconstruction kernel results in low noise images with sharper edges as compared to FBP. The reduction of noise with IR leads to a sharper image compared to FBP.

*Kilic et al* [22], *Vorona et al* [23] and *Ho et al* [24] all found acceptable diagnostic image quality using IR at reduced dose levels. Since only ASIR and iDose<sup>4</sup>

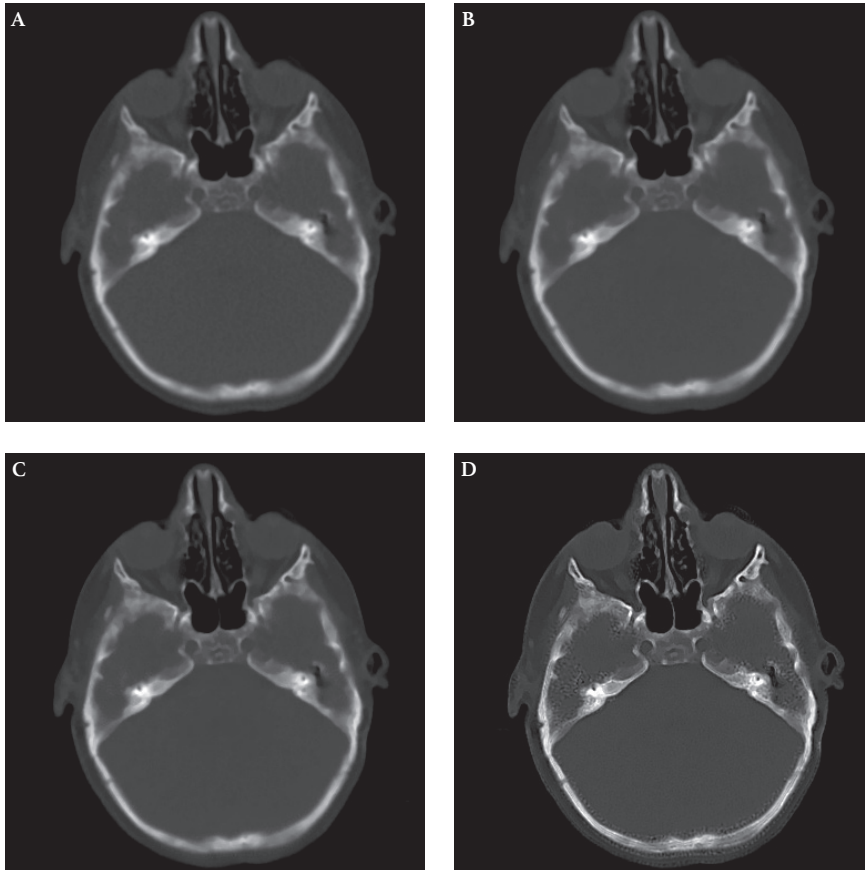


**Figure 2** – Head CT in an 8-year old boy reconstructed with different kernels: FBP (a), IMR level 3 Head Routine (b), IMR level 3 Head Sharp Routine (c), IMR level 3 Head Sharp Plus (d). With the sharpest filter (d) bones are better visualized.

80 kVp, 73 mAs, CTDIvol 2.8 mGy, DLP 56.1 mGy\*cm, ED 0.1 mSv

Noise 7.9 (a) – 4.6 (b) – 5.3 (c) – 13.4 (d); CNR 6.1 (a) – 10.0 (b) – 8.6 (c) – 3.4 (d)

have been investigated in pediatric head CT, other IR techniques should be investigated as well, and corroboration of the findings with ASIR and iDose<sup>4</sup> remain to be established for other CT vendors.

### *Chest Imaging*

The chest is the most widely investigated body part for pediatric IR. Although different IR algorithms were used and different dose reductions were achieved, all studies concluded that IR allowed for dose reduction with improved image quality [27-37].

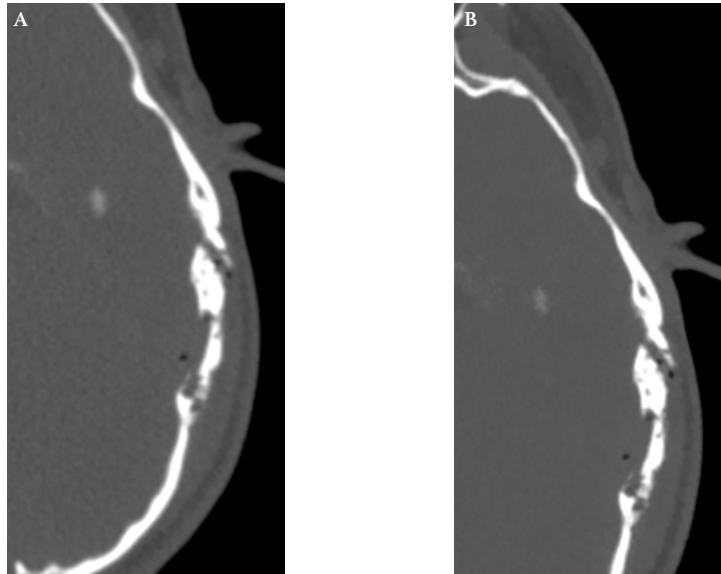


**Figure 3** – Head CT in a 15-year old boy with a skull fracture reconstructed with FBP (a) and IMR level 1 (b) with the same reconstruction kernel. Details of the skull fracture in this 15-year old boy are sharper with IMR compared to FBP.

120 kVp, 149 mAs, CTDIvol 10.1, DLP: 316.0 mGy\*cm, ED: 0.6 mSv  
 Noise 10.6 (a) – 7.3 (b); CNR 5.0 (a) – 7.8 (b); SNR 0.1 (a) – 0.3 (b)

The achieved dose reductions varied from 31% with ASIR up to 92% with the model-based iterative reconstruction technique Veo (MBIR-Veo, *GE Healthcare*) [26,31].

*Figure 4* shows a chest CT during inspiration in an 11-year old boy with lung nodules and lung consolidation due to a pulmonary aspergillus infection. Model-based IR resulted in a substantial decrease in image noise.

With IMR the extent of air trapping and visibility of small lung structures is better visualized compared to FBP. Furthermore, sharpness of lung structures also improves with the right IMR kernel. This is shown in *Figure 5*, which demonstrates a chest CT in a 7-year old boy with an immunodeficiency.

The smoothing effect of IR can potentially result in vanishing of small structures. However, by choosing the right kernel our experience is that small structures can be visualized adequately. Two other studies using MBIR-Veo reported that model-based IR improved visualization of small structures like lung fissures and small vessels [31,36]. However, more studies are necessary to evaluate the effect of model-based IR on visibility of small structures.

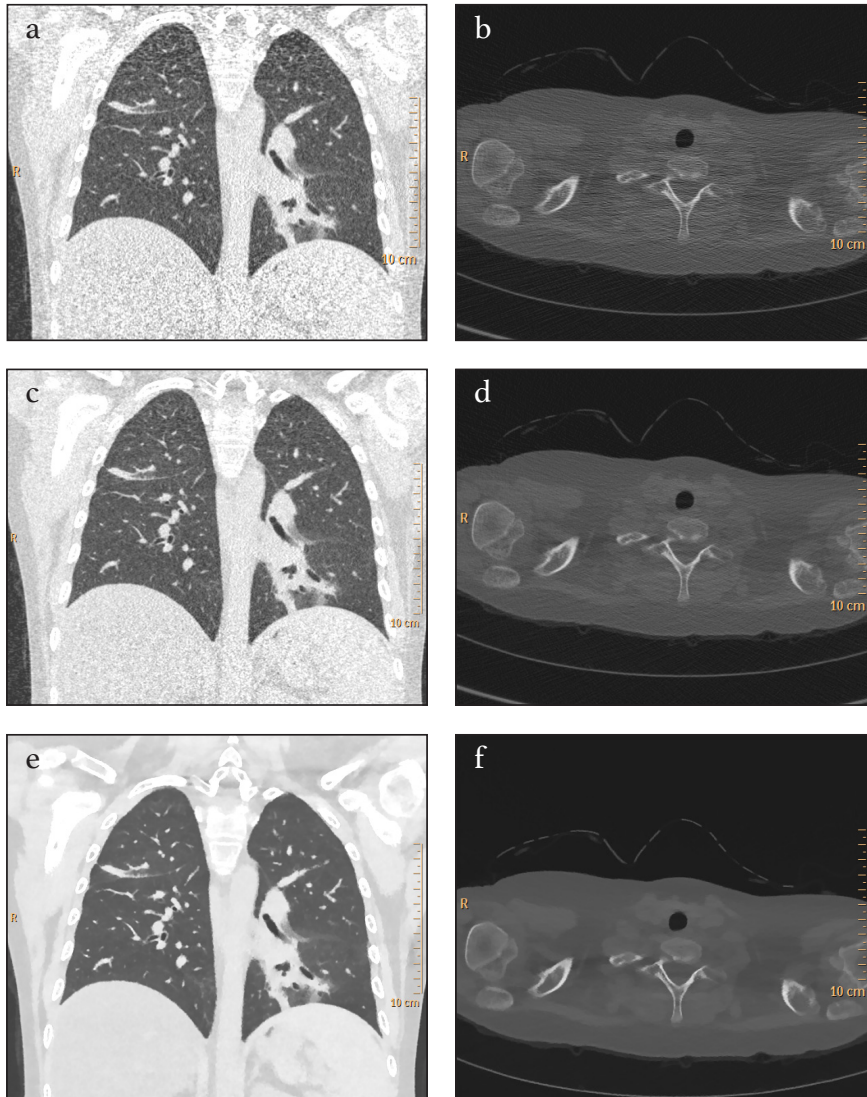


**Figure 4** – Chest CT during inspiration in an 11-year old boy with lung nodules and lung consolidation due to pulmonary aspergillus infection reconstructed with FBP (upper row), hybrid IR (iDose+ level 4; middle row) and MBIR (IMR level 3; bottom row). Note the virtual disappearance of streak artefacts in the shoulder area with IR.

80 kVp, 70 mAs, CTDI<sub>vol</sub> 1.3 mGy, DLP 38.4 mGy\*cm, ED 0.4 mSv

Noise 113.7 (a+b) – 79.4 (c+d) – 15.3 (e+f); CNR 0.6 (a+b) – 0.7 (c+d) – 3.0 (e+f)

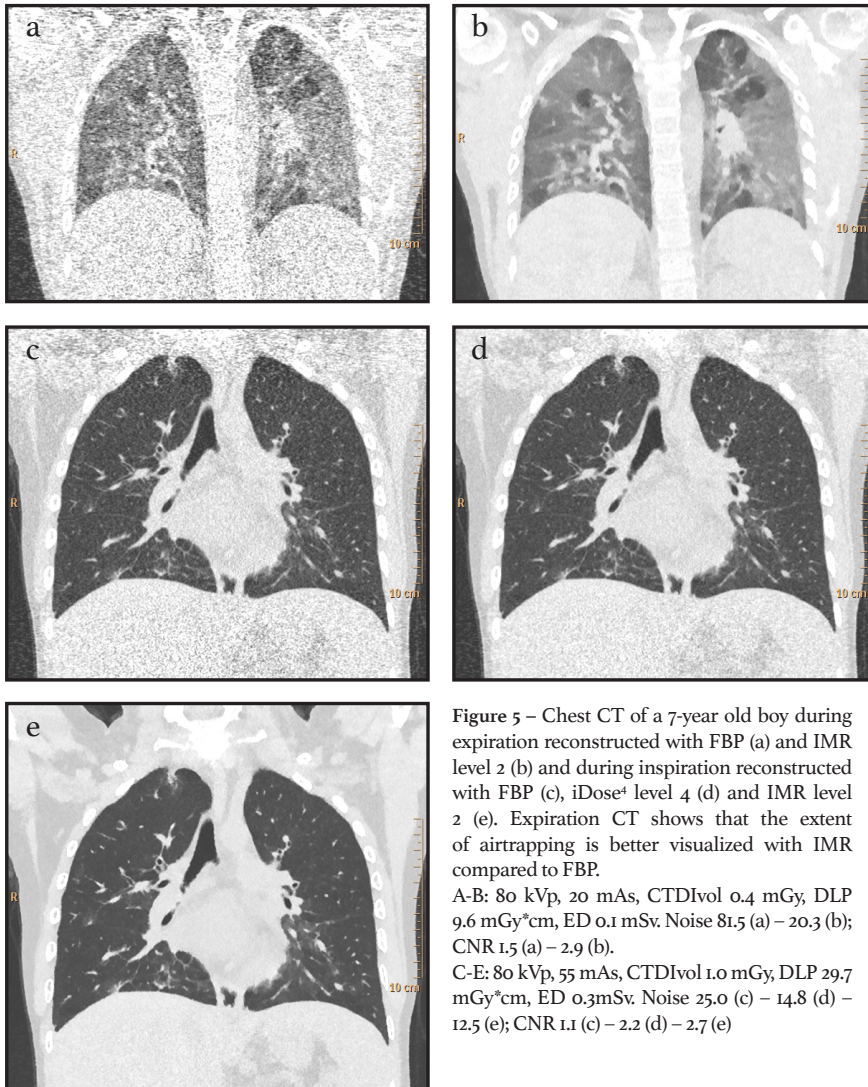


**Figure 5** – Chest CT of a 7-year old boy during expiration reconstructed with FBP (a) and IMR level 2 (b) and during inspiration reconstructed with FBP (c), iDose<sup>4</sup> level 4 (d) and IMR level 2 (e). Expiration CT shows that the extent of airtrapping is better visualized with IMR compared to FBP.

A-B: 80 kVp, 20 mAs, CTDIvol 0.4 mGy, DLP 9.6 mGy\*cm, ED 0.1 mSv. Noise 81.5 (a) – 20.3 (b); CNR 1.5 (a) – 2.9 (b).

C-E: 80 kVp, 55 mAs, CTDIvol 1.0 mGy, DLP 29.7 mGy\*cm, ED 0.3mSv. Noise 25.0 (c) – 14.8 (d) – 12.5 (e); CNR 1.1 (c) – 2.2 (d) – 2.7 (e)

### Abdomen

A feasibility study by *Vorona et al* [38] found that radiation dose can be decreased with 33% in contrast-enhanced pediatric abdominal CT with the use of ASIR 40% while maintaining diagnostic acceptability and image quality. Other studies also found that the radiation dose could be decreased in pediatric abdominal CT with IR [27,28,32-38]. However, the percentage of dose reduction is dependent

on the reference protocol and the  $CTDI_{vol}$  of the reference dose varied largely from 4.1 – 21.2 mGy.

An example of an abdominal CT reconstructed with FBP and IR is shown in Figure 6. This figure shows that IMR results in decreased streak artifacts and noise.

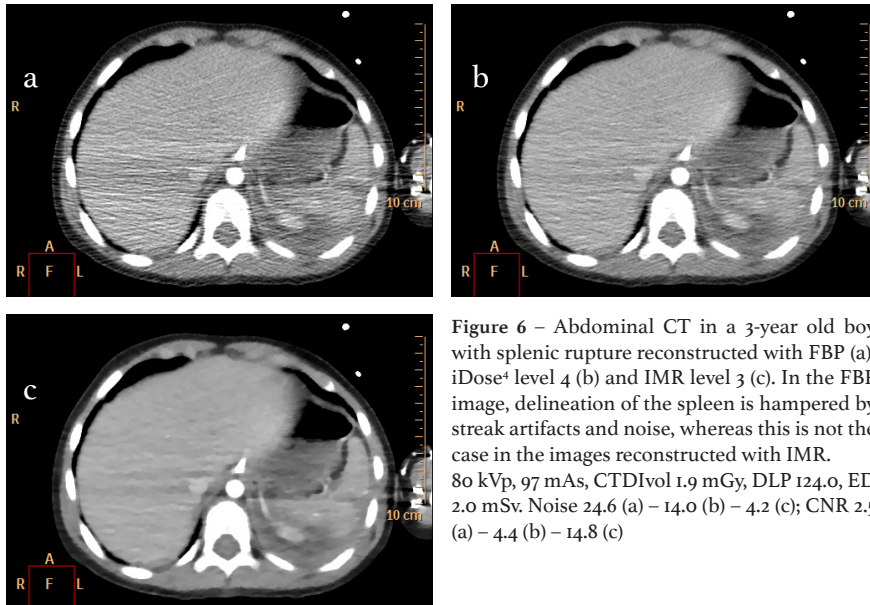


Figure 6 – Abdominal CT in a 3-year old boy with splenic rupture reconstructed with FBP (a), iDose+ level 4 (b) and IMR level 3 (c). In the FBP image, delineation of the spleen is hampered by streak artifacts and noise, whereas this is not the case in the images reconstructed with IMR.  
80 kVp, 97 mAs,  $CTDI_{vol}$  1.9 mGy, DLP 124.0, ED 2.0 mSv. Noise 24.6 (a) – 14.0 (b) – 4.2 (c); CNR 2.5 (a) – 4.4 (b) – 14.8 (c)

### Spine

There are no prior studies that evaluated the use of IR in pediatric spinal CT but in adults the use of IR in spinal CT has been investigated. At approximately 40% dose reduction the IR technique sinogram-affirmed iterative reconstruction (SAFIRE, *Siemens Healthcare*) provided better image quality for intervertebral discs, neural foramina and ligaments but the image quality for non-spinal soft tissues and vertebrae declined compared to FBP at normal dose [39]. *Omoumi et al* [40] also found that the image quality of soft tissue and trabecular bone decreased with SAFIRE. However, *Geyer et al* [41] found that the radiation dose could be reduced to a dose comparable to plain radiography with ASIR without loss of subjective image quality.

Whether the achieved dose reductions with IR in adult spinal CT also holds for pediatric spinal CT, remains to be investigated.

## Discussion

Radiation dose reduction for CT imaging is especially important in children. IR is a highly promising technique that has recently become available for clinical use and has the potential to vastly reduce the radiation dose for pediatric CT imaging. All major CT vendors have developed hybrid IR algorithms and some vendors introduced more advanced model-based IR algorithms recently [16,31]. Since the introduction of IR, substantial and clinically relevant dose reductions were reported for different pediatric CT protocols using IR [22,29,33,38]. Reported maximal dose reductions ranged from 32-92%, depending on the scanned body area and the IR algorithm. However, maximal dose reduction is dependent on the reference dose. Large differences between reference doses were found between studies (*Table 1*). This is partly due to different diagnostic aims between studies, and a reflection of the wide variety of imaging equipment as well as imaging protocols. Therefore it is important to interpret percentages of dose reduction with caution and to assess protocols by looking at dose in terms of  $CTDI_{vol}$ , DLP and/or effective dose.

All major vendors developed their own IR algorithms that are all slightly different from each other. Therefore, the findings with the IR algorithm of a vendor may not be applicable to IR algorithms of other vendors.

The two most mentioned disadvantages of IR are prolonged reconstruction times and a blotchier image appearance. IR leads to longer reconstruction because more computational power is required, however this does not result in a clinically significant delay [13]. Although a blotchy pixelated appearance have been reported in with IR in adults, this was not reported in pediatric CT studies with IR [42]. An explanation could be that relatively few articles on IR in pediatric CT have been compared to adult CT. Furthermore, *Sing et al* [33] suggest that pediatric radiologists may have a higher acceptance of image noise and artifacts compared to adult radiologists, since it is more important to have a low radiation dose in children compared to adults.

Most studies investigating IR used hybrid IR techniques because model-based IR techniques became only recently available. Model-based IR techniques are more advanced and therefore expected to reduce the radiation dose even further. However, because only two studies used model-based IR in pediatrics, some effects remain unclear, for example the visibility of small structures as mentioned earlier [31,36].

In conclusion, in our experience IR is a promising and potentially highly valuable technique that can be used to substantially reduce the amount of radiation in pediatric imaging. Future research should determine the maximum achievable radiation dose reduction in pediatric CT that is possible without loss of diagnostic image quality.

## References

- [1] Brenner DJ, Hall EJ, Computed tomography--an increasing source of radiation exposure. *N Engl J Med* 2007;357(22):2277-84.
- [2] Sun Z, Ng KH, Sarji SA, Is utilisation of computed tomography justified in clinical practice? Part IV: applications of paediatric computed tomography. *Singapore Med J* 2010;51(6):457-63.
- [3] ICRP, Khong PL, Ringertz H, et al., ICRP publication 121: radiological protection in paediatric diagnostic and interventional radiology. *Ann ICRP* 2013;42(2):1-63.
- [4] de Jong PA, Mayo JR, Golmohammadi K, et al., Estimation of cancer mortality associated with repetitive computed tomography scanning. *Am J Respir Crit Care Med* 2006;173(2):199-203.
- [5] Nosek AE, Hartin CW, Jr, Bass KD, et al., Are facilities following best practices of pediatric abdominal CT scans? *J Surg Res* 2013;181(1):11-5.
- [6] Zacharias C, Alessio AM, Otto RK, et al., Pediatric CT: strategies to lower radiation dose. *AJR Am J Roentgenol* 2013;200(5):950-6.
- [7] Townsend BA, Callahan MJ, Zurakowski D, Taylor GA, Has pediatric CT at children's hospitals reached its peak? *AJR Am J Roentgenol* 2010;194(5):1194-6.
- [8] Brooks RA, Di Chiro G, Principles of computer assisted tomography (CAT) in radiographic and radioisotopic imaging. *Phys Med Biol* 1976;21(5):689-732.
- [9] Beister M, Kolditz D, Kalender WA, Iterative reconstruction methods in X-ray CT. *Phys Med* 2012;28(2):94-108.
- [10] Willemink MJ, Leiner T, de Jong PA, et al., Iterative reconstruction techniques for computed tomography part 2: initial results in dose reduction and image quality. *Eur Radiol* 2013;23(6):1632-42.
- [11] Sucha D, Willemink MJ, de Jong PA, et al., The impact of a new model-based iterative reconstruction algorithm on prosthetic heart valve related artifacts at reduced radiation dose MDCT. *Int J Cardiovasc Imaging* 2014.
- [12] Zeng GL, Image reconstruction--a tutorial. *Comput Med Imaging Graph* 2001;25(2):97-103.
- [13] Willemink MJ, Schilham AM, Leiner T, Mali WP, de Jong PA, Budde RP, Iterative reconstruction does not substantially delay CT imaging in an emergency setting. *Insights Imaging* 2013;4(3):391-7.
- [14] Willemink MJ, de Jong PA, Leiner T, et al., Iterative reconstruction techniques for computed tomography Part 1: Technical principles. *Eur Radiol* 2013;23(6):1623-31.
- [15] Raman SP, Johnson PT, Deshmukh S, Mahesh M, Grant KL, Fishman EK, CT dose reduction applications: available tools on the latest generation of CT scanners. *J Am Coll Radiol* 2013;10(1):37-41.
- [16] Mehta D, Thompson R, Morton T, Dhanantwari A, Shefer E, Iterative Model Reconstruction: simultaneously lowered computed tomography radiation dose and improved image quality. *Med Phys* 2013;1(2):147-155.

- [17] Scibelli A, iDose<sup>4</sup> iterative reconstruction technique. Philips Healthcare Whitepaper. 2011; Available via [https://www.healthcare.philips.com/pwc\\_hc/main/shared/Assets/Documents/ct/idose\\_white\\_paper\\_452296267841.pdf](https://www.healthcare.philips.com/pwc_hc/main/shared/Assets/Documents/ct/idose_white_paper_452296267841.pdf) (Accessed 30 September 2013).
- [18] Funama Y, Taguchi K, Utsunomiya D, et al., Combination of a low-tube-voltage technique with hybrid iterative reconstruction (iDose) algorithm at coronary computed tomographic angiography. *J Comput Assist Tomogr* 2011;35(4):480-5.
- [19] Kligerman S, Read K, Dhanantwari A, et al., Iterative model reconstruction (IMR) a novel method of noise reduction to improve diagnostic confidence in obese patients undergoing CT pulmonary angiography (CTPA). Radiological Society of North America 2012. Scientific assembly and annual meeting 2012. (07/25).
- [20] Willeminck MJ, de Jong PA, Pediatric chest computed tomography at a radiation dose approaching a chest radiograph. *Am J Respir Crit Care Med* 2013;188(5):626-7.
- [21] Goo HW, CT radiation dose optimization and estimation: an update for radiologists. *Korean J Radiol* 2012;13(1):1-11.
- [22] Kilic K, Erbas G, Guryildirim M, et al., Quantitative and qualitative comparison of standard-dose and low-dose pediatric head computed tomography: a retrospective study assessing the effect of adaptive statistical iterative reconstruction. *J Comput Assist Tomogr* 2013;37(3):377-81.
- [23] Vorona GA, Zuccoli G, Sutcavage T, Clayton BL, Ceschin RC, Panigrahy A, The use of adaptive statistical iterative reconstruction in pediatric head CT: a feasibility study. *AJNR Am J Neuroradiol* 2013;34(1):205-11.
- [24] Ho C, Oberle R, Wu I, Kim E, Comparison of image quality in pediatric head computed tomography reconstructed using blended iterative reconstruction versus filtered back projection. *Clin Imaging* 2013.
- [25] Leipsic J, Labounty TM, Heilbron B, et al., Adaptive statistical iterative reconstruction: assessment of image noise and image quality in coronary CT angiography. *AJR Am J Roentgenol* 2010;195(3):649-54.
- [26] Mieville FA, Gudinchet F, Rizzo E, et al., Paediatric cardiac CT examinations: impact of the iterative reconstruction method ASIR on image quality--preliminary findings. *Pediatr Radiol* 2011;41(9):1154-64.
- [27] Brady SL, Moore BM, Yee BS, Kaufman RA, Pediatric CT: Implementation of ASIR for Substantial Radiation Dose Reduction while Maintaining Pre-ASIR Image Noise. *Radiology* 2013.
- [28] Brady SL, Yee BS, Kaufman RA, Characterization of adaptive statistical iterative reconstruction algorithm for dose reduction in CT: A pediatric oncology perspective. *Med Phys* 2012;39(9):5520-31.
- [29] Lee SH, Kim MJ, Yoon CS, Lee MJ, Radiation dose reduction with the adaptive statistical iterative reconstruction (ASIR) technique for chest CT in children: an intra-individual comparison. *Eur J Radiol* 2012;81(9):e938-43.

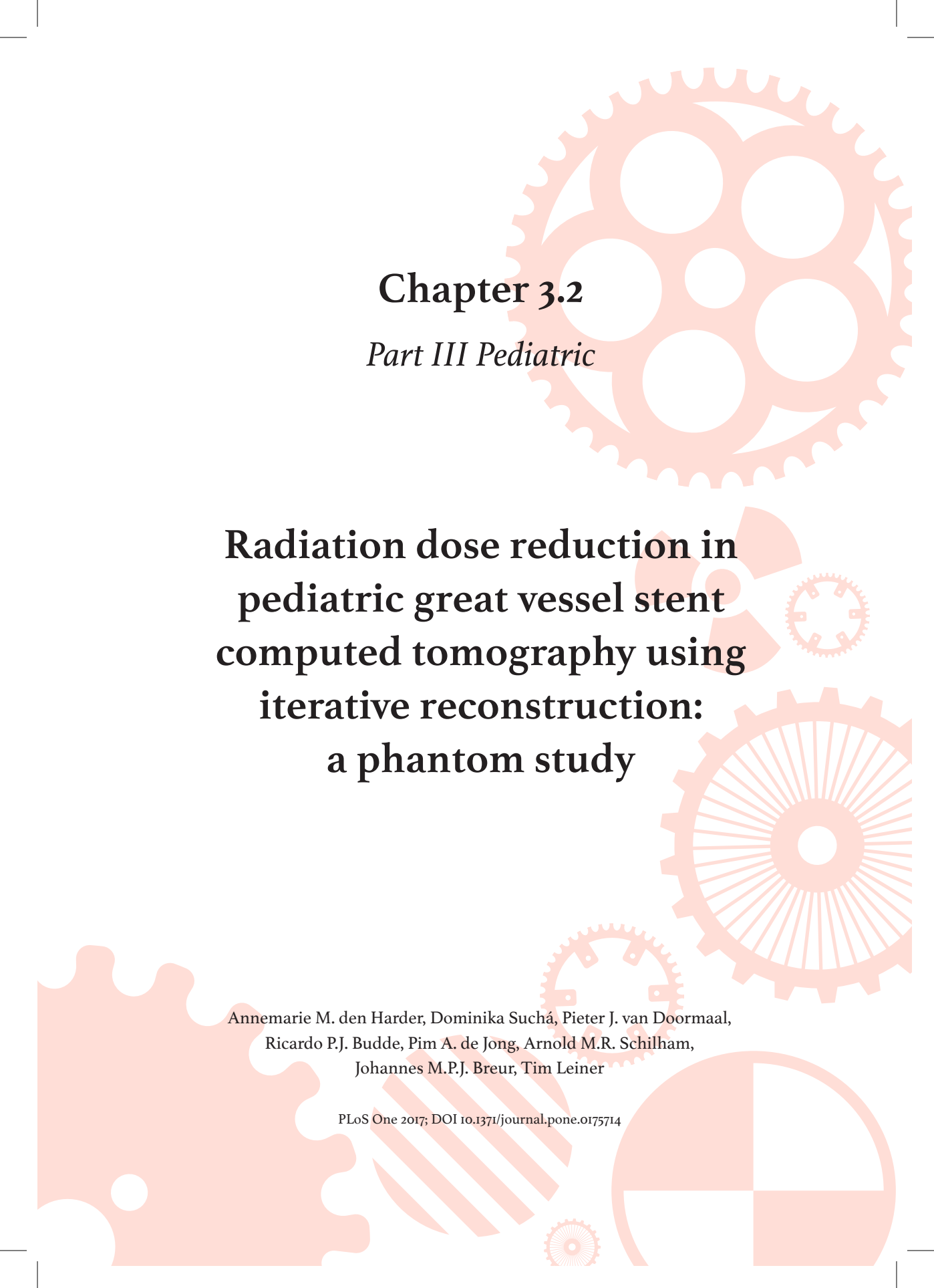
- [30] Lee Y, Jin KN, Lee NK, Low-dose computed tomography of the chest using iterative reconstruction versus filtered back projection: comparison of image quality. *J Comput Assist Tomogr* 2012;36(5):512-7.
- [31] Mieville FA, Berteloot L, Grandjean A, et al., Model-based iterative reconstruction in pediatric chest CT: assessment of image quality in a prospective study of children with cystic fibrosis. *Pediatr Radiol* 2013;43(5):558-67.
- [32] Mieville FA, Gudinchet F, Brunelle F, Bochud FO, Verdun FR, Iterative reconstruction methods in two different MDCT scanners: physical metrics and 4-alternative forced-choice detectability experiments--a phantom approach. *Phys Med* 2013;29(1):99-110.
- [33] Singh S, Kalra MK, Shenoy-Bhangle AS, et al., Radiation dose reduction with hybrid iterative reconstruction for pediatric CT. *Radiology* 2012;263(2):537-46.
- [34] Smith EA, Dillman JR, Goodsitt MM, Christodoulou EG, Keshavarzi N, Strouse PJ, Model-based iterative reconstruction: effect on patient radiation dose and image quality in pediatric body CT. *Radiology* 2014;270(2):526-34.
- [35] Gay F, Pavia Y, Pierrat N, Lasalle S, Neuenschwander S, Brisse HJ, Dose reduction with adaptive statistical iterative reconstruction for paediatric CT: phantom study and clinical experience on chest and abdomen CT. *Eur Radiol* 2013;Epub ahead of print.
- [36] Koc G, Courtier JL, Phelps A, Marcovici PA, Mackenzie JD, Computed tomography depiction of small pediatric vessels with model-based iterative reconstruction. *Pediatr Radiol* 2014.
- [37] Karmazyn B, Liang Y, Ai H, et al., Optimization of Hybrid Iterative Reconstruction Level in Pediatric Body CT. *AJR Am J Roentgenol* 2014;202(2):426-31.
- [38] Vorona GA, Ceschin RC, Clayton BL, Sutcavage T, Tadros SS, Panigrahy A, Reducing abdominal CT radiation dose with the adaptive statistical iterative reconstruction technique in children: a feasibility study. *Pediatr Radiol* 2011;41(9):1174-82.
- [39] Becce F, Ben Salah Y, Verdun FR, et al., Computed tomography of the cervical spine: comparison of image quality between a standard-dose and a low-dose protocol using filtered back-projection and iterative reconstruction. *Skeletal Radiol* 2013;42(7):937-45.
- [40] Omoumi P, Verdun FR, Salah YB, et al., Low-dose multidetector computed tomography of the cervical spine: optimization of iterative reconstruction strength levels. *Acta Radiol* 2013;Epub ahead of print.
- [41] Geyer LL, Korner M, Hempel R, et al., Evaluation of a dedicated MDCT protocol using iterative image reconstruction after cervical spine trauma. *Clin Radiol* 2013;68(7):e391-6.
- [42] Prakash P, Kalra MK, Kambadakone AK, et al., Reducing abdominal CT radiation dose with adaptive statistical iterative reconstruction technique. *Invest Radiol* 2010;45(4):202-10.
- [43] Han BK, Grant KL, Garberich R, Sedlmair M, Lindberg J, Lesser JR, Assessment of an iterative reconstruction algorithm (SAFIRE) on image quality in pediatric cardiac CT datasets. *J Cardiovasc Comput Tomogr* 2012;6(3):200-4.

## Chapter 3.1

- [44] Tricarico F, Hlavacek AM, Schoepf UJ, et al., Cardiovascular CT angiography in neonates and children: image quality and potential for radiation dose reduction with iterative image reconstruction techniques. *Eur Radiol* 2013;23(5):1306-15.
- [45] Nie P, Li H, Duan Y, et al., Impact of Sinogram Affirmed Iterative Reconstruction (SAFIRE) Algorithm on Image Quality with 70 kVp-Tube-Voltage Dual-Source CT Angiography in Children with Congenital Heart Disease. *PLoS One* 2014;9(3):e91123.







## Chapter 3.2

*Part III Pediatric*

# Radiation dose reduction in pediatric great vessel stent computed tomography using iterative reconstruction: a phantom study

Annemarie M. den Harder, Dominika Suchá, Pieter J. van Doormaal,  
Ricardo P.J. Budde, Pim A. de Jong, Arnold M.R. Schilham,  
Johannes M.P.J. Breur, Tim Leiner

PLoS One 2017; DOI 10.1371/journal.pone.0175714

## Abstract

### *Background*

To study dose reduction using iterative reconstruction (IR) for pediatric great vessel stent computed tomography (CT).

### *Methods*

Five different great vessel stents were separately placed in a gel-containing plastic holder within an anthropomorphic chest phantom. The stent lumen was filled with diluted contrast gel. CT acquisitions were performed at routine dose, 52% and 81% reduced dose and reconstructed with filtered back projection (FBP) and IR. Objective image quality in terms of noise, signal-to-noise ratio (SNR) and contrast-to-noise ratio (CNR) as well as subjective image quality were evaluated.

### *Results*

Noise, SNR and CNR were improved with IR at routine and 52% reduced dose, compared to FBP at routine dose. The lowest dose level resulted in decreased objective image quality with both FBP and IR. Subjective image quality was excellent at all dose levels.

### *Conclusion*

IR resulted in improved objective image quality at routine dose and 52% reduced dose, while objective image quality deteriorated at 81% reduced dose. Subjective image quality was not affected by dose reduction.

## Introduction

Coarctation of the aorta is a common congenital heart disease. The most frequent treatment for coarctation of the aorta is stent implantation [1]. After implantation, imaging follow-up is needed to detect complications like in-stent stenosis and aneurysm formation [2-4]. Guidelines propose to perform regular follow-up with CT angiography or magnetic resonance imaging at intervals of less than five years [4]. CT angiography is often the modality of first choice, because it is fast, widely available, non-invasive, associated with less metal artefacts compared to magnetic resonance imaging and this part of the aorta is difficult to visualize with ultrasound [5]. A large multi-institutional study showed that CT is used more than five times as often as MRI for follow-up after stent implantation [1]. However, concerns about the harmful effect of radiation have led to an increased focus on radiation dose reduction. Especially since aortic coarctation stents are predominantly implanted in children [1], who are more radiosensitive and have a longer expected lifetime to develop stochastic effects [6]. Furthermore, the regular CT follow-up in those patients can lead to a substantial cumulative dose. A substantial radiation dose reduction can be achieved by optimizing acquisition parameters and using iterative reconstruction (IR) [7]. A recent study showed that IR allows for a 25 – 41% radiation dose reduction in pediatric CT angiography [7], while studies in adults reported radiation dose reductions of up to 48% with IR for coronary CT [8]. Two phantom studies investigating the use of IR for prosthetic heart valve imaging reported a radiation dose reduction of 50 – 75% without a decrease in objective image quality [9,10]. In the current study we investigated the achievable radiation dose reduction with IR for CT angiography of aortic coarctation stents. To assess whether substantial radiation dose reduction for pediatric CT angiography is feasible, we performed an *in vitro* study. We evaluated the effect of dose reduction on objective and subjective image quality of commonly used stents to treat coarctation aortae.

## Materials and Methods

### *Phantom*

Five different stents were studied: (1) Advanta V12 covered stent made of stainless steel (Atrium Medica, length 25mm), (2) AndraStent 30-XL stent made of cobalt-chromium (Andramed, length 39mm), (3) Cheatham-Platinum stent made of 0.013” platinum / iridium wire (NuMED), (4) IntraStent Max LD made of stainless steel (EV3, length 36mm) and (5) Formula 535 stent made of

316L stainless steel (Cook Medical). An Atlas balloon (Bard BV) was used to inflate stent 1-4 to a diameter of 20 mm. Stent 5 (a premounted Formula 535 stent) was dilated to a diameter of 10 mm because this is the maximal vendor recommended size. To simulate a contrast-enhanced vessel, a balloon filled with diluted contrast-gel (20 times diluted) was placed inside every stent. The stents were placed at an angle of approximately 30 degrees in a plastic holder. The plastic holder was filled with gel without contrast and placed in a commercially available anthropomorphic chest phantom (D100, QRM GmbH, Moehrendorf, Germany) which simulates the radiation absorption of a small person [11]. The posterior-anterior distance is 200 mm and the distance from left to right is 300 mm. Images of the phantom setup are provided in *Figure 1*.

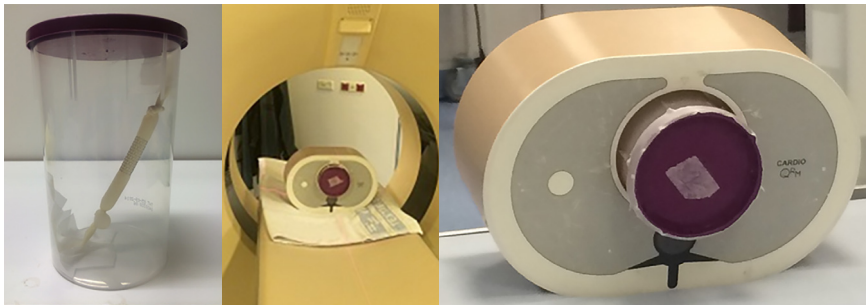


Figure 1 - Phantom set-up. A plastic holder containing a stent with inside a balloon (left image) was placed into an anthropomorphic chest phantom (middle and right image) [2].

### *CT acquisition protocol*

A 256-slice CT scanner (Brilliance iCT, Philips Healthcare, Best, The Netherlands) was used for image acquisition. The following parameters were used: collimation 128 x 0.625 mm, slice thickness 0.9 mm, rotation time 0.27 seconds and a matrix size of 512 x 512 pixels. A standard sequential cardiac CT protocol was used for all protocols with an ECG generator to simulate a heart rate of 60 beats/min. The tube voltage was 100 kV for the routine dose protocol and 80 kV for the low dose protocols. The tube current-time product was 195 mAs for the routine dose protocol and 195 mAs and 80 mAs respectively for the low dose protocols. Each stent was scanned eight times per protocol with small translations of the phantom to take interscan variation into account, resulting in a total of 120

acquisitions. Images were reconstructed with filtered back projection (FBP) and IR (iDose<sup>4</sup> level 3, Philips Healthcare, Best, The Netherlands). iDose<sup>4</sup> has seven levels of noise reduction, with a higher level implicating more noise reduction. iDose<sup>4</sup> level 3 was used as it is recommended by the vendor in this setting. Volumetric CT dose index (CTDI<sub>vol</sub>) based on a 32 cm phantom and dose-length product (DLP) were recorded for each scan. The scan length was 54 mm for the stents with a diameter of 20 mm and 73 mm for the stent with a diameter of 10 mm due to the length of this stent.

### *Image Quality*

Objective image quality was assessed by drawing a homogeneous region of interest (ROI) in the gel surrounding the stent with a diameter of approximately 20 mm and a smaller ROI in the contrast within the stent. Average CT values (HU) and standard deviation (SD) were obtained. Based on this, noise, contrast-to-noise ratio (CNR) and signal-to-noise ratio (SNR) were calculated [12]. Noise was defined as the SD of the ROI and the SNR as the ratio between the mean HU and the SD. The SNR was calculated for the ROI in the contrast within the stent. The CNR was computed using the following equation:

$$CNR = \frac{HU(\text{contrast within stent}) - HU(\text{gel})}{\sqrt{\frac{1}{2} \times (SD(\text{contrast within stent})^2 + SD(\text{gel})^2)}}$$

For each acquisition the relative difference in image quality was calculated as the percentage difference compared to FBP at routine dose (reference standard). Subjective image quality was assessed at the center and at the outlets of the stent by two radiologists using a 4-point scale and standardized scoring forms:

1. Poor, non-diagnostic image quality, in stent lumen not delineated due to severe artifacts or excessive noise
2. Moderate, limited diagnostic value, stent lumen is assessable but partially obscured due to moderate artifacts or noise
3. Good, diagnostic image quality, stent skeleton and lumen delineated with minor artifacts or noise
4. Excellent, excellent image quality with clear delineation of stent and lumen without artifacts or noise.

Subjective image quality was evaluated by two observers using one acquisition of each CT protocol and observers were blinded for stent type and acquisition protocol. One observer was a radiologist with 6 years' experience, the second observer was a pediatric cardiologist with 6 years' experience in cardiovascular CT.

### *Statistical analysis*

SPSS Statistics version 20.0 for Windows was used for statistical analysis. Data were compared using the Friedman test and post-hoc analyses were performed with the Wilcoxon signed-rank test to test for significant differences compared with the reference standard namely the routine dose CT protocol reconstructed with FBP. A p-value  $<0.05$  was considered statistically significant for the Friedman test and a Bonferroni correction was made for the post hoc Wilcoxon signed-rank test with a p-level set at 0.01. Inter-observer reproducibility for subjective image quality was assessed with the Cohen kappa coefficient and percentage of agreement. The kappa was interpreted as poor ( $k = 0.00-0.20$ ), fair ( $k = 0.21-0.40$ ), moderate ( $k = 0.41-0.60$ ), good ( $k = 0.61-0.80$ ) or excellent ( $k = 0.81-1.00$ ). Statistical significant differences in subjective image quality were tested using the Wilcoxon signed-rank test with a p-level set at 0.05.

## **Results**

An example of the stent images with different protocols is provided in *Figure 2*. The CTDI<sub>vol</sub> of the routine dose protocol (100 kV, 195 mAs) was 7.7 mGy while the low dose protocols were 3.7 mGy and 1.5 mGy respectively. This resulted in a relative dose reduction of 52% and 81% respectively. The DLP was 51.2 mGy\*cm, 23.6 mGy\*cm and 9.7 mGy\*cm respectively. The average attenuation of the balloon, simulating the contrast-enhanced vessel, was 875 HU and the average attenuation of the gel surrounding the balloon was 10 HU.

### *Objective image quality*

Results of the comparison with regard to objective image quality are shown in *Figures 3 – 5* and *Table 1*. At each radiation dose level, IR resulted in improved objective image quality compared to FBP. Noise was lower at routine dose with IR (-21.6%,  $p < 0.0005$ ), but increased at both reduced dose levels with 49.6% and 143.9% (FBP) and with 17.5% and 86.6% (IR). The SNR and the CNR were improved both at routine dose and at 52% reduced dose with IR, while FBP and the lowest dose level resulted in a decrease in SNR and CNR ( $p < 0.0005$ ). Full data are provided online [13].

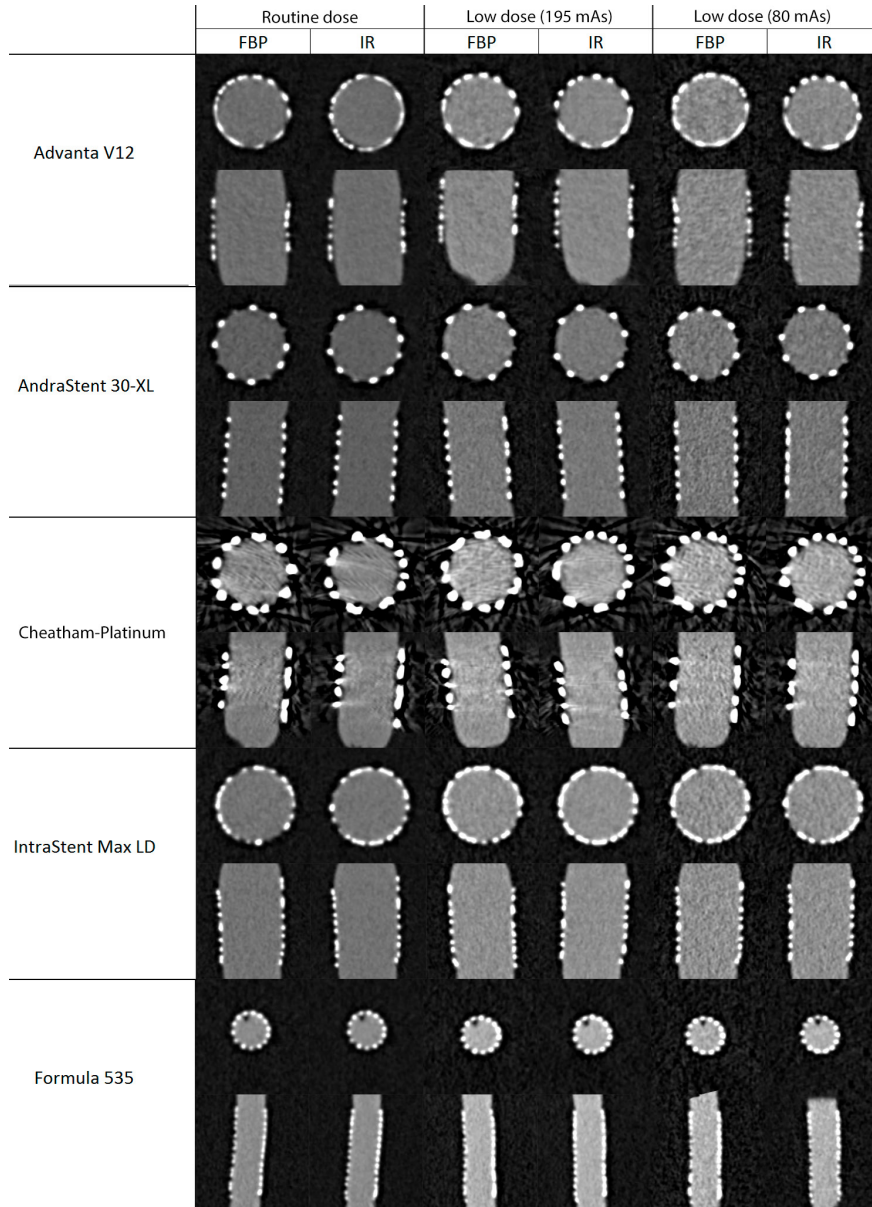


Figure 2 – Example of the stents acquired with different protocols: routine dose (195 mAs, 100kV), low dose (195 mAs, 80kV), low dose (80mAs, 80kV).

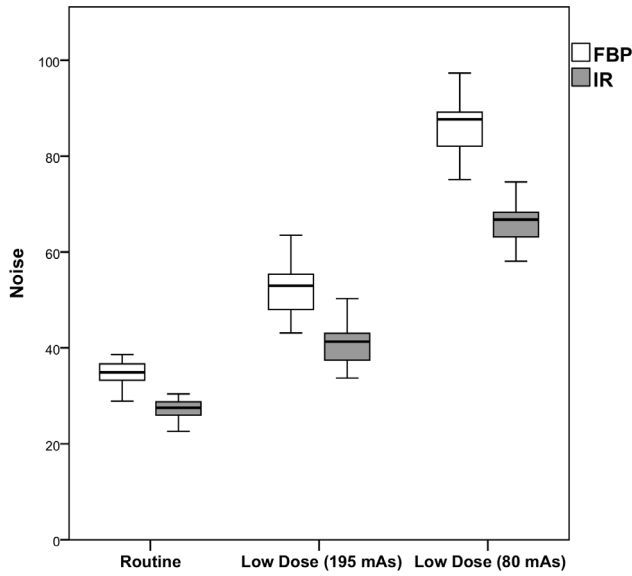


Figure 3 – Noise per dose level for FBP and IR. The white boxes represent the noise with FBP, while the gray boxes represent the noise with IR. IR resulted in a decrease in noise compared to FBP at the same dose level. *FBP Filtered Back Projection, IR Iterative Reconstruction*

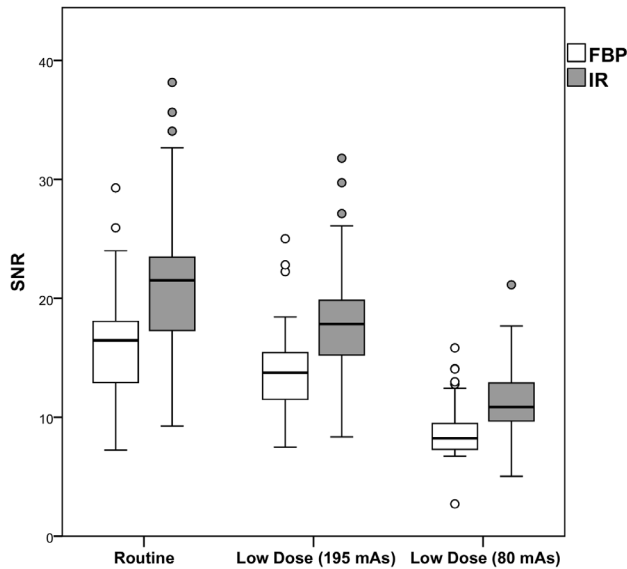


Figure 4 – SNR per dose level for FBP and IR. The white boxes represent the SNR with FBP, while the gray boxes represent the SNR with IR. IR resulted in an increase in SNR compared to FBP at the same dose level. *FBP Filtered Back Projection, IR Iterative Reconstruction, SNR Signal-to-noise ratio*

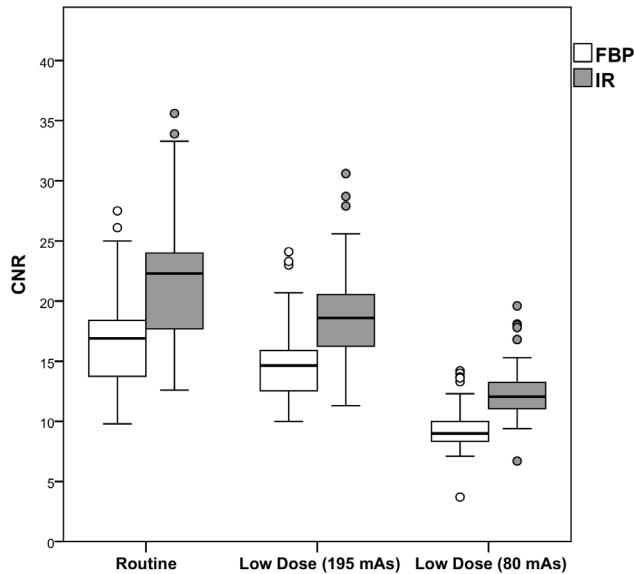


Figure 5 – CNR per dose level for FBP and IR. The white boxes represent the CNR with FBP, while the gray boxes represent the CNR with IR. IR resulted in an increase in CNR compared to FBP at the same dose level. *CNR Contrast-to-noise ratio, FBP Filtered Back Projection, IR Iterative Reconstruction*

Part III

Table 1 – Objective image quality. Values are presented as median [interquartile range].

	FBP	Relative change	IR	Relative change
<b>Noise</b>				
Routine	34.9 [33.2 – 36.7]	NA	27.5 [26.0 – 28.8]*	-21.6%
Low dose <sup>§</sup>	53.0 [48.0 – 55.5]*	49.6%	41.3 [37.4 – 43.1]*	17.5%
Low dose <sup>#</sup>	87.7 [82.0 – 89.3]*	143.9%	66.9 [62.9 – 68.3]*	86.6%
<b>SNR</b>				
Routine	16.48 [12.89 – 18.18]*	NA	21.52 [17.18 – 23.58]*	30.8%
Low dose <sup>§</sup>	13.75 [11.48 – 15.46]*	-13.8%	17.84 [14.99 – 19.84]*	10.6%
Low dose <sup>#</sup>	8.23 [7.30 – 9.53]*	-31.0%	10.86 [9.69 – 12.89]*	-46.5%
<b>CNR</b>				
Routine	16.9 [13.7 – 18.4]*	NA	22.3 [17.7 – 24.0]*	29.3%
Low dose <sup>§</sup>	14.7 [12.5 – 15.9]*	-12.1%	18.8 [16.4 – 20.6]*	11.9%
Low dose <sup>#</sup>	9.0 [8.3 – 10.1]*	-44.6%	12.1 [11 – 13.4]*	-28.7%

The relative difference is the percentage difference compared to FBP at routine dose (reference standard). The value represents the median relative change of the eight acquisitions. NA not applicable, \* p<0.01, <sup>§</sup>(80 kV, 195 mAs), <sup>#</sup>(80 kV, 80 mAs).

*Subjective image quality*

Inter-observer reliability for qualitative image quality scores was excellent ( $k = 0.81$ ). The percentage inter-observer agreement was 93%. Subjective image quality scores are displayed in *Table 2*. Overall, the image quality was excellent (median 4.0) with no differences between the routine and low dose protocols or between FBP and IR (all  $p$ -values  $>0.05$ ). Full data are provided online [13].

Table 2 – Subjective image quality scores. Scores are displayed as median [interquartile range].

	FBP		IR	
	Center	Outlets	Center	Outlets
<b>Routine dose</b> (100 kV, 195 mAs)	4.0 [3.0 – 4.0]	4.0 [3.0 – 4.0]	4.0 [3.8 – 4.0]	4.0 [3.8 – 4.0]
<b>Low dose</b> (80 kV, 195 mAs)	4.0 [3.8 – 4.0]	4.0 [3.8 – 4.0]	4.0 [3.8 – 4.0]	4.0 [3.8 – 4.0]
<b>Low dose</b> (80 kV, 80 mAs)	4.0 [3.8 – 4.0]	4.0 [3.8 – 4.0]	4.0 [3.8 – 4.0]	4.0 [3.8 – 4.0]

No significant differences compared to FBP at routine dose were observed. 1 poor, non-diagnostic image quality, 2 moderate, limited diagnostic value, 3 good, diagnostic image quality, 4 excellent, excellent image quality

**Discussion**

This in-vitro study showed that for pediatric great vessel stent CT imaging a radiation dose reduction of more than 81% is feasible without affecting subjective image quality. Although the objective image quality decreased with both FBP and IR at this dose level, the subjective image quality remained excellent and the use of IR resulted in improved objective image quality compared with FBP. The results of this study are relevant since risk estimates suggest that pediatric CT results in an increased radiation risk over adult CT [14]. This is worrisome, since the use of CT in pediatrics increased in the past decades [15]. To reduce the radiation dose burden, it is essential to increase awareness and decrease unnecessary CT examinations [16] as well as applying the As Low As Reasonably Achievable (ALARA) concept [17]. One of the strategies to achieve radiation dose reduction is applying IR techniques [8,18]. IR has also shown to allow for reduction of metal blooming artifacts, which is especially beneficial for the evaluation of stents [19]. Several studies have investigated the use of IR for stent

evaluation, but mainly in coronary artery stents [20-25]. Ebersberger et al.[26] investigated 37 implanted coronary artery stents at full and half radiation dose and found improved objective image quality and comparable subjective image quality at reduced radiation dose using IR. However, a relatively high radiation dose was used of 4.3 mSv at half radiation dose. A study performed by Wuest and colleagues [23] in 73 implanted coronary stents at a radiation dose of 0.3 mSv (DLP 22.6 mGy\*cm) found improved objective and subjective image quality with IR. Only one radiation dose level was used. To our best knowledge only one study investigated the effect of radiation dose reduction for great vessel stent imaging [27]. Two dose levels were used, namely 1.8 mSv (120 kVp, 80 mAs) and 0.6 mSv (80 kVp, 80 mAs) and results were compared to digital angiography. Both groups were comparable in body weight, age and stent size. There was good correlation with digital angiography at both dose levels. Subjective image quality was the same at the two dose levels, which is comparable to our study results.

In this study the dose was reduced with 52% and 81% compared to routine dose. However, routine dose levels may vary between hospitals. The current guidelines for aortic disease state that the estimated radiation dose of aortic CT is 10-15 mSv which is very high compared to current literature [28]. The American Association of Physicists in Medicine is currently working on reference protocols for CT, but there are no protocols for pediatric cardiac CT available yet. Our routine dose is however comparable to a previous study by Eichhorn et al. [27].

In our study the objective image quality decreased at low dose levels both with FBP and IR. A hybrid IR algorithm was used. Conventionally, FBP is used for image reconstruction, which creates images using projection data (backward projection). With true IR, both backward and forward projection steps are used, in which projection data are created using imaging data [29]. Hybrid iterative reconstruction is a blend of FBP and IR, and iterates in the projection data domain and image data domain. It reduces image noise because statistical properties of the acquisition are included in the reconstruction process. While model-based IR algorithms are more advanced and use both forward and backward projection steps between the projection domain and the image domain, thereby approaching true IR [6]. Further improvement in objective image quality can possibly be achieved with model-based IR algorithms which have shown to improve objective image quality further [6]. Another promising method to improve image quality further is the use of dual-energy CT which

enables the acquisition of mono-energetic images at different keV levels. Using a high keV-level blooming artifacts can be almost completely suppressed, however at the cost of reduced stent visibility [21]. First results show improved stent lumen visualization in coronary stents, however this effect might be less pronounced for large vessels stents but is currently unknown [21].

To our best knowledge, this study is the first to systematically assess the potential of IR for great vessel stent imaging. Radiation dose can be drastically reduced without affecting subjective image quality, and IR can be used to improve objective image quality at low dose levels. Since aortic coarctation is a congenital disease, stents are mainly implanted at young age and multiple follow-up examinations are often required. Therefore, radiation dose reduction for this indication is very important for daily practice. The current study contributes to a further reduction in radiation dose of CT angiography examinations in children after stent implantation. This study has however several limitations. It concerns an *in vitro* study, therefore the effect of motion artifacts is unknown. However, because of the *in vitro* set up we were able to repeat acquisitions and investigate multiple dose levels using the same phantom. Because we were only interested in the image quality of the stent, a short scan length was used which is not representative for the clinical situation where a larger scan length is used to depict the surrounding anatomical structures. This will result in a lower effective dose than feasible in clinical practice, therefore the CTDI<sub>vol</sub> was presented. Furthermore, future research should determine the diagnostic accuracy for pathology, since in our study no abnormalities like in-stent stenosis were present. Finally, only one hybrid IR algorithm was used, and results may be different with other hybrid and model-based IR algorithms. However, the overall results could be generalizable to other vendors and algorithms as we found substantial dose reduction to be feasible with routine FBP using subjective image quality was used as endpoint.

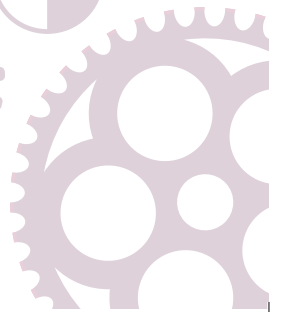
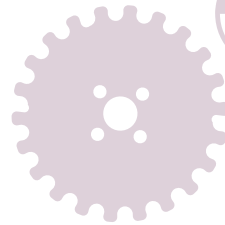
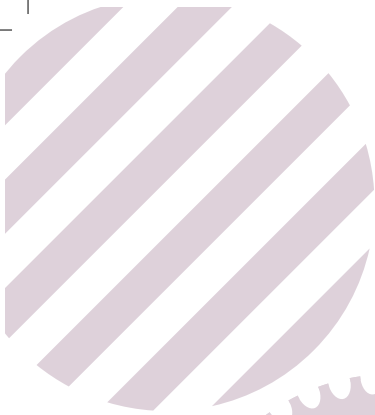
In conclusion, this study showed that in an *in vitro* setting, substantial CT radiation dose reduction can be achieved for pediatric great vessel stent imaging without affecting the subjective image quality. Using IR techniques is helpful as a significant improvement of the objective image quality was achieved by noise reduction, which resulted in an increase of SNR and CNR. Future research should determine the diagnostic accuracy with reduced dose acquisitions in an in-patient setting.

## References

- [1] Holzer R, Qureshi S, Ghasemi A, et al., Stenting of aortic coarctation: acute, intermediate, and long-term results of a prospective multi-institutional registry--Congenital Cardiovascular Interventional Study Consortium (CCISC). *Catheter Cardiovasc Interv* 2010;76(4):553-63.
- [2] den Harder AM, Sucha D, van Hamersvelt RW, et al., Imaging of pediatric great vessel stents: Computed tomography or magnetic resonance imaging? *PLoS One* 2017;12(1):e0171138.
- [3] Baumgartner H, Bonhoeffer P, De Groot NM, et al., ESC Guidelines for the management of grown-up congenital heart disease (new version 2010). *Eur Heart J* 2010;31(23):2915-57.
- [4] Warnes CA, Williams RG, Bashore TM, et al., ACC/AHA 2008 guidelines for the management of adults with congenital heart disease: a report of the American College of Cardiology/American Heart Association Task Force on Practice Guidelines (Writing Committee to Develop Guidelines on the Management of Adults With Congenital Heart Disease). Developed in Collaboration With the American Society of Echocardiography, Heart Rhythm Society, International Society for Adult Congenital Heart Disease, Society for Cardiovascular Angiography and Interventions, and Society of Thoracic Surgeons. *J Am Coll Cardiol* 2008;52(23):e143-263.
- [5] Taylor AM, Cardiac imaging: MR or CT? Which to use when. *Pediatr Radiol* 2008;38 Suppl 3:S433-8.
- [6] den Harder AM, Willemink MJ, Budde RP, Schilham AM, Leiner T, de Jong PA, Hybrid and model-based iterative reconstruction techniques for pediatric CT. *AJR Am J Roentgenol* 2015;204(3):645-53.
- [7] Habib Geryes B, Calmon R, Khraiche D, Boddaert N, Bonnet D, Raimondi F, Radiation dose reduction in paediatric coronary computed tomography: assessment of effective dose and image quality. *Eur Radiol* 2015.
- [8] Den Harder AM, Willemink MJ, De Ruiter QM, et al., Dose reduction with iterative reconstruction for coronary CT angiography: a systematic review and meta-analysis. *Br J Radiol* 2015;20150068.
- [9] Sucha D, Willemink MJ, de Jong PA, et al., The impact of a new model-based iterative reconstruction algorithm on prosthetic heart valve related artifacts at reduced radiation dose MDCT. *Int J Cardiovasc Imaging* 2014.
- [10] Habets J, Symersky P, de Mol BA, Mali WP, Leiner T, Budde RP, A novel iterative reconstruction algorithm allows reduced dose multidetector-row CT imaging of mechanical prosthetic heart valves. *Int J Cardiovasc Imaging* 2012;28(6):1567-75.
- [11] Quality Assurance in Radiology and Medicine (QRM) GmbH, Anthropomorphic cardio phantom; <http://www.qrm.de/content/pdf/QRM-Cardio-Phantom.pdf>. 2008;2013(May).

- [12] Sucha D, Willemlink MJ, de Jong PA, et al., The impact of a new model-based iterative reconstruction algorithm on prosthetic heart valve related artifacts at reduced radiation dose MDCT. *Int J Cardiovasc Imaging* 2014;30(4):785-93.
- [13] den Harder AM, Sucha D, van Doormaal PJ, et al., Radiation dose reduction in pediatric great vessel stent computed tomography using iterative reconstruction: A phantom study. *PLoS One* 2017;12(4):e0175714.
- [14] Brenner D, Elliston C, Hall E, Berdon W, Estimated risks of radiation-induced fatal cancer from pediatric CT. *AJR Am J Roentgenol* 2001;176(2):289-96.
- [15] Miglioretti DL, Johnson E, Williams A, et al., The use of computed tomography in pediatrics and the associated radiation exposure and estimated cancer risk. *JAMA Pediatr* 2013;167(8):700-7.
- [16] Donnelly LF, Reducing radiation dose associated with pediatric CT by decreasing unnecessary examinations. *AJR Am J Roentgenol* 2005;184(2):655-7.
- [17] Slovis TL, Children, computed tomography radiation dose, and the As Low As Reasonably Achievable (ALARA) concept. *Pediatrics* 2003;112(4):971-2.
- [18] Willemlink MJ, de Jong PA, Leiner T, et al., Iterative reconstruction techniques for computed tomography Part I: Technical principles. *Eur Radiol* 2013;23(6):1623-31.
- [19] Cho YJ, Schoepf UJ, Silverman JR, et al., Iterative image reconstruction techniques: cardiothoracic computed tomography applications. *J Thorac Imaging* 2014;29(4):198-208.
- [20] Ebersberger U, Tricarico F, Schoepf UJ, et al., CT evaluation of coronary artery stents with iterative image reconstruction: improvements in image quality and potential for radiation dose reduction. *Eur Radiol* 2013;23(1):125-32.
- [21] Mangold S, Cannao PM, Schoepf UJ, et al., Impact of an advanced image-based monoenergetic reconstruction algorithm on coronary stent visualization using third generation dual-source dual-energy CT: a phantom study. *Eur Radiol* 2015.
- [22] Almutairi A, Sun Z, Al Safran Z, Poovathumkadavi A, Albader S, Ifdailat H, Optimal Scanning Protocols for Dual-Energy CT Angiography in Peripheral Arterial Stents: An in Vitro Phantom Study. *Int J Mol Sci* 2015;16(5):11531-49.
- [23] Wuest W, May MS, Scharf M, et al., Stent evaluation in low-dose coronary CT angiography: effect of different iterative reconstruction settings. *J Cardiovasc Comput Tomogr* 2013;7(5):319-25.
- [24] Oda S, Utsunomiya D, Funama Y, et al., Improved coronary in-stent visualization using a combined high-resolution kernel and a hybrid iterative reconstruction technique at 256-slice cardiac CT-Pilot study. *Eur J Radiol* 2013;82(2):288-95.
- [25] Funama Y, Oda S, Utsunomiya D, et al., Coronary artery stent evaluation by combining iterative reconstruction and high-resolution kernel at coronary CT angiography. *Acad Radiol* 2012;19(11):1324-31.

- [26] Ebersberger U, Tricarico F, Schoepf UJ, et al., CT evaluation of coronary artery stents with iterative image reconstruction: improvements in image quality and potential for radiation dose reduction. *Eur Radiol* 2013;23(1):125-32.
- [27] Eichhorn JG, Long FR, Jourdan C, et al., Usefulness of multidetector CT imaging to assess vascular stents in children with congenital heart disease: an in vivo and in vitro study. *Catheter Cardiovasc Interv* 2008;72(4):544-51.
- [28] Erbel R, Aboyans V, Boileau C, et al., 2014 ESC Guidelines on the diagnosis and treatment of aortic diseases. *Kardiol Pol* 2014;72(12):1169-252.
- [29] den Harder AM, Willeminck MJ, de Jong PA, et al., New horizons in cardiac CT. *Clin Radiol* 2016;71(8):758-67.



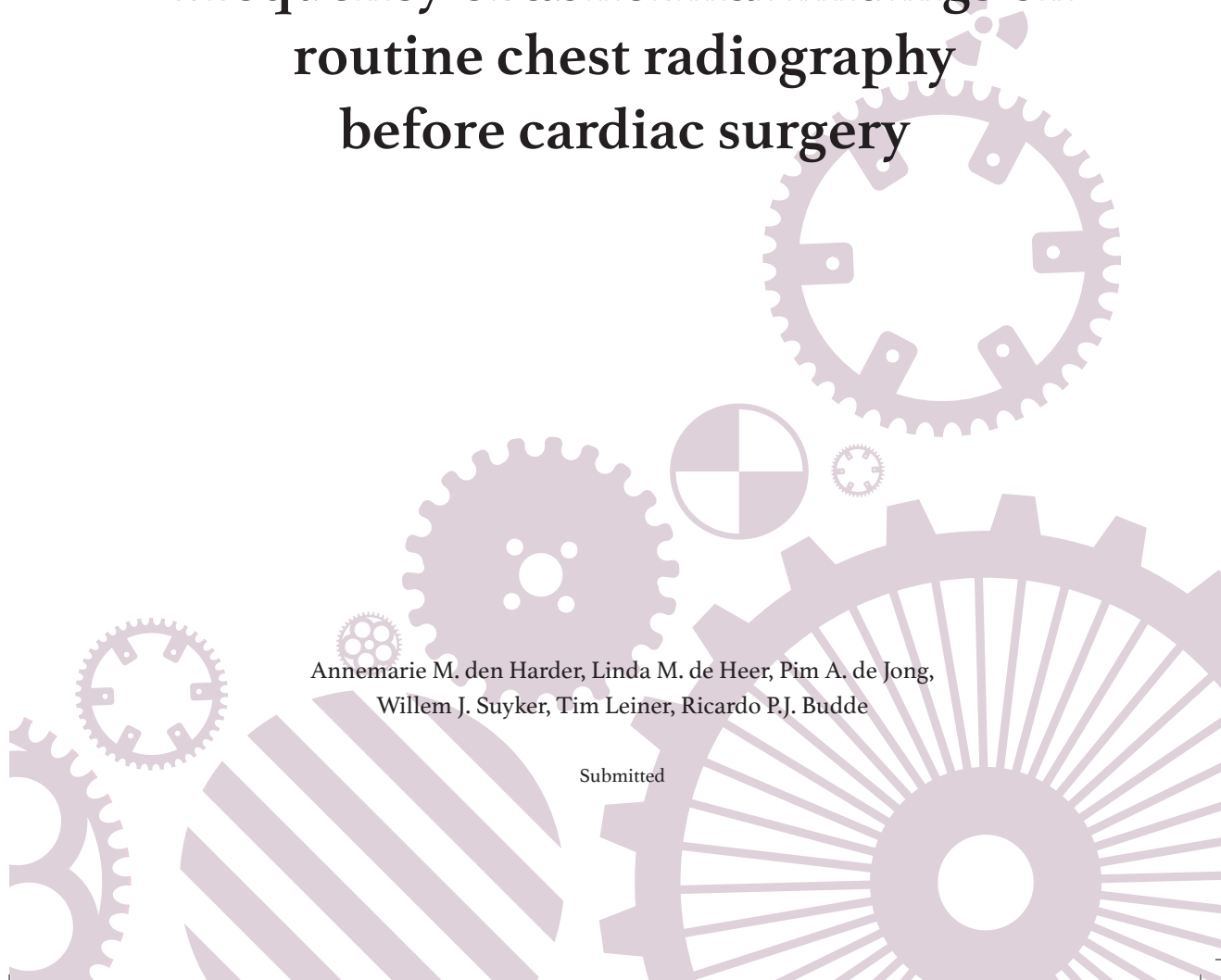
# Chapter 4.1

*Part IV Preoperative CT*

## Frequency of abnormal findings on routine chest radiography before cardiac surgery

Annemarie M. den Harder, Linda M. de Heer, Pim A. de Jong,  
Willem J. Suyker, Tim Leiner, Ricardo P.J. Budde

Submitted



## Abstract

### *Objective*

Preoperative chest radiograph screening is widely used prior to cardiac surgery. The objective of this study was to investigate the frequency of abnormal findings on a routine chest radiograph before cardiac surgery.

### *Methods*

In this retrospective cohort study 1,136 patients were included. Patients were scheduled for cardiac surgery and underwent a preoperative chest radiograph. The primary outcome was the frequency of abnormalities on the chest radiograph. Secondary outcome was the effect of those abnormalities on surgery.

### *Results*

Half of the patients (570/1,136; 50%) had one or more abnormalities on the chest radiograph. Most frequent abnormalities were cardiomegaly, aortic elongation, signs of chronic obstructive pulmonary disease, vertebral fractures or height loss, possible pulmonary or mediastinal mass, pleural effusion and atelectasis. In two patients (2/1,136; 0.2%), the chest radiograph led to postponement of surgery, while in none of the patients the surgery was cancelled. In 1 patient (1/1,136; 0.1%) the surgical approach was altered and in 15 patients (15/1,136; 1.3%) further analysis was performed without having an impact on the planned surgical approach.

### *Conclusions*

Although abnormalities are frequently found on preoperative chest radiographs prior to cardiac surgery, change in clinical management with regard to planned surgery or surgical approach occurs infrequently.

## Introduction

More than 30 billion dollars are spent annually on preoperative testing in the United States [1]. A conventional chest radiograph is performed before both cardiac and non-cardiac surgery in many hospitals as part of the routine work-up. Although the cost of a chest radiograph is relatively low (estimated at \$31 [2]) and the associated radiation risks are small, there are doubts about the efficacy of routinely performing preoperative chest radiographs. For non-cardiac surgery, several studies have demonstrated that a routine preoperative chest radiograph does not decrease morbidity or mortality [3]. The frequency of abnormal findings on a routine preoperative chest radiograph before non-cardiac surgery is 10%, but in only 0.1% this causes a modification of clinical management [4]. Therefore, it is recommended to only perform a preoperative chest radiograph if the results are expected to change perioperative management [5]. Despite these recommendations, routine chest radiographs are still performed frequently before non-cardiac surgery [6].

In cardiac surgery, however, the frequency of abnormal findings on routine preoperative chest radiography is unknown. Cardiac surgery guidelines do not give recommendations whether a routine chest radiograph should be performed before cardiac surgery [7-10]. Since cardiac surgery is associated with higher risks, routine chest radiography can possibly contribute to improved preoperative risk assessment.

To the best of our knowledge, there are no published studies that have investigated the frequency of abnormalities on routinely performed preoperative chest radiography in patients undergoing cardiac surgery. In the current study, we retrospectively investigated the frequency and types of abnormalities found on routinely performed chest radiographs in patients scheduled to undergo cardiac surgery, as well as the effect of the preoperative chest radiograph on planned surgery.

## Methods

A retrospective cohort study was performed at the University Medical Center Utrecht (UMCU). The UMCU is a tertiary referral center and one of sixteen hospitals in the Netherlands that performs cardiac surgery. The local institutional review board waived the need for informed consent (protocol number 15-359/C), because the study only involves retrospective analysis of recorded data.

### *Chest radiography*

A chest radiograph is part of the routine preoperative work-up at the UMCU. A chest radiograph in the lateral and posterior-anterior direction was made using a digital flat panel detector system with a tube potential of 125 kV (Philips Healthcare, Best, The Netherlands). The mAs-value was optimized per patient using automated exposure control. All radiographs were assessed and reported by a radiologist or radiology resident in the routine clinical care setting. No structured reporting was used. The reporting radiologist had access to previous imaging examinations as well as the electronic patient file.

### *Data collection and analysis*

A random selection of all chest radiographs ordered by the department of cardiothoracic surgery between May 2011 and August 2015 were automatically extracted from the Picture Archiving and Communication System (PACS). The chest radiograph reports were assessed by one observer (AH) and postoperative chest radiographs were excluded. Only preoperative chest radiographs of patients that underwent cardiac surgery were included, and therefore preoperative chest radiographs of patients scheduled to undergo thoracic surgery or minimally invasive procedures (e.g. video-assisted thoracoscopic surgery, lobectomy, mediastinoscopy, implantable cardioverter-defibrillator (ICD) replacement and procedures involving solely removal of sternal wires) were excluded. Subsequently, the report was assessed to see if any abnormalities were described. Abnormalities were divided in the following categories: pulmonary or mediastinal mass, consolidation, pleural effusion, cardiomegaly (cardiothoracic ratio  $\geq 50\%$ ), aortic elongation, aortic calcifications, signs of cardiac decompensation, vertebral fractures or height loss, atelectasis, signs of chronic obstructive pulmonary disease (COPD) or a diaphragmatic herniation.

Also the date of the most recent chest x-ray prior to the routine preoperative chest x-ray and/or chest computed tomography (CT) was recorded. Both non contrast-enhanced and contrast-enhanced cardiac and chest CT examinations were included as well as PET-CT examinations. If a previous imaging examination was mentioned in the referral letter without the exact date of the examination and the examination was not available in the PACS, the date of the referral letter was used. The electronic patient file of the cardiothoracic surgery department was used to determine if the chest radiograph results impacted the planned surgery. This was categorized as postponement of surgery, cancellation of surgery, change

in surgical approach or further diagnostic testing and analysis was needed. A direction relation between the abnormality described on the chest radiograph and the effect on surgery had to be mentioned.

For each patient baseline patient characteristics, type of surgery and postoperative complications were derived from the nationwide complication registry of the Dutch Association for Thoracic Surgery. This registry is based on the complication registry from the Society of Thoracic Surgeons (STS) and is mandatory for each patient undergoing cardiac surgery in the Netherlands. Completeness and accuracy of the nationwide complication registry is excellent (99% of the data are complete) [11].

Analysis was performed using SPSS version 20.0.0 (SPSS, International Business Machines, Armonk, NY, United States of America). Data are presented as mean  $\pm$  SD unless otherwise stated. Frequencies are provided as count and percentage. Data are presented using descriptive analysis.

## Results

### *Patient selection and baseline characteristics*

The chest radiograph reports of a total of 1,293 patients were screened. Overall, 157 patients were excluded because they underwent either thoracic surgery (n=119) or minimally invasive surgery (n=38; ICD replacements and procedures involving solely the removal of sternal wires). Ultimately, 1,136 patients were included. Baseline patient characteristics are provided in *Table 1*. Mean age was  $65 \pm 13$  years and 30% was female. Details regarding the surgical procedure are provided in *Table 2*. Most surgeries were elective (772/1,136; 70.2%) or within the same hospitalization for cardiac symptoms (324/1,136; 29.5%) while 0.4% (4/1,136) concerned emergency surgery. Seven percent of patients (76/1,136) underwent a reoperation. Isolated CABG (547/1,136; 48.2%), isolated valve surgery (270/1,136; 23.8%) and CABG combined with valve surgery (151/1,136; 13.3%) were the most common types of surgery. In seven patients (7/1,136; 0.6%) no surgery was performed because the surgery was considered too high risk (n=3), the patient denied surgery which was not related to the chest radiograph (n=1), the patient died before surgery (n=1) or because after further analysis it was decided the disease and symptoms were not severe enough to perform surgery (n=2).

Table 1 – Baseline characteristics

Variable	Participants (n=1,136)
Age yr (mean±SD)	65 ± 13
Gender (female/male)	345/791
EuroScore (mean±SD)	5.43 ± 5.48
Length m (mean±SD)	1.73 ± 0.09
Weight kg (mean±SD)	81 ± 16
BMI kg/m <sup>2</sup> (mean±SD)	27.1 ± 4.4
<b>Medical history</b>	<b>% (n)</b>
Hypertension	56.1% (637)
Diabetes	20.0% (227)
COPD	10.1% (115)
Poor mobility	1.7% (19)
CVA	5.7% (65)
Endocarditis	1.1% (12)
Angina pectoris	6.0% (67)
Recent myocardial infarction (<90 days)	13.1% (146)
Atrial fibrillation	14.1% (160)

Table 2 – Treatment characteristics

Variable	% (n)
Elective surgery	70.2% (772)
Within same hospitalization	29.5% (324)
Emergency surgery	0.4% (4)
Reoperation	6.8% (76)
<b>Type of surgery</b>	<b>% (n)</b>
Isolated CABG	48.2% (547)
Isolated valve surgery	23.8% (270)
Isolated aortic surgery	0.4% (5)
CABG combined with valve surgery	13.3% (151)
Double- or triple-valve surgery	3.2% (36)
Aortic surgery combined with CABG and/or valve surgery	3.8% (43)
Other*	7.4% (84)

\*Including 7 patients without surgery

*Abnormalities found on chest radiography*

Overall, 50% of the patients (570/1,136) had an abnormality on chest radiography. The frequency of abnormalities was as follows: a possible pulmonary or mediastinal mass (42/1,136; 3.7%), consolidation (19/1,136; 1.7%), pleural effusion (42/1,136; 3.7%), cardiomegaly (cardiothoracic ratio  $\geq 50\%$ , 336/1,136; 29.6%), aortic elongation (114/1,136; 10.0%), aortic calcifications (3/1,136; 0.3%), signs of cardiac decompensation (15/1,136; 1.3%), vertebral fractures or height loss (72/1,126; 6.3%), atelectasis (31/1,136; 2.7%), signs of COPD (90/1,136; 7.9%) and sliding diaphragmatic herniation (12/1,136; 1.1%).

In two patients (2/1,136; 0.2%), the chest radiograph led to postponement of surgery, in none of the patients the surgery was cancelled. In 1 patient (1/1,136; 0.1%) the surgical approach was altered and in 15 patients (15/1,136; 1.3%) further diagnostic testing and analysis was performed without affecting surgery. Postponement of surgery was caused by a suspicion of pulmonary infection in one patient, and due to additional tests in the other patient. In this patient, right-sided pleural effusion was seen for which a chest CT and thoracentesis was performed. The change in surgical approach was caused by extensive calcifications in the ascending aorta in a patient scheduled for conventional aortic valve replacement (*Figure 1*). Aortic cannulation and placement of an aortic crossclamp was not deemed possible in an area free of calcifications. This finding, combined with an impaired pulmonary function and decreased exercise tolerance, led to the decision to change the surgical approach to a transcatheter aortic valve implantation.

*Previous imaging*

The routine preoperative chest x-ray was made  $9 \pm 11$  days before surgery. Fifty-nine percent (669/1,136) of patients had undergone an additional chest x-ray in the year before surgery, on average  $58 \pm 58$  days before surgery. Twelve percent (138/1,136) of patients underwent a cardiac, chest and/or PET-CT in the year before surgery. Most patients who received a preoperative CT also underwent additional chest x-rays, therefore in total 63% (726/1,136) of patients had a recent chest x-ray and/or CT at the moment they received the routine preoperative chest x-ray.

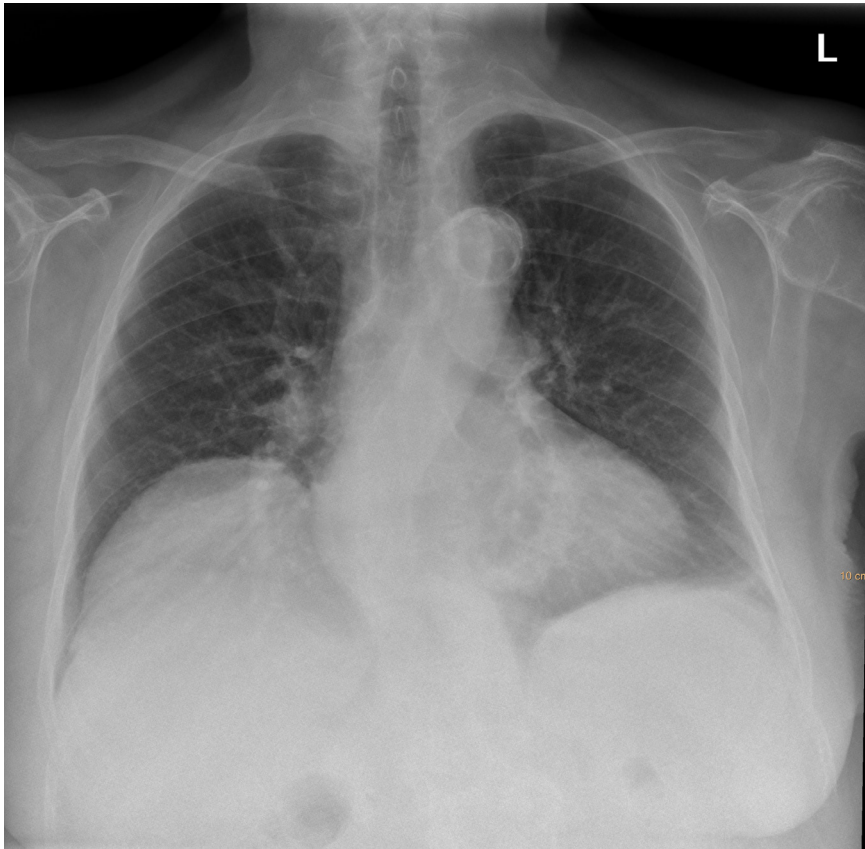


**Figure 1** – Chest radiograph of a 81-year old women in whom the surgical approach was altered due to extensive aortic calcifications.

### Discussion

This retrospective study provides insight into the frequency of abnormal findings on routine preoperative chest radiography in patients scheduled to undergo cardiac surgery. Although the vast majority of abnormal findings did not have a direct effect on the surgery, the information provided by routine preoperative screening chest radiography can substantially alter the surgical approach in selected cases.

The frequency of abnormal findings on routine preoperative chest radiography has been investigated extensively in non-cardiac surgery. A systematic review

and a meta-analysis [3,4], with considerably overlap in included studies, reported abnormal findings in 10% of the patients. Most common findings were associated with chronic disease, namely cardiomegaly and COPD, which is similar to the results in the current study. The frequency of abnormal findings in the current study was considerably higher. It is likely that some abnormalities are more common in patients undergoing cardiac surgery compared to non-cardiac surgery, such as cardiomegaly and elongation of the aorta. Furthermore, most studies in non-cardiac surgery were performed in the '70s and '80s, and advancements in chest radiography have improved the image quality which might have led to an increase in the frequency of abnormal findings [12]. Also, the definition of "abnormality" varies between studies and was relatively broad in the current study.

Even though cardiac surgery guidelines give no recommendations on the use of routine preoperative chest radiography, the National Collaborating Centre for Acute Care in the UK advises to perform preoperative chest radiography in all cardiac surgery patients based on consensus [13]. The costs associated with preoperative chest radiography are low, and if a preoperative chest radiograph could prevent one unnecessary surgery or prolonged hospitalization annually, those costs are easily compensated. Cost-effectiveness was not studied in the current study, but we showed that the frequency of abnormal findings is high. Although most abnormalities did not have an immediate impact on the surgery, in two cases the surgery was postponed and in one case the surgical approach was altered. Furthermore, a preoperative chest radiograph could also serve as a comparison for postoperative chest radiographs. However, in the current study most patients had recent previous imaging available which could also serve as comparison for postoperative chest radiographs.

An alternative would be to replace the preoperative chest radiograph by a preoperative chest CT. This offers the opportunity to improve visualization of pulmonary abnormalities and aortic atherosclerosis. The presence of atherosclerotic disease in the ascending aorta is associated with a five-fold increased risk of postoperative stroke [14], which is possibly caused by manipulation of the aorta during surgery causing embolization of atherothrombotic material. A recent review showed that a preoperative CT results in a change in surgical approach leading to decreased postoperative mortality and stroke in up to 17% of patients undergoing primary surgery [15]. Furthermore, the sensitivity of a chest CT for pulmonary nodules is high compared to a chest radiograph [16].

Finally, CT findings of for example emphysema may be able to more accurately predict problems in the intensive care unit postoperatively. Evidence for a routine preoperative CT is still weak, although an ongoing randomized clinical trial might provide more insight [17,18].

The current study has several limitations. First, it concerns a retrospective study. However, to the best of our knowledge, this is the first study investigating the frequency of abnormal findings on routine preoperative chest radiography in a population undergoing cardiac surgery. Second, we used the routine clinical care chest radiograph reports that were not reported in a structured format. Therefore, information provided in the (unstructured) report was dependent on the reporting radiologist, although this does reflect routine care. Also, the radiologist did have access to previous imaging.

In conclusion, this study shows that the incidence of abnormal findings on routine preoperative chest radiography in cardiac surgery is considerably higher compared to non-cardiac surgery. Although most abnormal findings were to be expected (e.g. cardiomegaly) and did not have a direct effect on the surgery, some findings can substantially alter the surgical approach in some cases. Future research should determine if it is cost-effective to replace the routine chest radiograph before cardiac surgery by a CT, which is expected to have a larger impact on the surgery.

## References

- [1] MacMahon H, Khan AR, Mohammed TL, et al., ACR Appropriateness Criteria routine admissions and preoperative chest radiography. *American College of Radiology* 2008;5.
- [2] Vijayasarithi A, Hawkins CM, Hughes DR, Mullins ME, Duszak R, Jr, How Much Do Common Imaging Studies Cost? A Nationwide Survey of Radiology Trainees. *AJR Am J Roentgenol* 2015;205(5):929-35.
- [3] Joo HS, Wong J, Naik VN, Savoldelli GL, The value of screening preoperative chest x-rays: a systematic review. *Can J Anaesth* 2005;52(6):568-74.
- [4] Archer C, Levy AR, McGregor M, Value of routine preoperative chest x-rays: a meta-analysis. *Can J Anaesth* 1993;40(11):1022-7.
- [5] Feely MA, Collins CS, Daniels PR, Kebede EB, Jatoi A, Mauck KF, Preoperative testing before noncardiac surgery: guidelines and recommendations. *Am Fam Physician* 2013;87(6):414-8.
- [6] Kirkham KR, Wijeyesundera DN, Pendrith C, et al., Preoperative Laboratory Investigations: Rates and Variability Prior to Low-risk Surgical Procedures. *Anesthesiology* 2016.
- [7] Kolh P, Windecker S, Alfonso F, et al., 2014 ESC/EACTS Guidelines on myocardial revascularization: the Task Force on Myocardial Revascularization of the European Society of Cardiology (ESC) and the European Association for Cardio-Thoracic Surgery (EACTS). Developed with the special contribution of the European Association of Percutaneous Cardiovascular Interventions (EAPCI). *Eur J Cardiothorac Surg* 2014;46(4):517-92.
- [8] Vahanian A, Alfieri O, Andreotti F, et al., Guidelines on the management of valvular heart disease (version 2012): the Joint Task Force on the Management of Valvular Heart Disease of the European Society of Cardiology (ESC) and the European Association for Cardio-Thoracic Surgery (EACTS). *Eur J Cardiothorac Surg* 2012;42(4):S1-44.
- [9] Hillis LD, Smith PK, Anderson JL, et al., 2011 ACCF/AHA Guideline for Coronary Artery Bypass Graft Surgery. A report of the American College of Cardiology Foundation/American Heart Association Task Force on Practice Guidelines. Developed in collaboration with the American Association for Thoracic Surgery, Society of Cardiovascular Anesthesiologists, and Society of Thoracic Surgeons. *J Am Coll Cardiol* 2011;58(24):e123-210.
- [10] Patel MR, Dehmer GJ, Hirshfeld JW, Smith PK, Spertus JA, ACCF/SCAI/STS/AATS/AHA/ASNC/HFSA/SCCT 2012 Appropriate use criteria for coronary revascularization focused update: a report of the American College of Cardiology Foundation Appropriate Use Criteria Task Force, Society for Cardiovascular Angiography and Interventions, Society of Thoracic Surgeons, American Association for Thoracic Surgery, American Heart Association, American Society of Nuclear Cardiology, and the Society of Cardiovascular Computed Tomography. *J Am Coll Cardiol* 2012;59(9):857-81.

## Chapter 4.1

- [11] Siregar S, Groenwold RH, Versteegh MI, et al., Data Resource Profile: adult cardiac surgery database of the Netherlands Association for Cardio-Thoracic Surgery. *Int J Epidemiol* 2013;42(1):142-9.
- [12] McAdams HP, Samei E, Dobbins J,3rd, Tourassi GD, Ravin CE, Recent advances in chest radiography. *Radiology* 2006;241(3):663-83.
- [13] National Collaborating Centre for Acute Care (UK), 2003.
- [14] van der Linden J, Hadjiniolaou L, Bergman P, Lindblom D, Postoperative stroke in cardiac surgery is related to the location and extent of atherosclerotic disease in the ascending aorta. *J Am Coll Cardiol* 2001;38(1):131-5.
- [15] den Harder AM, de Heer LM, Meijer RC, et al., Effect of computed tomography before cardiac surgery on surgical strategy, mortality and stroke. *Eur J Radiol* 2016;85(4):744--50.
- [16] Henschke CI, McCauley DI, Yankelevitz DF, et al., Early Lung Cancer Action Project: overall design and findings from baseline screening. *Lancet* 1999;354(9173):99-105.
- [17] ClinicalTrials.gov, Chest CT with iterative reconstructions as an alternative to conventional chest x-ray prior to heart surgery (CRICKET). 2014;2015.
- [18] den Harder AM, de Heer LM, Maurovich-Horvat P, et al., Ultra low-dose chest ct with iterative reconstructions as an alternative to conventional chest x-ray prior to heart surgery (CRICKET study): Rationale and design of a multicenter randomized trial. *J Cardiovasc Comput Tomogr* 2016.





## Chapter 4.2

*Part IV Preoperative CT*

# Can routine chest radiography be used to diagnose mild COPD? A nested case-control study

Annemarie M. den Harder, A.M. (Sander) Snoek, Tim Leiner,  
Willem J. Suyker, Linda M. de Heer, Ricardo P.J. Budde,  
Jan-Willem J. Lammers, Pim A. de Jong, Martijn J.A. Gondrie

European Journal of Radiology 2017; DOI 10.1016/j.ejrad.2017.05.007

## Abstract

### *Objectives*

To determine whether mild stage chronic obstructive pulmonary disease (COPD) can be detected on chest radiography without substantial overdiagnosis.

### *Methods*

A retrospective nested case-control study (case:control, 1:1) was performed in 783 patients scheduled for cardiothoracic surgery who underwent both spirometry and a chest radiograph preoperative. Diagnostic accuracy of chest radiography for diagnosing mild COPD was investigated using objective measurements and overall appearance specific for COPD on chest radiography. Inter-observer variability was investigated and variables with a kappa  $>0.40$  as well as baseline characteristics were used to make a diagnostic model which was aimed at achieving a high positive predictive value (PPV).

### *Results*

Twenty percent (155/783) had COPD. The PPV of overall appearance specific for COPD alone was low (37-55%). Factors in the diagnostic model were age, type of surgery, gender, distance of the right diaphragm apex to the first rib, retrosternal space, sternodiaphragmatic angle, maximum height right diaphragm (lateral view) and subjective impression of COPD (using both views). The model resulted in a PPV of 100%, negative predictive value (NPV) of 82%, sensitivity of 10% and specificity of 100% with an area under the curve of 0.811.

### *Conclusions*

Detection of mild COPD without substantial overdiagnosis was not feasible on chest radiographs in our cohort.

## Introduction

Chronic obstructive pulmonary disease (COPD) is a leading cause of chronic morbidity and mortality worldwide. Most patients have stage I or II COPD, as defined by the Global initiative for chronic Obstructive Lung Disease (GOLD) classification [1]. COPD is usually diagnosed and classified by spirometry. In patients with respiratory symptoms, a chest radiograph is generally the first test performed. Important signs of COPD are pulmonary emphysema and chronic bronchitis. Pulmonary emphysema is regularly suggested on chest radiography by the presence of bullae and the indirect signs of hyperinflation and vascular alterations [2]. However, sensitivity and specificity are low for the diagnosis of mild emphysema and there is considerable observer variation in the interpretation of these findings [3,4]. Radiographic signs of chronic bronchitis are bronchial wall thickening and increased lung markings [2]. The sensitivity of a chest radiograph for chronic bronchitis is also low, and the findings are non-specific since they are also often present, even in healthy non-smokers. Nevertheless, suspicion of COPD is often mentioned in chest radiography reports.

Since it is estimated that 60% of the individuals with COPD in the United States are undiagnosed, it is important to investigate if routine chest radiography could aid in the detection of undiagnosed COPD [5]. Recently the US preventive Services Task Force investigated if screening for COPD by using questionnaires or office-based pulmonary function testing is warranted to reduce undiagnosed COPD [6]. No benefit of COPD screening for all-cause mortality was found, but the annual rate of exacerbations was decreased due to improved pharmacologic treatment. The final recommendation was against screening in asymptomatic adults, since benefits did not outweigh potential harm [6]. However, this recommendation did not apply to symptomatic adults with respiratory symptoms, who frequently receive a chest radiograph. Clinicians were also encouraged to actively search for COPD in patients with risk factors like smoking. The objective of this study was to investigate the possibility to diagnose mild COPD based on a chest radiograph without substantial overdiagnosis using routine preoperative chest radiographs.

## Material and methods

This study was approved by our local institutional review board (protocol number 15/359). The IRB waived the requirement for informed consent because the study involved retrospective collection of recorded medical data.

The Standards for the Reporting of Diagnostic Accuracy Studies STARD guidelines for diagnostic studies were used [7].

In our hospital, patients scheduled for cardiothoracic surgery routinely receive a preoperative chest radiograph which is often combined with spirometry on the same day. From a database containing information about 1,295 randomly selected patients scheduled to undergo cardiothoracic surgery at the University Medical Center Utrecht between May 2011 and August 2015, patients with both a preoperative chest radiograph and spirometry were identified. A nested case-control design was used [8]. All cases along with a random sample of controls (case:control ratio 1:1) from the full cohort were analyzed.

Date of birth and smoking status (defined as never smoked, stopped, current or unknown) were extracted from the electronic patient record system. Type of surgery (cardiac or pulmonary), age, gender, length, weight and New York Heart Association (NYHA) functional classification of heart failure were derived from the nationwide complication registry of the Dutch Association for Thoracic Surgery. This registry is based on the complication registry from the Society of Thoracic Surgeons (STS). This registry has been shown to be complete and highly accurate [9].

#### *Spirometry*

Pulmonary function tests were carried out by experienced technicians according to current European Respiratory Society and American Thoracic Society guidelines [10] including forced expiratory volume in 1 second ( $FEV_1$ ), forced vital capacity (FVC) and  $FEV_1/FVC$  ratio. All pulmonary function tests were performed in our center. Reversibility of air flow limitation was not assessed. COPD was defined using the GOLD classification. All patients with a  $FEV_1/FVC$  below 0.70 were categorized using the following categories for severity:  $FEV_1 \geq 80\%$  as stage I,  $FEV_1$  50-79% as stage II,  $FEV_1$  30-49% as stage III and  $FEV_1 < 30\%$  as stage IV. Patients with stage III and stage IV were excluded from further analysis since clinical symptoms are usually present in these patients.

#### *Chest radiography*

A digital flat panel detector system was used with a tube potential of 125 kV while the mAs-value was determined using automated exposure control. Both posterior-anterior (PA) and a lateral chest radiograph were acquired. All chest radiographs were obtained in our center.

### *Measurements*

To assess if COPD was present, both objective and subjective measurements were used. Objective measurements assessed on the chest radiographs were based on the criteria described by Webb and Higgins [11] namely: distance from the apex of the right hemidiaphragm to the tubercle of the first rib, anterior rib level of the right hemidiaphragm, maximal height of the right hemidiaphragm (PA), maximal height of the right hemidiaphragm (lateral), retrosternal space and sternodiaphragmatic angle. Subjective criteria were: decreased vessel size (yes/no) and overall appearance of the chest radiograph specific for COPD (yes/no). Two senior radiology residents (AS, MG) and one board certified chest radiologist with over 10 years of experience in chest radiology (PJ) assessed if COPD signs were present on the chest radiograph. Observers were blinded for COPD status and did not have access to clinical information. To assess inter-observer variability, 30 randomly selected patients were scored by all three observers. Overall appearance of the chest radiograph specific for COPD were scored in all patients by all observers.

### *Statistical analysis*

Analysis was performed using SPSS version 20.0.0 (International Business Machines, Armonk, United States of America) and R software version 3.2.4 (R Foundation for Statistical Computing, Vienna, Austria). Inter-observer reproducibility was assessed using Krippendorff's alpha (10,000 bootstrap samples for inference) for discrete data. For continuous data the two-way random intraclass correlation coefficient (ICC, consistency, single measures) was used. Krippendorff's alpha and the ICC were interpreted as poor (0.00–0.20), fair (0.21–0.40), moderate (0.41–0.60), good (0.61–0.80) or excellent (0.81–1.00). Objective and subjective measurements with poor or fair inter-observer reproducibility were excluded from further analysis.

A simulated full cohort was used for further analysis by inflating the controls to achieve the original cohort size [8]. Univariate analysis was performed by building receiver operating characteristic (ROC) curves for continuous variables. The optimal cut-off point based on a predictive value of at least 80% was defined. If a PPV of 80% was not achieved, the cut-off value resulting in the highest PPV was chosen. Both these cut-off values and the cut-off values described by Webb and Higgins [11] were used to calculate positive predictive value (PPV), negative predictive value (NPV), sensitivity and specificity. The Chi<sup>2</sup>-test was used to determine if a cut-off value was preferred over continuous variables for

inclusion in the final model. Statistical significance was defined as  $p < 0.05$ . Binary logistic regression with backward step-wise elimination with a p-value of 0.20 for removal was used to make the final model. Objective and subjective measurements as well as age, gender and type of surgery were used. For overall appearance of the chest radiograph specific for COPD, only the score of the board certified radiologist was included. To develop a binary logistic model with sufficient power, at least 10 events per variable should be included [12]. A maximum number of 11 variables were included in the final model, depending on inter-observer reproducibility. Thus, at least 110 cases were included.

## Results

A flow diagram of the study is provided in *Figure 1*. In 61% (790/1,295) of all patients both a chest radiograph and spirometry were available. Twenty-one percent of patients (162/790) had COPD according to their spirometric assessment, namely GOLD stage I (86), stage II (69) and stage III (7), respectively. Since only patients with stage I and II COPD were included, ultimately 155 cases remained. The controls consisted of a random sample of 155 patients without COPD. In *Table 1* baseline characteristics of cases and controls are provided. Mean age was 67 years (cases) and 62 years (controls), respectively. Cases were more often male (81% versus 59%) and current smoker (27% versus 13%). Most patients underwent cardiac surgery (cases 58%, controls 87%).

### *Inter-observer reproducibility*

Results of inter-observer reproducibility are provided in *Table 2*. Distance of the right diaphragm to the first rib showed excellent observer agreement (ICC 0.834), while interobserver agreement for the sternodiaphragmatic angle and maximal height of the right diaphragm on the lateral view was good (0.625 and 0.643, respectively). Retrosternal space and overall appearance of the chest radiograph specific for COPD showed moderate agreement (0.532 and 0.484, respectively). Rib level of the right hemidiaphragm (0.345), maximal height of right diaphragm on PA (0.373) and decreased vessel size (0.286) scored fair and were therefore excluded from further analysis. The measurements included for further analysis are shown in *Figure 2*.

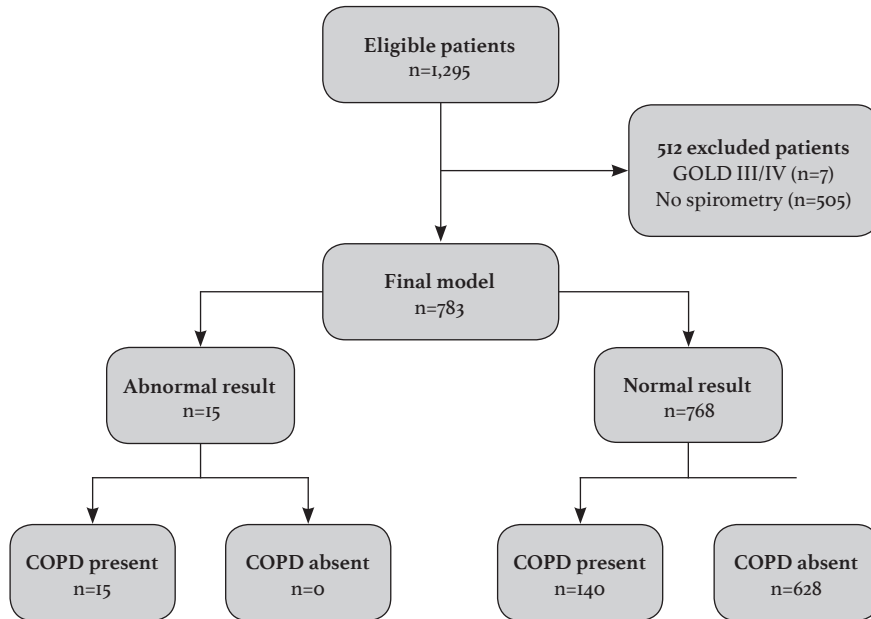


Figure 1: Flow diagram of the study. An abnormal or normal test result is based on the final model as provided in Figure 4.

Table 1 – Baseline characteristics of mild COPD cases and controls.

	Cases (n=155)	Controls (n=155)
Gender (male)	126 (81.3%)	91 (58.7%)
Age (mean ± SD)	66.5 ± 11.1	62.4 ± 13.9
Length (m, mean ± SD)	1.75 ± 0.09	1.72 ± 0.10
Weight (kg, mean ± SD)	79.3 ± 15.0	79.9 ± 14.8
<b>Smoking status</b>		
Never smoked	37 (23.9%)	71 (45.8%)
Stopped	61 (39.4%)	45 (29.0%)
Current	41 (26.5%)	20 (12.9%)
Unknown	16 (10.3%)	19 (12.3%)
<b>NYHA classification</b>		
1	22 (14.2%)	25 (16.1%)
2	58 (37.4%)	63 (40.6%)
3	25 (16.1%)	22 (14.2%)
4	2 (1.3%)	2 (1.3%)
unknown	48 (31.0%)	43 (27.7%)
<b>Type of surgery</b>		
Cardiac	90 (58.1%)	134 (86.5%)
Pulmonary	65 (41.9%)	21 (13.5%)

**Table 2** – Inter-observer reproducibility of 30 patients scored by all three observers.

Variable	Outcome	Interpretation
Distance right diaphragm to first rib <sup>†</sup>	0.834	Excellent
Maximal height right diaphragm (lateral) <sup>†</sup>	0.643	Good
Sternodiaphragmatic angle <sup>†</sup>	0.625	Good
Retrosternal space <sup>†</sup>	0.532	Moderate
Overall appearance of the chest radiograph specific for COPD <sup>*</sup>	0.484	Moderate
Maximal height right diaphragm (PA) <sup>†</sup>	0.373	Fair
Anterior rib level right hemidiaphragm <sup>*</sup>	0.345	Fair
Decreased vessel size <sup>*</sup>	0.286	Fair

Overall appearance of the chest radiograph specific for COPD was scored in all 310 patients. Objective and subjective measurements with poor or fair inter-observer reproducibility were excluded from further analysis. <sup>\*</sup>Intraclass correlation coefficient <sup>\*</sup>Krippendorff's alpha

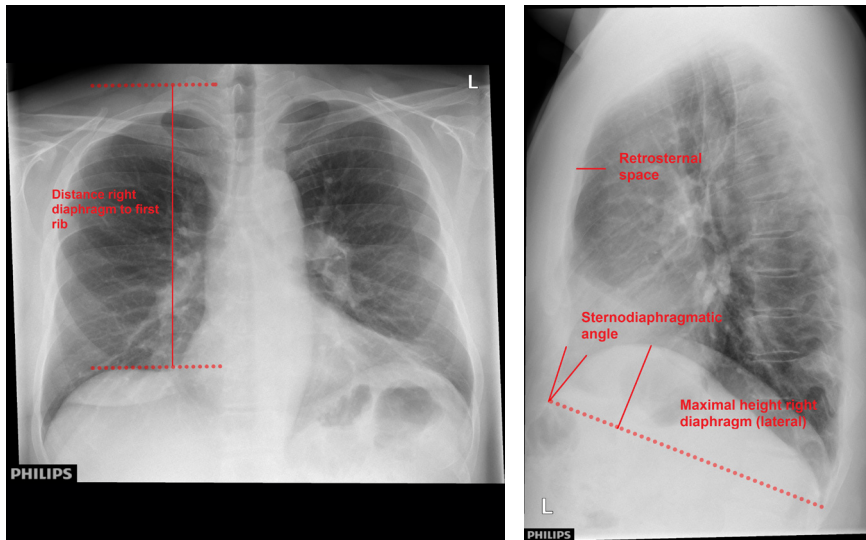


Figure 2: Measurements included for further analysis on posterior-anterior (left) and lateral (right) views.

### Univariate analysis

Results of univariate analysis are provided in *Table 3* and *Figure 3*. The area under the curve (AUC) was highest for increased distance of the apex of the right hemidiaphragm to the tubercle of the first rib (0.689). The maximal height of the right diaphragm (lateral) showed an AUC below 0.5 because an increase in height was associated with no COPD.

Table 3 – Univariate analysis for continuous variables. The Chi<sup>2</sup>-test was used to determine if a cut-off value was preferred over continuous outcomes.

	p-value (Chi <sup>2</sup> ) continuous	Optimal cut-off value	p-value (Chi <sup>2</sup> ) with cut-off
Age	0.001 (11.1)	>83 years	0.002 (9.8)
Distance right diaphragm to first rib	<0.001 (59.6)	>31.8cm	0.011 (6.5)
Retrosternal space	<0.001 (22.1)	>4.2cm	<0.001 (16.3)
Sternodiaphragmatic angle	<0.001 (12.4)	>87 degrees	<0.001 (22.9)
Maximal height right diaphragm (lateral)	<0.001 (23.4)	<2.8cm	<0.001 (12.2)

The optimal cut-off point based on a predictive value of at least 80% was defined. If a PPV of 80% was not achieved, the cut-off value resulting in the highest PPV was chosen.

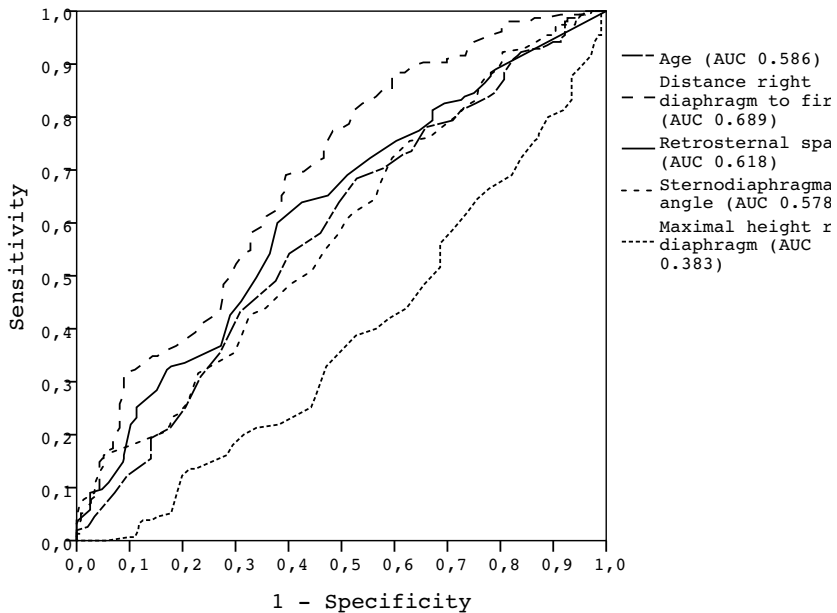


Figure 3 – Univariate analysis. ROC-curves of continuous variables.

Age >83 years, a distance of >31.8 cm of the apex of the right diaphragm to the first rib, a retrosternal space >4.2 cm, a sternodiaphragmatic angle of more than 87 degrees and a decreased maximal height of the right diaphragm on the lateral view of less than 2.8 cm were the optimal cut-off values for predicting COPD. The Chi<sup>2</sup>-test was used to determine if a cut-off value was preferred over

continuous outcomes. The Chi<sup>2</sup>-test was significant for all variables for both the cut-off values and the continuous outcomes. The continuous variables were more significant, except for the sternodiaphragmatic angle for which a cut-off value was preferred.

#### *Diagnostic accuracy*

In *Table 4* the diagnostic accuracy for all variables is provided. Because the optimal cut-off value for calculating the diagnostic accuracy was determined based on the optimal PPV as described in the methods, the PPV and specificity were high, which resulted in a low sensitivity. The diagnostic accuracy of overall appearance of the chest radiograph specific for COPD was poor. For the board certified radiologist, the PPV for overall appearance of the chest radiograph specific for COPD was 55%, NPV 84%, sensitivity 27% and specificity 95%. Only 26% (41/155) of the COPD cases were detected, while a similar proportion of 22% (34/155) of the patients without COPD were wrongly classified as having COPD. The results for the senior residents were similar, with a low PPV and sensitivity (*Table 4*).

The difference between the cut-off values provided by Webb and Higgins and the cut-off values determined by univariate analysis were small, with a slightly improved diagnostic accuracy for the cut-off values determined by univariate analysis in this study.

#### *Multivariate analysis*

The results of the multivariate analysis are shown in *Figure 4*. All variables were included in the final model (age, type of surgery, gender, distance of the right diaphragm to the first rib, width of retrosternal space, sternodiaphragmatic angle, maximal height of the right diaphragm on the lateral view and overall appearance of the chest radiograph specific for COPD based on the score of the board certified radiologist). The model calculates for each patient the predicted probability of having COPD, based on the variables in the model. To calculate the diagnostic accuracy of the final model, a cut-off value of the predicted probability should be chosen to determine which patients are classified as having COPD. As illustrated in *Figure 4*, choosing a low cut-off value will result in a high NPV and sensitivity, however at the cost of a low PPV and specificity. In routine clinical practice we think it is important in diagnosing COPD as an incidental finding to reach a high PPV to prevent substantial overdiagnosis. This can be achieved when only patients with a predicted probability of 0.97 or

Table 4 – Diagnostic accuracy of objective and subjective measurements.

Variables	COPD+, variable+	COPD-, variable-	COPD+, variable+	COPD-, variable-	PPV (%)	NPV (%)	Sensitivity (%)	Specificity (%)
Age	3	152	0	628	100.0	80.5	1.9	100.0
Gender	126	29	376	252	25.1	89.7	81.3	40.1
Type of surgery	65	90	84	554	43.7	86.0	41.9	86.8
Distance right diaphragm to first rib	2	153	0	628	100.0	80.4	1.3	100.0
Retrosternal space	5	150	0	628	100.0	80.7	3.2	100.0
Sternodiaphragmatic angle	7	148	0	628	100.0	80.9	4.5	100.0
Maximal height right diaphragm (lateral)	48	107	112	516	30.0	82.8	31.0	82.1
Overall appearance of the chest radiograph specific for COPD (board certified radiologist)	41	114	34	594	54.7	83.9	26.5	94.6
Overall appearance of the chest radiograph specific for COPD (resident 1)	41	114	37	591	52.6	83.8	26.5	94.1
Overall appearance of the chest radiograph specific for COPD (resident 2)	61	94	103	525	37.2	84.8	39.4	83.6
<b>Optimal cut-off final model</b>	<b>15</b>	<b>140</b>	<b>0</b>	<b>628</b>	<b>100.0</b>	<b>81.8</b>	<b>9.7</b>	<b>100.0</b>
Webb and Higgins criteria								
Distance right diaphragm to first rib	12	143	17	611	41.4	91.0	7.7	97.3
Retrosternal space	4	151	0	628	100.0	80.6	2.6	100.0
Sternodiaphragmatic angle	2	153	0	628	100.0	80.4	1.3	100.0
Maximal height right diaphragm (lateral)	43	112	101	527	29.9	82.5	27.7	83.9

PPV positive predictive value, NPV negative predictive value

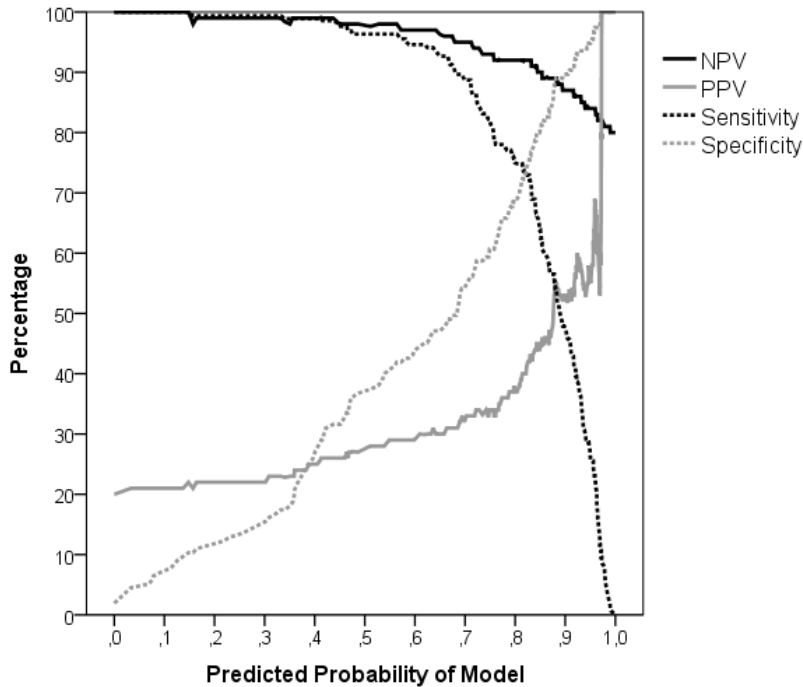


**Figure 4** – Multivariate analysis. The PPV, NPV, sensitivity and specificity are displayed as a function of the predicted probability of the model. The model calculates for each patient the predicted probability of having COPD, based on the variables in the model. The optimal model is achieved when only patients with a predicted probability of 0.97 (dotted x-axis reference line) or higher are classified as having COPD. This will result in a PPV of 100%, NPV of 82%, sensitivity of 10% and a specificity of 100%

higher are classified as having COPD. This will result in a PPV of 100%, NPV of 82%, sensitivity of 10% and a specificity of 100% (Table 4). Hence it is possible to detect 10% of patients with mild-COPD without any false-positives. However, as soon as more COPD patients are detected by also classifying patients with a lower predicted probability as having COPD, this results in a disproportionately large increase in the number of false-positives because the PPV rapidly declines with smaller predicted probabilities. The ROC curve of the shown model had an area under the curve of 0.811.

## Discussion

This study showed that, even when an extensive diagnostic model is used, the performance of chest radiography for diagnosing mild COPD is limited. Only a small proportion of 10% of proven COPD cases could be detected without additional diagnostic measurements. Scoring only a subjective impression of COPD on chest radiography resulted in more COPD patients (n=41, 26%), but 34 (22%) patients without COPD were wrongly classified as having COPD.

COPD is a large health problem and is one of the leading causes of morbidity and mortality worldwide [13]. Annually 133,575 deaths in the United States are caused by COPD [14]. The medical costs attributable to COPD were \$32 billion in the United States in 2010, and are expected to increase to \$49 billion in 2020 [15]. It is estimated that more than 100 million chest radiographs are performed in the United States annually [16]. If chest radiography would have diagnostic value for detecting COPD, this could potentially lead to a large reduction in the number of patients with undiagnosed COPD [5]. Radiologists often report features associated with COPD in chest radiography reports, thereby implying for referring clinicians that it is possible to detect or diagnose COPD from chest radiographs. On the other hand, because of the large number of chest radiographs, there is a substantial risk for overdiagnosis of COPD if the accuracy of chest radiography is limited. The current study was motivated by a paucity of data on the diagnostic accuracy of chest radiography for the detection of mild-stage, clinically undetected COPD [11]. The most important finding is that there is no role for chest radiography in the diagnosis of mild COPD, because the diagnostic accuracy is low. We found that chest radiography was unable to diagnose a reasonable proportion of mild COPD with high PPV.

This is the first large patient study investigating the diagnostic value of a two view chest radiography using modern equipment in mild COPD. In the '60s several small studies investigated the accuracy of a chest radiograph compared to pathology for the diagnosis of emphysema. Reid et al.[17] investigated 40 patients, including 19 patients without emphysema. All patients with emphysema did have radiographic findings of emphysema (specificity 100%), however patients without emphysema were often diagnosed as having emphysema leading to a sensitivity of 58%. Nicklaus et al.[4] studied 73 patients with no (n=20), moderate (n=22) and severe (n=31) emphysema. Only 26% of the patients with moderate emphysema were correctly diagnosed based on the subjective opinion of the radiologist, which increased to 32% based on objective signs. However, those

studies did not use pulmonary function tests as a reference standard, which is currently the golden standard to diagnose COPD. In a large study (n=1,000) by Reich and colleagues [18] the use of objective chest radiography measurements for the diagnosis of COPD was investigated. Two measurements correlated with the presence of COPD, namely decreased height of the right diaphragm ( $\leq 2.6$  cm) and increased height of the right lung ( $\geq 29.9$ cm). This identified 68% and 70% of patients with an abnormal pulmonary function test respectively. The same criteria were used in the current study, and although those signs are very specific for COPD, the sensitivity and positive predictive values for diagnosing mild COPD are low leading to substantial overdiagnosis. Partly based on this study, Webb and Higgins described several objective measurements for diagnosing COPD on a chest radiograph [11]. Because in clinical routine, most chest radiography reports are made by experienced residents, in our study the objective and subjective measurements were performed by both a board certified radiologist and two senior residents. This study proves that it is very difficult to diagnose mild COPD based on a chest radiograph, and based on these findings we suggest this should not be mentioned anymore in the report. Signs like a saber-sheath trachea [19,20] and a decreased cardiac size [21] are mainly present in patients with severe COPD, and were therefore not assessed in the current study. Therefore, the diagnostic accuracy of a chest radiograph for severe COPD might be higher. Severe COPD was not investigated in this study, but undiagnosed COPD is less of a problem in these patients since they usually have evident clinical symptoms.

Based on the findings of this study, specialists and general practitioners should be aware of the limited diagnostic value of chest radiographs for COPD. This should be discussed with patients to prevent unnecessary anxiety and confirmation with spirometry should be obtained when COPD is mentioned in chest radiography reports. We discourage radiologists to mention suspicion of COPD in chest radiograph reports. It is possible to detect COPD patients in some extent, however this will result in substantial overdiagnosis which is associated with a waste of resources on unnecessary care [22].

This study has several limitations. First of all, not all radiographs were scored but a nested case-control approach was adopted. In a nested case-control study, cases and controls are derived from a well-defined source cohort. Therefore, the sampling fraction is known and it is possible to calculate diagnostic accuracy measures, in contrast to case-control studies. Studies comparing the nested

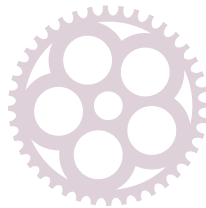
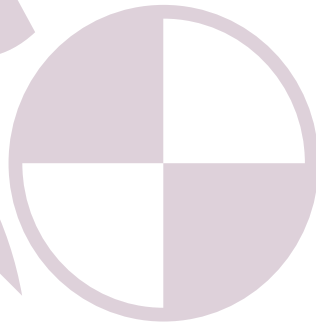
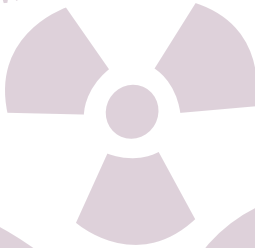
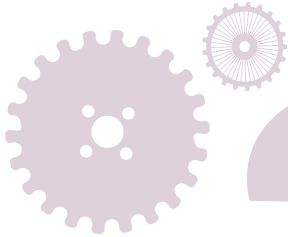
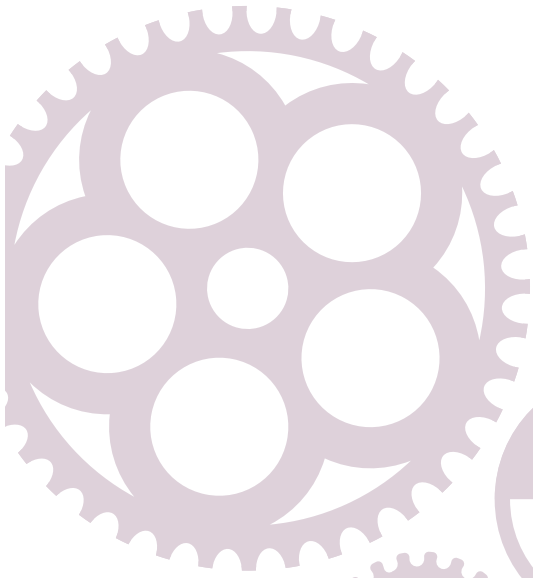
case-control design to a cohort design have found that this is a valid and efficient study design [8,23,24]. Second, only preoperative chest radiographs before cardiothoracic surgery were studied because in this patient population spirometry is routinely performed. We did not validate externally since the model was not clinically useful due to the limited number of COPD cases that can be detected. Third, in only 61% of patients with a chest radiograph, spirometry was performed. In nearly all patients undergoing cardiothoracic surgery chest radiographs are obtained, but spirometry is often omitted in emergency surgery and in patients who are operated within the same hospitalization for cardiac symptoms. Therefore, patients in whom spirometry data is missing are not a random sample but represent a patient group with more severe disease. However, it is unlikely that this bias affects the ability to diagnose mild COPD using routine pre-operative chest radiography. Fourth, the subjective score included in the final model was based on the score of one observer namely the board certified radiologist. We decided not to include the average subjective score, since this is not representative to clinical practice where a report is usually made by one radiologist. The subjective score of the most experienced observer was included in the final model in order to achieve an optimal diagnostic model. Fifth, the reversibility of the airflow limitation was not investigated, which is used to differentiate between COPD and asthma. Therefore, it is possible that patients with asthma were misclassified as having COPD and that COPD is overdiagnosed. Nevertheless, the conclusion remains that chest radiography has insufficient accuracy for the diagnosis mild COPD.

In conclusion this is the first large study investigating the diagnostic utility of two-view chest radiography with modern equipment for diagnosing mild COPD. Using an extensive diagnostic model, the diagnostic accuracy improved compared to a radiologists subjective impression only, however, the role for chest radiography in diagnosing mild COPD is very limited because only a small proportion of COPD cases could be detected. Increasing the number of detected COPD cases leads to a clinically unacceptable increase in false-positives. Our findings discourage diagnosing mild stage COPD on chest radiographs by radiologists where moderate and severe COPD is usually clinically already known. Hence in our view there is no added diagnostic value of chest radiography for moderate and severe COPD, although this cannot be concluded from the present study. If COPD is mentioned in chest radiography, this should trigger clinicians and general practitioners to seek confirmation with spirometry.

## References

- [1] Afonso AS, Verhamme KM, Sturkenboom MC, Brusselle GG, COPD in the general population: prevalence, incidence and survival. *Respir Med* 2011;105(12):1872-84.
- [2] Muller NL, Coxson H, Chronic obstructive pulmonary disease. 4: imaging the lungs in patients with chronic obstructive pulmonary disease. *Thorax* 2002;57(11):982-5.
- [3] Thurlbeck WM, Muller NL, Emphysema: definition, imaging, and quantification. *AJR Am J Roentgenol* 1994;163(5):1017-25.
- [4] Nicklaus TM, Stowell DW, Christiansen WR, Renzetti AD, Jr, The accuracy of the roentgenologic diagnosis of chronic pulmonary emphysema. *Am Rev Respir Dis* 1966;93(6):889-99.
- [5] Martinez FJ, O'Connor GT, Screening, Case-Finding, and Outcomes for Adults With Unrecognized COPD. *JAMA* 2016;315(13):1343-4.
- [6] Guirguis-Blake JM, Senger CA, Webber EM, Mularski RA, Whitlock EP, Screening for Chronic Obstructive Pulmonary Disease: Evidence Report and Systematic Review for the US Preventive Services Task Force. *JAMA* 2016;315(13):1378-93.
- [7] Bossuyt PM, Cohen JF, Gatsonis CA, Korevaar DA, STARD group, STARD 2015: updated reporting guidelines for all diagnostic accuracy studies. *Ann Transl Med* 2016;4(4):85,5839.2016.02.06.
- [8] Biesheuvel CJ, Vergouwe Y, Oudega R, Hoes AW, Grobbee DE, Moons KG, Advantages of the nested case-control design in diagnostic research. *BMC Med Res Methodol* 2008;8:48,2288-8-48.
- [9] Siregar S, Groenwold RH, Versteegh MI, et al., Data Resource Profile: adult cardiac surgery database of the Netherlands Association for Cardio-Thoracic Surgery. *Int J Epidemiol* 2013;42(1):142-9.
- [10] Miller MR, Crapo R, Hankinson J, et al., General considerations for lung function testing. *Eur Respir J* 2005;26(1):153-61.
- [11] Webb WR, Higgins CB, Emphysema and Chronic Obstructive Pulmonary Disease. In: Mitchell CW, editor. *Thoracic Imaging: Pulmonary and Cardiovascular Radiology*. : Wolters Kluwer | Lippincott Williams And Wilkins, 2010:554-555.
- [12] Harrell FE, Jr, Lee KL, Mark DB, Multivariable prognostic models: issues in developing models, evaluating assumptions and adequacy, and measuring and reducing errors. *Stat Med* 1996;15(4):361-87.
- [13] Boschetto P, Quintavalle S, Miotto D, Lo Cascio N, Zeni E, Mapp CE, Chronic obstructive pulmonary disease (COPD) and occupational exposures. *J Occup Med Toxicol* 2006;1:11.
- [14] Ford ES, Croft JB, Mannino DM, Wheaton AG, Zhang X, Giles WH, COPD surveillance--United States, 1999-2011. *Chest* 2013;144(1):284-305.

- [15] Ford ES, Murphy LB, Khavjou O, Giles WH, Holt JB, Croft JB, Total and state-specific medical and absenteeism costs of COPD among adults aged  $\geq$  18 years in the United States for 2010 and projections through 2020. *Chest* 2015;147(1):31-45.
- [16] National Council on Radiation Protection and Measurements, Ionizing Radiation Exposure of the Population of the United States. Report No 60 2009.
- [17] REID L, MILLARD FJ, Correlation between Radiological Diagnosis and Structural Lung Changes in Emphysema. *Clin Radiol* 1964;15:307-11.
- [18] Reich SB, Weinshelbaum A, Yee J, Correlation of radiographic measurements and pulmonary function tests in chronic obstructive pulmonary disease. *AJR Am J Roentgenol* 1985;144(4):695-9.
- [19] Greene R, "Saber-sheath" trachea: relation to chronic obstructive pulmonary disease. *AJR Am J Roentgenol* 1978;130(3):441-5.
- [20] Ciccarese F, Poerio A, Stagni S, et al., Saber-sheath trachea as a marker of severe airflow obstruction in chronic obstructive pulmonary disease. *Radiol Med* 2014;119(2):90-6.
- [21] Watz H, Waschki B, Meyer T, et al., Decreasing cardiac chamber sizes and associated heart dysfunction in COPD: role of hyperinflation. *Chest* 2010;138(1):32-8.
- [22] Macdonald H, Loder E, Too much medicine: the challenge of finding common ground. *BMJ* 2015;350:h1163.
- [23] Ernster VL, Nested case-control studies. *Prev Med* 1994;23(5):587-90.
- [24] Essebag V, Genest J,Jr, Suissa S, Pilote L, The nested case-control study in cardiology. *Am Heart J* 2003;146(4):581-90.



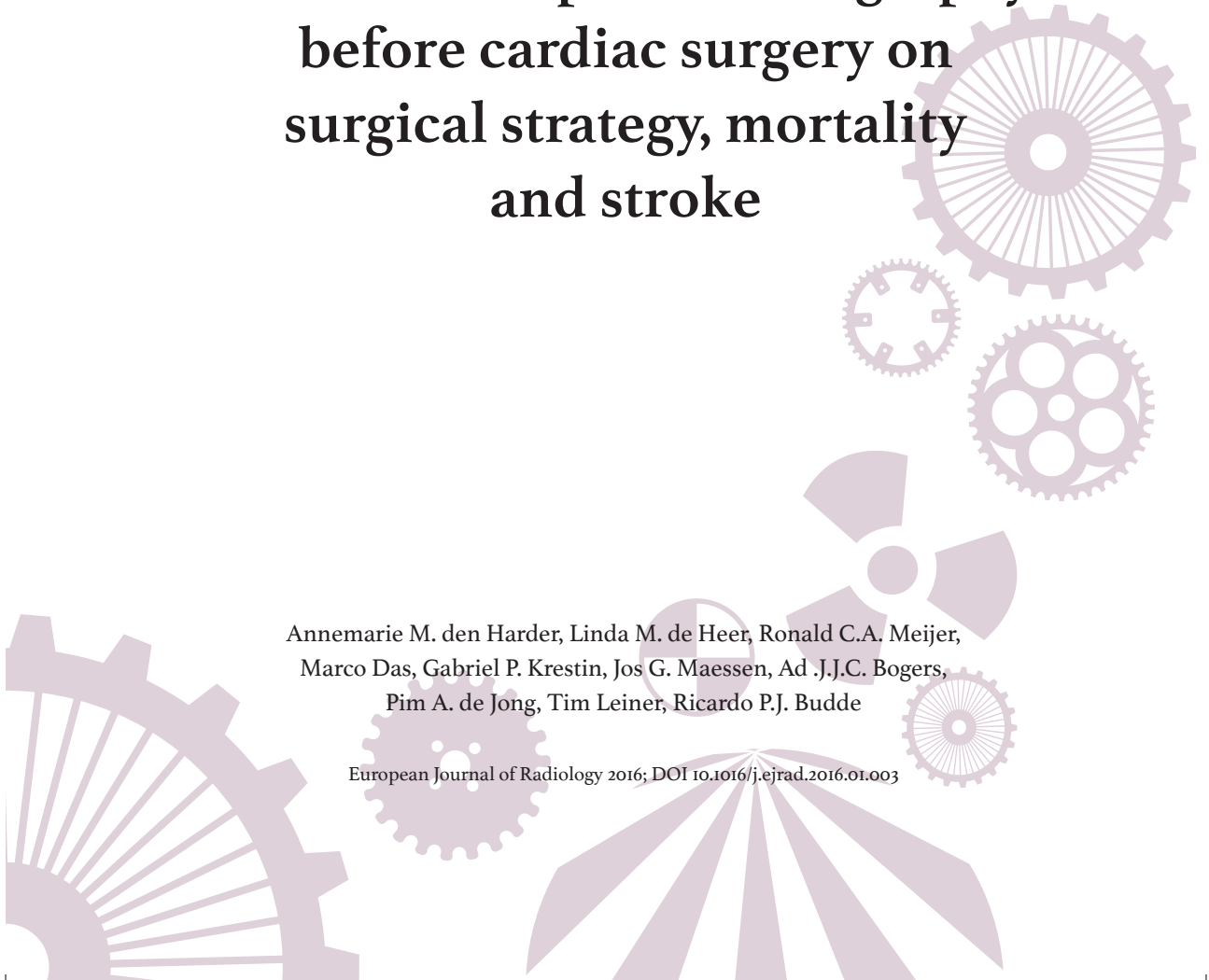
# Chapter 4.3

*Part IV Preoperative CT*

## Effect of computed tomography before cardiac surgery on surgical strategy, mortality and stroke

Annemarie M. den Harder, Linda M. de Heer, Ronald C.A. Meijer,  
Marco Das, Gabriel P. Krestin, Jos G. Maessen, Ad .J.J.C. Bogers,  
Pim A. de Jong, Tim Leiner, Ricardo P.J. Budde

European Journal of Radiology 2016; DOI 10.1016/j.ejrad.2016.01.003



## Abstract

### *Objective*

To investigate whether preoperative chest computed tomography (CT) decreases postoperative mortality and stroke rate in cardiac surgery by detection of calcifications and visualization of postoperative anatomy in redo cardiac surgery which can be used to optimize the surgical approach.

### *Methods*

The PubMed, EMBASE and Cochrane databases were searched and articles concerning preoperative CT in cardiac surgery were included. Articles not reporting mortality, stroke rate or change in surgical approach were excluded. Studies concerning primary cardiac surgery as well as articles concerning redo cardiac surgery were both included.

### *Results*

Eighteen studies were included (n=4,057 patients) in which 2,584 patients received a preoperative CT. Seven articles (n=1,754 patients) concerned primary surgery and eleven articles (n=2,303 patients) concerned redo cardiac surgery. None of the studies was randomized but 8 studies provided a comparison to a control group. Stroke rate decreased with 77–96% (primary surgery) and 18-100% (redo surgery) in patients receiving a preoperative CT. Mortality decreased up to 66% in studies investigating primary surgery while the effect on mortality in redo surgery varied widely. Change in surgical approach based on CT-findings consisted of choosing a different cannulation site, opting for off-pump surgery and cancellation of surgery.

### *Conclusions*

Current evidence suggests that preoperative CT imaging may lead to decreased stroke and mortality rate in patients undergoing primary cardiac surgery by optimizing surgical approach. In patients undergoing redo cardiac surgery stroke rate is also decreased but the effect on mortality is unclear. However, evidence is weak and included studies were of moderate quality.

## Introduction

One of the most devastating complications of cardiac surgery is a postoperative stroke. The reported incidence of postoperative stroke after cardiac surgery varies between 1.4–9.7% and strongly depends on the surgical procedure [1–4]. The majority of postoperative strokes are embolic in nature and aortic calcifications are the most important risk factor [2,5]. The risk of a postoperative stroke is up to fourfold higher in patients with aortic atherosclerosis [2,6]. This is explained by the need to clamp and manipulate the ascending aorta during cardiac surgery, thereby releasing material from aortic plaques and calcifications that may embolize to the brain [7]. This is an important problem since approximately 14% of cardiac surgery patients have significant ascending aorta calcifications [8]. Furthermore, stroke is a significant health burden and associated with high costs. The average costs in the United States for the first year after a stroke are estimated to be \$11,145 mainly due to rehabilitation costs [9]. Preoperative knowledge of the presence and extent of aortic calcifications may be used to optimize or even adapt surgical strategy to avoid manipulation of the calcified aorta with the aim of preventing stroke. Redo cardiac surgery is associated with increased mortality and morbidity due to previously altered anatomic relationships [10]. Preoperative visualization of this altered anatomy can identify structures at risk of injury [11,12].

Standard preoperative work-up prior to cardiac surgery includes imaging by chest x-ray, angiography and/or echocardiography [13–15]. Aortic calcifications are often not accurately detected on a chest x-ray due to inherent limitations imposed by the 2D superposition of structures [16,17]. Intraoperative epiaortic ultrasound has been described as a valuable intraoperative tool to assess wall characteristics of the ascending aorta and determine the presence of aortic wall calcifications and soft plaque. However, major drawbacks are the restriction to intraoperative use, limited anatomical coverage and the requirement for additional operating time.

An alternative technique that can be used to precisely assess cardiac and aortic anatomy is computed tomography (CT) of the chest. This modality offers excellent preoperative visualization of the location and extent of aortic calcifications allowing improved preoperative planning with adaptation of cardiac surgical strategy in case of severe calcifications. Furthermore, a preoperative CT can identify the altered anatomy in redo cardiac surgery.

The objective of this study is to systematically review the available literature with regard to the effect of preoperative CT on optimizing surgical strategy, and subsequent stroke rate and mortality.

### Materials and Methods

PubMed, EMBASE and Cochrane electronic databases were searched for relevant articles on January 20, 2015. No time restrictions were applied. Synonyms of preoperative, CT and cardiac surgery were combined. The search syntax is provided in *Table 1*. Duplicates were removed and articles were screened by one person using predefined in- and exclusion criteria. Inclusion criteria were articles concerning preoperative CT for cardiac surgery and reporting surgical modification based on CT findings, postoperative mortality or stroke rate. Exclusion criteria were case and congress reports, non-English language, articles concerning pediatric populations and articles concerning transcatheter aortic valve implantation. The reference lists of included articles were screened for additional articles.

The quality of included studies was assessed by one person using a modified Quality Assessment of Diagnostic Accuracy Studies (QUADAS) tool [18]. Since the QUADAS tool is designed for quality assessment of studies concerning diagnostic accuracy, not all items were applicable. Non-applicable items were left out. Two items concerning study design were added (prospective versus retrospective design and single center versus multicenter study design). In addition, two items concerning outcome were added, namely whether a definition of the primary outcome stroke was provided and the time interval over which the secondary outcome mortality was measured namely in-hospital mortality or 30-day mortality (*Table 2*).

Data concerning author, title, publication date, journal, patient characteristics, CT acquisition, type of surgery, stroke rate and mortality were extracted to a standardized data sheet. Subgroup analysis was performed for studies investigating primary cardiac operation and studies investigating redo cardiac surgery.

We performed a systematic review of the published literature on the effect of preoperative CT on surgical strategy and postoperative mortality and stroke rate in patients undergoing primary and redo cardiac surgery. Preoperative CT can provide previously unrecognized information about aortic calcifications that has the potential to change surgical strategy, and, possibly, reduce the incidence of postoperative stroke and mortality.

Table 1 – Search syntax. Date of search: January 20th 2015

Databases searched:	Search terms entered into databases:
PubMed In title and abstract	preoperat* OR (pre AND operat*) OR prior OR planning OR
EMBASE In title and abstract	before OR presurgical
Cochrane In title and abstract	AND  CT OR (computed AND tomograph*)  AND  (cardiac AND (surgery OR operat*)) OR (cardiothora* AND (surgery OR operat*)) OR (heart AND (surgery OR operat*)) OR CABG OR (bypass AND (surgery OR operat*)) OR (valve AND replacement) OR (valve AND (surgery OR operat*))

## Results

The search resulted in 4,371 unique articles. A flowchart is provided in *Figure 1*. Articles were excluded because they did not concern preoperative chest CT or did not report on the outcomes of surgical modification, mortality or stroke rate (n=4,343), non-English language (n=2), concerned a case report (n=3), was a congress report (n=1) or concerned children (n=1). A total of 19 articles were included. Two of the remaining articles [12,19] described the same study population. Only the most recent publication was included [12] therefore 18 unique articles were included.

Results of the critical appraisal are provided in *Table 2*. All studies clearly described their inclusion criteria. However, only four studies of the studies had a prospective study design and none of the studies was multicenter. Less than half of the studies (7 studies) described the CT acquisition in sufficient detail to permit its replication by not reporting if it was a contrast-enhanced CT and/or the used CT system and parameters. Four out of 13 studies investigating postoperative stroke provided a definition of stroke. All but one study investigating mortality defined if this was in-hospital or 30-day mortality.

Table 2 – Quality assessment.

	Were selection criteria clearly described?	Was the study prospective?	Was the study multicenter?	Were patients randomized?	Was the execution of the CT-scan described in sufficient detail to permit its replication?	Was a definition of stroke provided?	Was the time interval of mortality provided?
<b>Primary operation</b>							
Fukuda et al.[26]	Yes	Yes	No	No	No	No	Yes
Knollman et al.[21]	Yes	Yes	No	No	No	No	NA
Lee et al.[20]	Yes	No	No	No	No	Yes	No
Nishi et al.[44]	Yes	Yes	No	No	No	No	Yes
Park et al.[25]	Yes	No	No	No	Yes	No	Yes
Russo et al. [27]	Yes	No	No	No	Yes	NA	Yes
Takami et al. [28]	Yes	No	No	No	No	Yes	Yes
<b>Redo operation</b>							
Aviram et al.[10]	Yes	Yes	No	No	Yes	No	Yes
Aviram et al.[45]	Yes	No	No	No	Yes	NA	NA
Gasparovic et al.[46]	Yes	No	No	No	Yes	No	Yes
Goldstein et al. [12]	Yes	No	No	No	No	Yes	Yes
Imran Hamid et al.[22]	Yes	No	No	No	Yes	NA	Yes
Kamdar et al.[29]	Yes	No	No	No	Yes	NA	Yes
LaPar et al. [23]	Yes	No	No	No	No	No	Yes
Luciani et al.[47]	Yes	No	No	No	No	Yes	Yes
Morishita et al.[24]	Yes	No	No	No	No	No	Yes
Nikolaou et al.[30]	Yes	No	No	No	Yes	NA	Yes
Yamashiro et al. [48]	Yes	No	No	No	No	No	Yes

NA not applicable

None of the studies was randomized, leading to different patient populations. For the studies investigating primary cardiac operation, two studies with a control group only performed a CT-scan in high-risk patients with extensive atherosclerosis, history of cerebrovascular accident or transient ischemic attack, peripheral vascular disease or renal disease [20,21] while one study did not perform a CT-scan before emergency operations, if the CT-scanner was

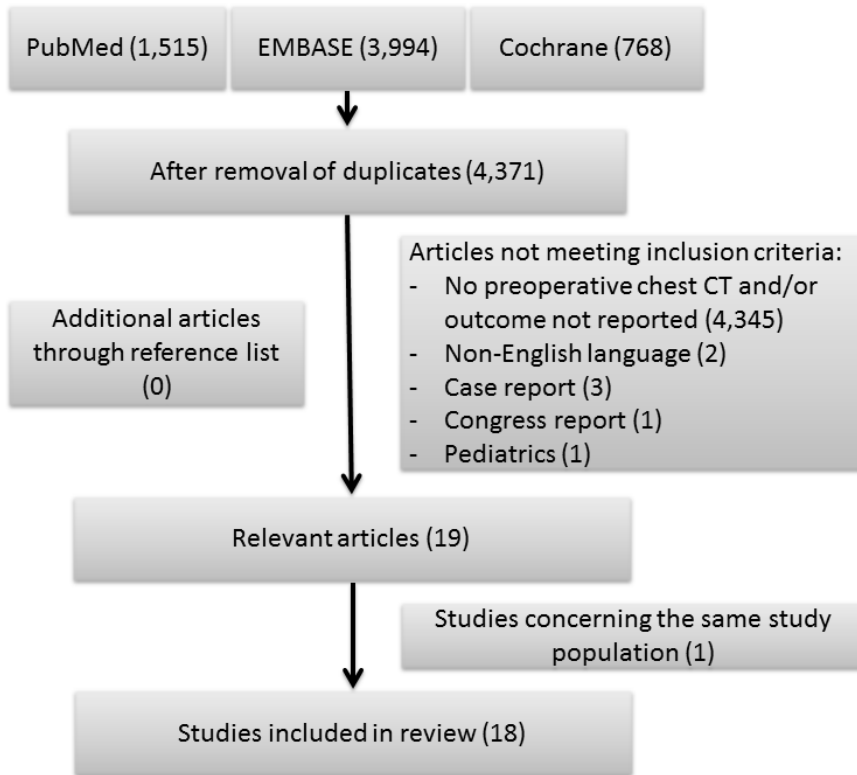


Figure 1: Flowchart of study inclusion

not available and in patients with renal failure or previous contrast reaction. For redo cardiac operation, in three retrospective studies a CT-scan was not performed routinely resulting in a control group of patients who did not receive a CT-scan [12,22,23]. One study only performed a CT-scan in high-risk patients with extensive atherosclerosis, history of stroke, peripheral vascular disease or renal disease [24] while emergency surgery, renal failure, previous contrast reaction or non-availability were reasons for not receiving a CT-scan in the remaining study [10].

The non-randomized study design led to a large heterogeneity between patients receiving a CT-scan and control groups. Also the type of surgery varied widely between studies. Therefore, due to the large clinical and methodological heterogeneity between studies, data were not pooled.

### *Primary operation*

Seven articles concerned patients receiving their primary operation. The total number of included patients was 1,754, of which 1,194 received a CT scan and 560 served as control group. There were no large differences in age, gender and history of stroke between the two groups. Baseline characteristics are provided in *Table 3*. Patients were operated between 1990 and 2008. The most commonly performed procedure was coronary artery bypass grafting (CABG) followed by valve replacement and combined CABG and valve replacement. Three studies used non-contrast enhanced CT while three studies used contrast-enhanced CT and one study did not report if contrast was administered.

Outcomes are provided in *Table 4*. The incidence of postoperative stroke ranged from 0.0 – 2.5 (median 0.7%) in the CT-group. Three studies used a control group, of which two studies reported the outcomes separately for the control group [20,25]. Lee et al.[20] and Park et al.[25] found a decrease of 77% (3.0% to 0.7%) and 96% (9.1% to 0.4%) respectively in stroke rate in favor of the CT group. The CT-group consisted of high risk patients in the study of Lee et al. [20] while Park et al.[25] excluded emergency operations and patients with renal failure or previous contrast reaction. Lee et al.[20] changed the surgical approach mainly by choosing an axillary artery cannulation site (10.5%) while Park and colleagues [25] mainly used an off-pump no-touch technique in 9.2% of the patients (*Table 4*).

Two studies compared 30-day mortality in the CT-group to a control group. Both Lee et al. [20] and Park et al. [25] found a decrease in mortality of 49% (13.5% to 7.0%) and 66% (5.3% to 1.8%) respectively in favor of the CT group. Main cause of death was stroke. Fukada et al.[26], Russo et al.[27] and Takami et al.[28] reported the in-hospital mortality for patients receiving a preoperative CT which was 1.0%, 4.0% and 0.0% respectively. No control group was used.

### *Redo cardiac surgery*

Eleven studies with in total 2,303 patients concerned redo cardiac surgery, often after primary CABG. Thirteen-hundred-ninety patients received a CT-scan while the remaining 913 patients served as control group. Included patients were operated between 1981 and 2011. The study population ranged from 6 – 610 patients. Two studies did not report if the CT-scan was contrast enhanced. All the remaining studies used contrast-enhanced CT. The most commonly performed procedure was valve surgery followed by combined CABG and valve replacement.

Table 3 – Baseline study characteristics.

Author	Year of publication	Patients operated (year)	Total number of patients	CT group (n)	Control group (n)	CT group						Control group					
						CT with contrast-enhancement	Only reoperations	CABG (%)	Valve surgery (%)	CABG + valve operation (%)	Aortic surgery (%)	Other (%)	CABG (%)	Valve surgery (%)	CABG + valve operation (%)	Aortic surgery (%)	Other (%)
<b>Primary operation</b>																	
Fukuda et al.[26]	2000	1990-1998	308	308	0	No	No	100	0	0	0	0	0	0	0		
Knollman et al.[21]	1998	NR	100	5	95	Yes	No	77*	14*	9*	0	0	0	0	0		
Lee et al.[20]	2007	2002-2005	503	114	389	No	No	58*	24*	16*	0*	3*	62	20	12		
Nishi et al.[44]	2009	2005-2008	300	300	0	No	No	30	60	10	0	0	NA	NA	0		
Park et al.[25]	2010	2006-2008	360	284	76	Yes	No	100	0	0	0	0	100	0	0		
Russo et al. [27]	2007	2004-2005	143	143	0	Yes	No	NR	NR	NR	NR	NR	NA	NA	0		
Takami et al. [28]	2008	1997-2007	40	40	0	NR	No	0	54	41	0	5	NA	NA	0		
<b>Redo operation</b>																	
Aviram et al.[10]	2009	2003-2006	73	28	45	Yes	Yes	21	32	36	11	0	58	31	9		
Aviram et al.[45]	2005	2003-2004	15	15	0	Yes	Yes	NR	NR	NR	NR	NR	NA	NA	2		
Gasparovic et al.[46]	2005	2003-2004	33	33	0	Yes	Yes	21	48	9	0	21	NA	NA	0		
Goldstein et al. [12]	2013	2004-2008	364	137	227	Yes	Yes	53*	24*	20*	0	3*	53*	24*	20*		
Imran Hamid et al.[22]	2014	2001-2011	544	162	382	Yes	Yes	15*	48*	14*	4*	19*	15*	48*	14*		
Kamdar et al.[29]	2008	2003-2006	167	167	0	Yes	Yes	25	24	49	2	0	NA	NA	7		
LaPar et al. [23]	2011	2002-2009	373	140	233	NR	Yes	14	70	10	0	6	23	56	14		
Luciani et al.[47]	2008	2000-2006	610	610	0	Partly	Yes	10	70	0	10	10	NA	NA	0		
Morishita et al.[24]	2003	1981-2000	90	64	26	NR	Yes	0	98	0	2	0	0	100	0		
Nikolaou et al.[30]	2012	2009-2010	28	28	0	Yes	Yes	21	57	18	0	4	NA	NA	0		
Yamashiro et al. [48]	2011	NR	6	6	0	Yes	Yes	0	50	0	50	0	NA	NA	0		

NR not reported; NA not applicable; \*Data were not provided separately for the CT-group and the control group. # These numbers represent the 'post-CT' group which also contained 159 patients without a CT

Table 4 – Outcomes.

Author	Change in surgical approach in patients receiving a preoperative CT															
	Postoperative stroke in CT group (%)	Postoperative stroke in control group (%)	30-day mortality in CT group (%)	30-day mortality in control group (%)	In-hospital mortality in CT group (%)	In-hospital mortality in control group (%)	Surgery cancelled (%)	Different cannulation site (%)	Off-pump surgery (%)	No-touch technique (%)	Deep hypothermic circulatory arrest (%)	Mycardial preservation technique (%)	Norminline incision (%)	Periheral arterial and venous dissection before incision (%)	Ascending aorta replacement (%)	Other/unknown (%)
<b>Primary operation</b>																
Fukuda et al.[26]	0.7	NA	NR	NA	1.0	NA	9.4	1.6	4.8							
Knollman et al.[21]	0.0	NR	NR	NR	NR	NR					Not reported					
Lee et al.[20]	0.7	3.0	7.0**	13.5*	NR	NR	10.5	3.5						2.6		
Nishi et al.[44]	0.7	NA	2.0	NA	NR	NA	4.3									
Park et al.[25]	0.4	9.1	1.8	5.3	NR	NR	2.5	9.2	1.4					2.1		
Russo et al. [27]	NR	NA	NR	NA	4.0	NA					Not reported					
Takami et al. [28]	2.5	NA	NR	NA	0.0	NA					Not reported					
<b>Redo operation</b>																
Aviram et al.[10]	0.0	2.2	3.6	8.9	NR	NR										35.7
Aviram et al.[45]	NR	NA	NR	NA	NR	NA	13.3				6.7					20.0
Gasparovic et al.[46]	7.0	NA	NR	NA	17.0	NA					Not reported					
Goldstein et al. [12]	3.6	4.4	10.9	11.0	NR	NR					Not reported					
Imran Hamid et al.[22]	NR	NR	NR	NR	11.0	9.0					Not reported					
Kamdar et al.[29]	NR	NA	2.5	NA	NR	NA	4.1	10.7		4.1			8.3	49.7		
LaPar et al. [23]	0.0	5.6	7.9	7.3	NR	NR					Not reported					
Luciani et al.[47]	1.6	NA	3.8	NA	NR	NA					Not reported					
Morishita et al.[24]	5.0	8.0	NR	NR	6.0	NR					Not reported					
Nikolaou et al.[30]	NR	NA	0.0	NA	NR	NA	7.1	3.5		14			7.1			14.2
Yamashiro et al. [48]	0.0	NA	NR	NA	0.0	NA					Not reported					

NR not reported; NA not applicable; \*Mortality not defined; #These numbers represent the 'post-CT' group which also contained 159 patients without a CT

The incidence of stroke ranged from 0.0 – 7.0 (median: 1.6)% for the CT-group. Four studies [10,12,23,24] used a control group and all studies found a decrease in stroke rate namely 2.2% to 0.0% [10], 4.4% to 3.6% [12], 5.6% to 0.0% [23] and 8.0% to 5.0% [24] in patients receiving a CT-scan.

The 30-day mortality decreased in patients receiving a CT-scan with 60% and 1% in the studies of Aviram et al.[10] and Goldstein et al.[12] while LaPar et al.[23] found a slight increase of 8%. Also Hamid et al.[22] found an increase of the in hospital mortality from 9.0% to 11.0% in patients receiving a preoperative CT. Three studies reported the effect of CT-scanning on surgical approach [10,29,30]. The most common change in surgical strategy was a different cannulation site (3.5–13.3%) and cancellation or postponing of surgery (4.1–13.3%). Also two studies reported a change to a non-midline approach [29,30].

## Discussion

We performed a systematic review of the published literature on the effect of preoperative CT on surgical strategy and postoperative mortality and stroke rate in patients undergoing primary and redo cardiac surgery. Preoperative CT can provide previously unrecognized information about aortic calcifications that has the potential to change surgical strategy, and, possibly, reduce the incidence of postoperative stroke and mortality.

The indication for a preoperative CT differs between primary and redo cardiac surgery. The main benefit in primary surgery seems to be visualization of the extent of aortic atherosclerosis. In redo cardiac surgery the main purpose is visualization of the (previously altered) anatomic relationships as well assessment of previous grafts [31]. Redo cardiac surgery is more complicated and preoperative CT evaluation has therefore become a procedure that is performed often [32]. We also found that change in surgical approach based on CT findings is higher in redo surgery patients. However, both in primary and redo cardiac surgery the most common change is a different cannulation site due to extensive aortic atherosclerosis. This can be visualized using different imaging modalities. A chest X-ray often only detects large calcified areas and underestimates atherosclerosis and is therefore not the best tool to quantify aorta atherosclerosis [33]. Furthermore, it is hard to determine the extensiveness and exact localization of the calcifications on a chest X-ray. With transesophageal ultrasound both calcified and noncalcified areas can be visualized but the trachea makes evaluation of the middle and distal part

of the ascending aorta impossible [34,35]. Manual palpation during surgery is unreliable and misses almost half of the soft plaques [36]. This problem could potentially be solved by using epiaortic intraoperative ultrasound, which is superior to both transesophageal ultrasound and manual palpation [34]. Disadvantages of epiaortic ultrasound are the operator dependency, the limited anatomical coverage and the poor acoustic window [37]. Intraoperative epiaortic ultrasound can reduce the risk of a postoperative stroke by modification of cannulation and clamping techniques [8,38]. The major drawback however is the intraoperative use after sternotomy. This can lead to modifications during the surgical procedure if intraoperative ultrasound shows unexpected findings. Furthermore, several studies have shown that intraoperative ultrasound is inferior to CT and leads to an underestimation of the calcium burden [21,28,39]. Preferably, this information should be available preoperatively, which also can prevent sternotomy and limit operation time in selected patients. A preoperative CT-scan offers the possibility to visualize ascending aorta atherosclerosis and this review shows that a preoperative CT has effect on surgical decision-making and postoperative complications. However, CT is also associated with radiation exposure with the small risk of radiation-induced malignancy. Recently several new technical developments have been introduced allowing non contrast-enhanced CT at submillisievert dose levels [40]. Therefore, radiation dose cannot be considered as a limitation for performing a preoperative CT anymore. Furthermore the radiation risk is negligible compared to the risk associated with the surgery. To visualize soft plaques contrast agent is needed but aortic calcifications are perfectly visualized without contrast. Therefore renal failure is no contraindication to perform a preoperative CT for this indication. Another drawback of performing a preoperative CT might be the additional costs of a CT-scan. Gada et al.[41] and Goldstein et al. [12] investigated the cost-effectiveness of a preoperative CT and both found that the performance of a preoperative CT is justified because it can lead to change in surgical approach and prevention of postoperative complications. Both studies were however performed in redo cardiac surgery patients. Furthermore, the costs associated with a stroke are very high compared to the relatively low costs of a CT-scan. However, future research should determine the cost-effectiveness of implementing a standard preoperative CT-scan in patients undergoing their primary cardiac surgery. This systematic review has several limitations. Most important, none of the included studies was randomized, which may have biased the results. Only,

three studies performed a CT-scan only in high risk patients with extensive atherosclerosis, history of stroke, peripheral vascular disease or renal disease but still found a decrease in stroke and mortality rate in these patients [20,21,24]. Two studies used emergency operations, non-availability of the scanner and patients with renal failure as a control group [10,25]. These two studies found the largest increase in stroke and mortality, which can possibly be explained because the control group contained high-risk patients which might overestimate the effect [42]. Furthermore, due to the large heterogeneity in included patients and study designs it was not possible to pool the data since the stroke and mortality rate strongly depended on the type of included patients. Randomized and outcome based studies are sparse and need to be performed in order to determine if a standard preoperative CT should be implemented. We are currently conducting a large randomized multicenter trial to investigate the effect a non-contrast enhanced preoperative CT on postoperative stroke rate which will provide more insights in the usefulness and cost-effectiveness of a preoperative CT for cardiac surgery in the future [43].

In conclusion, current evidence suggests that a preoperative CT may lead to decreased stroke and mortality rate in primary cardiac surgery by optimizing surgical approach. Current evidence is too weak for the implementation of a standard preoperative CT but ongoing and future research will provide more information. In redo cardiac surgery the stroke rate is decreased as well but the effect on mortality is unclear.

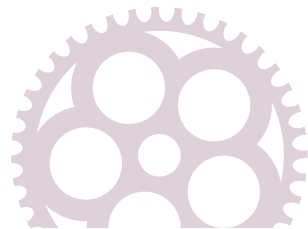
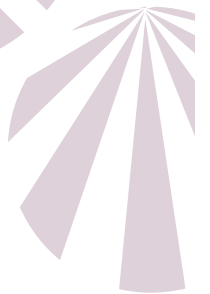
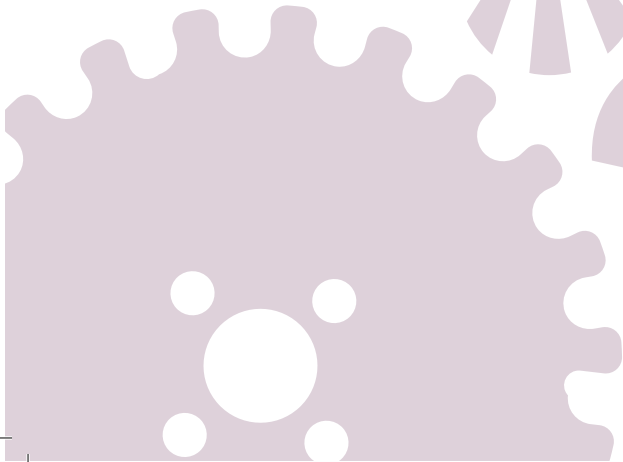
## References

- [1] Bucerius J, Gummert JF, Borger MA, et al., Stroke after cardiac surgery: a risk factor analysis of 16,184 consecutive adult patients. *Ann Thorac Surg* 2003;75(2):472-8.
- [2] Filsoufi F, Rahmanian PB, Castillo JG, Bronster D, Adams DH, Incidence, topography, predictors and long-term survival after stroke in patients undergoing coronary artery bypass grafting. *Ann Thorac Surg* 2008;85(3):862-70.
- [3] Messe SR, Acker MA, Kasner SE, et al., Stroke after aortic valve surgery: results from a prospective cohort. *Circulation* 2014;129(22):2253-61.
- [4] Hogue CW, Jr, Murphy SF, Schechtman KB, Davila-Roman VG, Risk factors for early or delayed stroke after cardiac surgery. *Circulation* 1999;100(6):642-7.
- [5] Rankin JM, Silbert PL, Yadava OP, Hankey GJ, Stewart-Wynne EG, Mechanism of stroke complicating cardiopulmonary bypass surgery. *Aust N Z J Med* 1994;24(2):154-60.
- [6] van der Linden J, Hadjiniolaou L, Bergman P, Lindblom D, Postoperative stroke in cardiac surgery is related to the location and extent of atherosclerotic disease in the ascending aorta. *J Am Coll Cardiol* 2001;38(1):131-5.
- [7] Selim M, Perioperative stroke. *N Engl J Med* 2007;356(7):706-13.
- [8] Wareing TH, Davila-Roman VG, Barzilai B, Murphy SF, Kouchoukos NT, Management of the severely atherosclerotic ascending aorta during cardiac operations. A strategy for detection and treatment. *J Thorac Cardiovasc Surg* 1992;103(3):453-62.
- [9] Mozaffarian D, Benjamin EJ, Go AS, et al., Executive summary: heart disease and stroke statistics-2015 update: a report from the american heart association. *Circulation* 2015;131(4):434-41.
- [10] Aviram G, Mohr R, Sharony R, Medalion B, Kramer A, Uretzky G, Open heart reoperations after coronary artery bypass grafting: the role of preoperative imaging with multidetector computed tomography. *Isr Med Assoc J* 2009;11(8):465-9.
- [11] Goldstein M.A., Roy S.K., Hebsur S., et al., Relationship between multi-detector cardiac computed tomographic angiography prior to reoperative cardiac surgery, length of stay and hospital charges. *J Am Coll Cardiol* 2011;57(14):E638.
- [12] Goldstein MA, Roy SK, Hebsur S, et al., Relationship between routine multi-detector cardiac computed tomographic angiography prior to reoperative cardiac surgery, length of stay, and hospital charges. *Int J Cardiovasc Imaging* 2013;29(3):709-17.
- [13] Glas KE, Swaminathan M, Reeves ST, et al., Guidelines for the performance of a comprehensive intraoperative epiaortic ultrasonographic examination: recommendations of the American Society of Echocardiography and the Society of Cardiovascular Anesthesiologists; endorsed by the Society of Thoracic Surgeons. *Anesth Analg* 2008;106(5):1376-84.
- [14] Svensson LG, Adams DH, Bonow RO, et al., Aortic valve and ascending aorta guidelines for management and quality measures. *Ann Thorac Surg* 2013;95(6 Suppl):S1-66.

- [15] Eagle KA, Guyton RA, Davidoff R, et al., ACC/AHA 2004 guideline update for coronary artery bypass graft surgery: a report of the American College of Cardiology/American Heart Association Task Force on Practice Guidelines (Committee to Update the 1999 Guidelines for Coronary Artery Bypass Graft Surgery). *Circulation* 2004;110(14):e340-437.
- [16] Mahnken A.H., Dohmen G., Koos R., Aortic valve calcifications on chest films: How much calcium do I need? *Acta Cardiol* 2011;66(4):505-8.
- [17] Mahnken AH, Wein BB, Sinha AM, Gunther RW, Wildberger JE, Value of conventional chest radiography for the detection of coronary calcifications: comparison with MSCT. *Eur J Radiol* 2009;69(3):510-6.
- [18] Whiting P, Rutjes AW, Reitsma JB, Bossuyt PM, Kleijnen J, The development of QUADAS: a tool for the quality assessment of studies of diagnostic accuracy included in systematic reviews. *BMC Med Res Methodol* 2003;3:25.
- [19] Maluenda G., Goldstein M.A., Lemesle G., et al., Perioperative outcomes in reoperative cardiac surgery guided by cardiac multidetector computed tomographic angiography. *Am Heart J* 2010;159(2):301-6.
- [20] Lee R, Matsutani N, Polimenakos AC, Levers LC, Lee M, Johnson RG, Preoperative noncontrast chest computed tomography identifies potential aortic emboli. *Ann Thorac Surg* 2007;84(1):38,41; discussion 42.
- [21] Knollmann F.D., Knorig J., Loebe M., et al., Preoperative screening for aortic calcification in cardiac surgery candidates. *Z Herz- Thorax- Gefasschir* 1998;12(3):121-9.
- [22] Imran Hamid U, Digney R, Soo L, Leung S, Graham AN, Incidence and outcome of re-entry injury in redo cardiac surgery: benefits of preoperative planning. *Eur J Cardiothorac Surg* 2014.
- [23] LaPar D.J., Ailawadi G., Irvine J.N., Lau C.L., Kron I.L., Kern J.A., Preoperative computed tomography is associated with lower risk of perioperative stroke in reoperative cardiac surgery. *Interact Cardiovasc Thorac Surg* 2011;12(6):919-23.
- [24] Morishita K, Kawaharada N, Fukada J, et al., Three or more median sternotomies for patients with valve disease: role of computed tomography. *Ann Thorac Surg* 2003;75(5):1476,80; discussion 1481.
- [25] Park KH, Lee HY, Lim C, et al., Clinical impact of computerised tomographic angiography performed for preoperative evaluation before coronary artery bypass grafting. *Eur J Cardiothorac Surg* 2010;37(6):1346-52.
- [26] Fukuda I, Unno H, Kaminishi Y, Strategies for preventing stroke after coronary artery bypass grafting. *Jpn J Thorac Cardiovasc Surg* 1998;46(1):38-45.
- [27] Russo V, Gostoli V, Lovato L, et al., Clinical value of multidetector CT coronary angiography as a preoperative screening test before non-coronary cardiac surgery. *Heart* 2007;93(12):1591-8.

- [28] Takami Y, Tajima K, Terazawa S, Okada N, Fujii K, Sakai Y, Safer aortic crossclamping during short-term moderate hypothermic circulatory arrest for cardiac surgery in patients with a bad ascending aorta. *J Thorac Cardiovasc Surg* 2009;137(4):875-80.
- [29] Kamdar AR, Meadows TA, Roselli EE, et al., Multidetector computed tomographic angiography in planning of reoperative cardiothoracic surgery. *Ann Thorac Surg* 2008;85(4):1239-45.
- [30] Nikolaou K, Vicol C., Vogt F., et al., Dual-source computed tomography of the chest in the surgical planning of repeated cardiac surgery. *J Cardiovasc Surg* 2012;53(2):247-55.
- [31] Gilkeson RC, Markowitz AH, Ciancibello L, Multisection CT evaluation of the reoperative cardiac surgery patient. *Radiographics* 2003;23 Spec No:S3-17.
- [32] Roselli EE, Reoperative cardiac surgery: challenges and outcomes. *Tex Heart Inst J* 2011;38(6):669-71.
- [33] Marschall K, Kanchuger M, Kessler K, et al., Superiority of transesophageal echocardiography in detecting aortic arch atheromatous disease: identification of patients at increased risk of stroke during cardiac surgery. *J Cardiothorac Vasc Anesth* 1994;8(1):5-13.
- [34] Bergman P, van der Linden J, Atherosclerosis of the ascending aorta as a major determinant of the outcome of cardiac surgery. *Nat Clin Pract Cardiovasc Med* 2005;2(5):246,51; quiz 269.
- [35] Konstadt SN, Reich DL, Quintana C, Levy M, The ascending aorta: how much does transesophageal echocardiography see? *Anesth Analg* 1994;78(2):240-4.
- [36] Roysse AG, Roysse CF, Epiaortic ultrasound assessment of the aorta in cardiac surgery. *Best Pract Res Clin Anaesthesiol* 2009;23(3):335-41.
- [37] Akhtar N.J., Markowitz A.H., Gilkeson R.C., Multidetector Computed Tomography in the Preoperative Assessment of Cardiac Surgery Patients. *Radiol Clin North Am* 2010;48(1):117-39.
- [38] Duda AM, Letwin LB, Sutter FP, Goldman SM, Does routine use of aortic ultrasonography decrease the stroke rate in coronary artery bypass surgery? *J Vasc Surg* 1995;21(1):98,107; discussion 108-9.
- [39] Fukuda I, Gomi S, Watanabe K, Seita J, Carotid and aortic screening for coronary artery bypass grafting. *Ann Thorac Surg* 2000;70(6):2034-9.
- [40] den Harder AM, Willeminck MJ, de Ruyter QM, et al., Achievable dose reduction using iterative reconstruction for chest computed tomography: A systematic review. *Eur J Radiol* 2015.
- [41] Gada H, Desai MY, Marwick TH, Cost-effectiveness of computed tomographic angiography before reoperative coronary artery bypass grafting: a decision-analytic model. *Circ Cardiovasc Qual Outcomes* 2012;5(5):705-10.
- [42] John R, Choudhri AF, Weinberg AD, et al., Multicenter review of preoperative risk factors for stroke after coronary artery bypass grafting. *Ann Thorac Surg* 2000;69(1):30,5; discussion 35-6.

- [43] ClinicalTrials.gov, Chest CT with iterative reconstructions as an alternative to conventional chest x-ray prior to heart surgery (CRICKET). 2014;2015.
- [44] Nishi H, Mitsuno M, Tanaka H, Ryomoto M, Fukui S, Miyamoto Y, Who needs preoperative routine chest computed tomography for prevention of stroke in cardiac surgery? *Interact Cardiovasc Thorac Surg* 2010;11(1):30-3.
- [45] Aviram G, Sharony R, Kramer A, et al., Modification of surgical planning based on cardiac multidetector computed tomography in reoperative heart surgery. *Ann Thorac Surg* 2005;79(2):589-95.
- [46] Gasparovic H, Rybicki FJ, Millstine J, et al., Three dimensional computed tomographic imaging in planning the surgical approach for redo cardiac surgery after coronary revascularization. *Eur J Cardiothorac Surg* 2005;28(2):244-9.
- [47] Luciani N, Anselmi A, De Geest R, Martinelli L, Perisano M, Possati G, Extracorporeal circulation by peripheral cannulation before redo sternotomy: indications and results. *J Thorac Cardiovasc Surg* 2008;136(3):572-7.
- [48] Yamashiro S, Yukiko K, Kise Y, Arakaki R, Cardiac and Aortic Reoperation for Patients with Functional Grafts after CABG. *Ann Vasc Dis* 2011;4(4):299-305.



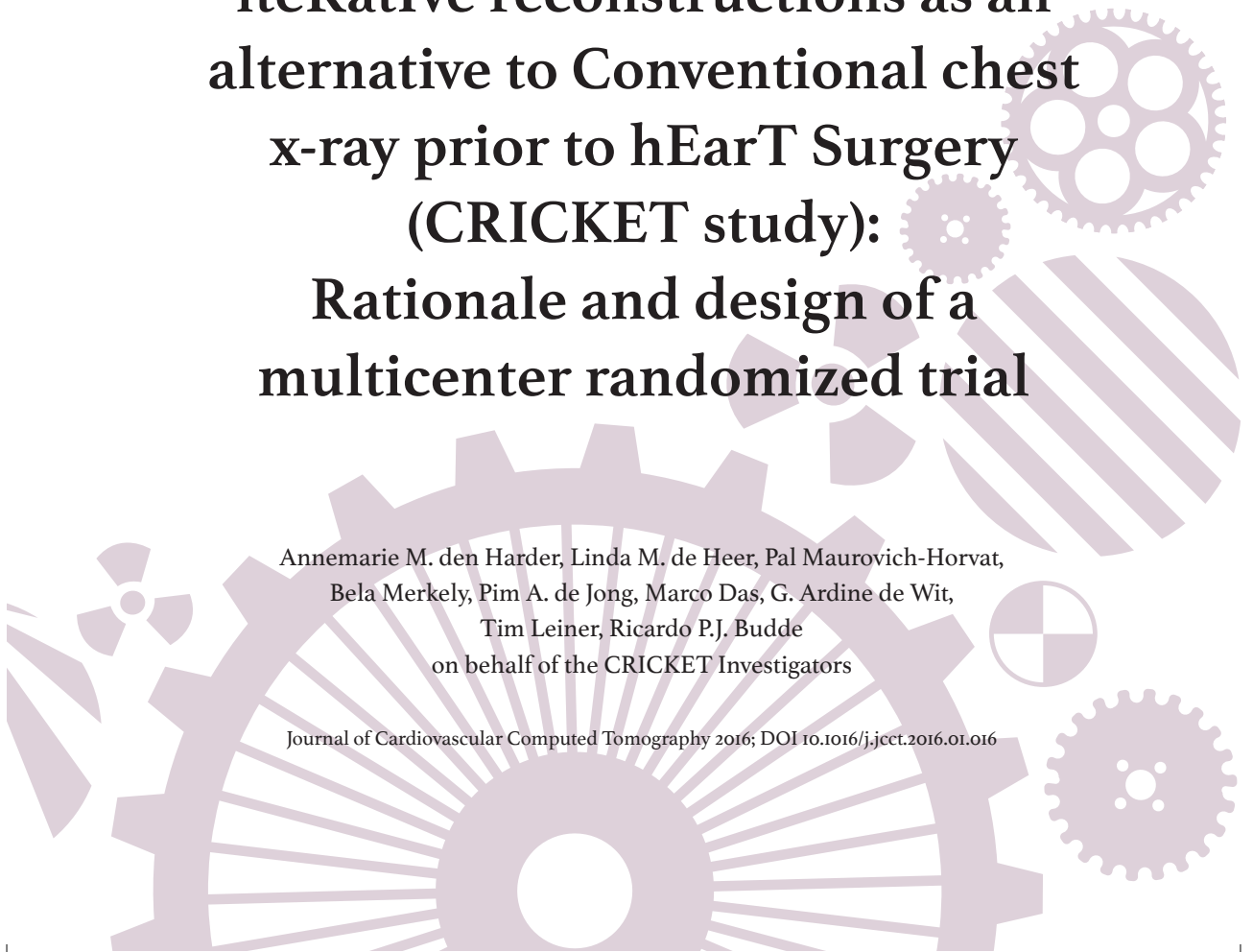
# Chapter 4.4

*Part IV Preoperative CT*

## **Ultra low-dose Chest ct with iteRatIve reconstructions as an alternative to Conventional chest x-ray prior to hEarT Surgery (CRICKET study): Rationale and design of a multicenter randomized trial**

Annemarie M. den Harder, Linda M. de Heer, Pal Maurovich-Horvat,  
Bela Merkely, Pim A. de Jong, Marco Das, G. Ardine de Wit,  
Tim Leiner, Ricardo P.J. Budde  
on behalf of the CRICKET Investigators

Journal of Cardiovascular Computed Tomography 2016; DOI 10.1016/j.jcct.2016.01.016



## Abstract

### *Background*

Stroke after cardiac surgery is a devastating complication with a persistently high incidence of 1.4 – 9.7%. Postoperative strokes are mainly embolic and can be provoked by manipulation and clamping of the aorta during cardiac surgery which can result in the embolization of atherothrombotic material and calcifications from the aortic wall. Computed tomography (CT) can offer preoperative visualization of aortic calcifications at submillisievert dose levels. We hypothesize that preoperative knowledge regarding the location and extent of aortic calcifications can be used to optimize surgical strategy and decrease postoperative stroke rate.

### *Methods/Design*

The CRICKET study (ultra low-dose Chest ct with iterative reconstructions as an alternative to Conventional chest x-ray prior to hEarT Surgery) is a prospective multicenter RCT to evaluate if a non contrast-enhanced chest CT before cardiac surgery can decrease postoperative stroke rate by optimizing surgical strategy. Patients scheduled to undergo cardiac surgery aged 18 years and older are eligible for inclusion. Exclusion criteria are pregnancy, a chest/cardiac CT in the past three months, emergency surgery, concomitant or prior participation in a study with ionizing radiation and unwillingness to be informed about unrequested findings. Subjects (N=1,724) are randomized between routine care, including a chest x-ray, or routine care with an additional low dose chest CT. The primary objective is to investigate whether the postoperative in-hospital stroke rate is reduced in the CT arm compared to the routine care arm of the randomized trial. The secondary outcome measures are altered surgical approach based on CT findings and cost-effectiveness.

## Introduction

Postoperative stroke is a major complication in 1.4 – 9.7% of patients undergoing cardiac surgery [1]. The stroke rate strongly depends on the surgical procedure, with increasing rates being seen in valve surgery, especially when combined with coronary artery bypass grafting (CABG). Stroke is associated with high postoperative mortality and a longer period of hospitalization [2]. A recent editorial highlights the fact that the incidence of stroke after isolated CABG, the most commonly performed cardiac surgical procedure, has not decreased over the past 10 years and occurs in 2.2% of patients [3]. Although various interventions and modifications of surgical technique have been tried, randomized trials to demonstrate their benefit are lacking which is partly due to the relatively low incidence of stroke which makes it more difficult to perform adequately powered trials. Postoperative strokes are mainly embolic in nature and often provoked by intraoperative manipulation of the aortic root and ascending aorta, which can result in the embolization of atherothrombotic material and calcifications from the aortic wall [1,4]. During surgery the ascending aorta is clamped to initiate cardiopulmonary bypass. Patients with ascending aorta atherosclerosis have an almost five-fold higher risk of developing a postoperative stroke [5]. Although intraoperative manual palpation can be used to detect aortic atherosclerosis it has only modest reliability [6]. Intraoperative direct epiaortic ultrasound is a valuable tool, but has a limited anatomical coverage and is operator dependent [7]. Furthermore, direct intraoperative ultrasound is only possible after sternotomy has been performed. This is a major drawback as it would be preferable to have detailed knowledge about aortic anatomy prior to surgery. In patients with extensive aortic calcifications this may even lead to the choice for alternative therapies because operative risk may outweigh benefits.

Unenhanced computed tomography (CT) can offer preoperative visualization of aortic calcifications as a marker of ascending aortic atherosclerosis. CT provides a 3D dataset with a high spatial resolution and offers the possibility to preoperatively plan surgical strategy. Recent technical innovations including iterative reconstruction allow a low radiation dose [8]. Several small, non-randomized studies indicate that a preoperative CT in cardiac surgery can possibly reduce postoperative stroke rate by adapting surgical strategy to avoid manipulation of the atherosclerotic aorta [9].

The CRICKET study (ultra low-dose Chest ct with iterative reconstructions as an alternative to Conventional chest x-ray prior to hEarT Surgery) was developed

to investigate whether a management strategy that includes preoperative chest CT compared to routine preoperative chest x-ray can reduce the stroke rate after cardiac surgery. Furthermore this study investigates the cost-effectiveness and cost-utility since a CT is associated with higher costs compared to chest radiography. Here we describe the rationale and design of this multicenter randomized controlled clinical trial (RCT).

## Methods

### 2.1 Overall study design and participants

The CRICKET study is a prospective, multicenter RCT to investigate if preoperative chest CT in patients scheduled for cardiac surgery can lower postoperative stroke rate by optimizing surgical strategy compared to standard chest x-ray. The study is registered at [www.clinicaltrials.gov](http://www.clinicaltrials.gov) (NCT02173470). All sites currently participating in this study are academic medical centers in Europe. Patient inclusion started in September 2014 and is expected to be finished in 2018.

Patients scheduled to undergo cardiac surgery aged 18 years and older are eligible for inclusion. Exclusion criteria are pregnancy, a chest or cardiac CT in the past three months, emergency surgery, concomitant or previous participation in a study that exposed the patient to radiation and unwillingness to be informed about unexpected findings on the CT scan such as lung nodules and vertebral fractures (*Table 1*). Patients scheduled for transcatheter aortic valve implantation (TAVI) are not eligible for inclusion, because these patients routinely receive preoperative contrast enhanced CT.

**Table 1** – Inclusion and exclusion criteria

Inclusion criteria	Exclusion criteria
Scheduled to undergo cardiac surgery ≥ 18 years old	Pregnant women Chest/cardiac CT in past 3 months Emergency surgery Participation in a study that prohibits the patient from participating in a study that exposes the patient to radiation Unwillingness to be informed about unrequested findings on the CT scan

### *2.2 Study objectives*

The primary study objective is to investigate if information about aortic calcifications derived from preoperative unenhanced low dose CT of the chest can lower in-hospital stroke rate after cardiac surgery by optimizing surgical strategy. The secondary objectives are (1) to investigate change in surgical approach, based on information derived from the preoperative chest CT, and (2) to assess the cost-effectiveness and cost-utility of the chest CT based strategy compared to routine care from a societal perspective.

### *2.3 Ethical considerations*

The institutional review board of the University Medical Center Utrecht reviewed and approved the study protocol (NL47293.041.13). Furthermore, the radiation safety committee and executive board of each center approved the study. The risk due to radiation was estimated to be low to intermediate according to the ICRP guideline Radiological Protection in Biomedical Research [10]. Subjects will only be included in the study after written informed consent is provided. Four centers are currently participating in this trial: University Medical Center Utrecht, Maastricht University Medical Center, Erasmus Medical Center Rotterdam (all located in The Netherlands) and the Heart and Vascular Center of Semmelweis University, Budapest, Hungary.

### *2.4 Sample size calculation*

Pilot data based on the largest and most comprehensive study reported in literature suggest that a 4-fold reduction in stroke rate (from 3.0% to 0.7%) is possible in patients undergoing a CT before cardiac surgery [11]. The local incidence of a postoperative stroke was 1.9% in 2010 in University Medical Center Utrecht. Since this is relatively low compared to literature a slightly higher expected stroke rate of 2.0% was used for sample size calculation. Given a 0.05 type-1 error and a 0.80 type-2 error, 1,724 patients are necessary to detect a reduction in stroke rate from 2.0% to 0.5%. Patients that withdraw before the CT scan is performed, will be replaced by new patients to reach the required number of included patients. Patients that withdraw after the CT scan is performed will not be replaced.

### *2.5 Patient recruitment and randomization*

All patients eligible for inclusion are asked by a physician, physician-assistant or nurse(-practitioner) to participate in the trial when they visit the hospital

for preoperative tests. After signing informed consent, patients are randomized using a web-based randomization procedure. Patients are randomized on a 1:1 basis to either the control or intervention group. The control group receives routine care including a preoperative chest x-ray. The patients in the intervention group receive an additional low dose non contrast-enhanced chest CT scan the day before surgery (*Figure 1*). Randomization is performed in blocks of eight in which the number of patients in the control and intervention group are divided equally. Randomization is stratified per center.

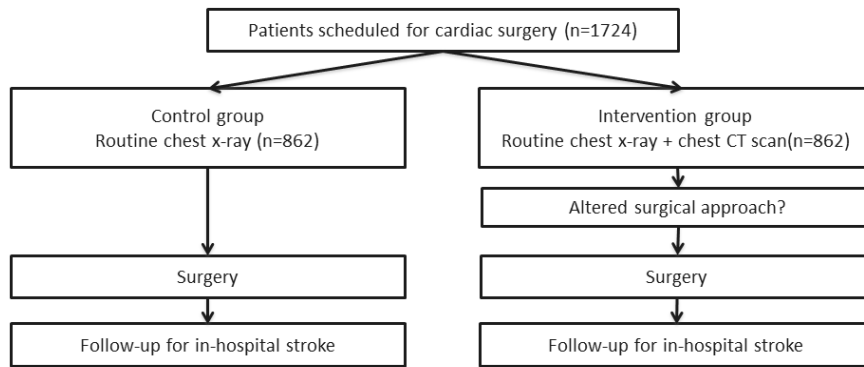


Figure 1 – Flowchart of study inclusion

### 2.6 CT protocol

All CT acquisitions are performed with state-of-the-art multidetector row CT (MDCT) systems (64-slice or higher). No contrast agent is administered. Kilovoltage (kV) will be reduced (aim 80 KV) as well as milliAmpere second (mAs) settings (aim as low as possible) with an effective radiation dose below 1 mSv for all acquisition settings. Images are reconstructed with iterative reconstruction with a slice thickness of 1 mm. First a locator image is made to select the acquisition region ranging from neck to liver. After this the acquisition is performed. Patients are instructed to hold their breath during acquisition. No ECG gating is necessary, since the focus is on aortic calcifications.

### 2.7 Adverse events

All unrequested findings on chest CT that require further investigations and/or medical treatment are documented as an adverse event. We expect this will mainly concern patients with pulmonary nodules. Patients with pulmonary nodules will receive follow-up according to local routine based on volumetric measurements. Since the intervention in this study concerns only an additional low-dose CT-scan without the use of contrast agents, it is not expected that serious adverse events occur due to this addition.

### 2.8 Data evaluation

A standardized report is made of the CT scan to describe aortic calcifications as well as pulmonary and other findings. The location and extent of the aortic calcifications is reported as well as the presence of pulmonary nodules, emphysema, infiltrates and other abnormalities. In case of pulmonary nodules, the location and size or volume is described. A written report is communicated to the surgeon, who has also access to the images.

A standardized form filled out by the treating surgeon before surgery is used to assess if adaptations to the initially intended surgical approach are made based on CT findings. If the surgical approach is not altered, the surgeon has to describe if this is because of the absence of aortic calcifications or if there is another reason. In case the surgical approach is altered, the surgeon can choose between the most common reasons (on-pump changes in off-pump surgery, no surgery, percutaneous approach) or give a different reason.

Baseline characteristics such as age, type of surgery, co-morbidities, history of stroke as well as surgery and CT characteristics are derived from the electronic patient file, the nationwide complication registry of the Dutch Association for Thoracic Surgery and the Picture Archiving and Communication System (PACS). A detailed overview is provided in *Appendix A*. The national registry from the Dutch Association for Thoracic Surgery started in 2007 and is based on the complication registry from the Society of Thoracic Surgeons (STS) [12]. For this study stroke is defined as central neurological defects that either recover spontaneously (transient ischemic attack) or become permanent. Completeness and accuracy of stroke data of the nationwide registry is excellent [12]. The participating center in Hungary does not use the same complication registry, therefore these data will be prospectively acquired using the definitions of the Dutch complication registry.

### 2.9 Data analysis

The number of in hospital postoperative strokes will be compared between the control and intervention group using a Chi-square test. A p-value of  $<0.05$  will be considered statistically significant. The number of patients in whom the surgical strategy is altered based on CT findings in the intervention arm is presented using descriptive statistics. A p value  $<0.05$  is considered statistically significant.

As CT scanning is more expensive compared to the routine chest X-ray it is important to know whether these excess expenses result in better patient outcomes and/or cost savings related to these improved patient outcomes. Therefore, an economic evaluation will be performed at the end of the study.

### Discussion

The CRICKET study is the first multicenter RCT to assess if cardiac surgical strategy can be further optimized by subjecting patients to preoperative non contrast-enhanced chest CT. The primary objective is to investigate if information about aortic atherosclerosis can lower stroke rate while the secondary objectives are to investigate alteration of surgical approach based on information derived from the preoperative chest CT and to assess the cost-effectiveness and cost-utility of the chest CT based strategy compared to routine care.

Several studies investigated the effect of a preoperative CT on stroke rate. The largest study was performed by Lee et al.[11] who introduced a non contrast-enhanced chest CT in patients at high risk of stroke and compared this to patients that underwent surgery before the introduction of chest CT. In total 503 patients were included and a decrease in postoperative stroke rate from 3.0% to 0.7% after the introduction of chest CT was found. A study by Park and colleagues [13] retrospectively compared patient receiving a preoperative CT to patients undergoing cardiac surgery without a preoperative CT. Postoperative stroke rate decreased from 9.0% to 0.4% in favor of the patients receiving a preoperative CT. Furthermore, several studies have investigated a preoperative CT in redo cardiac surgery and all found a decrease in stroke rate [14-17]. A major limitation of the aforementioned studies is that none of the studies was randomized. Furthermore, the studies lack power to prove the benefit of a preoperative CT to reduce the postoperative stroke rate. Since the incidence of a postoperative stroke is relatively small, a large number of patients is required to achieve sufficient power.

The CRICKET study will be the first multicenter RCT to assess whether a preoperative non contrast-enhanced chest CT can reduce the stroke rate in cardiac surgery by optimizing surgical strategy.

### **Conclusion**

The results of the CRICKET study will help to clarify whether it is useful to perform a preoperative chest CT in cardiac surgery to optimize surgical strategy. The multicenter design affords broad generalization of the study. The findings of the CRICKET study will be valuable for current guidelines for preoperative imaging in cardiac surgery.

### **Acknowledgments**

This work is funded by the Dutch Organization for Health Research and Development (grant number 837001403). A list of the CRICKET investigators and participating centers is provided in the *appendix B*.

## Appendix A – Database variables

### *Baseline variables*

Age, gender, length, weight, smoking status, randomization, EuroSCORE

### *Medical history*

Diabetes, hypertension, use of statins, peripheral vascular disease, myocardial infarction, COPD, extracardiac arteropathy, poor mobility, neurological dysfunction, TIA, CVA, active endocarditis, creatinine level, chronic kidney failure, dialysis, pulmonary hypertension, AV gradient >120mmHg, pacemaker dependency, atrial fibrillation, left ventricular function, NYHA classification, angina pectoris, urgency of operation, preoperative critical state, reoperation

### *Medication*

Use of anticoagulants, use of inhalation medication

### *CT (if applicable)*

Kilovoltage, milliampereseconds, iterative reconstruction method and level, CTDIvol, dose-length product, aortic calcifications (visibility of CT aortic calcifications on chest x-ray, >half of the circumference, >1cm of the ascending aorta, ventral calcifications in ascending aorta), coronary calcifications (LM, LAD, LCX, RCA), pulmonary nodules (number, diameter, volume), aortic valve calcification, other

### *Surgery*

Date of surgery, type of surgery, on or off pump surgery, altered surgical approach, location aortic cannulation, duration of heart-lung machine, duration of aortic clamping

### *Postoperative*

TIA, CVA, pneumonia, prolonged ventilation (>24 hours), pulmonary embolism, atrial fibrillation, total days in hospital, total days on intensive care unit, discharge to home or other hospital

## Appendix B – CRICKET investigators

### *University Medical Center Utrecht*

Tim Leiner, Pim de Jong, Annemarie den Harder, Ricardo Budde, Shanta Kalaykhan-Sewradj, Linda de Heer, Ronald Meijer, Anneke Hamersma, Robert Valkenburg, Remko Kockelkoren, Ardine de Wit, Mieke Goedvolk, Frederiek de Heer

### *Erasmus Medical Center Rotterdam*

Ricardo Budde, Gabriel Krestin, Myriam Hunink, Ad Boogers, Jos Bekkers, Bardia Arabkhani

### *Maastricht University Medical Center*

Marco Das, Joachim Wildberger, Jos Maessen, Debbie Blyau, Bas Kietselaer

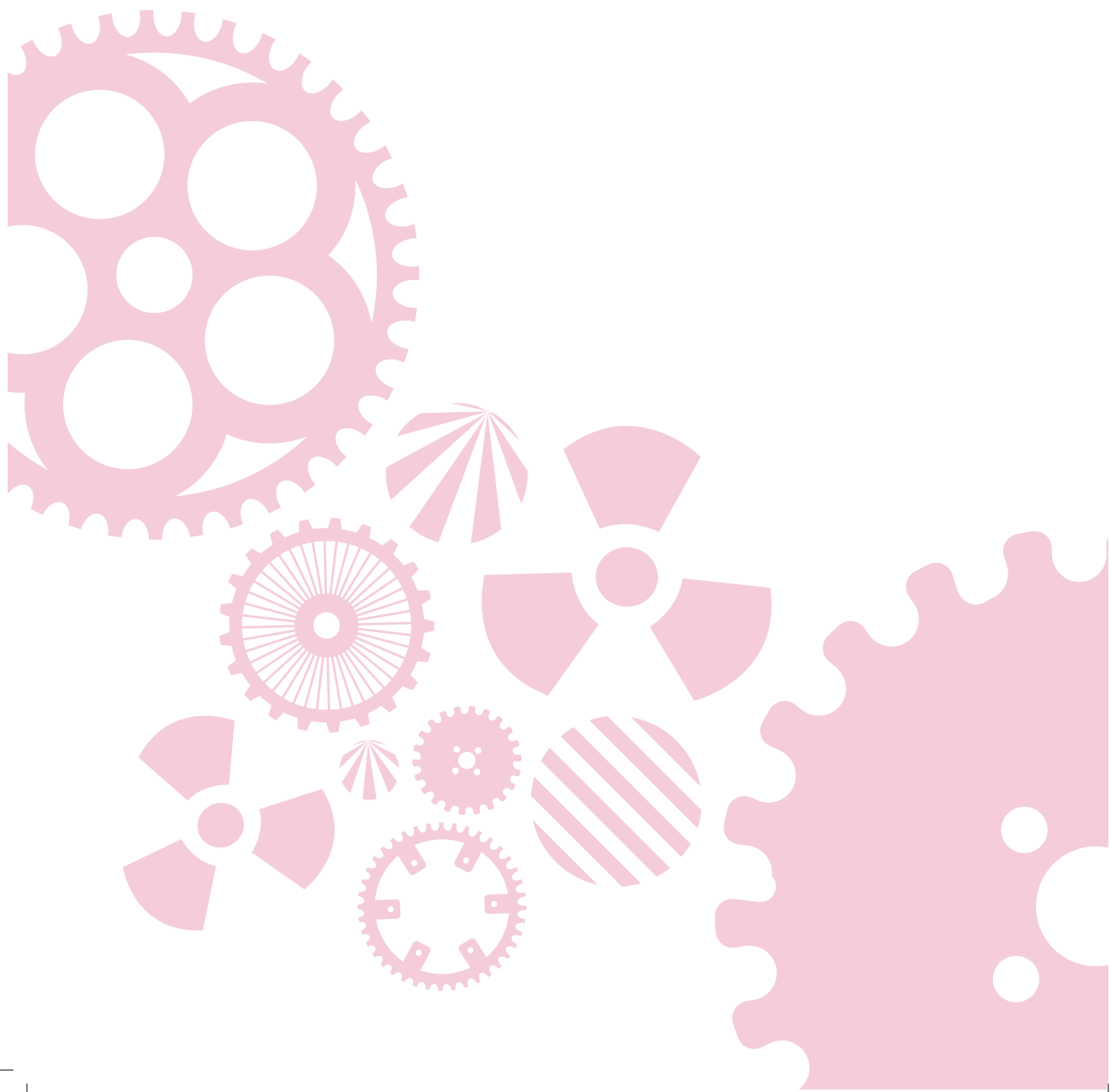
### *The Heart and Vascular Center of Semmelweis University*

Pál Maurovich-Horvat, Béla Merkely, Júlia Karady, Bálint Szilveszter, Kálmán Benke, Cao Chun, Zoltán Szabolcs, István Hartyánszky

## References

- [1] Selim M, Perioperative stroke. *N Engl J Med* 2007;356(7):706-13.
- [2] Anyanwu AC, Filsoufi F, Salzberg SP, Bronster DJ, Adams DH, Epidemiology of stroke after cardiac surgery in the current era. *J Thorac Cardiovasc Surg* 2007;134(5):1121-7.
- [3] Mack M, Can we make stroke during cardiac surgery a never event? *J Thorac Cardiovasc Surg* 2015.
- [4] Hogue CW, Jr, Murphy SF, Schechtman KB, Davila-Roman VG, Risk factors for early or delayed stroke after cardiac surgery. *Circulation* 1999;100(6):642-7.
- [5] van der Linden J, Hadjinikolaou L, Bergman P, Lindblom D, Postoperative stroke in cardiac surgery is related to the location and extent of atherosclerotic disease in the ascending aorta. *J Am Coll Cardiol* 2001;38(1):131-5.
- [6] Royse AG, Royse CF, Epiaortic ultrasound assessment of the aorta in cardiac surgery. *Best Pract Res Clin Anaesthesiol* 2009;23(3):335-41.
- [7] Akhtar N.J., Markowitz A.H., Gilkeson R.C., Multidetector Computed Tomography in the Preoperative Assessment of Cardiac Surgery Patients. *Radiol Clin North Am* 2010;48(1):117-39.
- [8] den Harder AM, Willemink MJ, de Ruitter QM, et al., Achievable dose reduction using iterative reconstruction for chest computed tomography: A systematic review. *Eur J Radiol* 2015.
- [9] den Harder AM, de Heer LM, Meijer RC, et al., Effect of computed tomography before cardiac surgery on surgical strategy, mortality and stroke. *Eur J Radiol* 2016;85(4):744--50.
- [10] Radiological Protection in Biomedical Research. A report of Committee 3 adopted by the International Commission on Radiological Protection. *Ann ICRP* 1991;22(3):1,28, v-xxiv.
- [11] Lee R, Matsutani N, Polimenakos AC, Levers LC, Lee M, Johnson RG, Preoperative noncontrast chest computed tomography identifies potential aortic emboli. *Ann Thorac Surg* 2007;84(1):38,41; discussion 42.
- [12] Siregar S, Groenwold RH, Versteegh MI, et al., Data Resource Profile: adult cardiac surgery database of the Netherlands Association for Cardio-Thoracic Surgery. *Int J Epidemiol* 2013;42(1):142-9.
- [13] Park KH, Lee HY, Lim C, et al., Clinical impact of computerised tomographic angiography performed for preoperative evaluation before coronary artery bypass grafting. *Eur J Cardiothorac Surg* 2010;37(6):1346-52.
- [14] Lapar DJ, Ailawadi G, Irvine JN, Jr, Lau CL, Kron IL, Kern JA, Preoperative computed tomography is associated with lower risk of perioperative stroke in reoperative cardiac surgery. *Interact Cardiovasc Thorac Surg* 2011;12(6):919-23.
- [15] Morishita K, Kawaharada N, Fukada J, et al., Three or more median sternotomies for patients with valve disease: role of computed tomography. *Ann Thorac Surg* 2003;75(5):1476,80; discussion 1481.

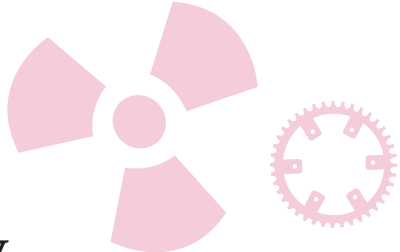
- [16] Aviram G, Mohr R, Sharony R, Medalion B, Kramer A, Uretzky G, Open heart reoperations after coronary artery bypass grafting: the role of preoperative imaging with multidetector computed tomography. *Isr Med Assoc J* 2009;11(8):465-9.
- [17] Goldstein MA, Roy SK, Hebsur S, et al., Relationship between routine multi-detector cardiac computed tomographic angiography prior to reoperative cardiac surgery, length of stay, and hospital charges. *Int J Cardiovasc Imaging* 2013;29(3):709-17.



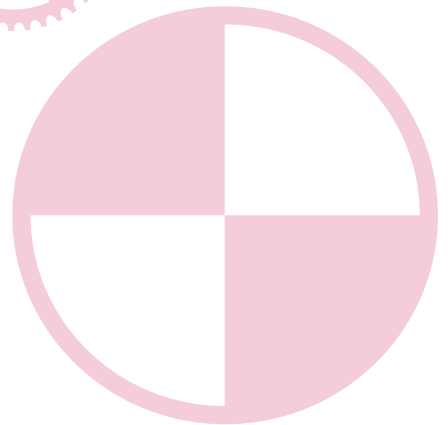
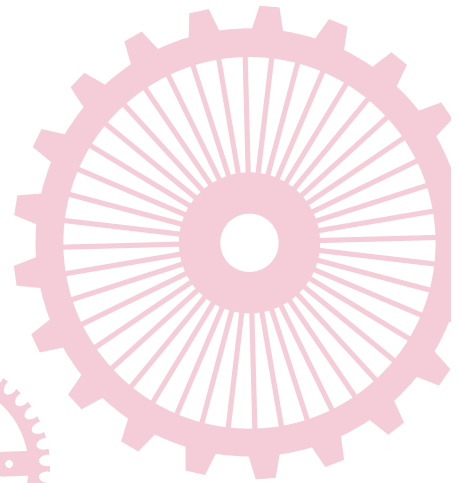
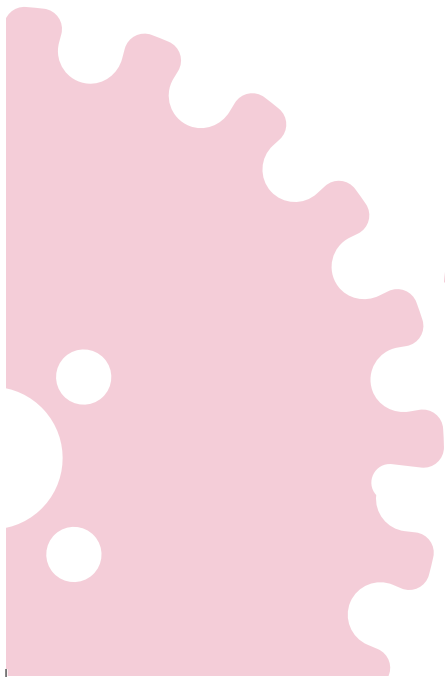


# Chapter 5.1

*Part V Discussion*



## Summary



This thesis studied the application of CT iterative reconstruction in a clinical setting. The potential dose reduction and effect on imaging-based quantification methods and diagnostic accuracy were investigated. Since iterative reconstruction can potentially reduce CT radiation dose to submillisievert dose levels, the secondary aim of this thesis was to investigate whether conventional imaging could be replaced by CT for imaging prior to cardiac surgery.

*Part I Clinical implementation of iterative reconstruction in cardiac CT*

Coronary CT angiography (CCTA) is associated with a relatively high radiation dose. Therefore, iterative reconstruction is particularly attractive for this indication. In **chapter 1.1** a meta-analysis was performed investigating the achievable radiation dose reduction for CCTA using iterative reconstruction. Ten studies comparing FBP at routine dose with iterative reconstruction at reduced dose were included. The pooled effective radiation dose decreased from 4.2 mSv with FBP to 2.2 mSv with iterative reconstruction, a 48% decrease. Both objective and subjective image quality were equal or improved with iterative reconstruction at low radiation dose in most studies. The following chapters (1.2 – 1.4) focused on the coronary calcium score, which is derived from a non contrast-enhanced CT acquisition. In **chapter 1.2** fifteen ex vivo hearts were scanned in a phantom at four different radiation dose levels. Images were reconstructed with FBP, hybrid iterative reconstruction and model-based iterative reconstruction. There was no effect on the coronary calcium score when using FBP and low levels of hybrid iterative reconstruction, while high levels of hybrid iterative reconstruction and model-based iterative reconstruction resulted in a significant underestimation of the coronary calcium score. Objective image quality improved with hybrid and especially with model-based iterative reconstruction. This phantom study was the basis of a clinical study (**chapters 1.3 and 1.4**), in which 30 patients underwent a routine dose acquisition for coronary calcium scoring, followed by three low dose acquisitions with 40%, 60% and 80% reduced dose. FBP resulted in several non-interpretable acquisitions at 60% and 80% reduced dose while acquisitions were interpretable using hybrid and model-based iterative reconstruction. Model-based iterative reconstruction resulted in an underestimation of the calcium score, and hereby confirmed the results of the phantom study. Similar to the phantom study, the calcium mass was not affected by dose reduction or reconstruction technique. In conclusion, hybrid iterative reconstruction can be safely implemented in clinical practice for coronary calcium scoring at reduced dose levels.

*Part II Clinical implementation of iterative reconstruction in thoraco-abdominal CT*

Chest CT scans are commonly performed, and the number of CT scans of the chest is expected to rise substantially with the anticipated implementation of lung cancer screening with chest CT in the USA. **Chapter 2.1** reports the results of 24 studies investigating the potential of dose reduction with iterative reconstruction in patients undergoing chest CT. The radiation dose of contrast-enhanced chest CT scanning can be reduced to 1.4 mSv, while submillisievert dose levels are achievable for non contrast-enhanced chest CT when using iterative reconstruction. A common indication for chest CT is follow-up of pulmonary nodules to assess potential growth. In **chapter 2.2** the effect of dose reduction and iterative reconstruction on pulmonary nodule volume was assessed. Dose reduction and hybrid iterative reconstruction did not affect pulmonary nodule volume, while model-based iterative reconstruction resulted in lower pulmonary nodule volumes at reduced dose. Therefore, hybrid iterative reconstruction can be safely implemented for pulmonary nodule volumetry, while caution should be taken with model-based iterative reconstruction.

To assist radiologists in the identification of pulmonary nodules, computer-aided detection (CAD) software can be used which automatically identifies potential pulmonary nodules. In **chapter 2.3** the accuracy of CAD software was investigated in the same study population as **chapter 2.2**. CAD correctly identified the majority of pulmonary nodules (82 – 96%) at routine and reduced dose levels with FBP, hybrid and model-based iterative reconstruction. However, high level hybrid iterative reconstruction and model-based reconstruction resulted in a significant increase in the number of false-positive findings with the CAD software at reduced dose. In **chapter 2.4**, thoracic aortic calcifications and aortic valve calcifications were studied, which are associated with cardiovascular disease and mortality. Iterative reconstruction resulted in improved subjective image quality and enabled accurate quantification of thoracic aortic and aortic valve calcifications. In **chapter 2.5** application of iterative reconstruction in CT assessment of urolithiasis was studied. Twenty patients underwent a routine dose acquisition followed by 40%, 60% and 80% reduced dose acquisitions. The sensitivity for detection of stones decreased to 50% at the lowest dose level, while this remained 100% when using model-based iterative reconstruction. Also, hybrid iterative reconstruction outperformed FBP. Assessment of possible extra-urinary tract pathology was feasible at 40% and 60% reduced dose, while the lowest dose level resulted in non-evaluable images.

*Part III Clinical implementation of iterative reconstruction in pediatric CT*

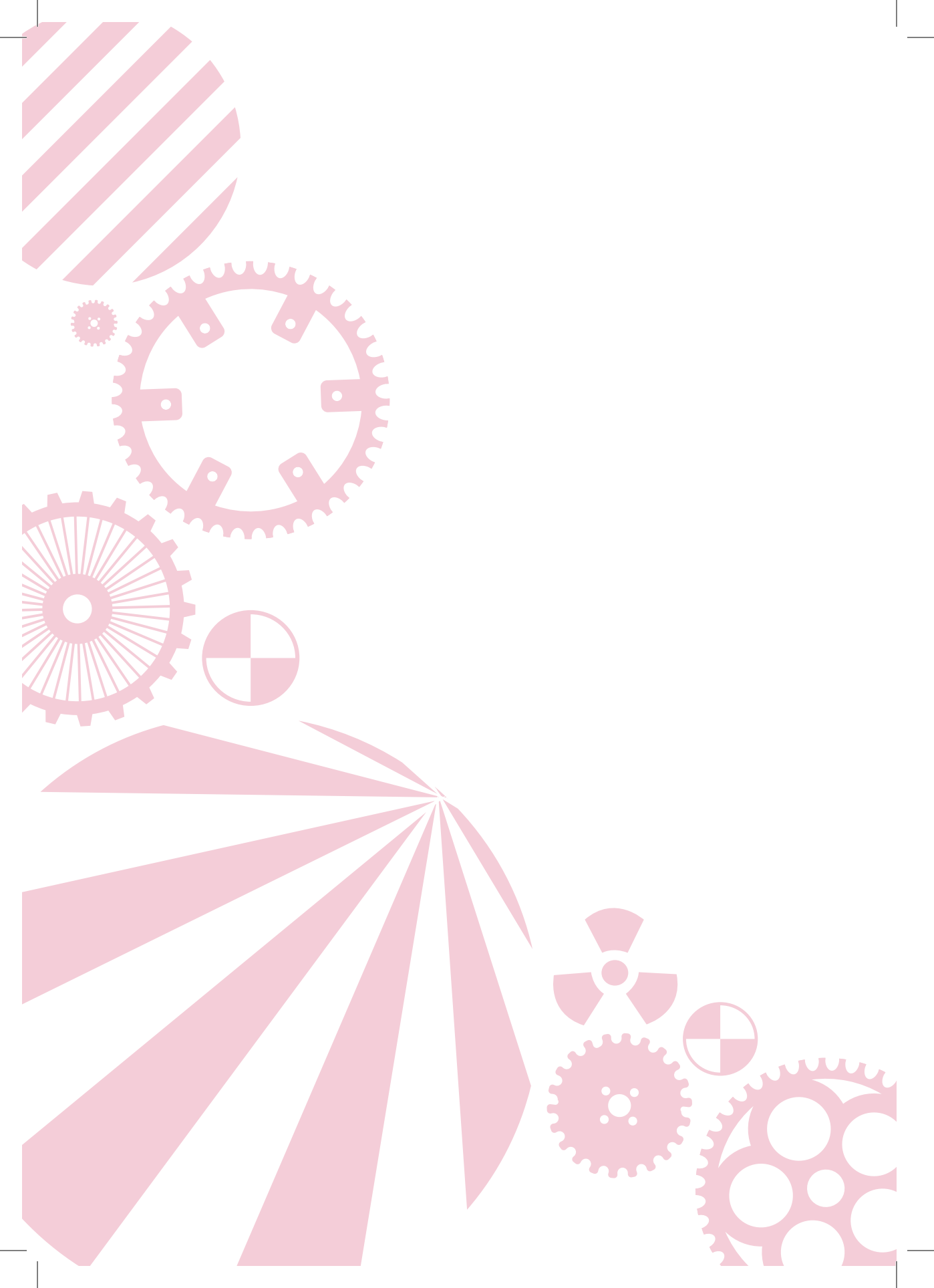
Radiation dose reduction is especially important in children, who are more sensitive to the effects of ionizing radiation and have a much longer time to develop harmful radiation effects. In **chapter 3.1** the results of literature regarding the application of iterative reconstruction in pediatrics is summarized and examples of image quality with FBP and iterative reconstructions are shown. Since most studies are performed in adults, the maximal achievable dose reduction in pediatric CT is still unclear. Therefore, in **chapter 3.2** the achievable dose reduction for imaging of pediatric great vessel stents is studied. Five different great vessel stents, commonly used to treat aortic coarctation, were imaged at routine dose and two reduced dose levels (52% and 81% dose reduction) and reconstructed with FBP and hybrid iterative reconstruction. Subjective image quality remained excellent, while objective image quality improved with hybrid iterative reconstruction.

*Part IV The rationale and need for CT prior to cardiac surgery*

Chest radiographs are routinely obtained prior to cardiac surgery in many hospitals. In **chapter 4.1** the frequency of abnormal findings on preoperative chest radiographs prior to cardiac surgery was investigated in a cohort of 1,136 patients. Half of the patients had one or more abnormalities on the preoperative chest radiograph, however, surgical strategy was altered in just a single patient (0.1%) based on those findings, while in 15 patients (1.3%) further analysis was performed without impacting the planned surgery. A commonly mentioned abnormality on chest radiographs is suspicion of COPD. In **chapter 4.2** the diagnostic accuracy of a chest radiograph for diagnosing mild COPD was studied in a nested case-control study. The diagnostic accuracy was limited in comparison to spirometry, therefore suggesting the presence of mild COPD on a chest radiograph using specific imaging markers results in substantial overdiagnosis.

In addition to better visualization of the pulmonary parenchyma, preoperative chest CT also provides improved visualization of aortic calcifications compared to conventional chest radiography. Calcifications in the ascending aorta, an important risk factor for postoperative stroke due to the intraoperative manipulation of the aorta, can be clearly depicted on chest CT. This knowledge can be used intra-operatively to adapt surgical strategy, potentially resulting in a decreased risk of clinically relevant postoperative strokes. **Chapter 4.3** summarizes what is currently known on this topic, and shows that the

postoperative stroke rate can be decreased with 77 – 96% based on the current literature. However, the quality of the currently published studies is weak with small sample sizes and non-randomized study designs. Therefore, in **chapter 4.4** a sufficiently powered randomized controlled study is proposed. This study is ongoing, with currently over 400 patients included.



# Chapter 5.2

## *Part V Discussion*

### General Discussion

Based on:

Willemink MJ, den Harder AM, de Jong PA, Leiner T.

*De toekomst van de CT-scan:*

*Gaat CT de conventionele rontgendiagnostiek vervangen?*

Ned Tijdschr Geneeskd 2014

den Harder AM, Willemink MJ, de Jong PA, Schilham AMR, Rajiah P, Takx

RAP, Leiner T. *New horizons in cardiac CT*. Clin Radiol 2016

In this thesis, we have shown in several prospective studies that iterative reconstruction enables dose reduction to submillisievert levels in a clinical setting for coronary calcium scoring and pulmonary nodule assessment while image quality and interpretability are maintained. Furthermore, based on literature research we found an achievable dose reduction of around 50% for cardiothoracic CT using iterative reconstruction with preserved image quality. Although these results are promising, iterative reconstruction can also affect commonly used imaging-based quantification methods such as the coronary calcium score and pulmonary nodule volumetry. These unwanted effects are more prominent when using more advanced fully model-based iterative reconstruction algorithms.

### Low dose coronary calcium scoring

The coronary calcium score is used for cardiovascular risk assessment. American Heart Association (AHA) guidelines recommend a non contrast-enhanced cardiac CT for coronary calcium scoring in asymptomatic patients at low to intermediate risk (6-10%, 10-year risk) and intermediate risk (10-20%, 10-year risk) [1]. In addition, coronary calcium scoring can potentially be used for population based cardiovascular screening. A currently ongoing Dutch study, the ROBINSICA trial (Risk Or Benefit IN Screening for Cardiovascular disease) [2], investigates the role of coronary calcium score for cardiovascular screening in people without diagnosed cardiovascular disease but with a possible increased risk of cardiovascular disease. Study participants are randomized between no screening, risk assessment based on classical risk factors and risk assessment using the coronary calcium score. Risk assessment is followed by preventive treatment. The goal of the study is to investigate if population screening for cardiovascular disease can reduce cardiovascular morbidity and mortality, and whether this strategy is cost-effective. Furthermore, the role of the coronary calcium score for population cardiovascular screening is studied. Complete follow-up is expected in 2022.

Coronary calcium screening can also be used in patients presenting with acute chest pain to rule out obstructive coronary disease [3,4]. In these patients, coronary CT angiography (CCTA) can be used as well which offers the advantage of also identifying non-calcified atherosclerotic plaques. A recent trial investigating the use of CCTA in patients suspected of acute coronary syndrome in the emergency department showed that this can safely reduce the costs and

frequency of outpatient testing after the initial emergency department visit [5]. Compared to high-sensitivity troponin assays, which can rule out acute coronary syndrome fast and accurate, CCTA did however not improve the identification of patients with significant coronary artery disease or shorten the hospital stay. Furthermore, the radiation dose of CCTA is substantially higher compared to a non-contrast-enhanced cardiac CT for coronary calcium scoring [6].

Quantification of coronary calcium was first described in 1990 by Agatston et al [7]. Several cohort studies have investigated the prognostic value of the coronary calcium score, mainly using electron-beam CT systems [8-12]. Currently coronary calcium scoring is predominantly performed on newer generation multi-detector row CT systems which are capable of advanced reconstruction techniques that enable imaging at much lower radiation dose [13]. A consensus document on how to perform coronary calcium scoring on multi-detector CT systems was developed, but no recommendation regarding reconstruction technique was provided [14]. In this thesis, it was shown that iterative reconstruction can result in an underestimation of the coronary calcium score, thereby reclassifying patients to lower risk categories [15]. This has also been described in several other patient studies and is more pronounced when using fully model-based iterative reconstruction algorithms [16-19]. There are several solutions to overcome this problem. First, it is possible to use correction factors in order to achieve agreement with the conventional calcium score derived with FBP [20]. A disadvantage of this method is that this correction factor is dependent on the specific algorithm and strength of the noise reduction, resulting in multiple conversion factors. Furthermore, large datasets are warranted to determine accurate conversion factors. Another possibility is to use the calcium mass instead of the coronary calcium score, which has shown to be more stable and less affected by reconstruction algorithm [15,21]. Calcium mass is also less affected by different scan starting positions [22] and differences in CT systems [23,24]. Interscan variation with iterative reconstruction was not studied in this thesis, however with FBP absolute differences ranging from 7% (highest risk category, calcium score >400) to 147% (low risk, calcium score >0 – 10) between acquisitions have been reported, while those differences were smaller for the calcium mass [22]. However, although it has been shown that the calcium mass is more reproducible, it is not widely accepted and implemented and most outcome studies only report the Agatston coronary calcium score. Therefore, outcome data concerning the calcium mass, necessary for risk stratification, are lacking. Finally, a completely different approach to reduce image noise in low-

dose CT scan based on convolution neural networks was recently described by Wolterink et al. [25]. This technique, which works in the image domain, utilizes a trained convolutional neural network (CNN) jointly with an adversarial CNN to estimate routine-dose CT images from low-dose CT images and hence reduce noise, without the need for iterative reconstruction.

In the current thesis radiation dose reduction for coronary calcium scoring was investigated by reducing the tube current while keeping the tube voltage fixed at 120 kVp. A tube voltage of 120 kVp correlates well with results derived from electron beam CT [26]. Since the tube voltage is exponentially related to the radiation dose, while this relationship is linear for the tube current, reducing the tube voltage is an attractive option to reduce radiation dose even further [27]. Reducing the tube voltage for coronary calcium scoring will result in increased blooming artifacts from calcium and higher HU-values [28]. This can be corrected for by using a higher HU-threshold for defining calcium, for example 147 HU (instead of the conventional 130 HU) when using 100 kV which was proposed by Nakazato and colleagues [26,29]. However, others argue that this is incorrect since the Agatston score is a multi-threshold measurement with a 4-step weighting function, therefore each threshold should be adapted [30]. Besides the fixed tube voltage, there are other limitations of the coronary calcium score according to Agatston. Although extensively used, increasing evidence suggests that this score might be too simplistic as it does not account for the distribution of coronary calcium. Furthermore, the calcium score is based on the size and the density of coronary calcifications whereby an increased density results in a higher coronary calcium score. It therefore assumes that a higher density of the coronary calcium spots is associated with a higher risk. Differences in calcification pattern however have been associated with different clinical outcomes. For instance, calcifications with a higher density appear to be associated with lower cardiovascular disease risk [31]. Furthermore, a diffuse distribution of coronary calcium over multiple affected vessels has been associated with worse outcomes. Thus, information about calcification pattern has the potential to improve risk prediction [32,33].

While the value of the coronary calcium assessment for cardiovascular risk assessment is unquestionable, the method as described by Agatston seems to be outdated. There is need for an improved quantification method which takes into account differences between reconstruction algorithms, low tube voltage acquisitions and the density and distribution of coronary calcifications in order to improve accurate and precise cardiovascular risk assessment [34].

## Future of Pulmonary Nodule Assessment

Based on the favorable results of National Lung Screening Trial [35], lung cancer screening is advised by the United States Preventive Services Task Force while the European Society of Radiology and the European Respiratory Society also recommend lung cancer screening using low-dose CT at certified multidisciplinary medical centers [36,37]. Considering the high frequency with which small incidental pulmonary nodules are encountered, low dose accurate pulmonary nodule assessment and follow-up is very important. We have shown that reliable pulmonary nodule volumetry is possible at radiation dose levels of 0.6 mSv using hybrid iterative reconstruction [38], while fully model-based iterative reconstruction results in an underestimation of around 10% at this dose. Since several image-acquisition and reconstruction parameters can influence pulmonary nodule volumetry [39], recent guidelines advise to use similar techniques for follow-up examinations compared to the initial examination while at the same time using a low radiation dose [40]. When using model-based iterative reconstruction at both the initial and follow-up examination, pulmonary nodule volume underestimation might not be an issue anymore.

Currently solid tumors are often measured using the diameter. Response evaluation criteria in solid tumors (RECIST) are also based on diameters [41]. For pulmonary nodules it has been shown that volumetry is more reproducible than diameter measurements [42]. The current guidelines of the British Society of Radiology therefore advise to use volumetry [43]. They note however that there are differences between software packages in nodule volumetry which have to be addressed. The recent guidelines from the Fleischner Society are cautious regarding nodule volumetry due to the reported differences between software packages [40], but will provide a more extensive recommendation in a separate white paper expected in the near future.

Due to the expected rise in the number of chest CT acquisitions, computer-aided detection of pulmonary nodules might gain importance. In this thesis it was shown that computer-aided detection of pulmonary nodules has a high sensitivity, also at low radiation dose levels in combination with iterative reconstruction [44]. Computer-aided detection can be especially useful as a second reader, since it has been shown to detect pulmonary nodules that are missed by radiologists [45].

It is expected that submillisievert radiation dose levels will become the standard for lung cancer screening chest CT acquisitions and follow-up of pulmonary nodules, and iterative reconstruction will be an important tool to achieve this.

### Future of Iterative Reconstruction

CT iterative reconstruction has rapidly been adopted in the past few years. While the search term “iterative reconstruction” in combination with “computed tomography” in PubMed resulted in 71 publications in 2010, last year over 300 articles were published on this topic (*Figure 1*). Iterative reconstruction algorithms are increasingly used in routine clinical practice, and on the newest generation CT systems the option to use FBP is sometimes not available anymore. Advancements such as iterative reconstruction have contributed to the decrease in radiation dose associated with CT examinations over the past years. A study examining CT radiation dose between 2010 and 2015 in almost 80,000 patients reported a radiation dose reduction of 43% over the years in adult chest, abdomen and pelvis exams [46]. Although these results might not be applicable to every center, it is representative of the general trend in radiation dose reduction worldwide which has been seen in the past years.

Dose reduction is most important in children, who are 10 times more sensitive to the effects of ionizing radiation and have a longer lifetime to develop harmful effects of radiation exposure [47-49]. Although application of iterative reconstruction is therefore especially attractive for CT acquisitions in children, only a limited number of studies focused on children [50]. The Dutch regulations

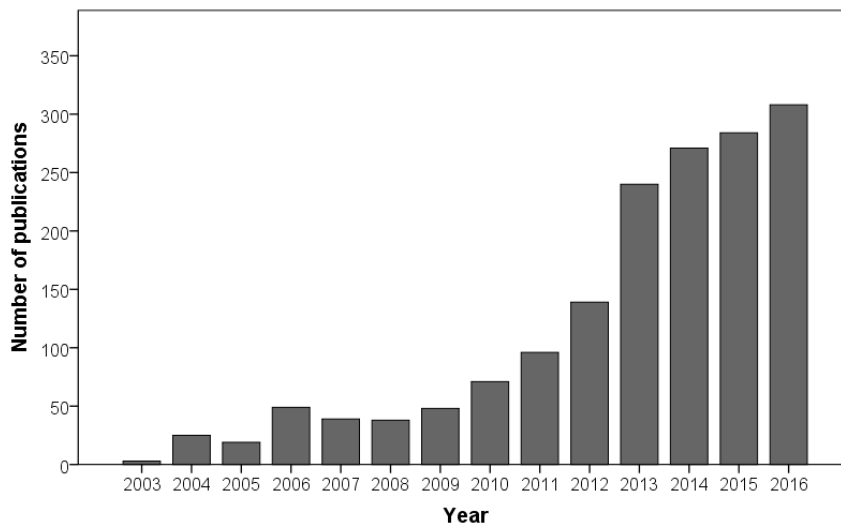


*Figure 1* – Number of studies in PubMed published over time when searching for “iterative reconstruction” combined with “computed tomography”

only allow non-therapeutic research in children when this is indispensable for the development of health care in children [51]. Since research on iterative reconstruction often requires additional acquisitions for research purpose without having a direct benefit for the study participant, it is more challenging to obtain approval of the ethical review board for this type of research in children. However, despite the advantage of reduced dose, two disadvantages of iterative reconstruction are commonly mentioned, namely prolonged reconstruction time and an artificial image appearance. To date, the additional reconstruction time of hybrid reconstruction is negligible [52], while this is in the order of several minutes for model-based iterative reconstruction [53]. Therefore, this limitation is no longer an issue. The second disadvantage is that iterative reconstruction results in a different image appearance. It takes time for a radiologist to become accustomed to this different image appearance. More important is the question if this affects the diagnostic power and if image-derived measurements are altered. In this thesis we have shown that the diagnostic power for CT assessment of urolithiasis is preserved with iterative reconstruction, as well as the sensitivity of pulmonary nodule detection. Although some studies have been performed, the literature on the diagnostic accuracy with iterative reconstruction remains scarce [54]. Results can differ between diagnostic tasks, and therefore task-based diagnostic accuracy evaluated is warranted. A good example of a study investigating the diagnostic accuracy of iterative reconstruction is the study performed by Moscariello and colleagues [55]. In this study, a full dose CCTA reconstructed with FBP was compared to a CCTA at half dose reconstructed with iterative reconstruction. The diagnostic accuracy of both acquisitions for stenosis detection was compared with invasive coronary angiography as the reference standard. The authors concluded that iterative reconstruction did not result in a loss of diagnostic information compared to FBP.

All major CT vendors developed their own iterative reconstruction algorithms. Since the exact working mechanism of those algorithms is proprietary information, results derived with a specific iterative reconstruction algorithm cannot directly be applied to other algorithms. It is important to be aware that different iterative reconstruction algorithms might have different effects on image quality and image-derived measurements. Therefore it is essential that quantitative measurements are validated for each iterative algorithm specifically before implementing this in clinical practice. Overall, the benefits of iterative reconstruction outweigh the disadvantages and one could even argue that it is unethical not to apply it in clinical practice.

### Replacement of conventional imaging by low dose CT

In the last part of this thesis the potential replacement of conventional chest radiography prior to cardiothoracic surgery by low dose CT was discussed. We are currently conducting a clinical trial in which patients are randomized between an additional low dose CT or conventional imaging only [56]. The aim of this trial is to assess if this affects the surgical procedure and complications after surgery. To date, over 400 patients have been included, and the additional low dose CT resulted in changes in clinical management in several patients. An example is shown in *Figure 2*, which shows the conventional chest radiograph in a 70-year old male on which no aortic calcifications were described.

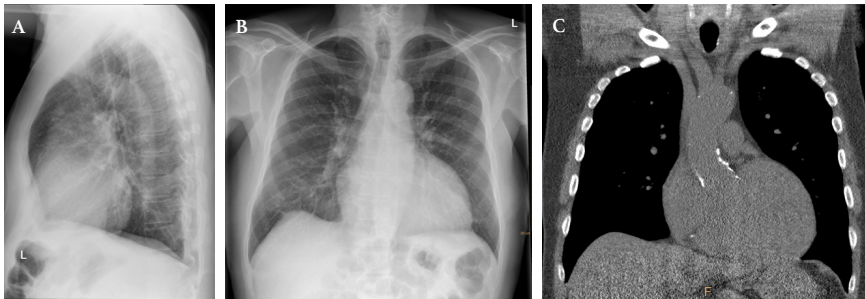


**Figure 2** – Conventional chest radiograph (left) and low dose CT (right) in a 70-year old male scheduled for coronary bypass surgery. The chest x-ray was made 9 days before the low dose CT. The CT showed calcifications in the ascending aorta which were not described on the chest radiograph. Based on those findings the surgeon decided to use a different cannulation site in an area free of calcifications. Scan parameters: tube voltage 80 kV, tube current 40 mAs, reconstruction with iDose level 3. Radiation dose: dose length product (DLP) 29.3 mGy\*cm, volumetric CT dose index (CTDIvol) 0.76 mGy, effective dose 0.43 mSv

The additional low dose chest CT for research purposes showed calcifications in the ascending aorta and based on those findings, a different aortic cannulation site was chosen. If replacement of conventional imaging by low dose CT can prevent postoperative complications, a routine preoperative chest CT might become cost-effective.

In patients suspected of pneumonia, the chest radiograph is often false-negative [57-59], while a CT is more sensitive [60,61]. Therefore, this might be another indication for replacement of the conventional chest radiograph by a low dose CT. A recent audit by the British Thoracic Society in 8,526 patients showed that

15% of patients coded as having pneumonia did not have pneumonia according to the international criteria [62]. Most of them (95%) did however receive antibiotic treatment. This reflects the difficulties with diagnosing pneumonia based on clinical symptoms and chest radiography. Several studies have investigated the role of CT for diagnosing pneumonia. At UMC Utrecht a study in patients with chemotherapy induced febrile neutropenia was performed, and an improved detection of pulmonary infiltrates with CT compared to chest radiography was reported [63]. Claessens and colleagues [64] performed an additional chest CT in 319 patients with a clinically suspected community-acquired pneumonia. CT findings markedly affected the diagnosis and clinical management such as the initiation (16%) or discontinuation (9%) of antibiotics. Several other studies on this topic are currently ongoing ([www.clinicaltrials.gov](http://www.clinicaltrials.gov), NCT03140163 & NCT02264483). Furthermore, UMC Utrecht initiated the CAP-NEXT study which is scheduled to start enrolling later this year. This study investigates whether a CT can help to diagnose community-acquired pneumonia in an earlier stage or to find a different diagnosis in order to reduce unnecessary use of antibiotics [65].

The associated radiation might not be a limiting factor for the use of CT anymore, with radiation dose levels approaching the radiation dose associated with conventional imaging [66-68]. However, since a CT is more than three times as expensive as conventional imaging, the cost-effectiveness of replacing conventional imaging with low dose CT for certain indications needs to be studied. Furthermore, a CT yields hundreds of images which have to be assessed and therefore requires more time for a radiologist to assess. Currently, a lot of research is performed in the field of machine-learning algorithms which is expected to eventually take over part of the workload of radiologists [69,70]. While computer-aided detection software is developed for a specific task, the goal of machine-learning algorithms is to detect if there is any abnormality in the image.

## Conclusion

CT iterative reconstruction is a powerful tool to substantially reduce patient radiation dose and is increasingly becoming embedded in routine clinical care. However, for each clinical indication the type and strength of the algorithm needs to be chosen with care to obtain accurate results with good image quality. We expect this will also lead to replacement of conventional imaging for specific indications.

## References

- [1] Greenland P, Alpert JS, Beller GA, et al., 2010 ACCF/AHA guideline for assessment of cardiovascular risk in asymptomatic adults: a report of the American College of Cardiology Foundation/American Heart Association Task Force on Practice Guidelines. *J Am Coll Cardiol* 2010;56(25):e50-103.
- [2] <http://www.robinsca.nl/>. ;Accessed 06/2017.
- [3] Georgiou D, Budoff MJ, Kaufer E, Kennedy JM, Lu B, Brundage BH, Screening patients with chest pain in the emergency department using electron beam tomography: a follow-up study. *J Am Coll Cardiol* 2001;38(1):105-10.
- [4] Greenland P, Bonow RO, Brundage BH, et al., ACCF/AHA 2007 clinical expert consensus document on coronary artery calcium scoring by computed tomography in global cardiovascular risk assessment and in evaluation of patients with chest pain: a report of the American College of Cardiology Foundation Clinical Expert Consensus Task Force (ACCF/AHA Writing Committee to Update the 2000 Expert Consensus Document on Electron Beam Computed Tomography) developed in collaboration with the Society of Atherosclerosis Imaging and Prevention and the Society of Cardiovascular Computed Tomography. *J Am Coll Cardiol* 2007;49(3):378-402.
- [5] Dedic A, Lubbers MM, Schaap J, et al., Coronary CT Angiography for Suspected ACS in the Era of High-Sensitivity Troponins: Randomized Multicenter Study. *J Am Coll Cardiol* 2016;67(1):16-26.
- [6] Hadamitzky M, Distler R, Meyer T, et al., Prognostic value of coronary computed tomographic angiography in comparison with calcium scoring and clinical risk scores. *Circ Cardiovasc Imaging* 2011;4(1):16-23.
- [7] Agatston AS, Janowitz WR, Hildner FJ, Zusmer NR, Viamonte M, Jr, Detrano R, Quantification of coronary artery calcium using ultrafast computed tomography. *J Am Coll Cardiol* 1990;15(4):827-32.
- [8] LaMonte MJ, FitzGerald SJ, Church TS, et al., Coronary artery calcium score and coronary heart disease events in a large cohort of asymptomatic men and women. *Am J Epidemiol* 2005;162(5):421-9.
- [9] Vliegenthart R, Oudkerk M, Hofman A, et al., Coronary calcification improves cardiovascular risk prediction in the elderly. *Circulation* 2005;112(4):572-7.
- [10] Kondos GT, Hoff JA, Sevrukov A, et al., Electron-beam tomography coronary artery calcium and cardiac events: a 37-month follow-up of 5635 initially asymptomatic low- to intermediate-risk adults. *Circulation* 2003;107(20):2571-6.
- [11] Arad Y, Goodman KJ, Roth M, Newstein D, Guerci AD, Coronary calcification, coronary disease risk factors, C-reactive protein, and atherosclerotic cardiovascular disease events: the St. Francis Heart Study. *J Am Coll Cardiol* 2005;46(1):158-65.

- [12] Taylor AJ, Bindeman J, Feuerstein I, Cao F, Brazaitis M, O'Malley PG, Coronary calcium independently predicts incident premature coronary heart disease over measured cardiovascular risk factors: mean three-year outcomes in the Prospective Army Coronary Calcium (PACC) project. *J Am Coll Cardiol* 2005;46(5):807-14.
- [13] Becker CR, Kleffel T, Crispin A, et al., Coronary artery calcium measurement: agreement of multirow detector and electron beam CT. *AJR Am J Roentgenol* 2001;176(5):1295-8.
- [14] McCollough CH, Ulzheimer S, Halliburton SS, Shanneik K, White RD, Kalender WA, Coronary artery calcium: a multi-institutional, multimanufacturer international standard for quantification at cardiac CT. *Radiology* 2007;243(2):527-38.
- [15] den Harder AM, Wolterink JM, Willeminck MJ, et al., Submillisievert coronary calcium quantification using model-based iterative reconstruction: A within-patient analysis. *Eur J Radiol* 2016;85(11):2152-9.
- [16] Szilveszter B, Elzomor H, Karolyi M, et al., The effect of iterative model reconstruction on coronary artery calcium quantification. *Int J Cardiovasc Imaging* 2016;32(1):153-60.
- [17] Hecht HS, de Siqueira ME, Cham M, et al., Low- vs. standard-dose coronary artery calcium scanning. *Eur Heart J Cardiovasc Imaging* 2015;16(4):358-63.
- [18] Obmann VC, Klink T, Heverhagen JT, et al., Impact of Hybrid Iterative Reconstruction on Agatston Coronary Artery Calcium Scores in Comparison to Filtered Back Projection in Native Cardiac CT. *Rofo* 2015;187(5):372-9.
- [19] van Osch JA, Mouden M, van Dalen JA, et al., Influence of iterative image reconstruction on CT-based calcium score measurements. *Int J Cardiovasc Imaging* 2014;30(5):961-7.
- [20] Caruso D, De Cecco CN, Schoepf UJ, et al., Correction Factors for CT Coronary Artery Calcium Scoring Using Advanced Modeled Iterative Reconstruction Instead of Filtered Back Projection. *Acad Radiol* 2016;23(12):1480-9.
- [21] den Harder AM, Willeminck MJ, Bleys RL, et al., Dose reduction for coronary calcium scoring with hybrid and model-based iterative reconstruction: an ex vivo study. *Int J Cardiovasc Imaging* 2014;30(6):1125-33.
- [22] Rutten A, Isgum I, Prokop M, Coronary calcification: effect of small variation of scan starting position on Agatston, volume, and mass scores. *Radiology* 2008;246(1):90-8.
- [23] Dijkstra H, Greuter MJ, Groen JM, et al., Coronary calcium mass scores measured by identical 64-slice MDCT scanners are comparable: a cardiac phantom study. *Int J Cardiovasc Imaging* 2010;26(1):89-98.
- [24] Ulzheimer S, Kalender WA, Assessment of calcium scoring performance in cardiac computed tomography. *Eur Radiol* 2003;13(3):484-97.

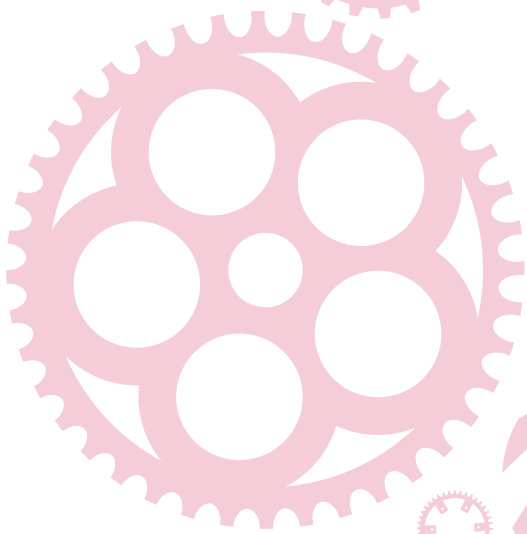
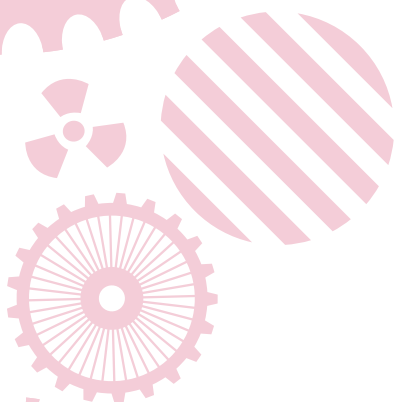
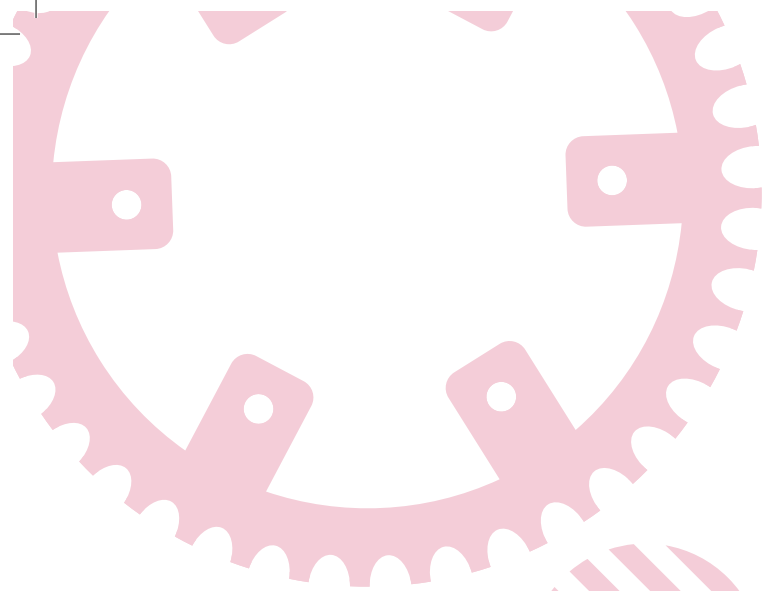
- [25] Wolterink JM, Leiner T, Viergever MA, Isgum I, Generative Adversarial Networks for Noise Reduction in Low-Dose CT. *IEEE Trans Med Imaging* 2017.
- [26] Nakazato R, Dey D, Gutstein A, et al., Coronary artery calcium scoring using a reduced tube voltage and radiation dose protocol with dual-source computed tomography. *J Cardiovasc Comput Tomogr* 2009;3(6):394-400.
- [27] Gunn ML, Kohr JR, State of the art: technologies for computed tomography dose reduction. *Emerg Radiol* 2010;17(3):209-18.
- [28] McQuiston AD, Muscogiuri G, Schoepf UJ, et al., Approaches to ultra-low radiation dose coronary artery calcium scoring based on 3rd generation dual-source CT: A phantom study. *Eur J Radiol* 2016;85(1):39-47.
- [29] Marwan M, Mettin C, Pflederer T, et al., Very low-dose coronary artery calcium scanning with high-pitch spiral acquisition mode: comparison between 120-kV and 100-kV tube voltage protocols. *J Cardiovasc Comput Tomogr* 2013;7(1):32-8.
- [30] Deprez FC, Vlassenbroek A, Ghaye B, Raaijmakers R, Coche E, Controversies about effects of low-kilovoltage MDCT acquisition on Agatston calcium scoring. *J Cardiovasc Comput Tomogr* 2013;7(1):58-61.
- [31] Criqui MH, Denenberg JO, Ix JH, et al., Calcium density of coronary artery plaque and risk of incident cardiovascular events. *JAMA* 2014;311(3):271-8.
- [32] Blaha MJ, Budoff MJ, Tota-Maharaj R, et al., Improving the CAC Score by Addition of Regional Measures of Calcium Distribution: Multi-Ethnic Study of Atherosclerosis. *JACC Cardiovasc Imaging* 2016;9(12):1407-16.
- [33] Tota-Maharaj R, Al-Mallah MH, Nasir K, Qureshi WT, Blumenthal RS, Blaha MJ, Improving the relationship between coronary artery calcium score and coronary plaque burden: addition of regional measures of coronary artery calcium distribution. *Atherosclerosis* 2015;238(1):126-31.
- [34] Berman DS, Arnson Y, Rozanski A, Coronary Artery Calcium Scanning: The Agatston Score and Beyond. *JACC Cardiovasc Imaging* 2016;9(12):1417-9.
- [35] Prosch H, Implementation of lung cancer screening: promises and hurdles. *Transl Lung Cancer Res* 2014;3(5):286-90.
- [36] Kauczor HU, Bonomo L, Gaga M, et al., ESR/ERS white paper on lung cancer screening. *Eur Radiol* 2015.
- [37] Moyer VA, U.S. Preventive Services Task Force, Screening for lung cancer: U.S. Preventive Services Task Force recommendation statement. *Ann Intern Med* 2014;160(5):330-8.
- [38] den Harder AM, Willeminck MJ, van Hamersvelt RW, et al., Pulmonary Nodule Volumetry at Different Low Computed Tomography Radiation Dose Levels With Hybrid and Model-Based Iterative Reconstruction: A Within Patient Analysis. *J Comput Assist Tomogr* 2016;40(4):578-83.

- [39] Hochhegger B, Marchiori E, Alves GR, Guimaraes MD, Irion K, Influences in CT scan lung nodule volumetry. *Chest* 2014;146(2):e69-70.
- [40] MacMahon H, Naidich DP, Goo JM, et al., Guidelines for Management of Incidental Pulmonary Nodules Detected on CT Images: From the Fleischner Society 2017. *Radiology* 2017;161659.
- [41] van Persijn van Meerten EL, Gelderblom H, Bloem JL, RECIST revised: implications for the radiologist. A review article on the modified RECIST guideline. *Eur Radiol* 2010;20(6):1456-67.
- [42] Hein PA, Romano VC, Rogalla P, et al., Linear and volume measurements of pulmonary nodules at different CT dose levels - intrascan and interscan analysis. *Rofo* 2009;181(1):24-31.
- [43] Callister ME, Baldwin DR, Akram AR, et al., British Thoracic Society guidelines for the investigation and management of pulmonary nodules. *Thorax* 2015;70 Suppl 2:iii-ii54.
- [44] den Harder AM, Willeminck MJ, van Hamersvelt RW, et al., Effect of radiation dose reduction and iterative reconstruction on computer-aided detection of pulmonary nodules: Intra-individual comparison. *European Journal of Radiology* 2016;85:346-351.
- [45] Liang M, Tang W, Xu DM, et al., Low-Dose CT Screening for Lung Cancer: Computer-aided Detection of Missed Lung Cancers. *Radiology* 2016;281(1):279-88.
- [46] Kovacs WC, Yao J, Bluemke DA, Folio LR, Opportunities to Reduce CT Radiation Exposure, Experience Over 5 Years at the NIH Clinical Center. *Radiat Prot Dosimetry* 2017.
- [47] Brenner DJ, Hall EJ, Computed tomography--an increasing source of radiation exposure. *N Engl J Med* 2007;357(22):2277-84.
- [48] ICRP, Khong PL, Ringertz H, et al., ICRP publication 121: radiological protection in paediatric diagnostic and interventional radiology. *Ann ICRP* 2013;42(2):1-63.
- [49] Sun Z, Ng KH, Sarji SA, Is utilisation of computed tomography justified in clinical practice? Part IV: applications of paediatric computed tomography. *Singapore Med J* 2010;51(6):457-63.
- [50] den Harder AM, Willeminck MJ, Budde RP, Schilham AM, Leiner T, de Jong PA, Hybrid and model-based iterative reconstruction techniques for pediatric CT. *AJR Am J Roentgenol* 2015;204(3):645-53.
- [51] Visser HK, Medical research in children: the pros and cons of extending the legal boundaries. *Ned Tijdschr Geneeskd* 2010;154:A2395.
- [52] Willeminck MJ, Schilham AM, Leiner T, Mali WP, de Jong PA, Budde RP, Iterative reconstruction does not substantially delay CT imaging in an emergency setting. *Insights Imaging* 2013;4(3):391-7.
- [53] Yuki H, Oda S, Utsunomiya D, et al., Clinical impact of model-based type iterative reconstruction with fast reconstruction time on image quality of low-dose screening chest CT. *Acta Radiol* 2016;57(3):295-302.

## Chapter 5.2

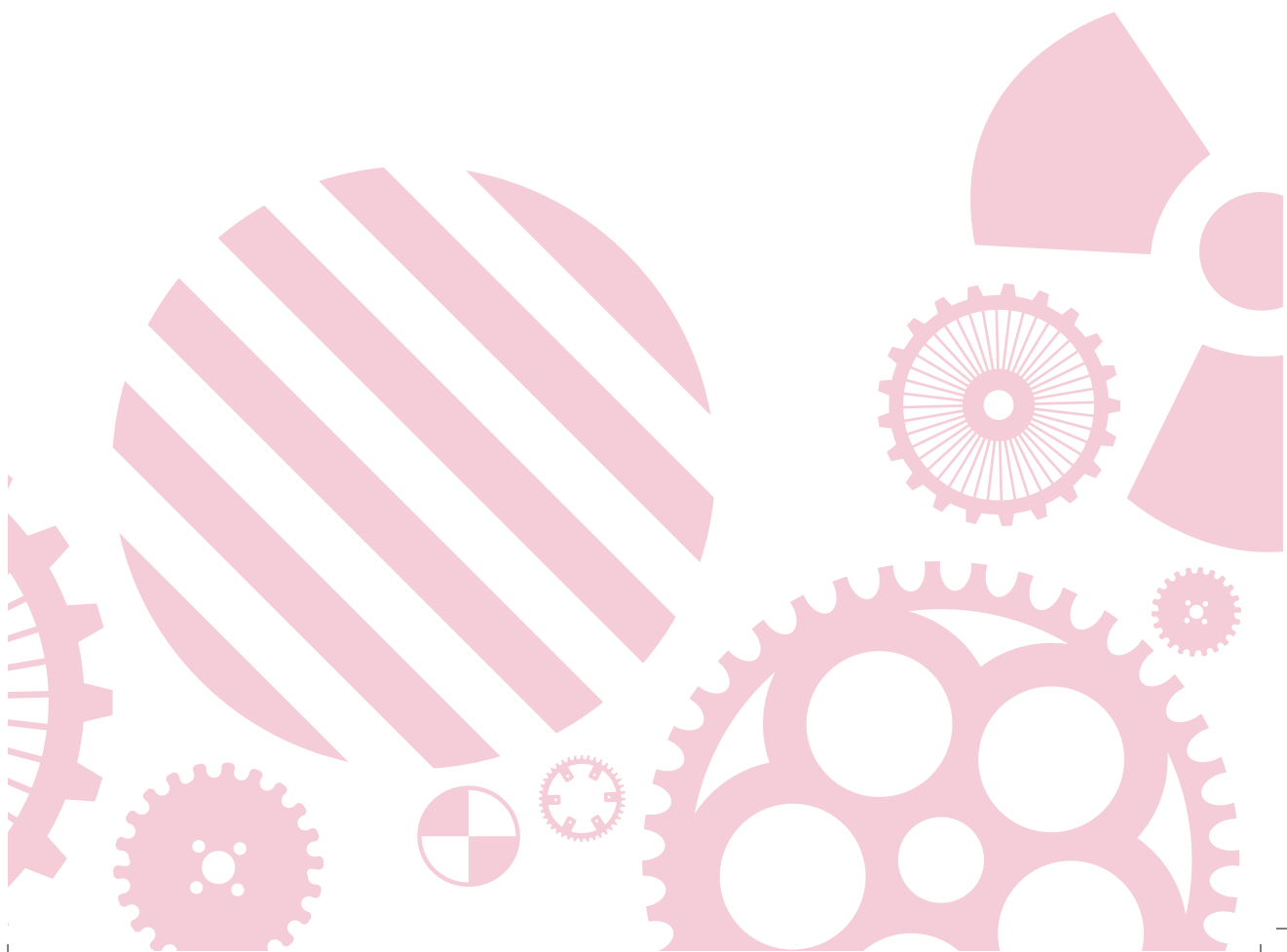
- [54] den Harder AM, Willeminck MJ, de Ruiter QM, et al., Achievable dose reduction using iterative reconstruction for chest computed tomography: A systematic review. *Eur J Radiol* 2015;84(11):2307-13.
- [55] Moscariello A., Takx R.A.P., Schoepf U.J., et al., Coronary CT angiography: Image quality, diagnostic accuracy, and potential for radiation dose reduction using a novel iterative image reconstruction technique-comparison with traditional filtered back projection. *Eur Radiol* 2011;21(10):2130-8.
- [56] den Harder AM, de Heer LM, Maurovich-Horvat P, et al., Ultra low-dose chest ct with iterative reconstructions as an alternative to conventional chest x-ray prior to heart surgery (CRICKET study): Rationale and design of a multicenter randomized trial. *J Cardiovasc Comput Tomogr* 2016;10(3):242-5.
- [57] Hagaman JT, Rouan GW, Shipley RT, Panos RJ, Admission chest radiograph lacks sensitivity in the diagnosis of community-acquired pneumonia. *Am J Med Sci* 2009;337(4):236-40.
- [58] Maughan BC, Asselin N, Carey JL, Sucov A, Valente JH, False-negative chest radiographs in emergency department diagnosis of pneumonia. *R I Med J* (2013) 2014;97(8):20-3.
- [59] Cereser L, Zuiani C, Graziani G, et al., Impact of clinical data on chest radiography sensitivity in detecting pulmonary abnormalities in immunocompromised patients with suspected pneumonia. *Radiol Med* 2010;115(2):205-14.
- [60] Self WH, Courtney DM, McNaughton CD, Wunderink RG, Kline JA, High discordance of chest x-ray and computed tomography for detection of pulmonary opacities in ED patients: implications for diagnosing pneumonia. *Am J Emerg Med* 2013;31(2):401-5.
- [61] Hayden GE, Wrenn KW, Chest radiograph vs. computed tomography scan in the evaluation for pneumonia. *J Emerg Med* 2009;36(3):266-70.
- [62] Daniel P, Bewick T, Welham S, Mckeever TM, Lim WS, British Thoracic Society, Adults miscoded and misdiagnosed as having pneumonia: results from the British Thoracic Society pneumonia audit. *Thorax* 2017;72(4):376-9.
- [63] Gerritsen MG, Willeminck MJ, Pompe E, et al., Improving early diagnosis of pulmonary infections in patients with febrile neutropenia using low-dose chest computed tomography. *PLoS One* 2017;12(2):e0172256.
- [64] Claessens YE, Debray MP, Tubach F, et al., Early Chest Computed Tomography Scan to Assist Diagnosis and Guide Treatment Decision for Suspected Community-acquired Pneumonia. *Am J Respir Crit Care Med* 2015;192(8):974-82.
- [65] CAP-NEXT: DiagNostic intervention study of low-dose CT and MultipleX PCR on antibiotic Treatment and outcome of Community-Acquired Pneumonia. (Accessed May 2017).
- [66] Willeminck MJ, de Jong PA, Pediatric chest computed tomography at a radiation dose approaching a chest radiograph. *Am J Respir Crit Care Med* 2013;188(5):626-7.

- [67] Newell JD, Jr, Fuld MK, Allmendinger T, et al., Very low-dose (0.15 mGy) chest CT protocols using the COPDGene 2 test object and a third-generation dual-source CT scanner with corresponding third-generation iterative reconstruction software. *Invest Radiol* 2015;50(1):40-5.
- [68] Lee SW, Kim Y, Shim SS, et al., Image quality assessment of ultra low-dose chest CT using sinogram-affirmed iterative reconstruction. *Eur Radiol* 2014;24(4):817-26.
- [69] Kruskal JB, Berkowitz S, Geis JR, Kim W, Nagy P, Dreyer K, Big Data and Machine Learning-Strategies for Driving This Bus: A Summary of the 2016 Intersociety Summer Conference. *J Am Coll Radiol* 2017.
- [70] Wong KKL, Wang L, Wang D, Recent developments in machine learning for medical imaging applications. *Comput Med Imaging Graph* 2017;57:1-3.



# Dutch summary

*(Nederlandse samenvatting)*



Computer tomografie (CT) is een 3D methode waarmee heel snel overall in het lichaam gekeken kan worden zonder de huid te openen. CT speelt daarom een belangrijke rol in het vaststellen van ziekte (diagnose) en het meten of een behandeling wel of niet aanslaat. De afgelopen decennia is het aantal CT-scans dat per jaar wordt gemaakt enorm toegenomen. In het jaar 1991 waren dit 400.000 CT-scans in Nederland, terwijl dit in 2014 1,4 miljoen bedroeg [1]. Bij het maken van een CT-scan wordt de patiënt blootgesteld aan mogelijk schadelijke röntgenstraling [2-4]. Een CT-scan wordt daarom alleen gemaakt wanneer dit medisch gezien noodzakelijk is [5]. Tevens dient de hoeveelheid röntgenstraling die wordt toegediend zo laag mogelijk gehouden te worden [6]. Een lagere hoeveelheid röntgenstraling resulteert echter ook in een slechtere beeldkwaliteit. Daarom dient de balans tussen een zo laag mogelijke hoeveelheid röntgenstraling maar toch voldoende beeldkwaliteit om de diagnose te kunnen stellen te worden gezocht.

Diverse technische ontwikkelingen hebben het mogelijk gemaakt om de stralingsdosis te verlagen [7]. Één van deze technieken is een ingewikkeld wiskundig algoritme dat iteratieve reconstructie wordt genoemd [8]. Om de data die geproduceerd worden door een CT-scanner om te zetten in beelden, is altijd een reconstructietechniek nodig. Een veelgebruikte, relatief eenvoudige, reconstructietechniek is filtered back projection (FBP). FBP kan echter minder goed overweg met de ruizige data die wordt verkregen als de stralingsdosis wordt verlaagd. Iteratieve reconstructie is een meer ingewikkelde methode die al in de jaren '70 werd beschreven [9]. Lange tijd was toepassing van iteratieve reconstructie echter niet mogelijk door een gebrek aan rekenkracht van de CT-hardware. Door de verbeterde rekenkracht was het mogelijk om in 2009 de eerste iteratieve reconstructie algoritmes op de markt te brengen [8]. Alle grote CT-fabrikanten hebben inmiddels één of meerdere iteratieve reconstructie algoritmes op de markt gebracht. Deze algoritmes kunnen worden onderverdeeld in hybride en model-gestuurde algoritmes. Hybride iteratieve reconstructie is een mengvorm van FBP en iteratieve reconstructie. Model-gestuurde algoritmes zijn meer geavanceerd dan hybride algoritmes, waardoor hier potentieel meer dosisreductie haalbaar mee is [10]. Verschillende fantoomstudies (onderzoek in namaakorganen of lichaamsdelen) hebben aangetoond dat het mogelijk is om de stralingsdosis te verlagen zonder dat de beeldkwaliteit wordt aangetast door iteratieve reconstructie toe te passen [10]. Het doel van dit proefschrift was de kansen en uitdagingen rondom het invoeren van iteratieve reconstructie in de patiëntenzorg te onderzoeken.

*Deel I: Invoeren van iteratieve reconstructie bij CT-scans van het hart*

**Hoofdstuk 1.1** geeft een literatuuroverzicht van de tot nu toe behaalde resultaten met iteratieve reconstructies bij CT-scans van het hart. De resultaten van 10 studies zijn hierbij samengenomen. Hieruit bleek dat de stralingsdosis met 48% kan worden verminderd door gebruik te maken van iteratieve reconstructie. **Hoofdstuk 1.2 – 1.4** beschrijft onderzoek naar de kalkscore in de kransslagaders. Deze score wordt bepaald door het maken van een scan van het hart zonder contrast en geeft weer hoeveel kalk zich in de kransslagaders bevindt. De kalkscore kan gebruikt worden om het risico op hart- en vaatziekten te voorspellen. In **hoofdstuk 1.2** wordt een studie beschreven waarbij 15 menselijke harten buiten het lichaam in een fantoom dat lijkt op de menselijke borstkast worden gescand. Ieder hart werd vier keer gescand, op een steeds lagere stralingsdosis. Uit deze studie bleek dat met iteratieve reconstructie de beeldkwaliteit verbetert. Bij het gebruik van meer geavanceerde model-gestuurde iteratieve reconstructie wordt de kalkscore echter onderschat. In **hoofdstuk 1.3 en 1.4** wordt een groep van 30 patiënten beschreven die naast de scan met een normale dosis ook drie scans kregen waarbij de stralingsdosis met 40%, 60% en 80% werd verlaagd. Met de conventionele reconstructietechniek, FBP, was er zoveel ruis dat een aantal scans niet meer te beoordelen waren op 60% en 80% verlaagde dosis, terwijl dit wel mogelijk was met iteratieve reconstructie. Ook bij deze studie zorgde model-gestuurde iteratieve reconstructie voor een onderschatting van de kalkscore. Hybride iteratieve reconstructie kan echter wel veilig worden gebruikt in de patiëntenzorg met een verlaagde stralingsdosis.

*Deel II: Invoeren van iteratieve reconstructie bij CT-scans van de longen en de buik*

In **hoofdstuk 2.1** wordt een literatuuroverzicht gegeven van de studies naar iteratieve reconstructie van CT-scans van de longen. Op basis van 24 studies wordt geconcludeerd dat de stralingsdosis gehalveerd kan worden voor CT-scans van de longen waarbij contrast wordt toegediend en met 72% indien er geen contrast wordt toegediend. Een veelvoorkomende reden voor het maken van een CT-scan van de longen is de aanwezigheid van longnodules. Een longnodule is een klein gebiedje (vlekje) van weefsel in de longen. Dit kan komen door een infectie, maar het kan ook kwaadaardig zijn. Om te beoordelen of deze longnodules groeien, wordt het volume van de longnodule gemeten. **Hoofdstuk 2.2** beschrijft of het verlagen van de stralingsdosis en het gebruik van iteratieve reconstructie deze meting beïnvloedt. Hieruit blijkt dat dosisreductie en hybride iteratieve reconstructie het meten van het volume van longnodules

niet verstoren. Echter treedt er bij het gebruik van model-gestuurde iteratieve reconstructie een onderschatting op van het volume.

Specifieke software kan de radioloog helpen om longnodules op te sporen. **Hoofdstuk 2.3** beschrijft het effect van dosisreductie en iteratieve reconstructie op de nauwkeurigheid van deze software. Hieruit blijkt dat op alle dosislevels en met alle reconstructietechnieken de longnodules goed kunnen worden opgespoord met de software. Wel zorgt met name model-gestuurde iteratieve reconstructie voor een toename van het aantal fout-positieve bevindingen (de computer vindt dingen geen nodule blijken te zijn) op lage dosis met de software. **Hoofdstuk 2.4** beschrijft de invloed van iteratieve reconstructie op het meten van de hoeveelheid kalk in de grote lichaamsslagader en op de hartklep tussen het hart en de grote lichaamsslagader (aortaklep). Met iteratieve reconstructie wordt de beeldkwaliteit verbeterd en kan het kalk nauwkeurig worden gemeten. **Hoofdstuk 2.5** focust op de stralingsdosis van CT-scans bij patiënten met nierstenen. Hierbij worden 20 patiënten gescand op normale dosis en op 40%, 60% en 80% verlaagde stralingsdosis. Op de scan met een 80% lagere stralingsdosis werden, met de conventionele reconstructietechniek FBP, de helft van de nierstenen gemist terwijl deze wel zichtbaar waren bij gebruik van model-gestuurde iteratieve reconstructie. Het beoordelen van eventuele andere oorzaken van buikpijn was mogelijk met 40% en 60% verlaagde dosis, maar niet op het laagste dosislevel.

### *Deel III: Invoeren van iteratieve reconstructie bij CT-scans van kinderen*

**Hoofdstuk 3.1** laat verschillende voorbeelden zien van FBP en iteratieve reconstructie. Tevens wordt een overzicht van de literatuur over iteratieve reconstructie bij CT-scans van kinderen getoond. De meeste studies worden echter uitgevoerd in volwassenen, waardoor het nog onduidelijk is met hoeveel de stralingsdosis verlaagd kan worden in kinderen door gebruik te maken van iteratieve reconstructie. **Hoofdstuk 3.2** beschrijft de resultaten van een fantoomstudie die gedaan is met verschillende stents die vaak gebruikt worden bij de behandeling van kinderen met een vernauwde lichaamsslagader (coarctatio aorta). Deze stent is een metalen buisje wat in de lichaamsslagader wordt geplaatst om deze te verwijden en open te houden. Hieruit blijkt dat de stralingsdosis voor deze indicatie verlaagd kan worden met 81% zonder dat de beeldkwaliteit wordt aangetast.

*Deel IV: CT voorafgaand aan een hartoperatie*

Deel 1 – 3 van dit proefschrift hebben we laten zien dat de stralingsdosis aanzienlijk verlaagd kan worden door gebruik te maken van iteratieve reconstructie. Als de stralingsdosis geen belemmering meer vormt, kunnen 2D röntgenfoto's, zoals een longfoto, voor sommige indicaties mogelijk vervangen worden door een 3D CT-scan met een lage stralingsdosis. Daarom wordt in deel 4 onderzocht of de longfoto die standaard wordt gemaakt voor een hartoperatie vervangen kan worden door een lage dosis CT-scan. **Hoofdstuk 4.1** beschrijft hoe vaak er afwijkingen worden gezien op de longfoto voorafgaand aan een hartoperatie. Hiervoor werd onderzoek gedaan in 1.136 patiënten, waarbij bij de helft één of meerdere afwijkingen op de longfoto werden beschreven. Echter, deze afwijkingen hadden zelden gevolgen voor het beleid. Slechts in 1 patiënt (0.1%) werd de operatie aangepast. In 15 patiënten (1.3%) vond verder onderzoek plaats zonder dat het invloed had op de geplande hartoperatie. Eén van de afwijkingen die regelmatig werd beschreven op de longfoto is de verdenking op COPD, een chronisch obstructieve longziekte. **Hoofdstuk 4.2** beschrijft in hoeverre het mogelijk is om milde COPD te herkennen op een longfoto. Dit blijkt zeer moeilijk te zijn waarbij veel patiënten ten onrechte de diagnose COPD krijgen.

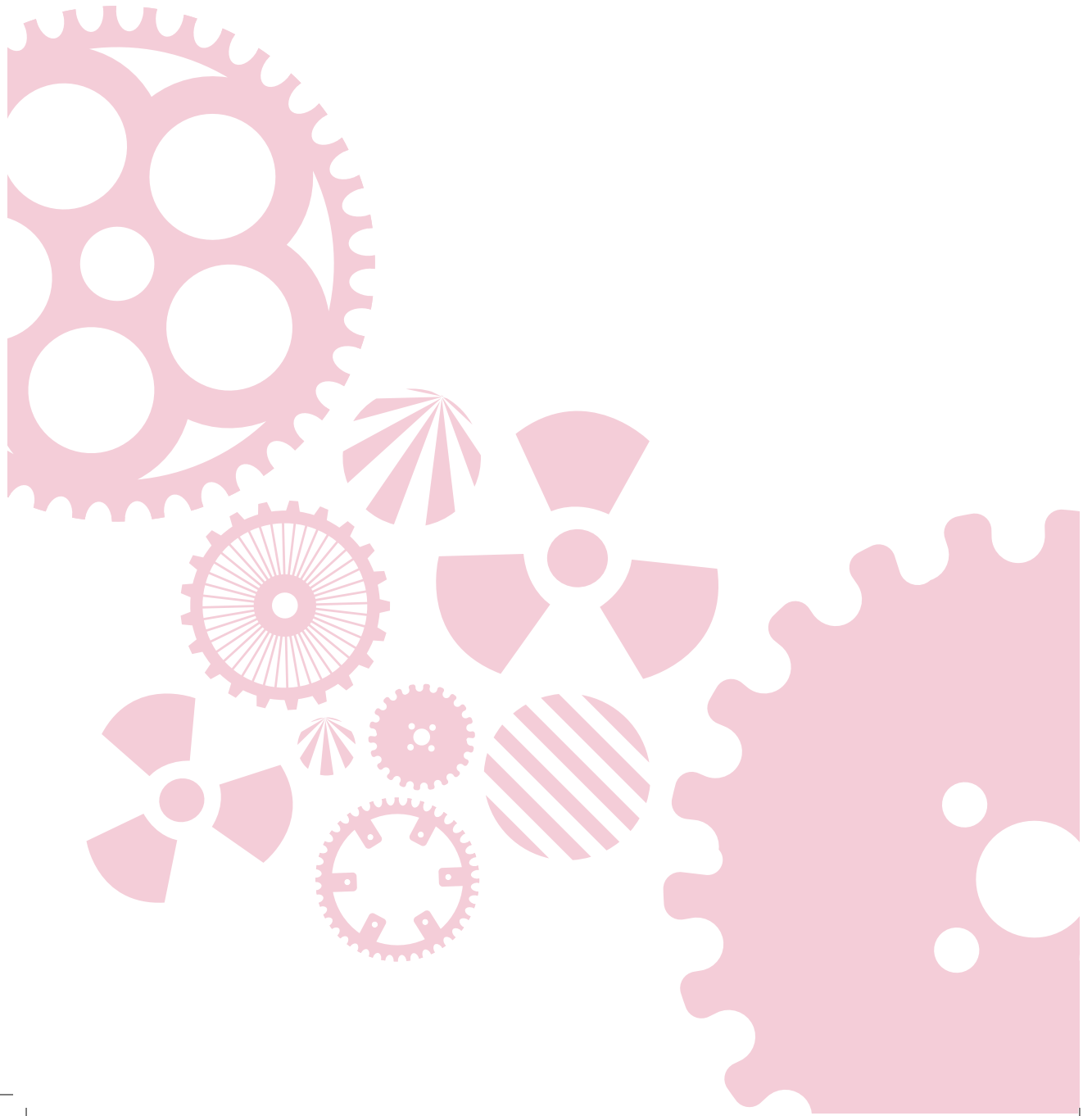
Een CT-scan voorafgaand aan hartchirurgie kan verschillende voordelen bieden ten opzichte van een longfoto. Op een CT-scan kan kalk in de grote lichaamsslagader duidelijk worden afgebeeld terwijl dit op een longfoto soms moeilijk te zien is. Kalk in de grote lichaamsslagader zorgt voor een hoger risico tijdens de operatie. Tijdens de hartoperatie wordt vaak gebruik gemaakt van een hart-long machine om de pompfunctie van het hart tijdelijk over te nemen. Om deze aan te sluiten wordt er een klem op de grote lichaamsslagader gezet. Indien er zich kalk in de grote lichaamsslagader bevindt, kan dit ervoor zorgen dat kleine stukjes kalk loslaten van de wand. Deze kalkstukjes kunnen met het bloed naar de hersenen schieten waardoor ze een herseninfarct kunnen veroorzaken. Indien de chirurg voor de operatie weet waar dit kalk zich bevindt, kan hier rekening mee worden gehouden tijdens de operatie. In **hoofdstuk 4.3** wordt samengevat wat er op dit moment bekend is over dit onderwerp. Uit de literatuur blijkt dat het aantal herseninfarcten met 77 – 96% kan worden verminderd door gebruik te maken van een CT-scan in plaats van

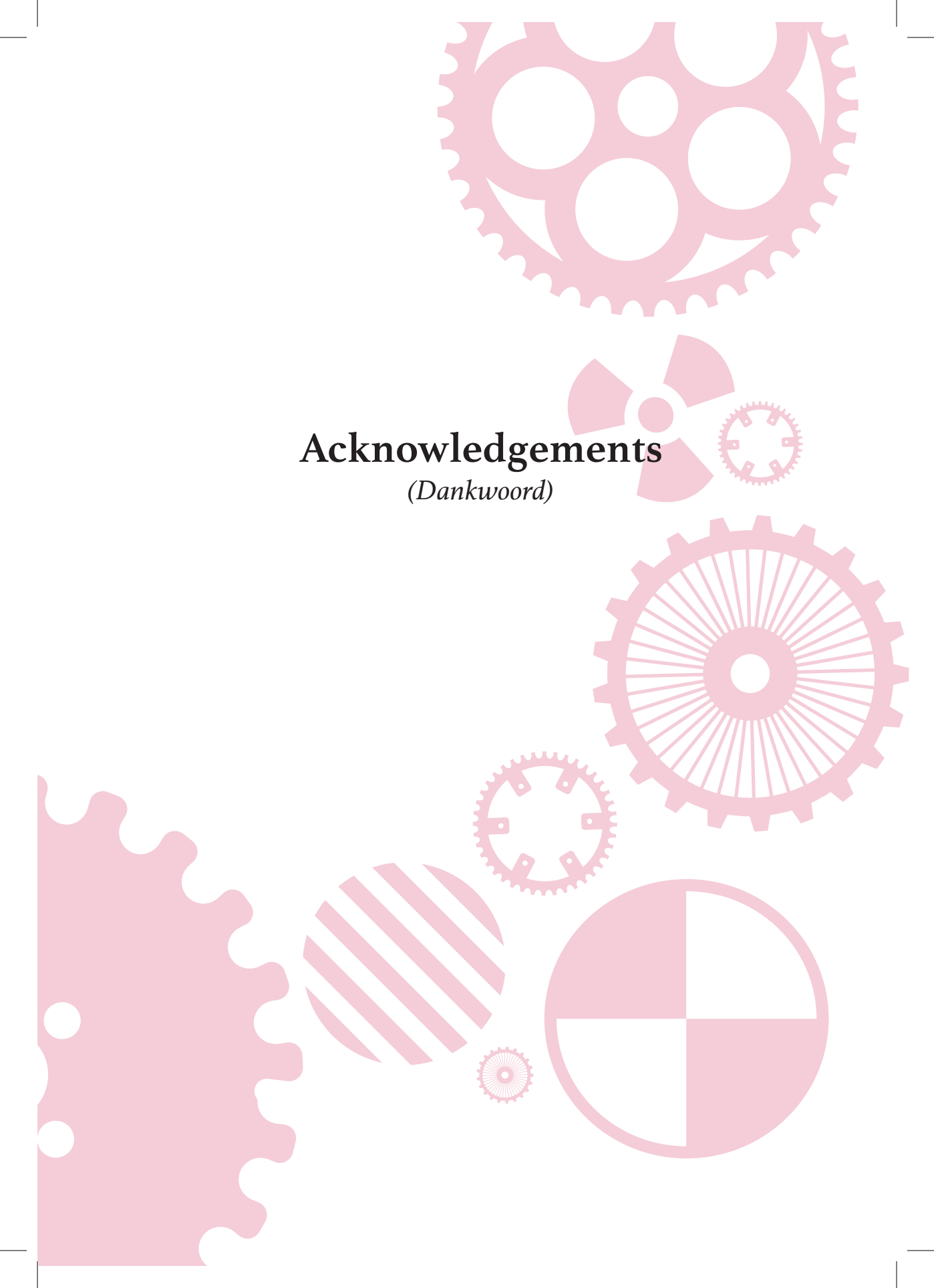
## Dutch summary

een longfoto voor de hartoperatie. De kwaliteit van de studies is echter matig waarbij er kleine patiëntengroepen zijn bestudeerd zonder gebruik te maken van randomisatie. Bij randomisatie krijgen patiënten op basis van loting wel of geen CT-scan. Hierdoor ontstaat een gelijke verdeling tussen beide groepen. In **hoofdstuk 4.4** wordt daarom het design van een gerandomiseerde studie met voldoende patiënten aantallen beschreven. Deze studie is op dit moment bezig waarbij er al meer dan 400 patiënten meedoen.

## Referenties

- [1] Rijksinstituut voor Volksgezondheid en Milieu (RIVM), Trends in het aantal CT-onderzoeken. ;2017/03/28.
- [2] Brenner DJ, Hall EJ, Computed tomography--an increasing source of radiation exposure. *N Engl J Med* 2007;357(22):2277-84.
- [3] Smith-Bindman R, Lipson J, Marcus R, et al., Radiation dose associated with common computed tomography examinations and the associated lifetime attributable risk of cancer. *Arch Intern Med* 2009;169(22):2078-86.
- [4] Berrington de Gonzalez A, Mahesh M, Kim KP, et al., Projected cancer risks from computed tomographic scans performed in the United States in 2007. *Arch Intern Med* 2009;169(22):2071-7.
- [5] Malone J, Guleria R, Craven C, et al., Justification of diagnostic medical exposures: some practical issues. Report of an International Atomic Energy Agency Consultation. *Br J Radiol* 2012;85(1013):523-38.
- [6] Frush DP, Applegate K, Computed tomography and radiation: understanding the issues. *J Am Coll Radiol* 2004;1(2):113-9.
- [7] Lell MM, Wildberger JE, Alkadhi H, Damilakis J, Kachelriess M, Evolution in Computed Tomography: The Battle for Speed and Dose. *Invest Radiol* 2015;50(9):629-44.
- [8] Willemink MJ, de Jong PA, Leiner T, et al., Iterative reconstruction techniques for computed tomography Part 1: technical principles. *Eur Radiol* 2013;23(6):1623-31.
- [9] Fleischmann D., Boas F.E., Computed tomography-old ideas and new technology. *Eur Radiol* 2011;21(3):510-7.
- [10] Willemink MJ, Leiner T, de Jong PA, et al., Iterative reconstruction techniques for computed tomography part 2: initial results in dose reduction and image quality. *Eur Radiol* 2013;23(6):1632-42.





# Acknowledgements

*(Dankwoord)*

## Dutch summary

Veel mensen hebben de afgelopen jaren bijgedragen aan de totstandkoming van dit proefschrift. Ik wil iedereen hiervoor hartelijk bedanken, en een aantal mensen in het bijzonder noemen.

Professor dr. Leiner, beste Tim, heel hartelijk dank voor je begeleiding de afgelopen jaren. Bedankt voor de vrijheid die ik kreeg in het uitvoeren van projecten en de sturing die je daarbij gaf. Door je enthousiasme en uitgebreide kennis ontstonden er steeds weer nieuwe ideeën voor onderzoek. Ook wil ik je graag bedanken voor de mogelijkheden die ik kreeg voor het bezoeken van congressen. Mijn presentatieskills zijn hierdoor een stuk verbeterd!

Professor dr. de Jong, beste Pim, ondanks je overvolle agenda stond je deur altijd open. Ik heb veel van je geleerd over zowel de geschreven als de ongeschreven regels bij het uitvoeren van onderzoek. Je bent een voorbeeld wat betreft snel, efficiënt maar ook grondig werken. Ook de samenwerking bij het begeleiden van studenten heb ik als zeer prettig ervaren.

Dr. Budde, beste Ricardo, dank voor je begeleiding, vooral rondom de CRICKET studie. Jij leerde mij om vol te houden als het trager ging dan ik zou willen. Ondanks dat je tijdens mijn promotie naar het Erasmus Medisch Centrum vertrok, bleef de samenwerking goed en leidde dit juist tot nieuwe samenwerkingsverbanden.

Graag wil ik de leden van de leescommissie bedanken voor de beoordeling van dit proefschrift: professor dr. Velthuis, professor dr. Suyker, professor dr. Lammers, professor dr. van der Schouw en professor dr. Krestin.

Martin Willeminck, zonder jou was ik nooit bij de radiologie terecht gekomen. Je maakte mij als student enthousiast voor het doen van onderzoek en ik werd hierdoor uiteindelijk je collega. Naast het doen van veel mooie projecten wist jij ook altijd precies wanneer welke congressen waren, wat resulteerde in interessante en gezellige congresbezoeken. Helaas ging dit soms ten koste van je Uber-rating, maar er zijn ergere dingen in het leven. Robbert van Hamersvelt, je bent een gezellige collega en het was fijn om een promovendus op hetzelfde onderzoeksgebied te hebben om mee te sparren. Niels van der Werf, het is fijn dat jij het cardiac CT-team bent komen versterken en het was leuk om je beter te leren kennen in Washington. Jelmer Wolterink and Ivana Isgúm, thank you for your collaboration in several research projects, especially the UPOD-

imaging project. Arnold Schilham, dank voor je technische input tijdens de iDose meetings en je nuttige commentaar op de manuscripten. Martijn Gondrie, Sander Snoek, Pieter Jan van Doormaal en Frank Wessels, bedankt voor het meedenken en scoren bij diverse onderzoeksprojecten. Dominika Suchá, bedankt voor je hulp bij de stent fantoomprojecten. Alle radiologen en arts-assistenten die geholpen hebben bij het superviseren van CT-scans voor de CRICKET studie, heel hartelijk bedankt.

Professor dr. Suyker en Linda de Heer, hartelijk dank voor de fijne samenwerking. Zonder jullie was het laatste deel van dit proefschrift niet tot stand gekomen. Ondanks jullie volle OK-programma maakten jullie altijd tijd om mee te denken over gezamenlijk onderzoek tussen de radiologie en de hartchirurgie. Ook wil ik graag het planningssecretariaat van de CTC bedanken voor de talloze studie-enveloppen die jullie hebben verstuurd. Hans Breur, je ben altijd enthousiast voor nieuwe projecten op het gebied van coarctatio aorta en door de goede samenwerking resulteerde dit uiteindelijk in diverse mooie papers. Imo Höfer, Mark de Groot, Saskia Haitjema en Wouter Veldhuis bedankt voor de fijne samenwerking in het UPOD-imaging team en de mooie projecten die hieruit voortgekomen zijn.

Julien Milles, thank you for your input during the iDose meetings and your collaboration in several projects. I also want to thank Walter Giepmans, Franca de Brouwer and Peter van de Riet for the pleasant cooperation with Philips Healthcare.

Sara Boccalini, it was nice to work with you on the aortic coarctation project in which your extensive clinical knowledge was very useful. We still have to run a race together someday. Laurens Swart, bedankt voor je hulp bij het opzetten van de CRICKET studie in Rotterdam. Professor Bogers en professor Krestin, bedankt voor de hulp bij het initiëren van de CRICKET studie in Rotterdam.

Dr. Pál Maurovich-Horvat, thank you for the participation of the Semmelweis center in the CRICKET study and your hospitality during my visits to Budapest. I would also like to thank Júlia Karady, Bálint Szilveszter, Kálmán Benke, Cao Chun, Zoltán Szabolcs, István Hartyánszky, Barabás Imre, Simon Judit and Sarolta Borzsák for their contributions to the CRICKET study.

## Dutch summary

Martijn Boomsma, bedankt voor de fijne samenwerking bij het emfyseemproject. Helaas kwam de CRICKET niet van de grond, maar hopelijk volgen er nog meer mooie samenwerkingsprojecten tussen Utrecht en Zwolle.

Graag wil ik de CT-laboranten bedanken voor de hulp bij het maken van talloze CT-scans voor de Circle2 studie en CRICKET studie. In het bijzonder Karin Thijn, Robert Valkenburg, Anne Manders en Nils van Veen. Het trialbureau, in het bijzonder Shanta Kalaykhan, Anneke Hamersma, Saskia van Amelsvoort en Cees Haaring, dank voor jullie onmisbare ondersteuning. Het secretariaat, in het bijzonder Marja Kool en Carin Marcus, bedankt voor jullie hulp. Tevens wil ik graag het technisch cluster (in het bijzonder Rudy van der Lek) en de multimedia bedanken. Roy Sanders, bedankt voor je hulp bij de vormgeving van het proefschrift.

Bjorn Blomberg, Esther Pompe, Remko Kockelkoren en Anouk Eikendal, bedankt voor de fijne tijd die we samen hebben gehad. Remko en Esther, graag wil ik jullie in het bijzonder bedanken voor de hulp bij de CRICKET studie als ik niet in huis was. Dhabia al Samarrai, Josanne de Maar, Caren van Roekel, Margot Reinders, Bianca den Dekker, Ludwike van Kalmthout en Frans Kouw, het is gezellig dat jullie de afdeling zijn komen versterken. Ik hoop dat ik na mijn vertrek nog steeds welkom ben op de “pannenkoekenparties”.

Wieke Haakma, met jou is het altijd gezellig op het werk. Van selfies bij de koffiecorner tot het uitzoeken van hoe je plaatjes in de mail plakt, ik ga het missen. Bedankt dat je mijn paranimf wilt zijn.

De Stockholmers, Lily, Joey, Bart, Bob en Matthijs, hopelijk kunnen we binnenkort de naam van de groep weer veranderen. Hoewel we inmiddels over het hele land verspreid zijn is het altijd gezellig om elkaar weer te zien! Marissa, ondanks dat we in sommige dingen totaal verschillend zijn kunnen we het goed met elkaar vinden. Ik hoop dat mijn outfit jouw kritische blik kan doorstaan. Lucia, vanaf het begin van de studie kennen we elkaar al. Het is altijd leuk om weer bij te kletsen.

Lily, we kenden elkaar eigenlijk nog niet zo heel lang toen we besloten om een coschap te gaan lopen in Afrika maar het klikte meteen. Wie weet krijgen we onze aanhang nog eens zover om terug te gaan. Dankjewel dat je mijn paranimf wilt zijn, hopelijk zonder tutu.

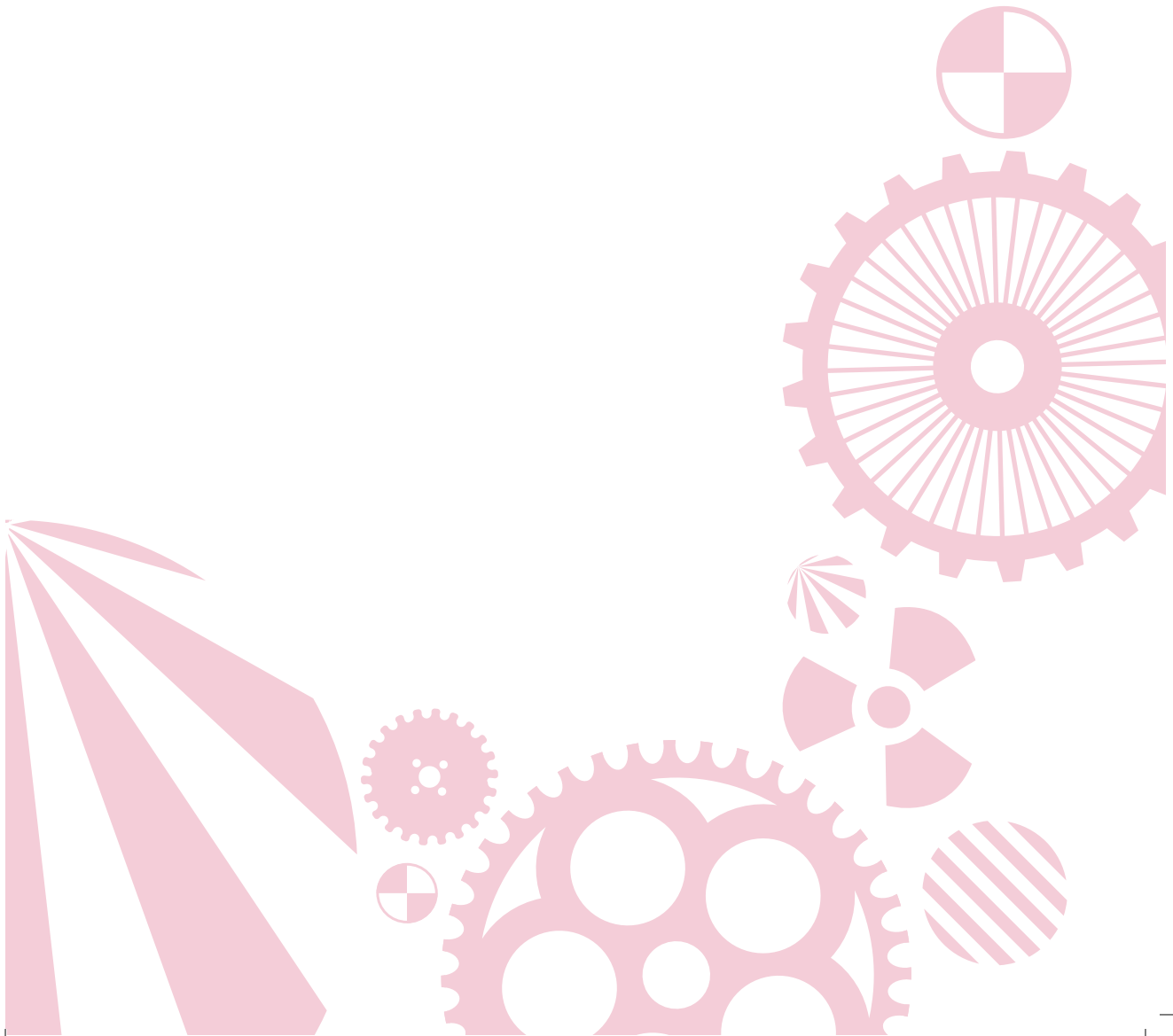
Eva en Irene, echte A-vrienden. Jullie staan garant voor ontspanning op de dinsdagavond. Ik hoop dat we elkaar nog regelmatig blijven zien zonder al te veel paashaas-incidenten.

Niek, het is een eer dat je speciaal voor de verdediging naar Nederland komt. Ik zal extra mijn best doen. Willemijn, hartelijk dank voor je hulp bij het ontwerp van dit proefschrift. Ik ben er trots op. Elsbeth, hard op weg om ook een medicus te worden. Wie weet versla ik je nog eens bij de Sylvestercross. Lieneke, het is altijd gezellig om je weer te zien. Ik houd van je droge humor. Papa en mama, hartelijk dank voor de ondersteuning en ik hoop dat het na het lezen van de samenvatting van dit boekje wat duidelijker is wat ik al die jaren heb gedaan.

Matthijs, ik ontmoette jou een paar maanden voordat ik aan mijn promotie avontuur begon. Je maakte alle ups en downs mee en steunde mij onvoorwaardelijk. Ook was het erg gezellig dat je mee ging op de intercontinentale congressen (je wist het goed uit te kiezen). Ik hoop dat we nog lang van elkaar kunnen genieten.



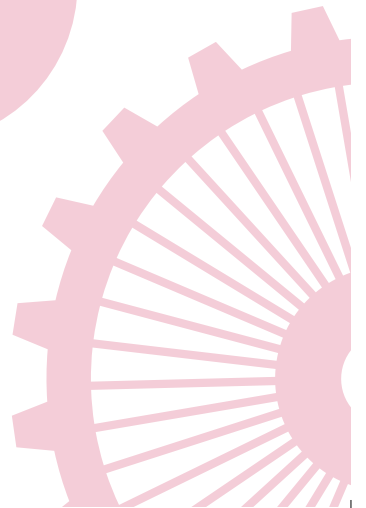
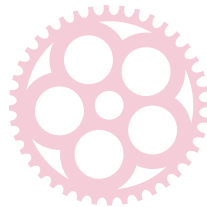
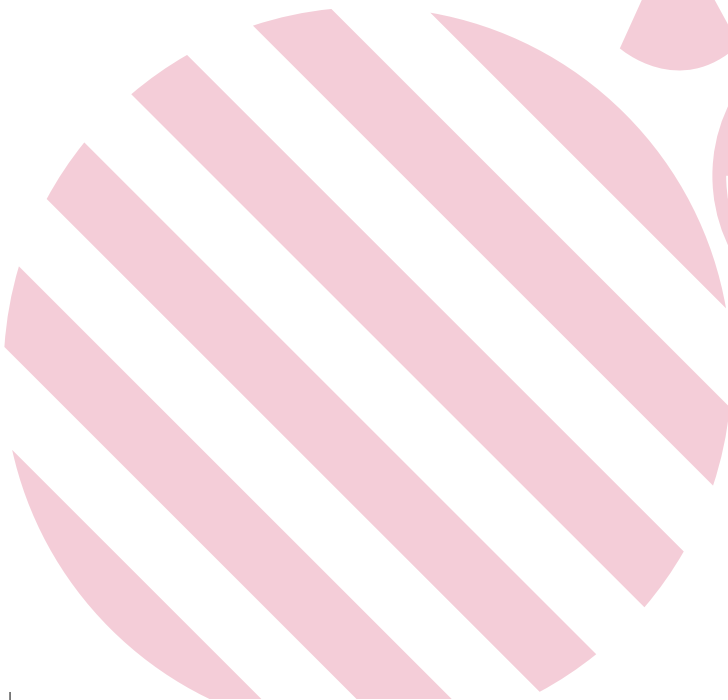
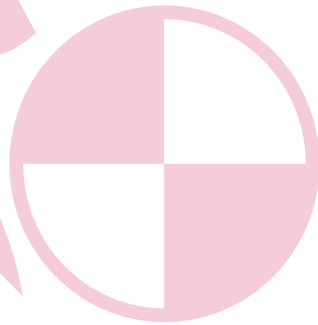
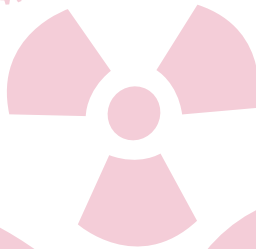
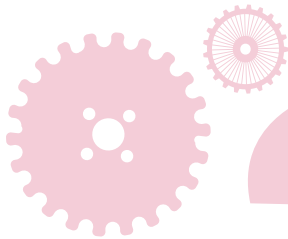
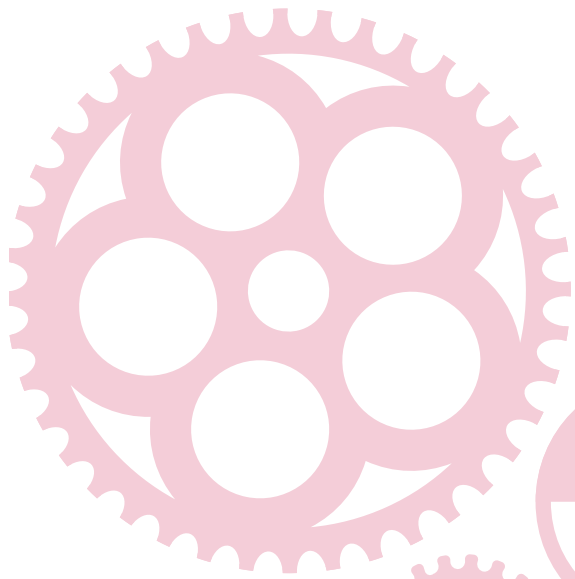
# Curriculum Vitae



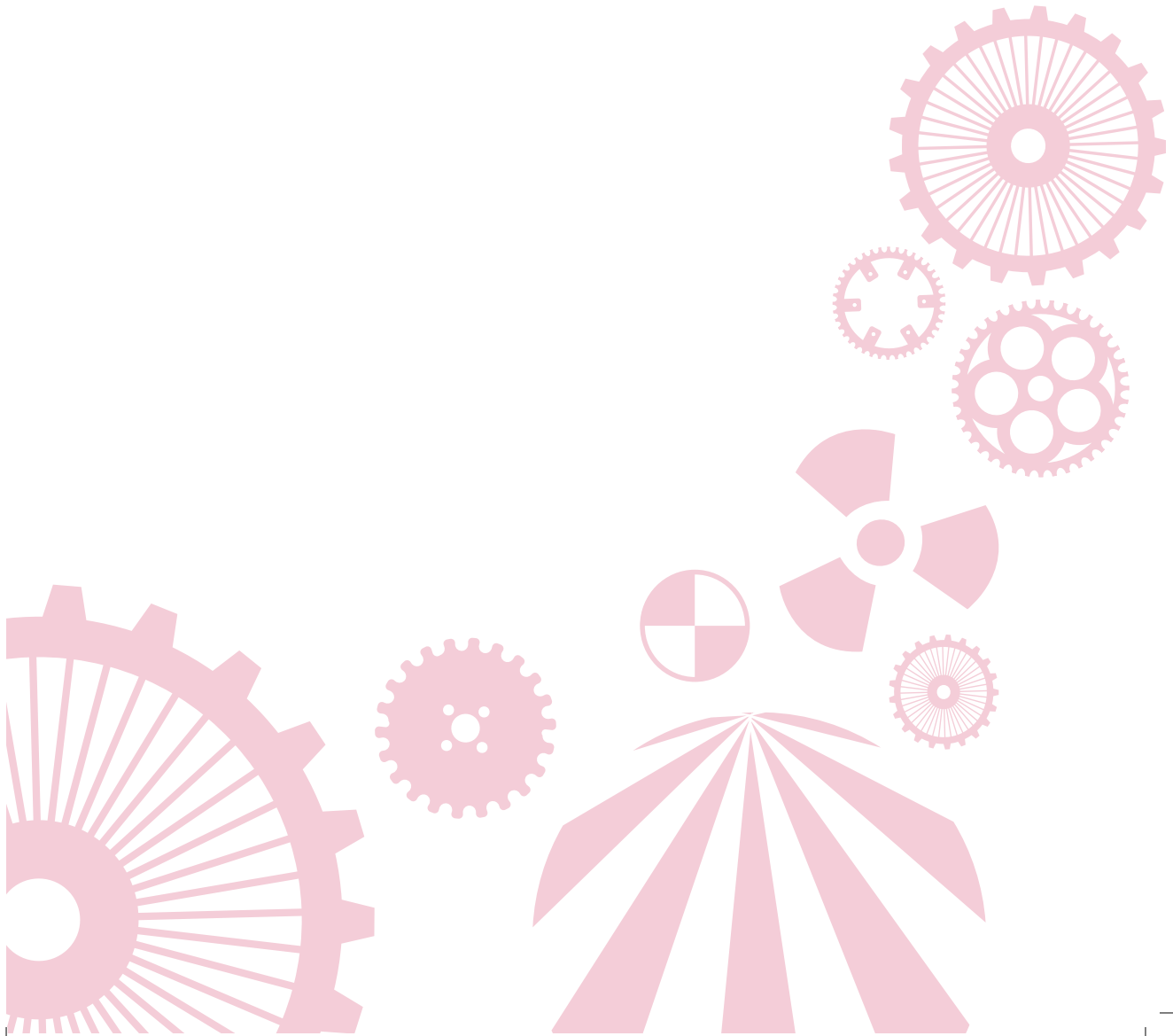




Annemarie den Harder was born on December 12, 1990 in Ouderkerk aan de Amstel, The Netherlands. In 2008, she obtained her pre-university education degree. That same year she started medical school at the University of Utrecht. During the master years of her study she performed research at the Department of Radiotherapy in the context of the Masters Honors Program. After receiving her medical degree in May 2014, she started her PhD at the Department of Radiology of the University Medical Center Utrecht (UMCU). Her research focused on low dose computed tomography imaging under supervision of professor Tim Leiner (UMCU), professor Pim de Jong (UMCU) and dr. Ricardo Budde (Erasmus Medical Center). During her PhD she followed the postgraduate Master's program in Clinical Epidemiology and was member of the Medical Imaging PhD Candidates Council. In November 2017 she will start as a hospitalist in training at the Jeroen Bosch Hospital under supervision of dr. Paetrick Netten.



# List of publications



### Publications in international journals

Boccalini S, **den Harder AM**, Witsenburg M, Breur JPMJ, Krestin GP, van Beynum IM, Stagnaro N, Marasini M, de Jong PA, Leiner T, Budde RPJ. Complications after Stent Placement for Aortic Coarctation: a Pictorial Essay of CT Angiography. *J Thorac Imaging* 2017 (in press)

**den Harder AM**, Bangert F, van Hamersvelt RW, Leiner T, Milles J, Schilham AMR, Willemink MJ, de Jong PA. The Effects of Iodine Attenuation on Pulmonary Nodule Volumetry using Novel Dual-Layer Computed Tomography Reconstructions. *Eur Radiol* 2017 Jul 10

**den Harder AM**, Willemink MJ, van Doormaal PJ, Wessels FJ, Lock MTWT, Schilham AMR, Budde RPJ, Leiner T, de Jong PA. Radiation dose reduction for CT assessment of urolithiasis using iterative reconstruction: a prospective intra-individual study. *Eur Radiol* 2017 Jul 4

**den Harder AM**, Snoek AM, Leiner T, Suyker WJ, de Heer LM, Budde RPJ, Lammers JJ, de Jong PA, Gondrie MJA. Can routine chest radiography be used to diagnose mild COPD? *Eur J Radiol* 2017 Jul;92:159-165

Jacob KA, Rozemeijer R, **den Harder AM**, Suyker WJ. Aortic homograft replacement in a patient with a circumferential porcelain aorta: A case report. *J Thorac Cardiovasc Surg* 2017 Aug;154(2):409-411

**den Harder AM**, Suchá D, van Doormaal PJ, Budde RPJ, de Jong PA, Schilham AMR, Breur JMPJ, Leiner T. Radiation dose reduction in pediatric great vessel stent computed tomography using iterative reconstruction: A phantom study. *PLoS One* 2017 Apr 14;12(4):e0175714

van Hamersvelt RW, Schilham AMR, Engelke K, **den Harder AM**, de Keizer B, Verhaar HJ, Leiner T, de Jong PA, Willemink MJ. Accuracy of bone mineral density quantification using dual-layer spectral detector CT: a phantom study. *Eur Radiol* 2017 Apr 3

**den Harder AM**, Suchá D, van Hamersvelt RW, Budde RPJ, de Jong PA, Schilham AMR, Bos C, Breur JMPJ, Leiner T. Imaging of pediatric great vessel stents: computed tomography or magnetic resonance imaging? *PLoS One* 2017 Jan 31;12(1):e0171138

**den Harder AM**, Wolterink JM, Willemink MJ, Schilham AMR, de Jong PA, Budde RPJ, Nathoe HM, Išgum I, Leiner T. Submillisievert coronary calcium quantification using model-based iterative reconstruction: a within patient analysis. *Eur J Radiol* 2016 Nov;85(11):2152-2159

van Hamersvelt RW, **den Harder AM**, Willemink MJ, Schilham AMR, Lammers JJ, Nathoe HM, Budde RPJ, Leiner T, de Jong PA. Aortic Valve and Thoracic Aortic Calcification Measurements: How Low Can We Go in Radiation Dose? *J Comput Assist Tomogr* 2017 Jan;41(1):148-155

**den Harder AM**, Willemink MJ, van Hamersvelt RW, Vonken EP, Schilham AMR, Lammers JJ, Luijk B, Budde RPJ, Leiner T, de Jong PA. Pulmonary Nodule Volumetry at Different Low Computed Tomography Radiation Dose Levels With Hybrid and Model-Based Iterative Reconstruction: A Within Patient Analysis. *J Comput Assist Tomogr* 2016 Jul-Aug;40(4):578-83

**den Harder AM**, de Heer LM, Meijer RC, Das M, Krestin GP, Maessen JG, Bogers AJ, de Jong PA, Leiner T, Budde RP. Effect of computed tomography before cardiac surgery on surgical strategy, mortality and stroke. *Eur J Radiol* 2016 Apr;85(4):744-50

**den Harder AM**, Willemink MJ, de Jong PA, Schilham AMR, Rajiah P, Takx RAP, Leiner T. New horizons in cardiac CT. *Clin Radiol* 2016 Feb 27. pii: S0009-9260(16)00044-1

**den Harder AM**, de Heer LM, de Jong PA, Leiner T, Budde RPJ, on behalf of the CRICKET investigators Ultra low-dose chest ct with iterative reconstructions as an alternative to conventional chest x-ray prior to heart surgery (CRICKET study): Rationale and design of a multicenter randomized trial. *J Cardiovasc Comput Tomogr* 2016 Jan 30

**den Harder AM**, Willemink MJ, van Hamersvelt RW, Vonken EJ, Milles J, Schilham AMR, Lammers JW, de Jong PA, Leiner T. Effect of radiation dose reduction and iterative reconstruction on computer-aided detection of pulmonary nodules: Intra-individual comparison. *Eur J Radiol* 2016 Feb;85(2):346-51

**den Harder AM**, Willemink MJ, de Ruiters QM, de Jong PA, Schilham AMR, Krestin GP, Leiner T, Budde RPJ. Dose reduction with iterative reconstruction for coronary CT angiography: a systematic review and meta-analysis. *Br J Radiol* 2016;89(1058):20150068

## List of publications

**den Harder AM**, Frijlingh M, Ravesloot CJ, Oosterbaan AE, van der Gijp A. The Importance of Human-Computer Interaction in Radiology E-learning. *J Digit Imaging* 2016 Apr;29(2):195-205

Willemink MJ, **den Harder AM**, Foppen W, Schilham AMR, Rienks R, Laufer EM, Nieman K, de Jong PA, Budde RPJ, Nathoe HM, Leiner T. Finding the optimal dose reduction and iterative reconstruction level for coronary calcium scoring. *J Cardiovasc Comput Tomogr* 2016 Jan-Feb;10(1):69-75

**den Harder AM**, Willemink MJ, de Ruiter QM, Schilham AMR, Krestin GP, Leiner T, de Jong PA, Budde RPJ. Achievable dose reduction using iterative reconstruction for chest computed tomography: A systematic review. *Eur J Radiol* 2015 Nov;84(11):2307-13

Willemink MJ, Abramiuc B, **den Harder AM**, van der Werf NR, de Jong PA, Budde RPJ, Wildberger JE, Vliegenthart R, Willems TP, Greuter MJ, Leiner T. Coronary calcium scores are systematically underestimated at a large chest size: A multivendor phantom study. *J Cardiovasc Comput Tomogr* 2015 Sep-Oct;9(5):415-21

**den Harder AM**, Willemink MJ, Budde RPJ, Schilham AMR, Leiner T, de Jong P. Hybrid and model-based iterative reconstruction for pediatric computed tomography. *AJR Am J Roentgenol* 2015 Mar;204(3):645-53

Burbach JPM, **den Harder AM**, Intven M, van Vulpen M, Verkooijen HM, Reerink O. Impact of radiotherapy boost on pathological complete response in patients with locally advanced rectal cancer: a systematic review and meta-analysis. *Radiother Oncol* 2014;30:S0167-8140

**den Harder AM**, Willemink MJ, Bleys RLAW, de Jong PA, Budde RPJ, Schilham AMR, Leiner T. Dose reduction for coronary calcium scoring with hybrid and model-based iterative reconstruction: an ex vivo study. *Int J Cardiovasc Imaging* 2014;30(6):1125-33

**den Harder AM**, van Gils GH, Kotte ANTJ, van Vulpen M, Lips IM. The effect of magnesium oxide on interfraction prostate motion and the amount of rectal filling during prostate cancer radiotherapy: analysis of a double blind placebo-controlled randomized clinical trial. *Strahlenther Onkol* 2014;190(8):776

### **Publications in national journals**

**den Harder AM**, Willemink MJ, de Jong PA, Budde RPJ, Schilham AMR, Leiner T. Nooit durven vragen ...: Wat is iteratieve reconstructie? *Imago 2015 (Augustus)*

Willemink MJ, **den Harder AM**, de Jong PA, Leiner T. De toekomst van de CT-scan: Vervangt CT de conventionele rontgendiagnostiek? *Ned Tijdschr Geneesk 2014;158(0)A7438*

### **Book chapter**

**den Harder AM**, Schilham AMR, Willemink MJ. CT of the Heart, Chapter Image Reconstruction (*expected in 2018*)

### **Conference presentations**

**den Harder AM**, Wolterink JM, de Jong PA, de Groot MCH, Isgum I, Veldhuis WB, Haitjema S, Hoefler IE, Leiner T. Towards understanding the role of the hematological system in the pathophysiology of coronary calcifications: A cohort study. *Annual meeting Society of Cardiovascular Computed Tomography, Washington, United States, July 2017 (oral presentation)*

**den Harder AM**, Willemink MJ, van Doormaal PJ, Wessels FJ, Lock MTWT, Schilham AMR, Budde RPJ, Leiner T, de Jong PA. Radiation dose reduction for CT assessment of urolithiasis using iterative reconstruction: a prospective intra-individual study. *Radiologendagen, Rotterdam, The Netherlands, May 2017 (oral presentation)*

**den Harder AM**, de Heer LM, de Jong PA, Suyker WJ, Leiner T, Budde RPJ. Incidence of abnormal findings on routine chest radiography before cardiac surgery: a routine clinical care study. *Radiologendagen, Rotterdam, The Netherlands, May 2017 (oral presentation)*

**den Harder AM**, Snoek AM, Leiner T, Suyker WJ, de Heer LM, Budde RPJ, Lammers JWJ, de Jong PA, Gondrie MJA. Can routine chest radiography be used to diagnose mild COPD? A nested case-control study. *Radiologendagen, Rotterdam, The Netherlands, May 2017 (oral presentation)*

## List of publications

**den Harder AM**, Snoek AM, Leiner T, Suyker WJ, de Heer LM, Budde RPJ, Lammers JWJ, de Jong PA, Gondrie MJA. Use of chest radiography for diagnosing mild COPD. *Scientific Meeting European Society of Thoracic Imaging, Krakow, Poland, October 2016 (oral presentation)*

**den Harder AM**, de Heer LM, de Jong PA, Suyker WJ, Leiner T, Budde RPJ. Value of routine chest x-ray before cardiac surgery. *Scientific Meeting European Society of Cardiac Radiology, Krakow, Poland, October 2016 (oral presentation)*

**den Harder AM**, Wolterink JM, Willemink MJ, Schilham AMR, de Jong PA, Budde RPJ, Nathoe HM, Isgum I, Leiner T. Low-dose coronary calcium scoring with model-based iterative reconstruction. *Annual meeting Society of Cardiovascular Computed Tomography, Orlando, United States, June 2016 (poster presentation)*

**den Harder AM**, Willemink MJ, van Hamersvelt RW, Vonken EJ, Schilham AMR, Lammers JW, Budde RPJ, Leiner T, de Jong PA. Influence of computed tomography dose reduction and iterative reconstruction on pulmonary nodule volumetry. *European Congress of Radiology, Vienna, Austria, March 2016 (oral presentation)*

**den Harder AM**, Wolterink JM, Willemink MJ, Schilham AMR, de Jong PA, Budde RPJ, Nathoe HM, Isgum I, Leiner T. Submillisievert coronary calcium quantification using model-based iterative reconstruction: a within-patient analysis. *Netherlands Heart Days, Piscadera Bay, Curacao, January 2016, (oral presentation)*

**den Harder AM**, Suchá D, Martens JPJ, van Hamersvelt RW, Schilham AMR, Bos C, Budde RPJ, Breur JMPJ, Leiner T. Pediatric aortic stents: which modality is best for follow-up imaging? A phantom study. *Netherlands Heart Days, Piscadera Bay, Curacao, January 2016, (poster presentation)*

**den Harder AM**. Gaat CT de conventionele radiodiagnostiek vervangen? *Nederlandse Vereniging Medische Beeldvorming en Radiotherapie Voorjaarscongres, Leeuwarden, The Netherlands, April 2015 (oral presentation)*

**den Harder AM**, Willemink MJ, Foppen W, Schilham AMR, Budde RPJ, de Jong PA, Leiner T. Achievable dose reduction for coronary calcium scoring with iterative reconstruction. *European Congress of Radiology, Vienna, Austria, March 2015 (poster presentation)*

**den Harder AM**, Willemink MJ, de Ruiters QMB, de Jong PA, Schilham AMR, Leiner T, Budde RPJ. Dose reduction with iterative reconstruction for cardiac computed tomography angiography: a systematic review and meta-analysis. *European Congress of Radiology, Vienna, Austria, March 2015 (oral presentation)*

**den Harder AM**, Suchá D, Breur JMPJ, Martens J, Budde RPJ, Bos C, Leiner T. Reliability and agreement of pediatric stent diameter measurements with computed tomography. *Scientific Meeting European Society of Cardiac Radiology, Paris, France, October 2014 (poster presentation)*

**den Harder AM**, Willemink MJ, Bleys RL, de Jong PA, Budde RPJ, Schilham AMR, Leiner T. Dose reduction for coronary calcium scoring with iterative reconstruction. *European Congress of Radiology, Vienna, Austria, March 2014 (oral presentation)*

